Causality and Communication: Relativistic astrophysical jets and the implementation of science communication training in astronomy classes

by

Susanna Kohler

B.S., University of California, Santa Barbara, 2008

M.S., University of Colorado Boulder, 2010

A thesis submitted to the

Faculty of the Graduate School of the

University of Colorado in partial fulfillment

of the requirements for the degree of

Doctor of Philosophy

Department of Astrophysics and Planetary Sciences

2014

This thesis entitled:
Causality and Communication: Relativistic astrophysical jets and the implementation of science communication training in astronomy classes
written by Susanna Kohler
has been approved for the Department of Astrophysics and Planetary Sciences

_____
Mitchell C. Begelman

_____
Prof. Seth Hornstein

_____
Prof. Phil Armitage

_____
Prof. Noah Finkelstein

_____
Prof. Andrew Hamilton

Date _____

The final copy of this thesis has been examined by the signatories, and we find that both the content and the form meet acceptable presentation standards of scholarly work in the above mentioned discipline.

IRB protocol #13-0430

Kohler, Susanna (Ph.D., Astrophysics)

Causality and Communication: Relativistic astrophysical jets and the implementation of science communication training in astronomy classes

Thesis directed by Prof. Mitchell C. Begelman

Part I: Relativistic jets emitted from the centers of some galaxies (called active galaxies) exhibit many interesting behaviors that are not yet fully understood: acceleration and collimation over vast distances, for instance, and occasional flaring activity. In the first part of my thesis, I examine the possibility of collimation and acceleration of relativistic jets by the pressure of the ambient medium surrounding the jet base. I discuss the differences in predicted jet behavior due to including the effects of a magnetic field threading the jet interior, and I describe the conditions that create some observed jet shapes, such as the "hollow cone" structure seen in M87 and similar jets. I also discuss what happens when the pressure outside of the jet drops so slowly that the jet shocks repeatedly, generating entropy at its boundary. Finally, I examine the spectra of the 40 brightest gamma-ray flares from blazars (active galaxies with jets pointed toward us) recorded by the Fermi Gamma-ray Space Telescope in its first four years of operation. I develop models to describe the observed behavior of these flares and discuss the physical implications of these models.

Part II: The ability to clearly communicate scientific concepts to both peers and the lay public is an important component of being a scientist. Few training programs exist, however, for scientists to obtain these skills. In the second part of my thesis, I examine the impact of two different training efforts for very early-career scientists: first, a short science communication workshop for science, technology, engineering and math (STEM) graduate students, and second, science communication training integrated into existing astrophysics classes for undergraduate STEM majors and early STEM graduate students. I evaluate whether the students' written communication skills demonstrate measurable improvement after training, and track students' attitudes toward science communication.

Dedication

Dedicated to my parents, for their boundless encouragement throughout this adventure.

Acknowledgements

A thesis is an exercise in patience, not just for the author, but for all of the people in the author's life. For everyone who has patiently supported me throughout my graduate career, I give you my deepest thanks — I could not have done this without you.

To my advisor, Mitch Begelman, I extend my first thanks. Not every advisor would find sign errors in pages of his student's algebra at 2 am — nor would every advisor handle it cheerfully as his student divides her attention to pursue education research as well. I cannot state enough how much I have appreciated your supportive patience as I've figured who I am and who I want to be.

I'm also grateful to my more recent advisor, Seth Hornstein. Thanks for making time for me and helping me to navigate this new world of education research, as well as for your patience with my last-minute emails and deadlines. I'm so pleased with the outcomes of this grand experiment!

To my research group, thank you for keeping my life surprisingly balanced. Greg, Eric, Phil and Mitch, your senses of humor have provided constant reminders that work is only work if you don't have hilarious people to share it with. And Greg and Eric, I can't imagine two guys I'd rather have shared an office with. I'd run a burro (or zebra) race for you guys any day of the year.

Finally, to my family and friends, I can never thank you enough for your overwhelming support throughout this adventure. Cara, Erin and Julia: meeting you ladies made every difficult part of the last six years worth it. Mom, Dad and Jessie: having you just a phone call away has often been the only thing keeping me sane. And François, your patience with the impact this journey has had on our lives has been been nothing short of monumental.

Contents

Chapter

1 Introduction 1

1.1 Causality and Communication 1

1.2 Outline of Remainder of Thesis 2

PART I: Relativistic Jets **3**

2 Preface to Part I 4

2.1 Overview of Relativistic Outflows 4

2.2 Classification of AGN 5

2.3 Phenomenology of AGN 6

2.4 Blazar Jets as Relativistic Outflows 7

2.5 Phenomenology of Blazar Jets 8

2.6 Spectral Energy Distributions of Blazars 10

3 Boundary Layers in Hydrodynamic Relativistic Jets 13

3.1 Preface 13

3.2 Introduction 14

3.3 Kompaneets Approximation 16

3.4 Self-Similar Treatment of the Boundary Layer 22

3.4.1 Self-Similar Solutions 24

3.4.2 Extension to the Kompaneets Model 32
3.5 Conclusion 35

4 Boundary Layers in Magnetized Relativistic Jets 40
4.1 Preface 40
4.2 Introduction 41
4.3 Self-Similar Treatment of the Magnetized Boundary Layer 42
4.3.1 Demonstration of Asymptotic Magnetic Dominance 45
4.3.2 Solutions in the Magnetic-Dominance Limit 46
4.4 Discussion of Results 49
4.5 Conclusion 53

5 Entropy Production in Relativistic Jet Boundary Layers 56
5.1 Preface 56
5.2 Introduction 57
5.3 Casting the problem 61
5.3.1 Isentropic solutions 61
5.3.2 Entropy-generating solutions 64
5.4 Deriving the boundary-layer flow 65
5.4.1 Fluid equations 67
5.4.2 Constructing self-similar solutions 68
5.5 Results 70
5.5.1 Radial scaling 70
5.5.2 Transverse scaling: a linear family of solutions 72
5.5.3 Entropy generation 74
5.5.4 Additional Isentropic Solutions 76
5.6 Conclusion 76

6 Spectral properties of the brightest gamma-ray flares of blazars 79

6.1 Preface . . . 79

6.2 Introduction . . . 80

6.3 Data analysis . . . 83

6.4 Results . . . 89

6.4.1 Spectral breaks . . . 89

6.4.2 Spectral curvature . . . 91

6.5 Discussion . . . 95

6.6 Conclusions . . . 99

PART II: Science Communication **101**

7 Preface to Part II 102

7.1 Background . . . 102

7.1.1 A Definition of Science Communication . . . 102

7.1.2 Importance of Science Communication . . . 103

7.1.3 Who Should Communicate Science? . . . 104

7.1.4 Impediments to Scientists as Communicators . . . 106

7.1.5 Availability of Communication Training for Scientists . . . 108

7.2 Statistical methods . . . 108

7.2.1 Types of quantitative data . . . 109

7.2.2 Parametric vs. non-parametric statistical analysis . . . 110

7.2.3 Interrater reliability . . . 111

7.2.4 Statistical significance . . . 113

7.2.5 Effect size . . . 116

7.2.6 Normalized gain and normalized change . . . 118

8 ComSciCon: Training Graduate Students to Communicate Science 120

8.1 Preface . . . 120

8.2 Introduction . . . 121

8.2.1 About ComSciCon 2013 . . . 121

8.2.2 Research Goals . . . 121

8.3 Methods . . . 122

8.3.1 Sample Selection and Participant Demographics . . . 122

8.3.2 Provided Training: Components of ComSciCon . . . 123

8.3.3 Instruments and Measures . . . 126

8.4 Results and Discussion . . . 127

8.4.1 General Goals and Beliefs of Participants . . . 128

8.4.2 Self-reported Impact . . . 133

8.4.3 Writing Sample Analysis . . . 134

8.4.4 Follow-Up . . . 137

8.5 Conclusion and the Future of ComSciCon . . . 138

9 Effects of Adding Science Communication Training to Astronomy Classes 141

9.1 Preface . . . 141

9.2 Introduction . . . 142

9.2.1 About This Study . . . 142

9.2.2 Preliminary study . . . 142

9.2.3 Research goals . . . 143

9.3 Methods . . . 144

9.3.1 Participants . . . 144

9.3.2 Training . . . 145

9.3.3 Instruments and measures . . . 146

9.4 Results and Discussion . . . 148

9.4.1 Writing sample analysis . . . 149
9.4.2 Attitudes survey analysis . . . 160
9.5 Conclusion . . . 167
9.5.1 Success of Training . . . 169
9.5.2 Timing of Training . . . 170
9.5.3 Recommendations . . . 170

10 Conclusion 172

Bibliography 175

Appendix

A Additional Derivations 182
A.1 Derivation of Governing Equations under the Kompaneets Approximation . . . 182

B ComSciCon Materials 187
B.1 ComSciCon 2013 Application . . . 187
B.2 Surveys . . . 190

C Science Communication Training in the Classroom Materials 203
C.1 Sample Training Materials . . . 203
C.1.1 Sample Lesson Plan Outlines . . . 203
C.1.2 In-Class Handout . . . 205
C.1.3 Sample Reading Assignment . . . 208
C.1.4 Sample Writing Assignment . . . 209
C.2 Attitudes Surveys . . . 210
C.3 Rubric . . . 218

Tables

Table

2.1 Comparison of properties of relativistic astrophysical jet systems 5

6.1 Statistically significant breaks discovered in the spectra of the 40 brightest Fermi gamma-ray flares 87

6.2 Log-parabola fit parameters for the brightest gamma-ray flares of blazars 93

8.1 Breakdown of study participants by STEM field 123

8.2 Learning goals targeted in Baram-Tsabari & Lewenstein (2013) 126

8.3 Normalized gains of participants' average scores 136

9.1 Summary of undergraduate and graduate classes targeted in this study 145

9.2 Learning goals targeted in the science communication training 147

9.3 Summary of study sample sizes for each participating class 149

9.4 Average normalized change g for the five classes studied 156

Figures

Figure

2.1 Cartoon illustrating physical and emission components of an AGN 9

2.2 Blazar jet half-opening angle vs. Lorentz factors 11

2.3 Variation of flux over time in blazar 3C 279 12

3.1 Diagram of the shocked boundary layer of a jet 17

3.2 Two examples of the solutions for the shock front and associated contact discontinuity 21

3.3 Dependence of the jet closure point on $\theta_0\Gamma_{j,0}$ 23

3.4 Pressure within the shock as scaled by the external pressure 28

3.5 Values of μ as a function of η for $2 < \eta < 8/3$ 30

3.6 Physical solutions for $q(\xi)$ within the shock 30

3.7 Shock front and contact discontinuity for two cases 34

3.8 Total integrated energy contained within the boundary layer at a given height 36

4.1 Special-case solution for $g(\xi)$ 49

5.1 Minimum angle of impact necessary to produce a shock 62

5.2 Plot of the deflection angle of flow across a shock for a range of impact angles 66

5.3 Radial scaling of the bulk Lorentz factor 71

5.4 Pressure within the shock as scaled by the external pressure 75

6.1 Time-integrated flare spectra of the 40 brightest gamma-ray blazar flares 84

6.2 Source-frame break energy vs. the peak flux of the flare 90
6.3 Change in photon index vs. the peak flux of the flare 92
6.4 Spectral curvature vs. duration of the flare 96
6.5 Spectral peak position vs. duration of the flare 97

7.1 Diagram of the linear model of science communication 105
7.2 The environments in which the three major actors in science communication work . 107

8.1 Perceived level of support for scientists who engage the public 129
8.2 Participants' self-reported career goals 130
8.3 Participants' self-reported previous training in science communication 132
8.4 Participants' reported confidence submitting an article to a popular science magazine 134
8.5 Participants' reported confidence in their ability to communicate 135
8.6 Participants' scores in five categories evaluating targeted learning goals 136

9.1 ASTR 1030 pre- and post-training writing sample score distributions 151
9.2 ASTR 2030 pre- and post-training writing sample score distributions 152
9.3 ASTR 3710 pre- and post-training writing sample score distributions 153
9.4 ASTR 5110 pre- and post-training writing sample score distributions 154
9.5 ASTR 5120 pre- and post-training writing sample score distributions 155
9.6 Average class pre- and post-training scores for each of the five classes 158
9.7 Comparison of average scores for STEM majors and non-majors in ASTR 2030 159
9.8 Students' initial perceptions of importance of science communication 161
9.9 Students' self-reported previous training in science communication 162
9.10 Perceived level of support for scientists who engage the public 163
9.11 Students' confidence submitting an article to a popular science publication 165
9.12 Students' reported confidence in their ability to communicate 166
9.13 Students' assessment of training impact 168

Chapter 1

Introduction

1.1 Causality and Communication

A thesis is usually very narrowly focused, but in my case, this presents a problem: how does one unite a thesis covering two topics as disparate as high-energy astrophysics research and science communication research? The title of this thesis, first suggested in humor by Phil Armitage, actually forges an insightful connection: both topics focus on the ideas of causality and communication.

In relativistic astrophysical jets, where the flow moves nearly at the speed of light, it can often outrun the soundspeed within the jet. This results in a loss of communication between the jet and its environment that can play a major role in the ultimate structure and dynamics of the system. If the environment downstream of the jet can't receive warning in the form of sound waves before the jet arrives, it is unable to move out of the way — which can result in shocks as the jet material slams into the ambient medium. We refer to this loss of communication between the jet and its environment as "loss of causal contact". My research on astrophysical jets primarily focuses on what happens to the jet after this loss of causality and communication has occurred.

In undertaking this research, it didn't take long to establish a fun parallel in my life: the process of trying to explain special relativistic astrophysics to a layperson **also** resulted in a prompt loss of communication. Though the sense of the word is different, the outcome was the same: the flow of information was not transmitted smoothly, because it was not being communicated effectively. It was this process of attempting to explain my astrophysics research to general audiences that first interested me in the theory behind specialized communication for different audiences, and led me

to pursue the research projects presented in the second half of thesis, in which I study ways to train future scientists to avoid the loss of communication that is so common when describing complex research topics.

1.2 Outline of Remainder of Thesis

Part I of this thesis contains the work that I've done on various aspects of relativistic jets. Chapter 2 provides an introduction and some background to astrophysical relativistic jets and their characteristics. Chapters 3 – 5 are reproductions of three papers (the first two published and the third submitted) I completed with Dr. Mitch Begelman on the structure of ultrarelativistic astrophysical jets. These are theory-based papers in which we propose models for how these jets are accelerated and collimated. Chapter 6 contains an observational paper I completed with Dr. Krzysztof Nalewajko, in which we perform spectral analysis of bright blazar flares detected by the Fermi Gamma-ray Space Telescope.

In Part II of this thesis, I transition to the research I have completed with Dr. Seth Hornstein in the field of science education research, with an emphasis on science communication. Chapter 7 provides an introduction and some background to science communication theory, as well as an overview of the statistical methods used in this part of the thesis. Chapters 8 and 9 detail the bulk of my research on the effectiveness of providing science communication training for science, technology, engineering and math (STEM) undergraduate and graduate students.

Appendix A contains some additional derivations not included in Chapter 3. Appendix B contains the text of the application for ComSciCon 2013 and all of the assessment instruments used in the ComSciCon study. Appendix C contains samples of all of the training materials and assessment instruments used in the study of science communication training in the classroom.

PART I

Relativistic Jets

Chapter 2

Preface to Part I

2.1 Overview of Relativistic Outflows

Relativistic jets exist throughout the universe in many forms. These jets can travel over vast distances, move at nearly the speed of light, and stem from sources that range from stellar-mass to billions of times that. The primary aspect that relativistic jets have in common is that they are all emitted from a region close to an accreting compact object, likely using energy extracted from the object itself or from the material feeding it.

Relativistic outflows tend to fall into three main categories: active galactic nuclei (AGN), microquasars (MQs), and gamma-ray bursts (GRBs). Table 2.1 summarizes a few properties of these three systems, and a brief description of each follows here:

Active galactic nuclei are particularly luminous compact regions at the centers of some galaxies. Their activity is inferred to be due to the accretion of material onto the supermassive black hole at the galaxy's center. The jets that are emitted from the poles of the accretion disk around the black hole can extend over distances of millions of light years.

Microquasars are galactic systems that are analogous to AGN, but on smaller scales. They result when a stellar-mass black hole in a binary star system accretes matter from its companion star. In a similar scenario to AGN, an accretion disk forms around the black hole, and jets that can extend over distances of roughly a light year are emitted from the poles of the disk.

Gamma-ray bursts are sudden flares of energy thought to be released when a high-mass star collapses in on itself, forming a black hole at its center. As material rapidly accretes onto this black

hole, extremely energetic jets are produced that punch through the remaining stellar envelope to escape at the surface. The jets typically extend over distances of only a few light hours, but they produce some of the highest luminosities observed in the universe.

While much of the work in the first part of this thesis is applicable to a broad range of astrophysical jets, we focus primarily on modeling the jets emitted from AGN; thus the remainder of this introduction will be spent further discussing these systems. I will provide some basic background necessary for understanding the next four chapters of this thesis, breaking down the classification of AGN and their basic phenomenology, discussing the properties and physics of blazar jets, and briefly reviewing characteristics of the spectra of blazars. The reader already familiar with these concepts can skip ahead to Chapter 3.

Table 2.1: Comparison of properties of relativistic astrophysical jet systems

	AGN	MQs	GRBs
Mass of central object	$10^6 - 10^{10}$ $M_\odot$	$1 - 10$ $M_\odot$	$1 - 10$ $M_\odot$
Luminosity	$10^{42} - 10^{48}$ erg s^{-1}	$10^{31} - 10^{37}$ erg s^{-1}	$10^{47} - 10^{52}$ erg s^{-1}
Terminal $\Gamma^\dagger$	$1 - 50$	$1 - 3$	$100 - 1000$

†where $\Gamma = (1 - (v/c)^2)^{-1/2}$ is the bulk Lorentz factor

2.2 Classification of AGN

AGN are the most powerful steady sources of luminosity in the universe. Unlike normal galaxies, whose spectra are dominated by starlight in the optical or dust in the IR, AGN have extremely broad spectra with large amounts of energy emitted from the radio or infrared all the way through X-rays or even gamma-rays (Fabian, 1999). AGN are often characterized by variability on timescales as short as a few days, which implies that emission must come a small region of order light days in size. AGN can be classified into different categories based on phenomenological features:

Seyfert galaxies have relatively slow, weak, poorly collimated flows (Marscher, 2010). These

galaxies have modest luminosities and are radio-quiet (i.e., radio emission is weak), yet they are well-studied because they generally lie near to us (Fabian, 1999). Seyfert spectra show prominent emission lines of highly ionized atoms that cannot be produced by stars (Rosswog & Brüggen, 2007).

Radio galaxies have spectra similar to normal elliptical galaxies, except that they exhibit an excess amount of energy in radio wavelengths. The category of radio galaxies includes Fanaroff-Riley type I galaxies, which have strong jets with relativistic speeds, and Fanaroff-Riley type II galaxies, which have some of the most luminous, highly focused and relativistic beams (Marscher, 2010).

Quasars are extremely luminous galactic nuclei that outshine their host galaxies. Their spectra are nearly featureless, and about 10% of quasars are radio-loud, a feature that is generally associated with having a collimated relativistic outflow (Fabian, 1999).

Blazars are AGN where the jet happens to be aligned (or nearly so) with our line of sight. Despite their cosmological distances, blazars are easily detected because their radiation has been boosted by special relativistic effects (this is discussed in more detail in §2.4). Blazars emit polarized light with a featureless, nonthermal spectrum typical of synchrotron radiation (radiation emitted when charged particles are accelerated radially); this synchrotron emission generally swamps any absorption or emission lines in the spectrum. Blazars are extremely luminous and highly variable, and are characterized by large X-ray and gamma-ray luminosities (Rosswog & Brüggen, 2007). The brightest blazars are further subclassified as flat-spectrum radio quasars (FSRQs) and BL Lacertae (BL Lac) objects, which both radiate most of their energy in MeV and GeV gamma-rays (Fossati et al., 1998).

2.3 Phenomenology of AGN

AGN are powered by the energy released as matter falls down the potential well of the central black hole. Because this matter carries angular momentum, it settles into a disk on scales much

smaller than a pc around the black hole, and viscous stresses then transport angular momentum outwards, releasing energy as the material is moved inwards. On larger scales, where angular momentum doesn't dominate the dynamics and temperatures are lower, molecular gas and dust is thought to form into a toroidal structure generally referred to as the dusty torus.

There exist two additional regions of material: 1) the Broad Line Region (BLR), an area consisting of fast-moving clouds orbiting fairly close in to the central black hole, extending approximately up to 0.1 pc for bright AGN (Kaspi et al., 1996), and 2) the Narrow Line Region (NLR), an area consisting of slower-moving clouds orbiting further out from the central black hole, extending approximately $10 - 1000$ pc out (Alexander & Hickox, 2012). A jet extending from the poles of the accretion disk in radio-loud galaxies such as blazars can interact with the clouds in both of these regions.

2.4 Blazar Jets as Relativistic Outflows

Very-long-baseline interferometry (VLBI) first allowed for resolution of structure within blazar jets, leading to the discovery that, in some cases, there were features within the jets that appear to be moving faster than the speed of light (e.g. Cohen et al., 1971, Jorstad et al., 2001). This was taken as the first evidence that blazar jets likely have relativistic velocities. For a special-relativistic object moving at velocity v at an angle of θ with respect to the line of sight, its apparent velocity is given by $v_{app} = v(\sin\theta)(1 - \beta\cos\theta)^{-1}$, where $\beta = v/c$. This is maximized at $v_{app} = v\Gamma$ when $\sin\theta = 1/\Gamma$, where $\Gamma = (1 - \beta^2)^{-1/2}$ is the bulk Lorentz factor. Thus, jets with apparent velocities significantly higher than c could indeed be observed if the outflow is relativistic and the jet is oriented at an angle near $\sin^{-1}(1/\Gamma)$. Complementing this evidence for relativistic jets are observations of blazar jet variability on timescales in the range of minutes to years. Assuming that variability is limited by the time it takes for a sound wave to cross the source, these timescales are far shorter than should be possible given the source size (Hoyle et al., 1966, Aharonian et al., 2005), providing another indication that the jets are likely relativistic.

It is not coincidence that the best-studied jets are those that are pointed toward us and have very high velocities. Relativistic motion also results in Doppler boosting, an amplification of the observed luminosity. The Doppler factor, given by $D = \Gamma^{-1}(1 - \beta\cos\theta)^{-1}$, is maximized for $\theta = 0$. Relativistic aberration causes most of the emission to be beamed into a cone of opening half-angle $\Theta \sim 1/\Gamma$, and if the emission is steady-state, the flux density is boosted by a factor of D^2. Thus it is as a result of the relativistic nature of blazar jets that they have become the best-studied variety of jets: the relativistic beaming of their radiation increases their observed brightness so that they're easy to detect — even at low emitted luminosities — so long as the jet points within a few degrees of the line of sight. Due to the same effect, AGN jets that are not pointed to within a very narrow angle of our line of sight will be much harder to detect, since their radiation will be similarly beamed away from us. Blazar observations themselves provide a clear example of this: while the jet that is pointed toward us is boosted in luminosity, the receding counter-jet is diminished and often isn't even detectable (e.g. Bridle & Perley, 1984).

2.5 Phenomenology of Blazar Jets

Blazar jets are modeled as being emitted along the poles of the AGN accretion disk and powered either by extraction of energy and angular momentum from the accretion disk itself (Blandford & Payne, 1982) or by extraction of the spin energy of the black hole (Blandford & Znajek, 1977). Because of the swamping of their spectra by the synchrotron radiation, no spectral features of the moving matter within jets are observed, preventing us from making reliable estimates about particle energy flux and mass, values of magnetic fields, or even the material composition of the jet. Observations lead us to assume that electrons are a necessary component since an excessively high magnetic field would be needed to produce the observed synchrotron radiation power (which is proportional to B^2/m^2) with only protons. Overall charge neutrality within the jet could be provided by either protons or positrons.

Hydrodynamic models of AGN jets consist of several successive regimes (see Figure 2.1). The

jet is launched with a high initial Lorentz factor — or accelerates to one fairly quickly — but it also initially contains a large amount of internal energy. In this regime, the jet is considered to be "pressure-dominated". As the jet propagates, however, the internal energy is gradually converted into kinetic energy, and the jet material is further accelerated until reaching a maximal point where all of the jet's energy is kinetic. In this regime the jet is "inertia-dominated," and it is now essentially a ballistic flow, coasting at a constant velocity until it is disturbed. Throughout this acceleration regime, which is expected to exist on scales of tens to thousands of Schwarzschild radii (approximately 0.1 pc, for a 10^8 $M_\odot$ black hole), the jet also undergoes collimation. Beyond this region, the jet propagates into the intergalactic medium and is gradually decelerated as it drives a shock into the material, eventually spreading out into large radio lobes where it deposits all of its energy.

Acceleration via adiabatic expansion occurs fairly gradually in relativistic hydrodynamic jets. Conversion of thermal energy into kinetic is governed by the relativistic Bernoulli equation, which states that $p \propto \Gamma^{-4}$ along streamlines, where p is the thermal pressure of the jet. Thus acceleration in relativistic jets occurs over long distances — a pressure drop by a factor of two corresponds to only a $\sim 20\%$ increase in the bulk Lorentz factor of a relativistic jet.

As discussed in Chapter 1, an important consideration when modeling relativistic jets is that of causal contact. Causal contact between two parts of a jet is lost when they are expanding away from each other faster than a sound wave can travel between them. In a relativistic jet, the sound speed as viewed in the lab frame is $c_s = \dfrac{c}{\Gamma\sqrt{3}}$ (it is decreased by a factor of Γ as a result of time dilation). Thus, in the case of a jet with a half-opening angle of Θ, the outer wall of the jet remains in causal contact with the jet center only if the opening angle obeys $\Gamma^{-1} > \sin\Theta \approx \Theta$. Indeed, this limiting value for maintaining causal contact provides a useful characteristic scale within the jet, as will be seen later. Observations confirm that blazar jets frequently have opening angles approximately of the order of Γ^{-1} (see Figure 2.2).

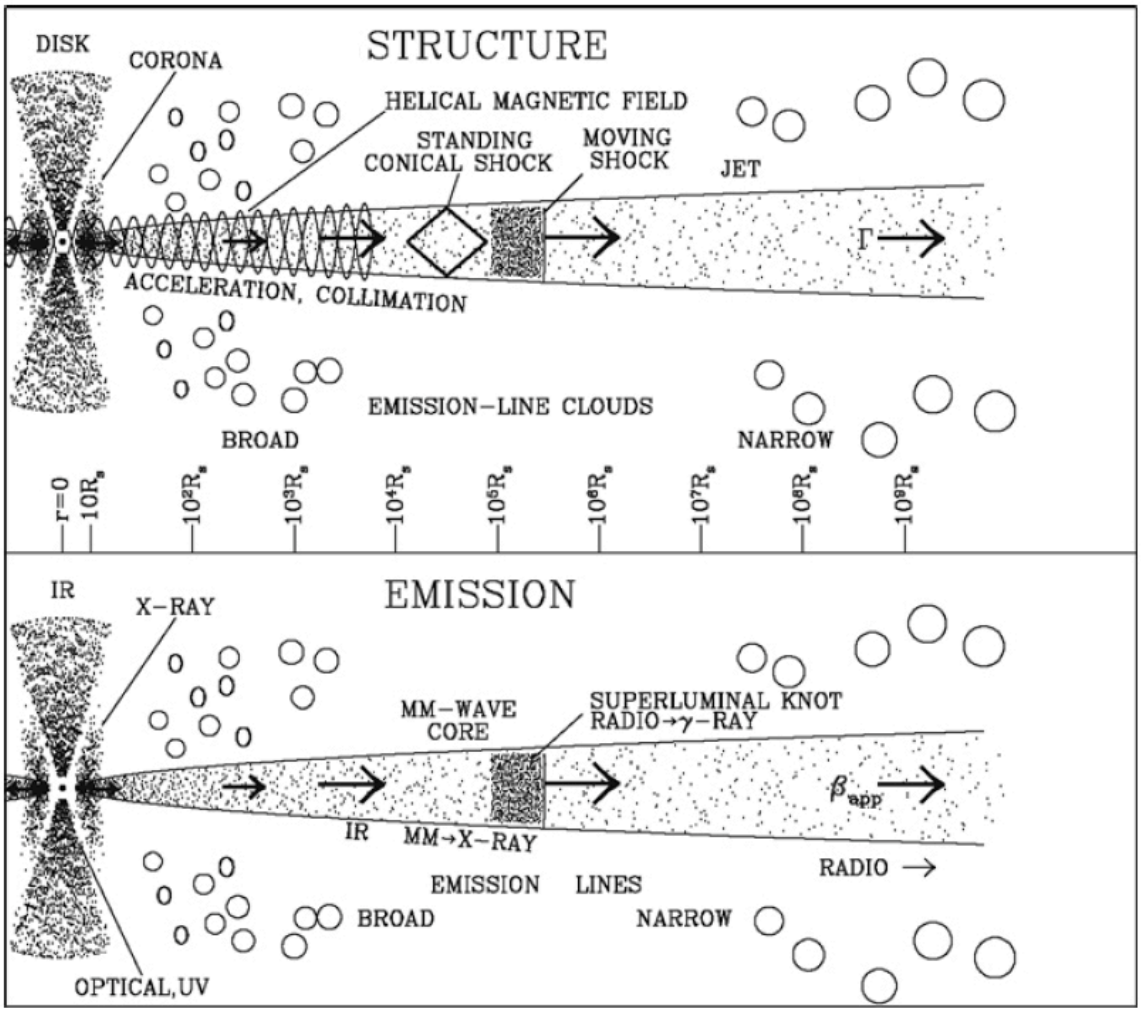

Figure 2.1: Cartoon illustrating the various physical and emission components of an AGN with a relativistic jet, shown on a logarithmic length scale. Adapted from Marscher, 2010.

2.6 Spectral Energy Distributions of Blazars

As previously mentioned, the emission from blazar jets is nonthermal, and the spectral energy distributions of blazars are very broad, with radiation extending from radio to gamma-ray frequencies. The continuum emission can generally be attributed to four main mechanisms: 1) the radio emission is dominated by synchrotron emission from the jet, 2) the infrared emission is primarily due to thermal radiation from the warm, dusty torus, 3) the optical/ultraviolet emission is largely due to thermal emission from the accretion disk and the hot gas around it, and 4) the

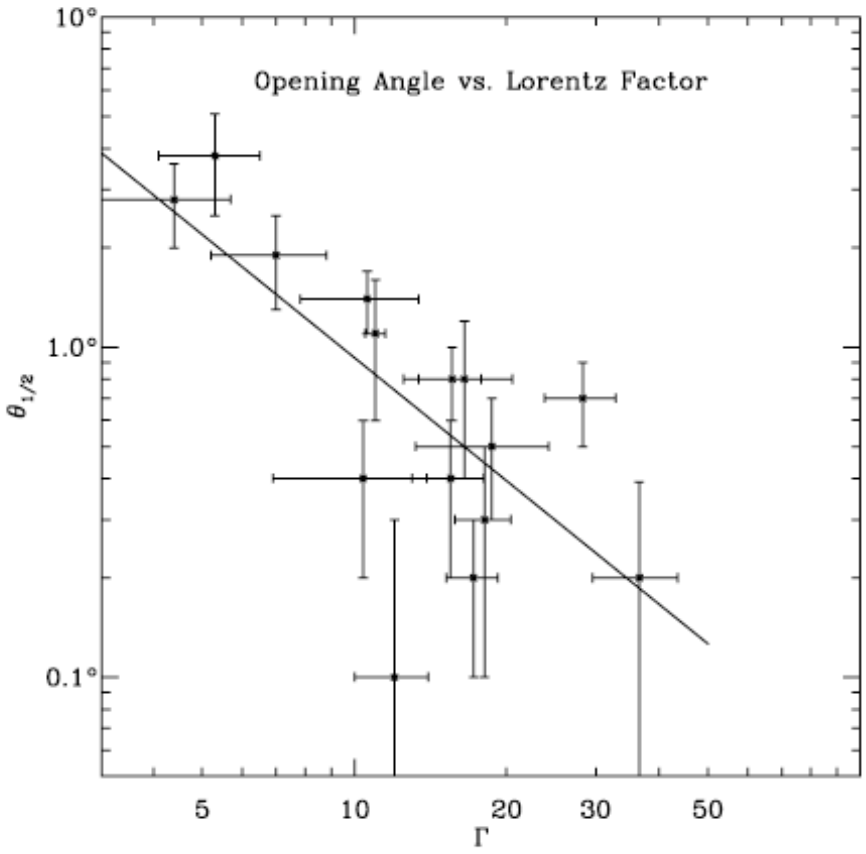

Figure 2.2: Blazar jet half-opening angle vs. Lorentz factors from 8 radio-loud quasars, 5 BL Lac objects, and 2 radio galaxies with blazar-like radio emission. The line corresponds to $\theta \propto \Gamma^{-1}$. From Marscher, 2006, adapted from Jorstad et al., 2005.

X-ray and gamma-ray emission is thought to be due to inverse Compton scattering of low-energy seed photons off of relativistic electrons in the jet.

One open question about emission from blazars is that of the source of the low-energy seed photons to produce the gamma-ray radiation we observe. It is unclear whether the source of the seed photons is internal to the jet (i.e., synchrotron emission from the jet itself; Maraschi et al. (1992)), externally located but near the central engine (e.g., coming from the BLR; Sikora et al. (1994a)), or located further from the source (e.g., emitted by the dusty torus; Wagner et al. (1995)). One way of placing constraints on the source of gamma-ray emission is to better understand the features seen in blazar spectra, including spectral "breaks", or sudden decreases in flux

observed above a certain energy. More will be said about this in Chapter 6.

Emission from blazars is inherently variable, often quite dramatically, on timescales as short as hours or even minutes (Marscher, 2010); an example of this can be seen in Figure 2.3. Analysis of blazar spectra frequently relies on first processing data by integrating over a large span of time — often weeks or months (e.g. Abdo et al. (2009), Abdo et al. (2010b), Poutanen & Stern (2010)). This process ignores the high level of variability, and possibly loses important information as a result. This is another topic that will be addressed in Chapter 6.

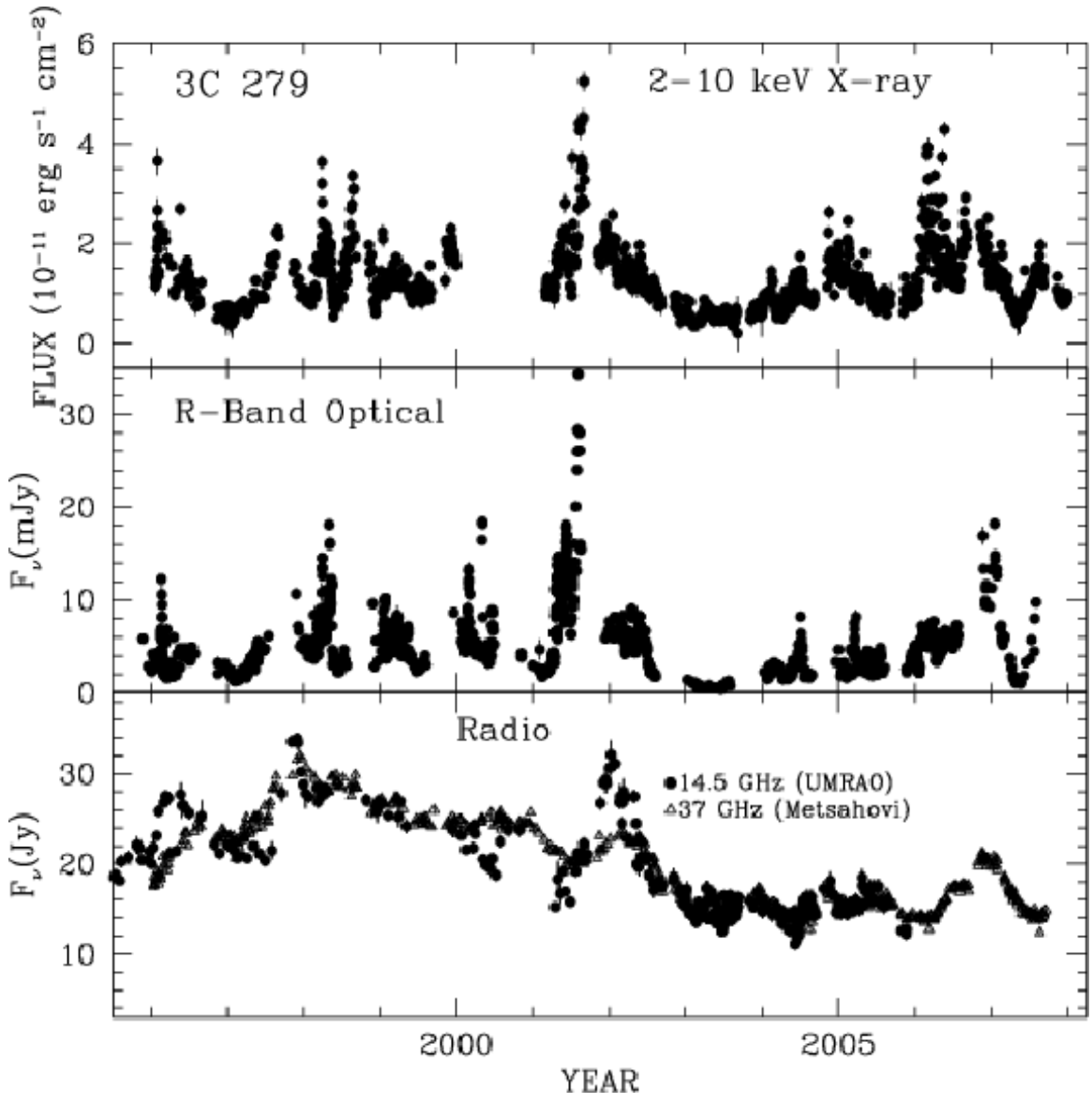

Figure 2.3: Variation of flux over time in blazar 3C 279 in radio, optical, and X-ray emission, as presented in Marscher, 2010.

Chapter 3

Boundary Layers in Hydrodynamic Relativistic Jets

3.1 Preface

This paper appeared in Monthly Notices of the Royal Astronomical Society, Volume 426, Issue 1, pp. 595-600 and was completed under the guidance of Dr. Mitch Begelman. This is the first of three papers examining the impact of the ambient medium on collimation and confinement of relativistic jets that have lost causal contact with their surroundings. This paper focuses on the purely hydrodynamic case. In addition, the solutions presented in this paper conserve energy within the boundary layer, and the flow is irrotational, isentropic, and behaves adiabatically; we relax some of these assumptions in Chapters 4 and 5 of this thesis.

Abstract

We study the collimation of relativistic hydrodynamic jets by the pressure of an ambient medium in the limit where the jet interior has lost causal contact with its surroundings. For a jet with an ultrarelativistic equation of state and external pressure that decreases as a power of spherical radius, $p \propto r^{-\eta}$, the jet interior will lose causal contact when $\eta > 2$. However, the outer layers of the jet gradually collimate toward the jet axis as long as $\eta < 4$, leading to the formation of a shocked boundary layer. Assuming that pressure-matching across the shock front determines the shape of the shock, we study the resulting structure of the jet in two ways: first by assuming that the pressure remains constant across the shocked boundary layer and looking for solutions to the shock jump equations, and then by constructing self-similar boundary-layer solutions that allow for

a pressure gradient across the shocked layer. We demonstrate that the constant-pressure solutions can be characterized by four initial parameters that determine the jet shape and whether the shock closes to the axis. We show that self-similar solutions for the boundary layer can be constructed that exhibit a monotonic decrease in pressure across the boundary layer from the contact discontinuity to the shock front, and that the addition of this pressure gradient in our initial model generally causes the shock front to move outwards, creating a thinner boundary layer and decreasing the tendency of the shock to close. We discuss trends based on the value of the pressure power-law index η.

3.2 Introduction

The idea that AGN outflows are highly collimated is supported by observations (e.g. Begelman et al., 1984, Jorstad et al., 2005), implying that confinement must occur. The cause of this confinement, which may occur at distances of just a few tens of Schwartzschild radii from the central black hole (Junor et al., 1999), is however not yet well-understood. It is generally accepted that some collimating agent is necessary, but this still allows for a variety of possibilities, both external (e.g. pressure confinement via an ambient static medium Eichler, 1982; Komissarov & Falle, 1997, inertial confinement via a slow outflow or wind surrounding the jet Komissarov, 1994b; Bromberg & Levinson, 2007) and internal (magnetic confinement via hoop stress due to the toroidal magnetic field component Benford, 1978; Begelman et al., 1984).

Pressure confinement is of particular interest because accretion disk winds surrounding an AGN provide an ideal external medium for interaction with the jet. Moreover, another collimating agent such as magnetic hoop stress cannot function alone; without an ambient medium to confine the globally-expansive magnetic field, collimation will not occur (Begelman, 1995; Komissarov et al., 2007, 2009; Komissarov, 2011). Thus pressure confinement may be relevant both on its own and in conjunction with other processes.

In this context, we note that numerical simulations that study confinement and acceleration

of the flow by MHD processes treat the action of the external medium as an applied boundary condition (e.g. Komissarov et al., 2007, 2009; Komissarov, 2011). In this work, we study the detailed physics of jet collimation by the external medium as a first step towards a complete treatment of both the action of the external medium and magnetic effects in collimating and accelerating relativistic jets.

The location and mechanism of jet collimation is interesting because it provides insight into energy dissipation within the jet. In a steady jet, there are two main sites where energy dissipation is likely to occur: at the jet spine, as a result of kink instabilities driven by the toroidal magnetic field (Begelman, 1998; Eichler, 1993), and at the interface between the jet and its environment, as a result of shear instabilities (Micono et al., 2000; Perucho et al., 2010; Barkov & Baushev, 2011) or collimation shocks, as we discuss here.

In the case of a jet with an opening half-angle of θ and a bulk Lorentz factor of Γ, the outer edge of the jet remains in causal contact with the jet center only if the opening angle obeys $\Gamma^{-1} > \sin\theta \approx \theta$. In this work, we assume a relativistic equation of state and examine the case where causal contact between the jet's spine and edge has been lost. Thus we model the jet as having a transverse structure consisting of two components: an inner region in which the flow is undergoing free expansion as it accelerates, and an outer shocked boundary layer region that results from the loss of causal contact within the jet. The geometrical shape that the jet assumes as it propagates is a direct result of its response to the collimating forces exerted by the ambient medium, and calculating that shape for the case of pressure confinement will be a major focus of this paper.

Our goal is to determine the basic jet structure and geometry under a simple set of collimation and acceleration assumptions, providing a model for the jet's steady-state configuration. This will allow more realistic initial conditions for simulations of instabilities and turbulence, which will in turn provide a model for AGN jets to which we can compare observational signatures.

While we specifically reference AGN jets in this work, our results can easily be extended to other relativistic outflows, such as a gamma-ray burst in the collapsar model, collimated by the

stellar envelope it breaks through, as discussed in Bromberg & Levinson, 2007 (hereafter BL07).

In this paper we use the shock conditions for a hydrodynamic, relativistic jet to derive the basic structure of the jet. This problem has been previously studied in the case of a "cold" (inertia-dominated) jet (Komissarov & Falle, 1997; Nalewajko & Sikora, 2009), but we now focus on the collimation behavior of a "hot" (pressure-dominated) jet.

We initially follow a similar approach to that of BL07, but deviate from its methods in our treatment of entropy distribution within the jet. Bromberg & Levinson, 2009 (BL09) performs a similar analytical inspection in the limit of small angles; we generalize this to all angles.

In §3.3 we find solutions for the jet shape using the Kompaneets approximation. In §3.4 we examine self-similar solutions for the boundary layer when a pressure gradient is allowed to form across the layer, and then revise our solutions from §3.3 to include this pressure gradient. In §3.5 we conclude, summarizing the results and discussing future work.

3.3 Kompaneets Approximation

We consider a cylindrically symmetric, ultrarelativistic jet injected into an ambient medium that has a power-law pressure profile. We wrap the physics of the shocked ambient medium into this external pressure profile and focus on the structure of the jet itself. In this stage of the treatment, we ignore magnetic fields and assume that the external pressure due to the ambient medium creates the sole collimating force on the jet.

We define R and z as dimensionless parameters in cylindrical coordinates describing the radial and axial distances as scaled by z_0, the height at which the jet initially encounters the external medium. The jet is injected with an initial opening half-angle of θ_0 and impacts the wall of the ambient medium at the point thus denoted as $(R_0 = \tan\theta_0, z_0 = 1)$. We assume the jet is injected from a point source with steady flow, and streamlines are conical and characterized by the angle θ_j.

We further suppose that the interior of the jet is undergoing free expansion. As relativistic

adiabatic expansion obeys $pV^{4/3} \sim const$, it therefore exhibits a corresponding pressure profile of $p_j \propto r^{-4}$, where r is the spherical radius defined as $r \propto (R^2 + z^2)^{1/2}$ in cylindrical coordinates. The gradual acceleration via adiabatic expansion of the jet interior is governed by the relativistic Bernoulli equation, which describes the conversion of thermal to kinetic energy as $p \propto \Gamma^{-4}$ along streamlines (see, e.g., Landau & Lifshitz, 1959).

Where the jet impacts the ambient medium with a supersonic normal velocity, a shocked layer will form, as indicated schematically in Figure 3.1. The layer is bounded on the inside by a shock front, and on the outside by a contact discontinuity. There is no mass flux across the contact discontinuity, and the pressure must be matched on either side of it. Adopting a pressure profile for the ambient medium of $p_s \propto r^{-\eta}$, for a parameter η, this fixes the pressure external to the jet and immediately inside the contact discontinuity.

We now adopt the Kompaneets approximation (Kompaneets, 1960; see e.g. BL07 and Komissarov & Falle, 1997), treating the pressure as a function only of z within the shocked layer. Thus the pressure profile of the external medium extends across the shocked layer with no pressure gradient in the axial direction, greatly simplifying the problem.

In this paper, we focus particularly on the less-explored case of an external pressure profile with $2 < \eta < 4$ (see e.g. BL07 for an example of treatment of this regime). An $\eta < 2$ implies that if the jet begins in causal contact it will remain in causal contact, suggesting that a shocked boundary layer would not form. For $\eta = 4$ the ambient pressure profile is equivalent to that of free expansion, matching the pressure within the jet, and an $\eta > 4$ would result in a rarefaction at the jet boundary (Begelman et al., 1984). Thus the regime between these two values is a logical place to examine.

Physically, this pressure profile range could describe multiple scenarios for the confining medium. The ram pressure of a head-on wind decreases as $p \propto r^{-2}$, and any obliquity would serve to steepen that pressure profile (Eichler, 1982). The range is similarly relevant if the confining medium were an accretion flow such as Bondi accretion ($p \propto r^{-5/2}$), and it would not be an unrealistic range for a disk corona, or a stellar envelope in a GRB collapsar model.

The flow parameters across the inside boundary of the shocked layer are governed by the rel-

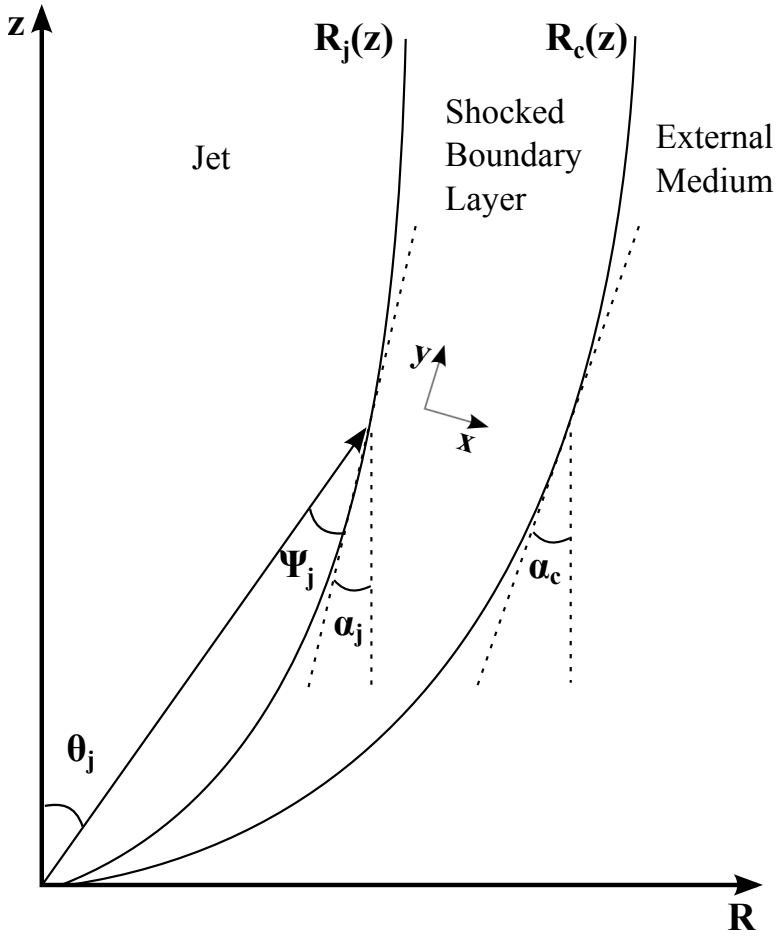

Figure 3.1: Diagram indicating the angles and orientation of the axes relative to the inner shock wall. θ_j is the angle the jet streamline makes with the z-axis. Ψ_j is the angle it makes with the shock normal, and α_j is the angle between the shock normal and the vertical.

ativistic oblique shock-jump conditions. These establish conservation of mass, momentum, energy, and tangential velocity:

$$n_j\Gamma_j\beta_{j,x} = n_s\Gamma_s\beta_{s,x} \tag{3.1}$$

$$w_j\Gamma_j^2\beta_{j,x} = w_s\Gamma_s^2\beta_{s,x} \tag{3.2}$$

$$w_j\Gamma_j^2\beta_{j,x}^2 + p_j = w_s\Gamma_s^2\beta_{s,x}^2 + p_s \tag{3.3}$$

$$\beta_{j,y} = \beta_{s,y} \tag{3.4}$$

where the x-direction is chosen perpendicular to the shock front and the y-direction is tangential (see Figure 3.1). The subscript j denotes quantities within the freely-expanding inner jet region, and the subscript s denotes quantities within the shocked boundary layer. Here $\beta = v/c$, and $w \equiv \epsilon + p$ where ϵ is the total proper energy density, given by $\epsilon = \rho + 3p$ with ρ defined as the proper rest mass density. Considering the case of an ultrarelativistic gas in the regime where the jet is still accelerating, we assume that $\rho \ll p$ and the equation of state is $p = \epsilon/3$, such that $w \approx 4p$.

Examining the geometry of the problem, we recognize that the angle of impact of the streamline with the shock front, $\sin\Psi_j$, can be represented in terms of θ_j and α_j, respectively the angle the streamline makes with the z-axis and the angle that the shock tangent makes with the z-axis. By noting that $\tan\alpha_j = dR_j/dz$, where R_j is the shape of the shock front, and assuming conical streamlines such that $\tan\theta_j = R_j/z$, we can combine the geometry of the problem with the general shock jump conditions to obtain a differential equation governing the shape of the inner shock wall,

$$\frac{\left(R_j - z\frac{dR_j}{dz}\right)^2}{\left(R_j^2 + z^2\right)\left(1 + \left(\frac{dR_j}{dz}\right)^2\right)} = \frac{1}{8\Gamma_j^2}\left(3\frac{p_s}{p_j} + 1\right). \tag{3.5}$$

This can be solved analytically for dR_j/dz and numerically integrated to find $R_j(z)$. A more detailed derivation of this equation is given in Appendix A.

To solve for the shape of the contact discontinuity separating the shocked layer from the ambient medium, denoted as R_c, we assume energy-momentum conservation through a volume of the shocked layer, as described in BL07. As in BL07, we assume that the flow parameters within the

shock depend only on the vertical distance z in order to make the problem analytically tractable. Making the further assumption that $|\boldsymbol{\beta}_j| \approx 1$, we obtain a differential equation (also derived in greater detail in Appendix A) similar to that in BL07 governing the contact discontinuity:

$$\frac{d}{dz}\left(p_s \Gamma_s^2 \beta_{s,z}(R_c^2 - R_j^2)\right) = 2p_j \Gamma_j^2 R_j \frac{\sin \Psi_j}{\cos \alpha_j}. \tag{3.6}$$

We insert into this the known expressions for p_s, p_j and Γ_j from the previous paragraphs. While a shock exists, Γ_s and $\beta_{s,z}$ are obtained from the original shock jump conditions; if the shock closes to the axis then Γ_s and $\beta_{s,z}$ are obtained by assuming adiabatic expansion within the fully-shocked jet. We then numerically integrate Eq (3.6) simultaneously with the differential equation for the inner shock wall, solving for both $R_j(z)$ and $R_c(z)$. Thus we obtain the shapes of the shock front and the contact discontinuity in terms of the initial pressure ratio $p_{s,0}/p_{j,0}$, the initial opening angle θ_0, the initial Lorentz factor $\Gamma_{j,0}$, and the pressure power-law index η.

Examining the effects of varying these four parameters, we see that under certain conditions the external pressure can drive the shock front back to the jet axis, resulting in a fully-shocked jet. The jet is more likely to close when $p_{s,0}/p_{j,0}$ is large and η is small. Initial under- or over-pressurization of the jet strongly affects whether or not it closes, but for physical scenarios we would expect that the pressure is approximately balanced where the jet first impacts the wall, $p_{s,0}/p_{j,0} = 1$. Increasing η can change whether or not the shock will reach the axis and, for cases where the jet does close, drives the point at which this occurs down the z-axis, further from the source. Two examples are shown in Figure 3.2: one in which the shock converges to the axis and one in which it doesn't. This demonstrates the effect that η can have when all other parameters are held constant.

Whether or not a jet closes and, if it does, the value of z at the point where the shock meets the axis is dependent upon the value of the product $\theta_0 \Gamma_{j,0}$, rather than on θ_0 or $\Gamma_{j,0}$ individually. Assuming that the initial pressure ratio and η are held constant, we find that all jets with the same value of $\theta_0 \Gamma_{j,0}$ close at the same point on the z-axis. Increasing $\theta_0 \Gamma_{j,0}$ causes the jet to close further down the axis from the source, until the point where it no longer closes. This dependence of the

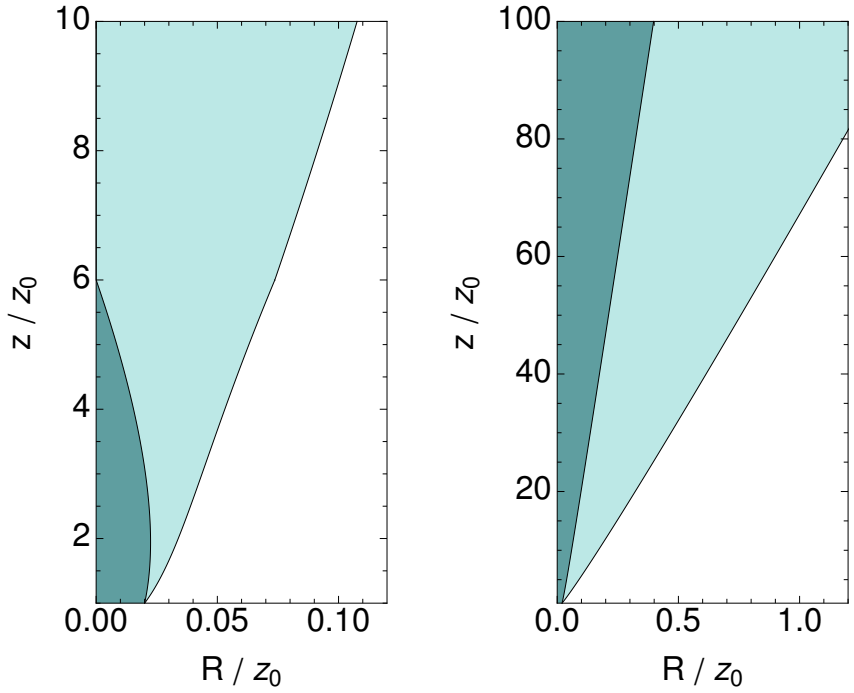

(a) $\eta = 7/3$ (b) $\eta = 11/3$

Figure 3.2: Two examples of the solutions for the shock front and associated contact discontinuity. In the first plot, $\eta = 7/3$; in the second $\eta = 11/3$. For both plots the remaining parameters are held constant at $p_{s,0}/p_{j,0} = 1$, $\Gamma_{j,0} = 50$, and $\theta_0 = 1/50$.

closure point on $\theta_0\Gamma_{j,0}$ is illustrated in Figure 3.3 for $2 < \eta \leq 3$, assuming $p_{s,0}/p_{j,0} = 1$. For $\eta > 3$, $\theta_0\Gamma_{j,0} < 1$ is required to produce a jet that closes.

We find that the shape of the contact discontinuity is initially dependent upon the values of the four parameters $p_{s,0}/p_{j,0}$, θ_0, $\Gamma_{j,0}$, and η. For large z, however, the contact discontinuity asymptotes to one of two shapes: if the shock closes to the axis, then the flow is governed by free expansion beyond that point and the contact discontinuity takes the shape $R_c \propto z^{\eta/4}$, as found in previous works such as BL07, BL09 and Levinson & Eichler, 2000. If the shock does not close to the axis, however, then the contact discontinuity takes the shape $R_c \propto z$, in contrast to these previous works.

The discrepancy between our work and previous studies appears to arise as a result of entropy treatment: in our work, we assume that as long as the shock has not yet closed to the axis, the continued addition of material into the boundary layer ensures that the boundary layer cannot have constant entropy throughout, and thus the layer is not governed by adiabatic expansion. We instead solve for all quantities directly from the shock jump equations, without making assumptions about the behavior of material within the boundary layer.

This difference in the behavior while the jet remains open is crucial, since this model for the jet can only be accurately applied in the regime in which it remains open. After the jet has closed, complex effects such as rarefaction waves or oblique shock reflections (e.g. Gomez et al., 1995) will likely arise, and this simple model no longer adequately describes the jet's behavior.

The conical asymptote that we find in this approximation will be an important factor in our ability to refine this model, as shown in §refsec:ss.

3.4 Self-Similar Treatment of the Boundary Layer

The Kompaneets assumption of constant pressure across the shocked layer is inconsistent with basic intuition: in a realistic large-scale jet, one would expect that the curvature of the streamlines as the jet collimates would go hand in hand with a force inwards along the radius of curvature.

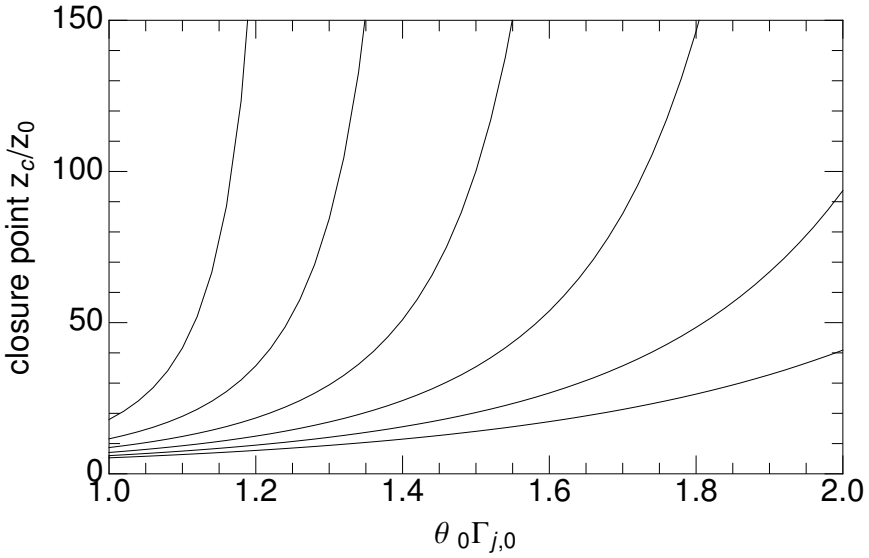

Figure 3.3: Dependence of the jet closure point on $\theta_0\Gamma_{j,0}$. The different curves correspond to various values of η, ranging from $\eta = 13/6$ on the right to $\eta = 3$ on the left, in increments of $1/6$. Here again, $p_{s,0}/p_{j,0} = 1$. The closure point does not depend on the value of $\Gamma_{j,0}$ individually.

Because of the special-relativistic length contraction along the direction of motion, the curvature appears to the fluid to be more extreme than it is in the lab frame by a factor of Γ, resulting in a sizable centripetal force for even slight curvature. Due to this centripetal force, a pressure gradient should then form across the boundary layer, with higher pressure at the outer wall of the jet and lower pressure at the shock front.

With this in mind, we now refine the model in §3.3 by including effects of a transverse pressure gradient within the boundary layer. Even assuming a steady state and axial symmetry, this problem intrinsically involves the solution of partial differential equations in two dimensions, so we simplify the problem by seeking self-similar solutions. In order to do so, we treat the streamlines as being very nearly conical (an assumption justified by the results of §3.3) and calculate their deviation from conical as a function of position within the boundary layer, thus examining the effects of a pressure gradient across the boundary layer.

3.4.1 Self-Similar Solutions

We assume that the opening angle of the jet is much greater than $1/\Gamma$, such that causal contact has been lost. We further suppose that the boundary layer that forms has a thickness that is of order $\Delta\theta \sim 1/\Gamma$, ensuring that the boundary layer is very thin compared to the width of the jet. The radius of curvature of the jet is then much larger than the width of the boundary layer, allowing us to treat the curvature as a small effect.

Given the assumption of nearly conical streamlines, we can in this case treat the entropy and the Bernoulli constant as being the same on all streamlines, implying potential flow. These assumptions are physically realizable if the majority of the material within the shock enters at approximately the same point near the base of the jet; we will later demonstrate that this assumption is self-consistent here.

The flow within the boundary layer is governed by the energy equation, momentum conser-

vation along streamlines, and mass conservation:

$$\rho = Ap^{3/4} \tag{3.7}$$

$$\frac{\Gamma w}{p^{3/4}} = B \tag{3.8}$$

$$\boldsymbol{\nabla} \cdot (\rho \boldsymbol{\beta} \Gamma) = 0 \tag{3.9}$$

where A and B are constants. We henceforth treat the problem in the spherical polar coordinates r, θ and ϕ for convenience in describing a jet with approximately radial streamlines. As the maximum transverse speed that can be achieved without a shock forming is of order $1/\Gamma$, we can therefore assume that β_θ is of this order, and β_r is of order one. Adopting this characteristic scale, we state that $\frac{\partial}{\partial \theta} \sim \Gamma \frac{\partial}{\partial r}$. Writing out β_r and employing the fact that $\beta_\theta^2 + \Gamma^{-2} \ll 1$, we have $\beta_r \approx 1 - \frac{1}{2}(\beta_\theta^2 + \Gamma^{-2})$. Using this, we then combine the flow equations, retaining terms only to lowest order.

If we now assume that the external pressure is a power law in spherical radius r, $p_e \propto r^{-\eta}$, then we can find self-similar solutions for the flow structure near the wall of the jet in the specific case of a pressure-dominated jet, or near enough to the jet source that the Lorentz factor is much less than its asymptotic value ($\Gamma \ll \Gamma_\infty$). In this limit, the equations reduce to a pair of coupled partial differential equations for the Lorentz factor Γ and the transverse velocity β_θ within the boundary layer:

$$\frac{1}{r}\frac{\partial}{\partial r}\left(\frac{r^2}{\Gamma^2}\right) + \frac{\partial}{\partial \theta}\left(\frac{\beta_\theta}{\Gamma^2}\right) = 0 \tag{3.10}$$

$$\frac{\partial}{\partial r}(r\beta_\theta) + \beta_\theta \frac{\partial \beta_\theta}{\partial \theta} + \frac{1}{2}\frac{\partial}{\partial \theta}\left(\frac{1}{\Gamma^2}\right) = 0. \tag{3.11}$$

We now seek self-similar solutions of the form

$$\frac{1}{\Gamma} = r^{-\eta/4} g(\xi), \quad p = r^{-\eta} g^4(\xi), \quad \beta_\theta = r^{-\eta/4} h(\xi), \tag{3.12}$$

where we have chosen the constant in the Bernoulli equation to be unity (i.e. $p\Gamma^4 = 1$) for simplicity. In these solutions g and h are functions of a similarity variable ξ that describes the distance from the contact discontinuity, normalized by the expected scale of the boundary layer,

$\xi \propto (\theta_c - \theta)/\Delta\theta$. The angular thickness of the boundary layer is expected to scale as $\Delta\theta = 1/\Gamma_c$, such that $\xi \propto r^{\eta/4}(\theta_c - \theta)$, where $\theta_c = \theta_c(r)$ is the location of the contact discontinuity.

The fact that the streamlines at θ_c must be parallel to the contact discontinuity, requiring that $\beta_\theta(\theta_c) = r d\theta_c/dr$, yields the further constraint that

$$\frac{d\theta_c}{dr} = h(0) r^{-(1+\eta/4)}. \tag{3.13}$$

Choosing the proportionality constant such that ξ is defined as

$$\xi = -\frac{1}{h(0)} r^{\eta/4}(\theta_c - \theta) \tag{3.14}$$

absorbs the boundary condition into the similarity variable and ensures collimating solutions (such that $h(0) < 0$).

The boundary condition $g(0) = 1$ is enforced so that the pressure is matched at the contact discontinuity, but $h(0)$ is allowed to range. Assuming solutions of this form, we define

$$w(\xi) = \frac{g(\xi)}{g(0)},\ q(\xi) = \frac{h(\xi)}{h(0)} \text{ and } \mu = \left(\frac{g(0)}{h(0)}\right)^2 \tag{3.15}$$

with $w(0) = q(0) = 1$. Further defining $x = (1 - \eta\xi/4)$, we obtain a set of coupled linear ordinary differential equations for $w(x)$ and $q(x)$ that can be cast to reflect the existence of a critical point:

$$(\mu w^2)' = \frac{\frac{8}{\eta}(1 - \frac{\eta}{4})(2x - q)\mu w^2}{\mu w^2 - 2(x - q)^2} \tag{3.16}$$

$$q' = \frac{\frac{8}{\eta}(1 - \frac{\eta}{4})\left(\mu w^2 + q(x - q)\right)}{\mu w^2 - 2(x - q)^2}. \tag{3.17}$$

The critical point occurs where the denominator of these equations goes to zero, forcing the numerators to also go to zero at this point in order to prevent q' and $(\mu w^2)'$ from diverging.

The critical point can be physically understood as a type of sonic point, in analogy with the critical points discussed in Blandford & Payne, 1982 (BP82). Setting the denominator in Eqs (3.16) and (3.17) equal to zero yields the constraint that $\Gamma^2 \beta_\xi^2 = 1/2$ at the critical point, where $\beta_\xi = \boldsymbol{\beta} \cdot \boldsymbol{\nabla}\xi / |\boldsymbol{\nabla}\xi|$. This constraint is mathematically equivalent to two conditions: that the speed of sound waves measured in the lab frame in the direction of $\boldsymbol{\nabla}\xi$ must vanish (analogous to BP82's condition

that the sound speed normal to the similarity surfaces is equal and opposite to the component of flow speed in the same direction), and that the sound speed along the similarity surfaces is equal to the fluid speed and carries no signals in this direction (analogous to BP82's condition that the wave signals are normal to the similarity surfaces).

The physical solutions for q and w are those that pass through the critical point; the solutions that don't pass through the critical point display unphysical behavior, such as crashing and becoming double-valued.

Requiring finite q' and $(\mu w^2)'$ at the critical point results in three possible sets of relations among q, w, μ and x specifically at the critical point. Each one of these sets of relations at the critical point applies uniquely to one of the three regions $\eta < 8/3$, $\eta = 8/3$, and $\eta > 8/3$ to produce physical solutions. Thus, while Eqs (3.16) and (3.17) must generally be solved numerically, we can use these constraints at the critical point to help identify the solutions of interest.

One such family of solutions occurs when $\mu = 1/2$ and $q(\xi) = w(\xi)$, i.e., when $h(\xi) = -\sqrt{2}g(\xi)$ everywhere. The solutions for $p \propto g(\xi)^4$ in this case are shown in Figure 3.4(a).

The most interesting result evident is that the structure of the solutions is divided based on the value of η. For $\eta = 8/3$ the solution is analytic and linear: $q = w = 1 - 2\xi/3$. This implies that the pressure decreases monotonically from the outer wall of the boundary layer ($\xi = 0$) inward, with $p \propto g(\xi)^4 \propto (1 - 2\xi/3)^4$, while the Lorentz factor Γ increases linearly inward.

For $\eta > 8/3$, within this special family, the solutions decrease monotonically and asymptote to zero, with the steepest decrease in q and w occurring for $\eta \approx 8/3$. The curve for $\eta = 4$ is roughly constant at $q = w \approx 1$.

Solutions for $\eta < 8/3$ within this special family are also possible, but they are not single-valued: at the critical point the derivatives diverge and the solutions do not continue to larger values of ξ. For these solutions to be physical, the boundary layer would have to be truncated at a point before where the solutions crash and become double-valued.

By looking beyond this special family of solutions, it is possible to identify a solution for every $2 < \eta < 4$ wherein the pressure is a monotonically decreasing, single-valued function of ξ.

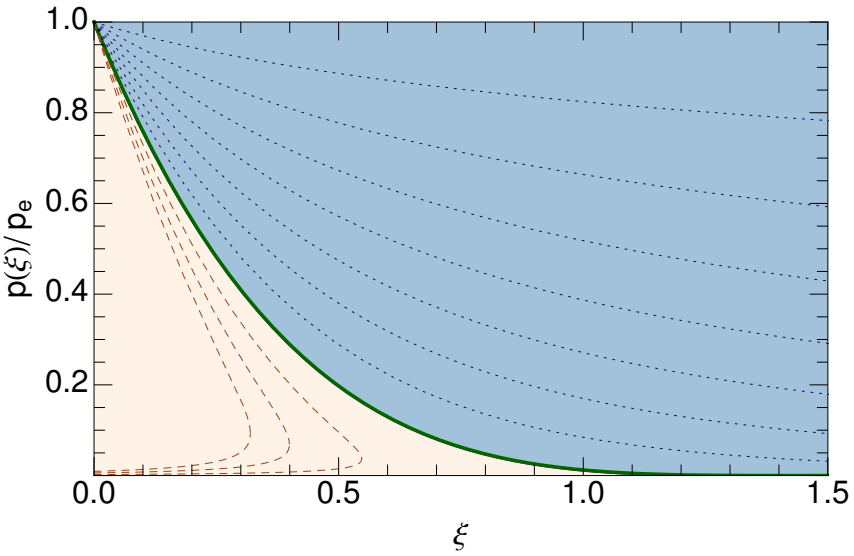

(a)

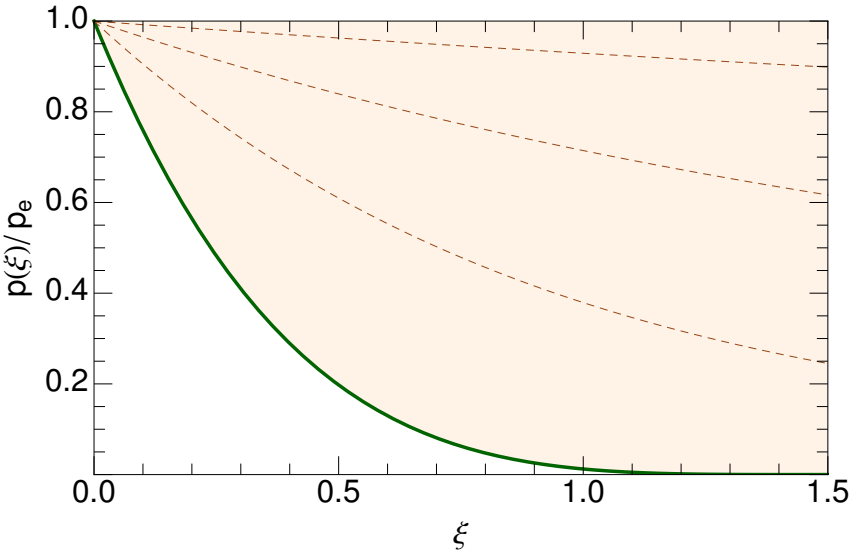

(b)

Figure 3.4: Pressure within the shock as scaled by the external pressure. The contact discontinuity is located at $\xi = 0$. (a) Curves for $2 < \eta < 4$ in increments of $1/6$ (beginning at $\eta = 13/6$ and ending at $\eta = 23/6$), for the special case that $h(\xi) = -\sqrt{2}g(\xi)$ everywhere. The value of η increases when viewing the curves from lower left of the graph to the upper right. The curves for $\eta > 8/3$ are physical, while the curves for $\eta < 8/3$ are not unless truncated. (b) Physical solutions for $2 < \eta \leq 8/3$ only, when the relation between g and h is allowed to vary. The value of η decreases when viewing the curves from lower left of the graph to the upper right. In both figures, the solid curve corresponds to $\eta = 8/3$; the orange region contains curves for $\eta < 8/3$ and the blue region contains curves for $\eta > 8/3$.

In the case of $\eta \geq 8/3$, the unique physical solutions are the solutions that belong to the special family where $\mu = 1/2$ and $q = w$. For $\eta < 8/3$, however, the value of μ is not fixed. Instead, for each value of η there is a single value of μ that yields the physical solution that traverses the critical point. For these solutions, μ varies from $\mu = 1/2$ for $\eta = 8/3$ to $\mu = \infty$ for $\eta = 2$ (see Figure 3.5). When $\eta < 8/3$ the solutions for w asymptote to zero, but the solutions for q become negative at finite ξ, as in the $\eta = 8/3$ case (where w and q reach zero simultaneously). The steepest decrease in q thus occurs for $\eta \approx 2$, whereas the steepest decrease in w now occurs for $\eta \approx 8/3$. The physical pressure solutions for $\eta < 8/3$ are plotted in Figure 3.4(b), and the physical solutions for $q(\xi)$ (describing the spatial dependence of the transverse velocity) are plotted in Figure 3.6.

Thus we find solutions that all display monotonically decreasing pressure from the contact discontinuity across the boundary layer, as we would expect for a pressure gradient arising from centripetal acceleration. Solutions for $\eta \approx 2$ have a nearly constant pressure across the boundary layer, but the pressure profiles become steeper as η increases to $8/3$. The pressure for $\eta = 8/3$ is the only solution that goes to zero at a finite value, thereby forming a boundary layer of thickness $\xi \sim 1$, or $\Delta\theta \sim 1/\Gamma$. Above $\eta = 8/3$ the pressure profiles begin to decrease more gradually again, and for $\eta \approx 4$ the profiles again approach a constant.

Physically, this has very interesting implications. For $\eta = 8/3$, the pressure dropping to zero at a fixed value of ξ implies that all of the jet material has piled up in the outer region of the boundary layer. Thus the jet is a hollow cone: the material is concentrated against the outer wall of the jet, and the inner region is essentially evacuated. This "edge pileup" has been studied as a possibility in quasar jets previously, e.g. Zakamska et al., 2008. Observationally, Zakamska et al. suggested this phenomenon as an alternative explanation for observed edge-brightening in jets, which is more commonly interpreted as a result of the Kelvin-Helmholtz instability occurring at the jet boundary.

For values of η near $8/3$, while the material is not immediately all piled up against the wall, the structure is not dissimilar. The region against the outer wall has the highest pressure, and the sharp pressure decrease interior to the outer wall suggests that most of the material is still in the

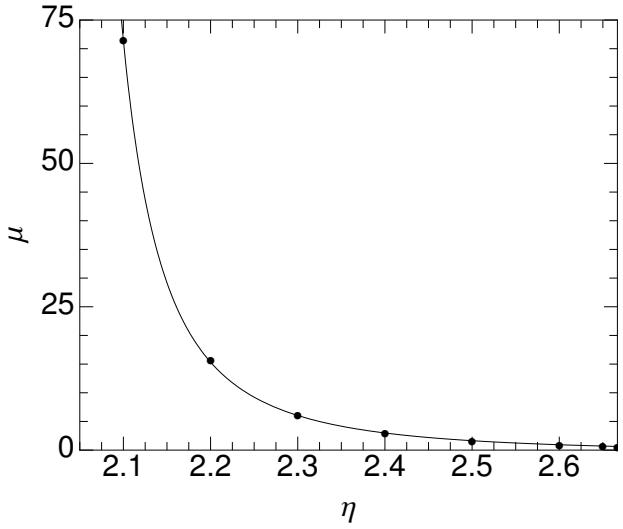

η	μ
2.0	∞
2.1	71.39
2.2	15.57
2.3	5.959
2.4	2.842
2.5	1.506
2.6	0.8270
2.65	0.5943
8/3	0.5

Figure 3.5: Some values of μ as a function of η for $2 < \eta < 8/3$, found empirically by seeking, for each value of η, the solution that passes through the critical point. A numerical fit to these data is shown on the left, and a table of values is given to the right.

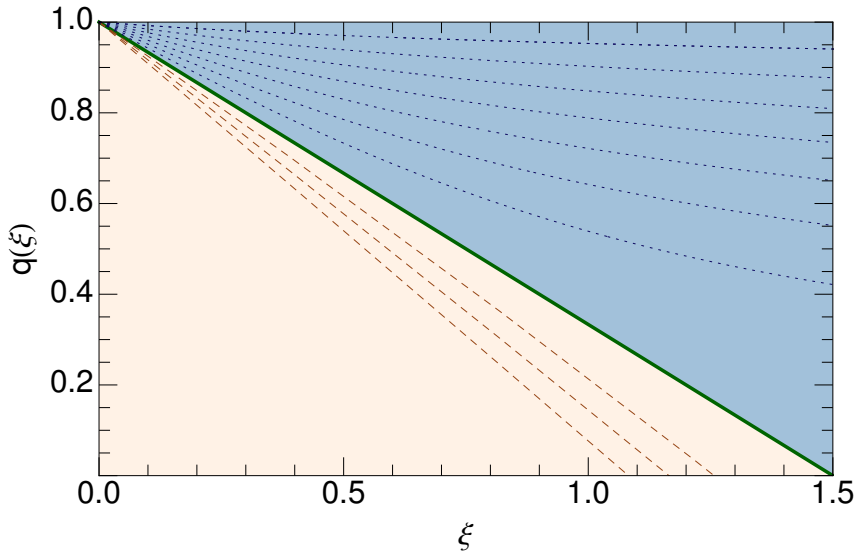

Figure 3.6: Physical solutions for $q(\xi)$ within the shock, where the relation between g and h has been allowed to vary. The contact discontinuity is located at $\xi = 0$. Curves for $2 < \eta < 4$, in increments of $1/6$ (again beginning at $\eta = 13/6$ and ending at $\eta = 23/6$), are plotted. The value of η increases when viewing the curves from lower left of the graph to the upper right, with the solid curve corresponding to $\eta = 8/3$. The coloring is the same as that in Figure 3.4.

outer region. While not truly a hollow cone, this structure could still account for observed edge-brightening in jets. Moving in either direction away from $\eta = 8/3$, however, this region becomes broader and the jet becomes more evenly distributed.

For large and small enough values of η, the pressure gradient becomes small and the deviation of the pressure within the shock from the external pressure is minimal, suggesting that the Kompaneets approximation is a valid approximation in this region. For values of η nearer to $8/3$, however, the Kompaneets approximation is clearly not a reasonable one.

The fact that the pressure profile begins level at $\eta = 2$, steepens as η approaches $8/3$, and then levels out again as η approaches 4 can be explained as the result of a tradeoff between two opposing effects: as η increases, the degree of collimation decreases. This causes a decrease in the centripetal force, and therefore the pressure gradient should decrease accordingly. But an increase in η also means an increase in the rate of jet acceleration (as measured by the increase of Γ with r), which will result in a steeper pressure gradient across the boundary. This acceleration effect appears to be stronger in the region where $2 < \eta < 8/3$, but the collimation effect wins out in the region where $8/3 < \eta < 4$. The two effects are in balance when $\eta = 8/3$, leading to maximal compression of the gas against the wall of the jet.

This dividing behavior at $\eta = 8/3$ is not entirely unexpected, as can be shown by a quick calculation. The power carried by a pressure-dominated jet is given by

$$L \propto p\Gamma^2 A, \tag{3.18}$$

where p is the pressure and A is the cross-sectional area of the region carrying most of the power. If we assume that the power is concentrated in an outer layer of width $\Delta\theta = 1/\Gamma$, then viewed end-on the cross-sectional area of that ring would be $A \propto r^2/\Gamma$, supposing that the jet is conical to first order with very slow collimation. Using the external pressure profile and employing the relativistic Bernoulli equation, we see then that

$$L \propto r^{-\eta/2} A = r^{-3\eta/4+2}. \tag{3.19}$$

If we demand that the jet power be distance-independent, thus containing a finite amount of energy in the boundary layer, then this scaling implies that $\eta = 8/3$ must be true.

For $\eta < 8/3$, we have L scaling with radius to some positive power, such that for $r \to \infty$, $L \to \infty$. Thus, given a roughly conical jet, the power carried cannot remain constant with $\eta < 8/3$. Reexamining Eq (3.19), however, we can see that if the area scaled as some smaller power of r rather than as described, then the jet power could be maintained as a constant despite the lower value of η. Thus, for $\eta < 8/3$, the jet must become more strongly collimated, causing the cross-sectional area to grow more slowly than in the conical case, in order for the jet power not to diverge.

For $\eta > 8/3$, it would appear that $L \to 0$ as $r \to \infty$. This is misleading, however, given that for this range in η, the integrals over ξ of the energy contained within the boundary layer diverge. Thus, in a total spatial integral of L over both ξ and r, the r-scaling of $L \to 0$ and the ξ-scaling of $L \to \infty$ can combine to counteract each other, making it possible to obtain physical solutions under which a finite amount of energy is contained within the boundary layer after all.

3.4.2 Extension to the Kompaneets Model

This self-similar construction provides an important view of the behavior within the boundary layer, but to properly understand observations of the large-scale AGN jets that we seek to model, we must examine how the boundary-layer physics fits into that of the jet as a whole.

To this end, we now attempt to extend the Kompaneets model by repeating §3.3 with the addition of a pressure gradient across the boundary layer. The form of this added pressure gradient will come from our self-similar boundary-layer model, and in this section we work in cylindrical coordinates to facilitate the matching.

Applying the self-similar model to the structure developed in §3.3 inherently renders the problem no longer self-similar, as length scales are introduced into the problem. Nonetheless, the combination of methods is instructive in the description of general trends that are expected when adding a pressure gradient to the Kompaneets model.

Because ξ is a function of distance from the contact discontinuity $(\theta_c - \theta)$, using the self-similar pressure solutions in the model in §3.3 requires that we already know the shape of this outer wall. As the self-similar model was developed with the assumption of an approximately conical contact discontinuity, we solve this problem by fitting a conical solution to each contact discontinuity found in §3.3 using the Kompaneets approximation and then using this fit as a fixed input for the location of the outer wall. As was shown in §3.3, approximating the contact discontinuity as conical is justified in the case of jets where the shock never closes to the axis, or in the region of the jet before the shock closes. It is this regime that we study.

We examine three representative cases — one for $\eta < 8/3$, one for $\eta = 8/3$, and one for $\eta > 8/3$ — and use these to infer the general behavior of the jet shape after the addition of a pressure gradient.

For $\eta = 7/3$, the physical self-similar solution is that for which $\mu = 4.575$. From this we fit an analytic function to the numerical solution for g, of the form

$$g(\xi) \quad = \quad a + \frac{b}{(\xi + c)} + \frac{d}{(\xi + e)^2}, \tag{3.20}$$

where $a, b, c, d,$ and e are constant parameters determined by the fit. We then modify the expression for the pressure within the boundary layer so that $p_s \propto r^{-\eta}\, g^4(\xi)$. We find that the results display the expected physical effect of adding this pressure gradient: the shock front moves outward to match the decreased pressure.

For $\eta = 8/3$, the solution for $g(\xi)$ was analytic:

$$g(\xi) \quad = \quad 1 - \frac{2}{3}\xi. \tag{3.21}$$

Using this function to add a pressure gradient into the case from §3.3, we again find that the shock wall moves outward to match the decreased pressure function. Two examples are shown in Figure 3.7: one in which the shock front initially closed to the axis in the Kompaneets approximation, and one in which it initially remained open. Due to the approximation of a conical contact discontinuity breaking down beyond the point where the shock front initially closes, we cannot

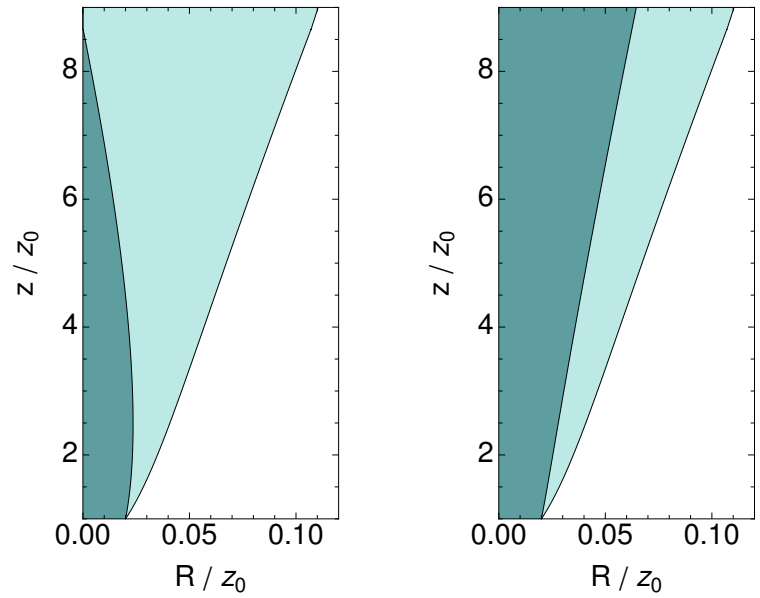

(a) $\eta = 8/3, \theta_0 = 1/50, \Gamma_0 = 50$

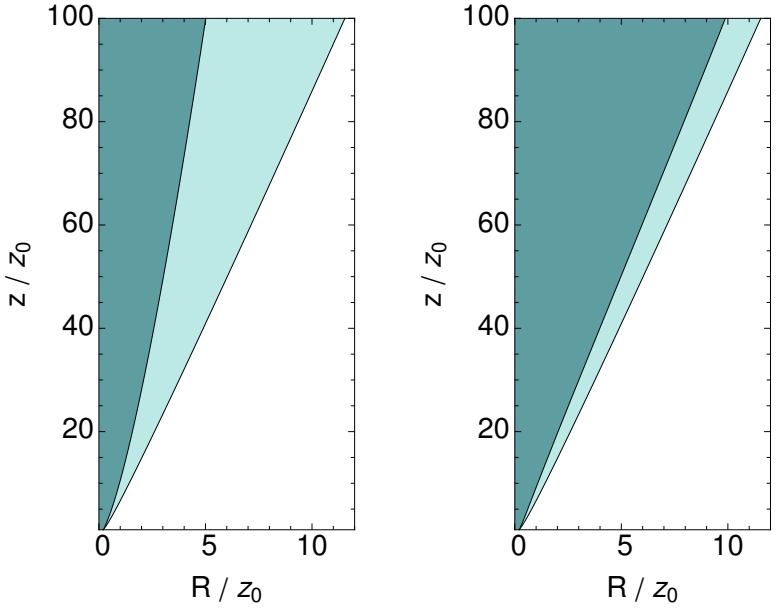

(b) $\eta = 8/3, \theta_0 = 2/10, \Gamma_0 = 10$

Figure 3.7: The shock front and contact discontinuity for two cases: one in which the jet originally closes (a) and one in which it originally remains open (b). Left plots demonstrate the jet under the Kompaneets approximation, from §3.3. Right plots indicate the new position of the shock front after the addition of the pressure gradient. The contact discontinuity remains unchanged in this approximation.

draw conclusions from these models in that regime. Nonetheless, it is clear that the addition of a pressure gradient either causes the shock front to converge to the axis at a distance further down the jet axis, or else it prevents the shock front from ever reaching the axis. Either way, one can see from Figure 3.7 that the addition of the pressure gradient causes the shocked boundary layer to become thinner.

For $\eta = 3$, we can again fit the function given by Eq (3.20) to the numerical solution of $g(\xi)$. This time the physical solution corresponds to $\mu = 1/2$. Again modifying the Kompaneets solution of §3.3 with this pressure gradient, we find that here too the shock moves outward and forms a thin boundary layer. As with the $\eta = 8/3$ solutions, cases that originally closed to the axis in the Kompaneets approximation either close further down the axis or no longer close.

We would hope that the energy within the shocked layer increases with radius, despite the message of the luminosity scaling worked out at the end of §3.4.1. As a test of this, for $\eta = 3$, we can integrate the total energy contained in the boundary layer in a slice across the jet at a fixed z:

$$L \propto \int_{R_j}^{R_c} p\Gamma^2 R dR. \tag{3.22}$$

Comparing this enclosed energy at a few different values of z (see Figure 3.8), we can see that although the total energy within the layer would be decreasing if ξ were fixed along the shock (the dashed curves show the fixed-ξ energy through a given value of z), the net energy instead increases as we go to higher z because we move to different values of ξ in the process of traveling along the shock. Thus the solution is entirely physical: the energy behind the shock increases with an increase in distance from the source, as is required.

3.5 Conclusion

We have evaluated the shape of the shocked boundary layer of a hot jet with an ultrarelativistic equation of state, in the case that it is injected into an ambient medium that has a power-law pressure profile of $p \propto r^{-\eta}$ with $2 < \eta < 4$. Using the shock jump conditions and momentum

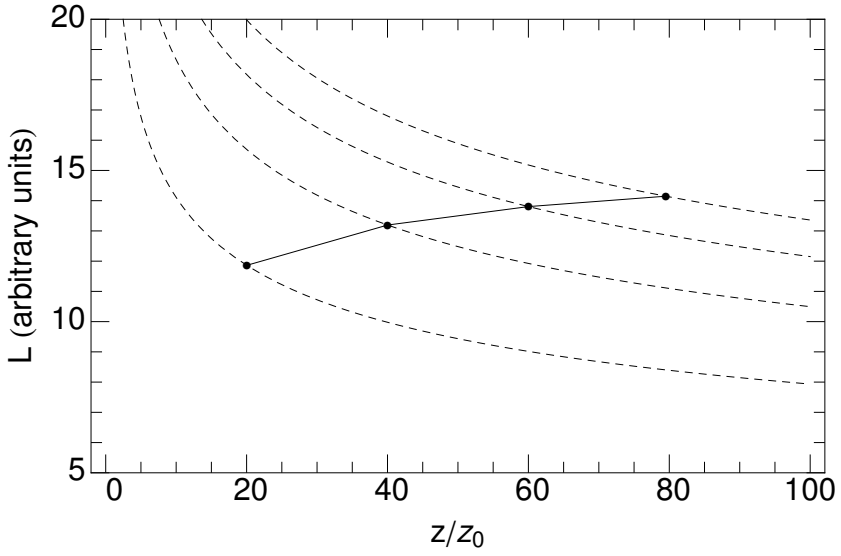

Figure 3.8: The total integrated energy contained within the boundary layer at a given height z for $\eta = 3$. L is given in arbitrary units. The dashed curves through the data points correspond to what the total-energy curve through each data point would be if ξ were instead a fixed value along the shock.

conservation and assuming that the pressure remains constant across the boundary layer, we found that whether the shocked layer closes to the axis — and where it closes, if it does — is dependent upon the values of the initial pressure ratio, the power-law index, the initial bulk Lorentz factor, and the product of the initial opening angle and initial Lorentz factor.

We also found that, in the Kompaneets approximation, the contact discontinuity asymptotes to the shape $R_c \propto z^{\eta/4}$ in the case where the shock has closed to the axis, but to a conical shape, $R_c \propto z$, in the case of a non-closing shock or in the region of the jet before the shock has closed.

Due to the expectation of a pressure gradient arising from the centripetal force created by the slight collimation of the jet, we then created a self-similar model of the boundary layer that allows for a pressure gradient across the layer. From this we found solutions for which pressure decreases monotonically across the boundary layer for all values of the power-law index η.

An η of 8/3 constitutes a special solution where the pressure goes to zero at a finite distance from the outer wall. For values of η greater or less than 8/3, the pressure approaches zero asymptotically. The curve for pressure steepens for values of η near 8/3 and approaches a constant value for $\eta \to 2$ or $\eta \to 4$.

The drastic decrease of the pressure inwards from the contact discontinuity for values of η near 8/3 suggests that most of the material is pushed up against the outer wall, creating a hollow-cone structure for the jet that may be observable as edge-brightening. It also indicates that the Kompaneets approximation is not valid for these values of η. For values of η near 2 or 4, however, the Kompaneets approximation may be reasonable, since the pressure decrease is very gradual.

To better understand these results, we then revised the Kompaneets solutions to include the pressure gradient of the self-similar boundary-layer model. We held the outer wall fixed and solved for the new position of the shock front by pressure-matching across the shock jump. We found that the addition of the pressure gradient caused the shock front to move outward in order to match the lower pressure, resulting in a thinner boundary layer and preventing the shock from closing to the axis in places where it originally had done so. We also confirmed that the total energy contained within the boundary layer was an increasing function of height z, as is required.

The inherent difficulty of examining this problem analytically required us to make several simplifying assumptions over the course of this work. One such assumption, made in §3.4 to obtain the boundary-layer solutions, is that all the material within the boundary layer is on the same adiabat. This would be true if the majority of the material entered the boundary layer at roughly the same location, however this is not the case in general. But for the boundary-layer solutions where the pressure drops rapidly (η near $8/3$), most of the material must be pushed up against the contact discontinuity early on. This suggests that it must all have entered the boundary layer near the jet base, which demonstrates self-consistency with the same-adiabat assumption for this regime. Nonetheless, in future work we intend to explore the possibility of treating the jet material on different adiabats.

It is widely believed that magnetic effects contribute to the collimation of relativistic jets (see e.g. Komissarov, 1999). While the models discussed here are purely hydrodynamic, they can have important applications both in interpreting the data obtained in three-dimensional general relativistic magnetohydrodynamics simulations that provide a self-consistent description of the jet launching mechanism (e.g. Beckwith et al., 2008, 2009; McKinney & Blandford, 2009) and in improving the physical content of boundary conditions imposed in simulations that study the role of magnetic fields in large-scale jet collimation (see e.g. Komissarov et al., 2007, 2009; Komissarov, 2011).

In the former case, the Poynting-flux dominated jet is sheathed by an unbound outflow (Hawley & Krolik, 2006), which may have important implications for the operation of current-driven instabilities (McKinney & Blandford, 2009). However, the numerical resolution used in these simulations is generally insufficient to adequately resolve the sharp density and pressure gradients present in these regions. Combining the models presented here with the conditions present in the ambient medium at the base of the jet (e.g. the disk corona) in these simulations will allow us to assess the extent to which numerical resolution affects simulation outcomes.

In the case of simulations that study the role of magnetic fields in large-scale jet collimation, the work presented here will allow a more complete physical treatment of the effects of the ambient

medium. In these simulations (Komissarov et al., 2007, 2009; Komissarov, 2011), this boundary is generally treated as a rigid wall, where fluid quantities (such as gas density and pressure) are simply copied across the boundary, while the normal component of vector quantities (e.g. velocity and magnetic field) is reflected. The models presented here will allow improvement of this treatment by specifying jump conditions for hydrodynamic quantities at this boundary, consistent with the shape of the wall — thereby including the collimating effect of the ambient medium.

These calculations mark the first step towards a more complete treatment of both the action of the external medium and magnetic effects in collimating and accelerating relativistic jets. The next step in this work is to include the effect of a toroidal magnetic field, allowing for magnetic confinement. Together, this work and its magnetized extension will provide us with an equilibrium model from which we can explore instabilities and radiative mechanisms of the jet near its base, leading to improved constraints on jet dissipation and associated radiative signatures. Through this work we hope to further our understanding of jet collimation and, in particular, boundary-layer behavior.

Chapter 4

Boundary Layers in Magnetized Relativistic Jets

4.1 Preface

This paper appeared in Monthly Notices of the Royal Astronomical Society, Volume 422, Issue 3, pp. 2282-2290 and was completed under the guidance of Dr. Mitch Begelman. This is the second of three papers examining the impact of the ambient medium on collimation and confinement of relativistic jets that have lost causal contact with their surroundings. This work focuses on how the results of Chapter 3 change with the addition of a toroidal magnetic field threading the jet. In particular, we examine the relative contributions of gas pressure and magnetic pressure to the jet's confinement, collimation, and acceleration.

Abstract

We study the collimation of relativistic magnetohydrodynamic jets by the pressure of an ambient medium, in the limit where the jet interior loses causal contact with its surroundings. This follows up a hydrodynamic study in a previous paper, adding the effects of a toroidal magnetic field threading the jet. As the ultrarelativistic jet encounters an ambient medium with a pressure profile with a radial scaling of $p \propto r^{-\eta}$ where $2 < \eta < 4$, it loses causal contact with its surroundings and forms a boundary layer with a large pressure gradient. By constructing self-similar solutions to the fluid equations within this boundary layer, we examine the structure of this layer as a function of the external pressure profile. We show that the boundary layer always becomes magnetically dominated far from the source, and that in the magnetic limit, physical self-similar solutions are

admitted in which the total pressure within the layer decreases linearly with distance from the contact discontinuity inward. These solutions suggest a 'hollow cone' behavior of the jet, with the boundary layer thickness prescribed by the value of η. In contrast to the hydrodynamical case, however, the boundary layer contains an asymptotically vanishing fraction of the jet energy flux.

4.2 Introduction

The outflows from active galactic nuclei (AGN) are thought to be highly relativistic (Begelman et al., 1984) and highly collimated (e.g. Jorstad et al., 2005), but the cause of this collimation is uncertain.

Because jet-launching is generally believed to be electromagnetically driven (e.g. Blandford & Payne, 1982; Contopoulos & Lovelace, 1994), one of the most commonly-accepted explanations for the observed collimation is that jets are threaded with magnetic fields that cause collimation via magnetic tension (e.g. Benford, 1978; Begelman, 1995). Supporting this theory, it has been demonstrated that both relativistic and non-relativistic hydromagnetic outflows must eventually become collimated (Chiueh et al., 1991; Heyvaerts & Norman, 1989). For magnetic fields acting alone, however, collimation will only happen on extremely large scales (Eichler, 1993; Begelman & Li, 1994; Begelman, 1995).

To cause jets to collimate on reasonable scales, there must be an additional mechanism at work. A logical culprit is confinement by the pressure of an external medium. Pressure confinement has been demonstrated to act effectively on its own (e.g. Levinson & Eichler, 2000; Bromberg & Levinson, 2007; Kohler et al., 2012), and accretion disk winds surrounding an AGN provide an ideal ambient medium to help to collimate the jet.

There have been many numerical studies of magnetized jets (e.g. Komissarov, 1999; Hawley & Krolik, 2006; Beckwith et al., 2008; McKinney & Blandford, 2009), with the goal of forming a self-consistent description of the jet-launching and collimation mechanisms. These numerical simulations have several restrictions, however, one of which being that the boundary of the jet,

rather than having its shape determined by pressure balance, is generally treated as a rigid wall (e.g. Komissarov et al., 2007, 2009; Komissarov, 2011; Tchekhovskoy et al., 2010). This construction doesn't allow the ambient pressure to affect collimation of the jet.

Treatments that do include effects of the external medium commonly focus on describing jets that remain in causal contact (e.g. Zakamska et al., 2008; Lyubarsky, 2011). As an ultrarelativistic jet expands into an ambient medium with a pressure profile $p \propto r^{-\eta}$, it will eventually lose causal contact if $\eta > 2$ and the opening angle is greater than $1/\Gamma$, where Γ is the bulk Lorentz factor of the fluid. Observations of gamma-ray bursts indicate that these relativistic jets largely have opening angles greater than $1/\Gamma$ (e.g. Piran, 2004; see Tchekhovskoy et al., 2010 for discussion), and AGN outflows with large Lorentz factors may similarly be causally disconnected; thus the poorly-studied regime of a jet that has lost causal contact is of physical interest.

In a previous paper (Kohler et al., 2012, hereafter KBB12) we developed a model describing the recollimation boundary layer of a purely hydrodynamic, "hot" (pressure-dominated) jet with an ultrarelativistic equation of state. In this model, we assumed that the pressure outside the jet decreases with r so rapidly that the jet interior loses causal contact with its boundary, resulting in a shocked boundary layer forming within the jet. Though the jet interior is causally disconnected, the boundary layer is nevertheless narrow enough to remain in causal contact itself. Assuming self-similarity as a function of r, we calculated how the transverse structure of the jet boundary layer depends on the value of η in the external pressure profile.

We now expand this work to include, in addition to collimation by the external medium, the effects of a magnetic field within the jet. We include only a toroidal field, as it is the toroidal field that dominates the dynamics at large radii, far outside the light cylinder (Begelman et al., 1984; Contopoulos, 1995; Beskin, 2009). In §4.3, we first demonstrate that seeding a jet with a magnetic field at the base will always cause it to become magnetically dominated at large radii. We then find self-similar solutions for the boundary layer of the jet in the limit of magnetic dominance. In §4.4 we discuss the results, and in §4.5 we conclude.

4.3 Self-Similar Treatment of the Magnetized Boundary Layer

We use spherical coordinates to model a hot, ultrarelativistic jet that is symmetric about the z-axis and has approximately radial streamlines – an approximation justified because the jet interior is causally disconnected from the environment. We assume that the jet is injected from a point source with steady flow, and we examine the jet in its steady-state configuration.

We focus on modeling the boundary layer of jet material that forms at the interface between the jet and the stationary ambient medium. This layer is bounded on the inside by a shock front or a rarefaction front, and on the outside by a contact discontinuity. There is no mass flux across the contact discontinuity, and the pressure must be matched on either side of it. The physics of the ambient medium is wrapped into the external pressure profile p_e.

We adopt a pressure profile for the ambient medium of $p_e \propto r^{-\eta}$, fixing the pressure external to the jet to be dependent only on the parameter η. We focus on the case of ambient pressure where $2 < \eta < 4$, as in our work in KBB12 or in, e.g., Bromberg & Levinson, 2007, because the jet interior is out of causal contact with the exterior for this range in η. Physically, this pressure profile range could describe a confining wind, an accretion flow, a disk corona, or even a stellar envelope in a GRB collapsar model (e.g. Bromberg et al., 2011).

As in KBB12, we assume that the opening angle of the jet is much greater than $1/\Gamma$, such that causal contact has been lost. We construct a boundary layer that remains in causal contact, such that its thickness is of order $\Delta\theta \sim 1/\Gamma$. The boundary layer is thus very thin compared to the width of the jet. The radius of curvature of the jet is then much larger than the width of the boundary layer, allowing us to treat the curvature as a small effect.

We begin with the equations for relativistic MHD (RMHD) in flat spacetime (e.g. Dixon, 1978; Komissarov, 1999; Zakamska et al., 2008), including the effects of a toroidal magnetic field within the jet. We ignore rotation since our regime of interest is far outside the light cylinder and, indeed, far outside the fast magnetosonic surface, rendering rotation effects unimportant. We again assume an ultrarelativistic equation of state such that the total proper energy density is given by

$\epsilon = \rho + 3p \approx 3p$, where ρ and p are, respectively, the proper rest mass density and the pressure of the fluid within the boundary layer.

The continuity equation remains unchanged with the addition of a magnetic field,

$$\nabla \cdot (\rho \boldsymbol{\beta} \Gamma) = 0, \tag{4.1}$$

where β and Γ are the velocity ($\boldsymbol{\beta} = \boldsymbol{v}/c$) and the bulk Lorentz factor of the fluid within the boundary layer. Assuming an energy equation of $p \propto \rho^{4/3}$ and taking $\theta \sim$ constant, the continuity equation becomes

$$\frac{1}{r^2}\frac{\partial}{\partial r}(r^2 p^{3/4} \Gamma \beta_r) + \frac{1}{r}\frac{\partial}{\partial \theta}(p^{3/4}\Gamma\beta_\theta) = 0 \tag{4.2}$$

in spherical coordinates.

Denoting the observer-frame magnetic field within the jet boundary layer as $\boldsymbol{B}$, and using the ideal MHD condition to express the observer-frame electric field as $\boldsymbol{E} = -\boldsymbol{v} \times \boldsymbol{B}$, the momentum equation can now be written as

$$\begin{aligned}(4p\Gamma^2 + B^2)(\boldsymbol{\beta}\cdot\nabla)\boldsymbol{\beta} + \nabla(p + \frac{1}{2}B^2\Gamma^{-2}) \\ -\boldsymbol{B}[\nabla\cdot(B\Gamma^{-2})] - \Gamma^{-2}(\boldsymbol{B}\cdot\nabla)\boldsymbol{B} = 0,\end{aligned} \tag{4.3}$$

where the parallel and perpendicular components of the momentum equation are obtained by taking the respective vector dot and cross product of $\boldsymbol{\beta}$ with Eq (4.3).

Finally, we add the equation for flux freezing,

$$\nabla \times (\boldsymbol{\beta} \times \boldsymbol{B}) = 0. \tag{4.4}$$

Writing this in spherical coordinates, and assuming a toroidal magnetic field $\boldsymbol{B} = B(r,\theta)\hat{\boldsymbol{\phi}}$, we have

$$\frac{\partial}{\partial r}(r\beta_r B) + \frac{\partial}{\partial\theta}(\beta_\theta B) = 0. \tag{4.5}$$

The full form of these four equations admit self-similar solutions only in the case where $\eta = 4$, which corresponds to a quasi-monopole flow with no collimation and therefore no distinct

boundary layer. For all other values of η, the full equations allow only for trivial solutions due to overconstraint of the system. We now demonstrate, however, that it is not appropriate to use these equations in their full form. They should instead be examined in the magnetically-dominated limit – where they do admit non-trivial self-similar solutions.

4.3.1 Demonstration of Asymptotic Magnetic Dominance

Suppose that the magnetic field takes the form $B = rp^{3/4}\Gamma f(r,\theta)$ where f is some function of r and θ. Inserting this into Eq (4.4), we obtain

$$\nabla \cdot (p^{3/4}\Gamma \boldsymbol{\beta} f) = 0 \tag{4.6}$$

which can be expanded and combined with Eq (4.1) to show that

$$\boldsymbol{\beta} \cdot \nabla f = 0, \tag{4.7}$$

indicating that the function f must be constant along streamlines.

Because the contact discontinuity is a streamline, we can therefore state that $B \propto rp^{3/4}\Gamma$ along the contact discontinuity. As in Zakamska et al., 2008, we now define a magnetization parameter β_B as the ratio of magnetic to gas pressure (the inverse of the usual plasma beta). Along the contact discontinuity this parameter is thus given by

$$\beta_B = \frac{B^2}{p\Gamma^2} \propto r^2 p^{1/2}. \tag{4.8}$$

Because pressure must be matched across the contact discontinuity, the external pressure $p_e \propto r^{-\eta}$ must be balanced at that point by the total internal pressure within the boundary layer, $p_{tot} = p + B^2/\Gamma^2$. We now examine β_B in two extreme cases: the limit where the pressure balance at the contact discontinuity is supplied solely by the gas pressure within the boundary layer, and the limit where the balance is supplied solely by the magnetic pressure within the layer.

In the gas pressure-dominated case, the internal gas pressure p is equivalent to the external pressure p_e, and must therefore scale in the same way, such that $p \propto r^{-\eta}$. Applying this to Eq (4.8)

demonstrates that in this case, $\beta_B \propto r^{(4-\eta)/2}$. Thus, for $2 < \eta < 4$, β_B scales as r to some positive power.

In the magnetically-dominated case, the external pressure is balanced by the magnetic pressure such that $B^2/\Gamma^2 \propto r^{-\eta}$. This scaling implies that the internal gas pressure is given by $p \propto r^{-(2/3)(\eta+2)}$, and we obtain $\beta_B \propto r^{(4-\eta)/3}$. Again, for $2 < \eta < 4$, β_B scales as r to some positive power.

Thus we see that in both extreme cases, β_B grows with increasing r. This suggests that no matter how small a magnetic field the jet is seeded with, the boundary layer will eventually become magnetically-dominated far from the jet source. With this in mind, we now repeat the calculations performed in KBB12 with the inclusion of a toroidal magnetic field, specifically in the limit where $\beta_B \gg 1$.

4.3.2 Solutions in the Magnetic-Dominance Limit

We first rederive the fluid equations in §4.3.1 in the limit where $\beta_B \gg 1$. Continuity and flux freezing are unchanged, but terms in the momentum equation containing $1/\beta_B$ are negligible in this limit.

We now make scaling arguments as in KBB12: we assume β_θ is of order $1/\Gamma$, since this is the maximum transverse speed that can be achieved without a shock forming, and β_r is of order one. With this characteristic scale, $\frac{\partial}{\partial\theta} \sim \Gamma\frac{\partial}{\partial r}$. Expressing β_r in terms of β_θ and Γ and employing the fact that $\beta_\theta^2 + \Gamma^{-2} \ll 1$, we have $\beta_r \approx 1 - \frac{1}{2}(\beta_\theta^2 + \Gamma^{-2})$. Using these scalings and keeping terms only to lowest order, the parallel and perpendicular components of the momentum equation are:

$$r\frac{\partial p}{\partial r} + \beta_\theta\frac{\partial p}{\partial\theta} + \frac{B}{\Gamma^2}\left(B + r\frac{\partial B}{\partial r} + \beta_\theta\frac{\partial B}{\partial\theta}\right) = 0 \tag{4.9}$$

$$B^2\left(r\frac{\partial\beta_\theta}{\partial r} + \beta_\theta + \beta_\theta\frac{\partial\beta_\theta}{\partial\theta} - \frac{1}{\Gamma^3}\frac{\partial\Gamma}{\partial\theta}\right) + \frac{\partial p}{\partial\theta} + \frac{B}{\Gamma^2}\frac{\partial B}{\partial\theta} = 0. \tag{4.10}$$

We now attempt to construct self-similar solutions in the following fashion:

$$\frac{1}{\Gamma} = g(\xi) r^{-x}, \qquad \beta_\theta = h(\xi) r^{-x},$$
$$B = b(\xi) r^{x-\eta/2}, \qquad p = a(\xi) r^{-\alpha}, \tag{4.11}$$

such that the external gas pressure is matched by the internal magnetic pressure, $B^2/\Gamma^2 \propto r^{-\eta}$. In these solutions x and α are constant free parameters describing the radial scaling, and g, h, b and a are functions of a similarity variable ξ (as in KBB12) that describes the distance from the contact discontinuity, normalized by the expected scale of the boundary layer, $\xi \propto (\theta_c - \theta)/\Delta\theta$. The angular thickness of the boundary layer is expected to scale as $\Delta\theta = 1/\Gamma_c$, such that $\xi \propto r^x(\theta_c - \theta)$, where $\theta_c = \theta_c(r)$ is the location of the contact discontinuity.

The fact that the streamlines at θ_c must be parallel to the contact discontinuity, requiring that $\beta_\theta(\theta_c) = r d\theta_c/dr$, yields the further constraint that

$$\frac{d\theta_c}{dr} = h_0 r^{-(x+1)}, \tag{4.12}$$

where $h_0 = h(\xi = 0)$ is a negative constant for collimating solutions. While the flow is very nearly radial, this expression describes the small deviation of the flow lines resulting from subtle collimation. Choosing the proportionality constant such that ξ is defined as

$$\xi = -\frac{1}{h_0} r^x (\theta_c - \theta) \tag{4.13}$$

absorbs the boundary condition into the similarity variable and ensures collimating solutions (such that $h_0 < 0$).

We now recast the fluid equations in terms of these functions. The continuity and flux-freezing equations are fully self-similar and become, respectively,

$$\left(3\frac{a'}{a} - 4\frac{g'}{g}\right)\left(x\xi - 1 + \frac{h}{h_0}\right) + \left(4x + 8 - 3\alpha + 4\frac{h'}{h_0}\right) = 0 \tag{4.14}$$
$$\frac{b'}{b}\left(x\xi - 1 + \frac{h}{h_0}\right) + \left(x - \frac{\eta}{2} + 1 + \frac{h'}{h_0}\right) = 0, \tag{4.15}$$

where primes denote differentiation with respect to ξ.

Now examining the parallel component of the momentum equation, one can see that the radial scaling does not automatically vanish:

$$\frac{b^2g^2}{a}\left[1+x-\frac{\eta}{2}+\frac{b'}{b}\left(x\xi-1+\frac{h}{h_0}\right)\right] + r^{\eta-\alpha}\left[\frac{a'}{a}\left(x\xi-1+\frac{h}{h_0}\right)-\alpha\right]=0. \tag{4.16}$$

Because we are specifically examining the regime where $\beta_B \propto B^2/(p\Gamma^2) \propto r^{\alpha-\eta} \gg 1$, however, we can assume that $r^{\eta-\alpha}$ will be very small for large r, rendering the second term negligible.

Using this logic, the parallel and perpendicular components of the momentum equation become, respectively,

$$\frac{b^2g^2}{a}\left[1+x-\frac{\eta}{2}+\frac{b'}{b}\left(x\xi-1+\frac{h}{h_0}\right)\right]=0 \tag{4.17}$$

$$h(1-x)+h'\left(x\xi-1+\frac{h}{h_0}\right)+\frac{g^2}{h_0}\left(\frac{g'}{g}+\frac{b'}{b}\right)=0. \tag{4.18}$$

Assuming that b, g, a and h are finite and non-zero, Eqs (4.15) and (4.17) imply that $h'=0$. This assumption results in Eq (4.15) becoming

$$\frac{b'}{b}=-\frac{x-\eta/2+1}{x\xi} \tag{4.19}$$

and yields the following general solutions for the functions describing the transverse behavior within the boundary layer:

$$h=h_0 \tag{4.20}$$

$$b=A\xi^{-(2+2x-\eta)/2x} \tag{4.21}$$

$$g=\pm\left[B\xi^{(2+2x-\eta)/x}-\frac{2h_0^2x(x-1)}{2+x-\eta}\xi\right]^{1/2} \tag{4.22}$$

$$\frac{a'}{a}=\frac{3\alpha-4-2\eta}{3x}\xi^{-1}-\frac{4}{3}(1-x)\left(\frac{g}{h_0}\right)^{-2}, \tag{4.23}$$

where A and B are constants of integration that are defined by the boundary conditions.

To produce physical solutions, we examine the special case where we prevent b' from having a singularity at $\xi=0$ by setting $x-\eta/2+1=0$, implying that b is a constant. In terms of boundary

conditions $h_0, g_0, b_0,$ and a_0, which serve as scaling factors and allow us to determine our functions self-consistently, the physical solutions within the boundary layer are therefore

$$h = h_0 \tag{4.24}$$

$$b = b_0 \tag{4.25}$$

$$g = -h_0 \left[\left(\frac{g_0}{h_0} \right)^2 - (4-\eta)\xi \right]^{1/2} \tag{4.26}$$

$$a = a_0 \left(\frac{h_0}{g_0} \right)^{4/3} \left[\left(\frac{g_0}{h_0} \right)^2 - (4-\eta)\xi \right]^{2/3}, \tag{4.27}$$

with the constraints $x = \frac{\eta}{2} - 1$ and $\alpha = \frac{2}{3}(\eta + 2)$, such that

$$\frac{1}{\Gamma} = g r^{1-\eta/2}, \qquad \beta_\theta = h r^{1-\eta/2},$$
$$B = b r^{-1}, \qquad p = a r^{-(2/3)(\eta+2)}. \tag{4.28}$$

A check for self-consistency shows that the density in the lab frame, given by $p^{3/4}\Gamma$, has no dependence upon θ and scales as r^{-2}, as is expected for nearly radial flow.

It should be noted that for the toroidal magnetic field and corresponding electric field to exist within the boundary layer, there must be a current distribution and charge distribution within the layer, and a current sheet and surface charge at the outer boundary where the magnetic and electric fields terminate. Calculating the current distribution within the jet from the solutions in Eq (4.28), one can see that longitudinal current within the jet is conserved in the case of approximately radial streamlines, providing another check of self-consistency.

4.4 Discussion of Results

The first important result of this solution is that, in the observer's frame, both the magnetic field B and the transverse jet velocity β_θ have only radial dependence; they are constant across the boundary layer. This is in direct opposition to the results from the strictly hydrodynamic limit (see KBB12, §3.1), where β_θ decreases monotonically from the outside of the boundary layer inward for all cases where $2 < \eta < 4$.

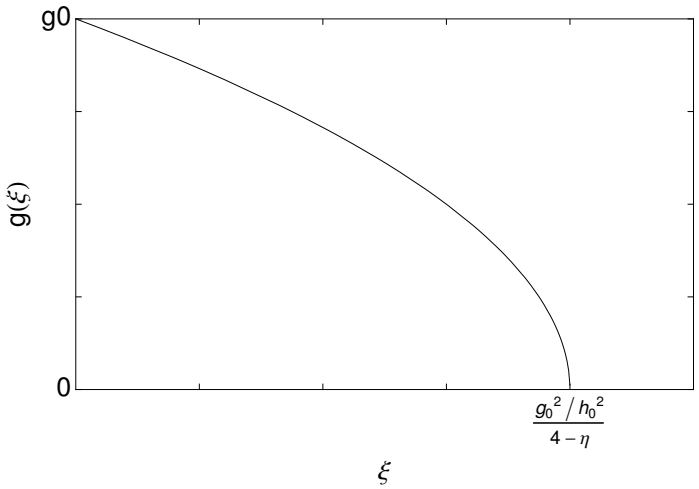

Figure 4.1: Special-case solution for $g(\xi)$ in terms of the pressure-profile parameter η and boundary conditions g_0 and h_0.

Another significant point is that the solution for the magnetic field has no dependence in either dimension on the parameter η, meaning that the magnetic field that develops within the boundary layer is not affected by the pressure profile of the medium that the jet passes through.

The Lorentz factor Γ, on the other hand, does have a radial dependence on η. As expected, we see that the jet is accelerated as it propagates outward: $\Gamma \propto r^{\eta/2-1}$ scales as a positive power of r.

We now examine the pressure profile within the boundary layer as prescribed by this solution. Since we have demonstrated that the magnetically-dominated regime is the relevant regime in this problem, the total pressure within the layer is approximately described by the magnetic pressure

$$\frac{B^2}{\Gamma^2} \propto b_0^2 h_0^2 \left[\left(\frac{g_0}{h_0} \right)^2 - (4-\eta)\xi \right]. \tag{4.29}$$

In KBB12 we demonstrated that in the strictly hydrodynamic case, the pressure monotonically decreases for all η, but decreases linearly with ξ only for the case where $\eta = 8/3$ (KBB12, §3.1). In this specific case, the pressure drops to zero within the boundary layer, indicating that all of the jet material is piled in a thin boundary layer in a 'hollow cone' structure. As the value of η gets further from $8/3$ in either direction, the pressure profile becomes less steep, implying that the boundary layer broadens and the structure of the jet becomes less like a hollow cone.

The magnetic case is a little more difficult to interpret due to the unspecified boundary conditions g_0 and h_0 in Eq (4.29), but we can make some qualitative observations. First, it is clear that the magnetic case parallels the hydrodynamic case in that all solutions for pressure (which, since magnetically dominated, scales as $1/\Gamma^2$ in the boundary layer) monotonically decrease with ξ for $2 < \eta < 4$. This means that the pressure is greatest at the contact discontinuity where it is matched with the external pressure, and it decreases inwards across the layer (see Fig. 4.1), as is expected due to the collimation.

A major contrast between the magnetic and hydrodynamic cases is that in the magnetic case it is true for **all** values of η that the pressure decreases linearly and vanishes at a critical value of ξ, in this case $\xi_{cr} = (g_0/h_0)^2/(4-\eta)$. Thus any jet can form a hollow cone structure in the magnetic

case, with a boundary layer of thickness $\Delta\xi = \xi_{cr}$. The impact of η, then, is instead to determine the thickness of the boundary layer: jets injected into an ambient medium with a pressure profile parametrized by a low η (a gradual decrease in external pressure) will therefore develop the most pronounced hollow-cone structure, whereas jets injected into a medium that has a higher η (a steep decrease in external pressure) will exhibit a thicker boundary layer.

The distinction between the magnetic and hydrodynamic cases is most evident, however, when examining the global energy constraints for these solutions, as in KBB12. In this case, we assume that all the power in the boundary layer is in the form of Poynting flux, given by $L \propto B^2 A$, where A is the cross-sectional area of the boundary layer. As we are assuming a boundary layer of width $\Delta\theta = 1/\Gamma$, the cross-sectional area of that ring is $A \propto r^2/\Gamma$, implying that the power within the boundary layer scales as $L \propto r^{1-\eta/2}$. Thus for $2 < \eta < 4$, the boundary layer contains less and less energy as one goes further out in r.

This loss of energy is indicative of a unique situation in the magnetic case: rather than being bounded on the inside by a shock front through which material is added, as in the hydrodynamic case, at large r the boundary layer instead appears to be bounded on the inside by a rarefaction front, through which material is leaving the layer and returning to the main jet.

We can verify the position of this rarefaction front by calculating the location of the surface at which the fluid motion normal to the surface is equivalent to the local speed of sound. This condition can be stated as

$$\beta_{\xi_r}^2 = \frac{\beta_f^2}{\Gamma^2\left(1-\beta_f^2\right)}, \tag{4.30}$$

where β_{ξ_r} is the velocity normal to the surface of the rarefaction front ξ_r, and β_f is the local sound speed, which is given by the relativistic expression for the fast magnetosonic speed in the hot-jet limit,

$$\beta_f^2 = \frac{\frac{4}{3}p + B^2}{4p + B^2}. \tag{4.31}$$

This calculation yields an approximate position for the rarefaction front of

$$\xi_r = \xi_{cr} - \frac{(\eta-2)^{3/2}}{(4-\eta)^{5/2}} \left(\frac{2a_0}{3b_0^2}\right)^{3/4} \left(\frac{g_0}{h_0}\right)^{1/2} r^{(\eta-4)/4}, \tag{4.32}$$

indicating that the rarefaction front occurs at a location just before the pressure within the boundary layer drops to zero, allowing matching across the front to the conditions in the interior of the jet. At large r, the position of the rarefaction front asymptotes to the location of the pressure zero-point.

Looking at how the Lorentz factor Γ scales with r along the rarefaction front, we see that $\Gamma \propto r^{3\eta/8-1/2}$. We know that the Lorentz factor scales as $\Gamma \propto r^{\eta/2-1}$ at the contact discontinuity, and we expect it to scale as $\Gamma \propto r$ in the jet interior to be consistent with free expansion (see also Lyubarsky, 2011). Thus, for $2 < \eta < 4$, the scaling of Γ at the rarefaction front is consistent with an intermediate acceleration between the two, providing a smooth transition between the boundary layer and the jet interior.

More insight into the boundary-layer energy loss can be attained by examining the position of the contact discontinuity (θ_c) and the inner boundary ($\theta_s = \theta(g = 0)$) as a function of radius. Using the solutions found in Eq (4.28), the width of the boundary layer is given by

$$\theta_c - \theta_s = -\frac{g_0^2/h_0}{4-\eta} r^{1-\eta/2}, \tag{4.33}$$

indicating that the width is decreasing in r.

Furthermore, integrating Eq (4.12) using the above equation allows us to find the form of the inner and outer boundaries individually:

$$\theta_c = \theta_0 - \frac{h_0}{\eta/2-1} r^{-(\eta/2-1)} \tag{4.34}$$

$$\theta_s = \theta_0 + \left(\frac{h_0}{4-\eta}\right)\left[\left(\frac{g_0}{h_0}\right)^2 - \frac{4-\eta}{\eta/2-1}\right] r^{-(\eta/2-1)}. \tag{4.35}$$

From this, we can see that the outer boundary is collimating, but less and less so with increasing r. The inner boundary, on the other hand, is *decollimating* when the condition

$$\left(\frac{g_0}{h_0}\right)^2 > \frac{4-\eta}{\eta/2-1} \tag{4.36}$$

is met, with the boundary conditions prescribed by matching across the rarefaction front to solutions for the jet interior (such as those described by Lyubarsky, 2011). When this condition is satisfied, the boundary layer intercepts fewer and fewer streamlines of new material from within the jet interior. The decollimation, too, weakens with increasing r, with the inner and outer boundaries meeting asymptotically.

These results suggest that the boundary layer of a magnetically dominated jet decreases in width with increasing distance from the source, and contains a decreasing amount of energy as material leaves the boundary layer across the rarefaction front to rejoin the jet interior. Nonetheless, a sharp pressure gradient is maintained across the layer, insulating the interior of the jet from the external medium.

4.5 Conclusion

We have evaluated the structure of a boundary layer within a hot, magnetohydrodynamic jet with an ultrarelativistic equation of state. We assumed that the jet as a whole is causally disconnected from its surroundings, but the boundary layer is thin and therefore in causal contact. We examined the impact on jet collimation of a toroidal magnetic field within the jet as well as an ambient medium with a pressure profile of $p \propto r^{-\eta}$, with $2 < \eta < 4$.

We first demonstrated that the basic RMHD equations can be used to show that any jet boundary layer seeded with a toroidal magnetic field at its base will eventually become magnetically dominated at large radii.

We then constructed self-similar solutions for the boundary layer in the limit where the jet pressure is dominated by magnetic pressure. We found a special case of physical solutions where the jet pressure decreases linearly across the boundary layer, dropping to zero at a location set by the boundary conditions and the value of the pressure profile parameter η. The boundary layer thickness is dependent upon the value of η, with increasing η producing an increasingly wide boundary layer.

We further found that the thickness of the boundary layer decreases with radial distance, and the boundary layer contains a decreasing amount of the jet energy. This suggests that the addition of a magnetic field fundamentally changes the jet at large radius: whereas in the hydrodynamic case the inner boundary of the layer is a shock front through which material enters the layer, in the magnetohydrodynamic case the layer is bounded on the inside by a rarefaction front through which material leaves the boundary layer and rejoins the interior of the jet.

We found the position of this rarefaction front to occur just inside the layer from the location where the pressure vanishes, providing a smooth transition between the boundary layer and the jet interior and allowing for matching across the rarefaction front to the conditions in the jet interior. This matching would prescribe the values of the boundary conditions within the layer, and could potentially yield a solution where the rarefaction front is gradually decollimating, intercepting fewer and fewer streamlines as radial distance from the source increases.

In spite of the thinning of the boundary layer with radial distance, a sharp pressure gradient is nonetheless maintained across the layer, causing it to function as an insulating buffer between the jet interior and the ambient medium. Unlike the hydrodynamic case, the solutions for the structure of a magnetized jet do not have clear observational implications. Though the boundary layer contains a decreasing amount of energy as one looks further from the source, the layer might nonetheless have a high emissivity, which could be observationally important if the flow within the boundary layer is pointed along our line of sight.

The results presented in this paper provide the premise for a more complete treatment in numerical simulations of the effects of the ambient medium on collimation, both by demonstrating the behavior of the jet when the outer wall is allowed to change its shape, and by providing models that can be used to assess the effects of numerical resolution on simulation outcomes.

Ultimately, these results provide a foundation for future work examining energy dissipation in magnetized jets and the associated radiative observational signatures.

Chapter 5

Entropy Production in Relativistic Jet Boundary Layers

5.1 Preface

This paper appeared in Monthly Notices of the Royal Astronomical Society, Volume 446, Issue 2, p.1195–1202 and was completed under the guidance of Dr. Mitch Begelman. This is the third of three papers examining the impact of the ambient medium on collimation and confinement of relativistic jets that have lost causal contact with their surroundings. In this paper, we return to the work of Chapter 3 and relax some of the strict assumptions made, including that the flow is irrotational, isentropic, and behaves adiabatically. Instead, we consider the case where the ambient pressure external to the jet decreases slowly, and entropy is generated within the boundary layer as a result of multiple shocks being driven into the flow.

Abstract

Hot relativistic jets, passing through a background medium with a pressure gradient $p \propto r^{-\eta}$ where $2 < \eta \leq 8/3$, develop a shocked boundary layer containing a significant fraction of the jet power. In previous work, we developed a self-similar description of the boundary layer assuming isentropic flow, but we found that such models respect global energy conservation only for the special case $\eta = 8/3$. Here we demonstrate that models with $\eta < 8/3$ can be made self-consistent if we relax the assumption of constant specific entropy. Instead, the entropy must increase with increasing r along the boundary layer, presumably due to multiple shocks driven into the flow as it gradually collimates.

The increase in specific entropy slows the acceleration rate of the flow and provides a source of internal energy that could be channeled into radiation. We suggest that this process may be important for determining the radiative characteristics of tidal disruption events and gamma-ray bursts from collapsars.

5.2 Introduction

Relativistic jets are becoming increasingly relevant as a component of high-energy astrophysical systems. Not only are these jets observed in the context of active galactic nuclei (AGN), microquasars, and gamma-ray bursts (GRBs), but they are now also considered to be an explanation of the flares seen from some tidal disruption events (TDEs), events in which a star is torn apart by the tidal forces exerted by a normally-dormant, massive black hole (Zauderer et al., 2011; Tchekhovskoy et al., 2014).

When a relativistic jet is launched, it slams into the gas and dust surrounding the source. Two things are thought to happen as these jets propagate outward. First, after they are launched with what are thought to be fairly modest speeds (Georganopoulos & Marscher, 1998), they are accelerated to Lorentz factors of typically a few for microquasars (Meier, 2003), 10-20 for blazars (Sikora et al., 1994b; Jorstad et al., 2005), and hundreds or even thousands for GRBs (Lithwick & Sari, 2001). Second, they experience some form of collimation that results in the relatively narrow jet opening angles observed in most blazars and GRBs (e.g. Doeleman et al., 2012; Jorstad et al., 2005; Sari et al., 1999; Goldstein et al., 2011). As jets from active galactic nuclei are observed to first become collimated near their source (Junor et al., 1999; Jorstad et al., 2005), we seek a description to explain simultaneous collimation and acceleration at the base of the jet, where the internal-energy-dominated flow first interacts with the ambient medium.

Close to the central black hole, inside the Alfvén surface, jets can be collimated by the inertia of the disk at the jet base, transmitted by magnetic tension along the flow (e.g. Blandford, 1976; Lovelace, 1976; Koide, 2004; Narayan et al., 2007). At larger scales, however, causal connection

between the disk and the flow is lost, creating a need for additional confinement by the pressure of an external medium (Begelman, 1995). Additionally, collimation by magnetic tension has been demonstrated to occur very slowly (Eichler, 1993; Tomimatsu, 1994; Begelman & Li, 1994; Beskin et al., 1998), and cannot explain the collimation scales observed.

In contrast to collimation where gas pressure is crucial, jet acceleration is generally assumed to be dominated by magnetic stresses. However, there are situations where other forces may play a dominant role. As an example, recent observations of TDEs indicate that some may exhibit powerful jets — but there is not enough magnetic flux available to power such a jet without invoking a relic field (see e.g. Tchekhovskoy et al., 2014). This provides additional motivation to study the effects of external pressure confinement on jet acceleration and collimation.

The environments around relativistic jets provide ideal scenarios for pressure confinement: there exist both static collimating environments such as the dusty torus of an AGN or the stellar envelope surrounding a GRB (e.g. Eichler, 1982; Komissarov & Falle, 1997), as well as the potential for collimation by dynamic means, such as by the ram pressure of a disk wind (e.g. Komissarov, 1994a; Bromberg & Levinson, 2007). Pressure confinement and magnetic tension could work together to collimate a flow, as we describe in Kohler & Begelman (2012). Alternatively, pressure confinement could act alone — a possibility which is our focus both in Kohler et al. (2012), hereafter KBB12, and in the current paper.

When a hydrodynamic, relativistic jet is injected into an ambient medium with a pressure profile that scales as $p \propto r^{-\eta}$ where $\eta > 2$, the jet interior will ultimately lose causal contact with its surroundings (Begelman et al., 1984). If $\eta < 4$, a shocked boundary layer forms at the interface between the flow and the ambient medium, and the outer region of the jet experiences a collimating force from the pressure of that environment.

The range of $2 < \eta < 4$ for the external pressure profile could describe many scenarios for a confining medium, such as the ram pressure of a disk wind (see Eichler, 1982), a disk corona, or a stellar envelope. This regime may be particularly relevant to the currently-explored topic of TDEs; in Coughlin & Begelman (2014), for example, the range calculated for the accretion disk that forms

around the central black hole in a TDE is $3/2 < \eta < 4$. Developing models of the jet flow in this range of ambient pressure profiles is therefore an important task for understanding the structure of the jets that form in a variety of interesting scenarios.

This problem has been previously approached in a variety of ways. Three-dimensional general relativistic MHD simulations such as Beckwith et al. (2008), Beckwith et al. (2009), and McKinney & Blandford (2009) provide self-consistent descriptions of the jet launching mechanism and propagation of a Poynting-flux-dominated jet sheathed by an unbound flow, but these simulations are limited by their inability to sufficiently resolve the sharp pressure and density gradients that occur in these regions. Other numerical studies of the large-scale collimation of jets treat the external medium as a rigid wall with a prescribed geometry, enclosing a cavity into which the jet is injected (e.g. Komissarov et al., 2007, 2009; Komissarov, 2011; Tchekhovskoy et al., 2010). Simulations that focus specifically on modeling gamma-ray burst jets breaking out of a stellar envelope — which generally describe either Poynting-flux-dominated jets (e.g., Proga et al., 2003; Bromberg et al., 2014) or thermally-accelerated jets (e.g., Aloy et al., 2005; Lazzati & Begelman, 2005) — often suffer from similar constraints on resolution and boundary conditions, as well as the additional complications of time-dependent jet behavior (though the inclusion of this time-dependent analysis is of course more realistic than steady-state idealizations).

Because of these limitations, simplified analytic models are extremely helpful for improving the physical content of the boundary conditions employed in numerical simulations, as well as for interpreting the extent to which numerical resolution affects the outcomes of these simulations. As such, we opted to pursue an analytic approach that instead treats the external pressure as a boundary condition, but leave the physical shape of the boundary free to be determined as a result of interaction between the jet and the ambient medium.

Simplified analytic treatments of this problem can also vary greatly in approach, however. Works such as Komissarov & Falle (1997), Nalewajko & Sikora (2009), and Lyubarsky (2009) focus on the interaction between a cold jet (dominated by inertia) and the ambient medium. In contrast, Levinson & Eichler (2000) assumed a hot jet (dominated by the internal energy), but examined

the structure and behavior of the jet in the limiting case where the jet becomes fully shocked upon impact. Other treatments, such as Zakamska et al. (2008), Begelman et al. (2008), and Lyubarsky (2011), focus on modeling jets that remain in causal contact.

In contrast to these studies, we are interested in the case where the jet loses causal contact as it propagates, forming a boundary layer of shocked jet material at the point of impact with the ambient medium. This problem was previously addressed in Bromberg & Levinson (2007); in this paper, the authors model the effects of both a stationary external medium and a disk wind on a hot, hydrodynamic jet that has lost causal contact when it impacts the external environment. The authors assume that the pressure remains constant across the boundary layer in this case, and they then examine the impact of the initial conditions, such as initial opening angle and Lorentz factor, on the structure of the jet as it balances its internal pressure with the pressure of the ambient medium.

In KBB12, we repeated their calculations, solving for the structure of a boundary layer just inside the contact discontinuity that separates the jet from its surroundings. We found results similar to those of Bromberg & Levinson (2007), though we treated the entropy within the boundary layer slightly differently, which resulted in a difference in the collimating behavior of the outer boundary of the jet (see KBB12 for details). We then took our analysis a step further, however: due to the curvature of the jet as it collimates, we expect a pressure gradient to form across the boundary layer, so we opted to refine the boundary-layer treatment to allow for varying pressure across different streamlines. In the limit of ultrarelativistic flow (bulk Lorentz factor $\Gamma \gg 1$), we found a method of constructing self-similar models specifically for the structure within the boundary layer (see, again, KBB12 for results). These models, however, only gave physically reasonable results for certain values of η: global energy conservation was only respected for the special case where $\eta = 8/3$. Our models in KBB12 were also simplified by the use of several underlying assumptions that are commonly adopted in analytic treatments; in particular, that the flow in these solutions was both irrotational and isentropic.

In this paper, as a follow-up to KBB12, we now propose a set of more general solutions to the

boundary-layer problem of a hot relativistic jet that has lost causal contact, and we demonstrate that these solutions provide physical results for the range of η that was not well-described by KBB12 (which is the interesting regime for astrophysical scenarios such as TDEs). These solutions, unlike in our previous paper, do not require the jet to be either adiabatic or irrotational, and they allow for entropy to be a varying function of position within the boundary layer.

Our motivation in this work is, as before, to create steady-state models of the underlying jet behavior, onto which effects such as instabilities and radiation can be added. Our models provide insight into the locations of the bulk of the jet luminosity, as well as the locations of energy dissipation, which indicate potential radiation signatures that can be used for comparison with observations.

In §5.3 we describe the problem, summarize the behavior of the solutions we found in KBB12, and explain why we seek a new family of solutions here. In §5.4 we describe how we obtain these new solutions, in §5.5 we discuss the results and their implications, and in §5.6 we conclude.

5.3 Casting the problem

We assume an axisymmetric, ultrarelativistic, hot jet. Flow launched from the source initially expands adiabatically, propagating outward on conical streamlines until it impacts the ambient medium. Given a particular bulk Lorentz factor for the flow, there exists a minimum angle of impact that will result in the flow shocking. For the flow to shock, the speed of sound waves measured in the lab frame in the direction perpendicular to the shock surface must vanish; this is equivalent to the condition that $\beta_\perp = 1/\sqrt{2}\Gamma$, as described in KBB12. From this, and using the definition of the bulk Lorentz factor $\Gamma = (1-\beta^2)^{-1/2}$, one can show that the minimum angle of impact that will result in a shock is given by

$$\sin\theta_i = \frac{1}{\sqrt{2}(\Gamma_i - 1)^{1/2}}, \tag{5.1}$$

where Γ_i is the bulk Lorentz factor at the point of impact. Plotting θ_i in Figure 5.1, we can see that the angle of impact necessary to result in a shock is fairly small even for low values of Γ_i, indicating

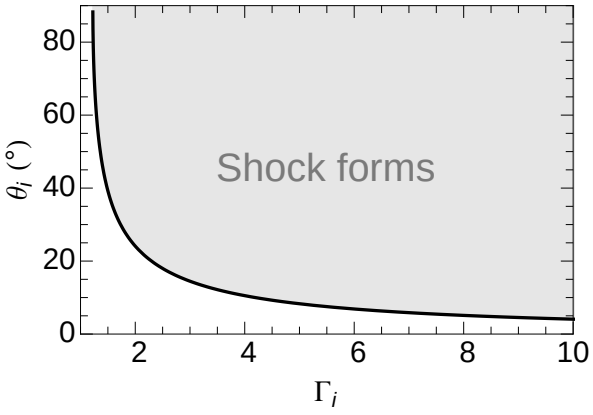

Figure 5.1: Minimum angle of impact necessary to produce a shock, plotted as a function of the initial bulk Lorentz factor of the flow at the point of impact. The shaded region corresponds to combinations of angle and Lorentz factor that will result in a shock forming.

that formation of a shocked boundary layer is a very likely result.

5.3.1 Isentropic solutions

As mentioned in §5.2, in KBB12 we sought self-similar solutions to the fluid equations within this shocked boundary layer. In this treatment we adopted several major simplifications to the problem: we assumed that the flow was adiabatic and isentropic, and that the flow was irrotational. In all solutions that we found, the overall shape of the jet remained very close to conical, but the relatively small amount of collimation due to the pressure of the ambient medium had a large impact on the behavior of the flow within the boundary layer.

The admitted solutions could be grouped into three families based upon how quickly the external pressure $p_e \propto r^{-\eta}$ dropped off. The behavior of each of those isentropic families is summarized briefly below.

(1) $\eta = 8/3$

Solutions for which the external pressure profile is exactly $p_e \propto r^{-8/3}$ are a special case of solutions: the pressure within the boundary layer decreases from the contact discontinuity inward, dropping to zero at a finite distance and forming a narrow boundary layer contain-

ing a fixed flux of jet energy. These "hollow cone" solutions are the only isentropic solutions to conserve energy globally; the power carried by the jet, given by $L \propto p\Gamma^2 A \propto r^{-3\eta/4+2}$ where p is the pressure and A is the cross-sectional area of the region carrying most of the power, is constant with radius in this case.

(2) $\eta > 8/3$

Solutions for which the external pressure profile drops off more steeply than $p_e \propto r^{-8/3}$ have pressure within the boundary layer that decreases from the contact discontinuity inwards, but this pressure drops off asymptotically. The resulting solutions demonstrate "hollow cone" behavior for values of η near $8/3$, but the boundary layer becomes wider and the cone progressively more filled as the value of η increases toward 4. For these solutions, the power carried by the boundary layer scales as r to a negative power. We demonstrated in KBB12, however, that because the transverse integrals of energy diverge, truncated solutions can still be constructed that conserve energy globally.

(3) $\eta < 8/3$

There exist isentropic solutions for which the external pressure profile drops off less steeply than $p_e \propto r^{-8/3}$, however, for these solutions the power carried by the boundary layer scales as r to a positive power. In KBB12, we argued that global energy could potentially be conserved if the jet cross-section gradually decreased with increasing radius, resulting in total energy remaining constant. We have since determined, however, that no such strongly-collimating solution can be constructed in a self-consistent way in the regime of $\eta < 8/3$. To find a set of solutions for the flow in this regime that **do** behave physically, we must now relax some of the assumptions we made in KBB12 about the behavior of the flow.

5.3.2 Entropy-generating solutions

Why might the regime of $\eta < 8/3$ not have physical solutions with fixed entropy, as we assumed in KBB12? We argue here that our assumption of isentropic flow over-constrained the problem in this regime. This can be more readily understood from a physical point of view: consider a boundary layer in contact with an ambient medium that has a slowly-decreasing pressure profile. Because the pressure outside the jet is significantly higher than inside, and because the flow impacts the ambient medium at an oblique angle, the initial shock that forms at the point of impact may not decrease the speed of the flow enough to prevent it from shocking again further downstream.

Figure 5.2 illustrates, in the observer frame, the angle by which the flow is deflected when crossing a shock, as a function of the impact angle, for a series of curves describing different upstream Mach numbers. The plot also indicates the values of the deflection and impact angles for which the speed of the flow is still greater than the sound speed, downstream of the shock; from this, it can be seen that for an oblique shock the flow can easily remain supersonic after shocking. In addition, we will later demonstrate that the flow continues to be accelerated after crossing to the downstream side of the shock. This acceleration makes it even more likely that the flow could shock again as it propagates outward in radius. One can imagine, then, the jet flow undergoing not just one, but a series of shocks, with each successively decreasing the speed perpendicular to the shock and deflecting streamlines closer to the shock tangent. This process would result in a gradually collimating flow, but each shock would also generate entropy, providing a source of internal energy.

Flow undergoing a series of shocks in this way would be difficult to model analytically; however, the motion can be approximated. By envisioning the flow as forming a single shocked boundary layer — but allowing the specific entropy within the layer to vary spatially — we can approximate the entropy generation that would occur over the course of a series of shocks. By not insisting that the fluid be irrotational, we provide the additional freedom needed for the flow to mimic the behavior of crossing multiple shocks.

Using this physical model, we now describe the construction of the problem under these terms and the solutions that are admitted as a result.

5.4 Deriving the boundary-layer flow

As in KBB12, we model a hot, ultrarelativistic jet that is cylindrically symmetric about the z axis. We assume that the jet is injected from a point source with steady flow and approximately radial streamlines, and we suppose that the ambient medium has a pressure profile that declines as $p_e \propto r^{-\eta}$ where r is spherical radius and η is some constant satisfying $2 < \eta < 4$ (see Bromberg & Levinson, 2007 for another treatment of this regime). For an external pressure that decreases at such a rate, the jet will lose causal contact and become gradually collimated by the ambient pressure; we now examine, in the steady-state limit, the shape that the jet takes as a result of this collimation.

When the jet plows into the external medium supersonically, a boundary layer of shocked jet material forms at the interface between the jet and the stationary ambient medium. We model this boundary layer with a thickness of order $\Delta\theta \sim 1/\Gamma$ such that the layer maintains causal contact, and we wrap the physics of the corresponding ambient medium into the pressure profile p_e.

In our model, the initial opening angle of the jet is assumed to be less than $\pi/2$ and greater than the minimum angle of impact for a shock, given by Eq (5.1), such that causal contact is lost across the jet and a shock forms when the jet impacts the ambient medium. We note that the initial opening angle does not otherwise play a role in establishing the structure that is formed across the boundary layer, because we construct here solutions of the boundary layer only, rather than attempting to solve for the entire structure of the jet. For further insight into the full jet structure, as well as details about how the initial conditions at the jet base affect the jet shape and behavior, we refer the reader to our previous paper, KBB12, as well as other works (e.g. Levinson & Eichler, 2000; Bromberg & Levinson, 2007).

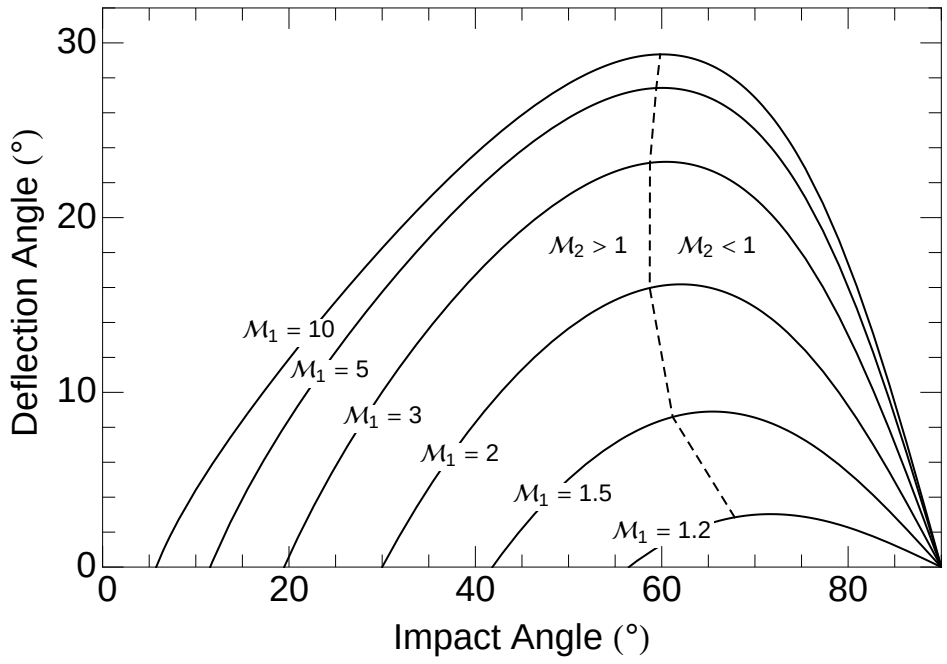

Figure 5.2: Plot of the deflection angle of flow across a shock for a range of impact angles, assuming that the flow is supersonic upstream of the shock. Individual curves correspond to different values of the upstream Mach number, $\mathcal{M}_1 = \sqrt{2}(\Gamma_1^2 - 1)^{1/2}$. The dashed line divides the parameter space into two regions: that in which the flow is subsonic downstream of the shock, and that in which it is still supersonic after shocking.

5.4.1 Fluid equations

The boundary layer of the jet is bounded on the inside by a shock front, through which jet material enters, and on the outside by a contact discontinuity, separating it from the ambient medium. To find solutions describing the fluid flow within the boundary layer, we start from the covariant form of the relativistic, hydrodynamic fluid equations (e.g. Dixon, 1978; Zakamska et al., 2008):

$$\nabla_\nu(\rho u^\nu) = 0 \tag{5.2}$$

$$\nabla_\nu T^{\mu\nu} = 0, \tag{5.3}$$

where

$$T^{\mu\nu} = wu^\mu u^\nu + pg^{\mu\nu} \tag{5.4}$$

is the stress-energy tensor. Here ρ is the proper rest mass density, w is the enthalpy, p is the pressure, $u^\mu = (\Gamma, \Gamma\boldsymbol{\beta})$ is the 4-velocity of a fluid element (with $\boldsymbol{\beta} = \boldsymbol{v}/c$), and $g^{\mu\nu}$ is the space metric. The enthalpy is defined as $w \equiv \epsilon + p$ where ϵ is the total proper energy density, given by $\epsilon = \rho + 3p$.

Assuming flat spacetime and time independence, and using number density n, these equations can be written in vector notation as

$$\nabla \cdot (n\Gamma\boldsymbol{\beta}) = 0 \tag{5.5}$$

$$\nabla \cdot (w\Gamma^2\boldsymbol{\beta}) = 0 \tag{5.6}$$

$$w\Gamma^2(\boldsymbol{\beta} \cdot \nabla)\boldsymbol{\beta} + \nabla p = 0, \tag{5.7}$$

describing continuity, energy conservation, and momentum conservation, respectively.

Treating the problem in the spherical polar coordinates r, θ and ϕ, we examine the ordering of the various terms in these equations. As the maximum transverse speed that can be achieved without a shock forming is of order $1/\Gamma$, we can assume that β_θ is of this order, and that β_r is of order one. Adopting this characteristic scaling, we state that $\frac{\partial}{\partial\theta} \sim \Gamma\frac{\partial}{\partial r}$. Writing out β_r and employing the fact that $\beta_\theta^2 + \Gamma^{-2} \ll 1$, we have $\beta_r \approx 1 - \frac{1}{2}(\beta_\theta^2 + \Gamma^{-2})$. Finally, we also assume that

$\theta \approx$ constant, i.e., that the streamlines are roughly radial; we will calculate their deviation from radial. Using all of these arguments, we hereafter retain terms only to lowest order.

5.4.2 Constructing self-similar solutions

As in KBB12, we construct a self-similar variable ξ that describes the distance into the boundary layer from the contact discontinuity, normalized by the expected scale of the boundary layer: $\xi \propto (\theta_c - \theta)/\Delta\theta$, where $\theta_c = \theta_c(r)$ is the position of the contact discontinuity. Assuming that $\rho \ll p$ such that $w \approx 4p$, we now search for solutions to the fluid equations that take the form

$$\begin{aligned} p &= g^4(\xi) r^{-\eta}, & \beta_\theta &= h(\xi) r^{-\delta}, \\ \frac{1}{\Gamma} &= j(\xi) r^{-\delta}, & n &= k(\xi) r^{-\alpha}. \end{aligned} \tag{5.8}$$

In these solutions δ and α are constant free parameters describing radial scaling, and g, h, j and k are arbitrary functions of the similarity variable ξ, with notation chosen for consistency with KBB12. The interior pressure has the same radial scaling as the pressure of the ambient medium because the gas pressure in the boundary layer must match the external pressure at the contact discontinuity. The boundary condition $g(0) = 1$ is enforced so that the pressures are matched at the contact discontinuity, but $h(0)$ is left free. Finally, the streamlines must be parallel to the contact discontinuity at its location, θ_c, which requires that $\beta_\theta(\theta_c) = r d\theta_c/dr$ and yields the further constraint that

$$\frac{d\theta_c}{dr} = h(0) r^{-(1+\delta)}. \tag{5.9}$$

In contrast to KBB12, where we did not specifically enforce that the boundary layer maintain constant power, we now impose this condition. The power carried by a pressure-dominated jet is given by $L \propto p\Gamma^2 A$, where A is the cross-sectional area of the jet. If we examine the jet's power concentrated in the boundary layer, which has width $\Delta\theta \sim 1/\Gamma$, then $L \propto p\Gamma r^2$. Using the pressure scaling $p \propto r^{-\eta}$ we see that for power to remain constant, the radial scaling of the Lorentz factor within the layer must be $\delta = \eta - 2$.

By taking the scalar and vector products of $\boldsymbol{\beta}$ with Eq (5.7), the momentum equation can be broken down into components parallel and perpendicular to the fluid motion, respectively. It can be shown (e.g., Landau & Lifshitz, 1959) that the parallel component of the momentum conservation equation can be reworked to obtain the relativistic Bernoulli equation:

$$\frac{\Gamma w}{n} = B \tag{5.10}$$

where B is a constant function along streamlines.

Unlike in KBB12, we make no assumptions that the flow is either irrotational or adiabatic. Instead, we obtain an additional equation by supposing that there is no flow across surfaces of constant ξ; that is, we claim that ξ is a streamfunction. Thus, to Eqs (5.5) – (5.7) we add one final equation:

$$\boldsymbol{\beta} \cdot \nabla \xi = 0. \tag{5.11}$$

This definition clarifies that the Bernoulli constant $B = B(\xi)$. Thus Eq (5.10) allows us to determine both the radial scaling for n and the transverse distribution for Γ: $\alpha = 2$ and $j(\xi) = \frac{4g^4(\xi)}{B(\xi)k(\xi)}$.

As the boundary layer is expected to scale as $\Delta\theta = 1/\Gamma_c$, where Γ_c is the Lorenz factor along the contact discontinuity, we can define our self-similar variable ξ as

$$\xi = -\frac{1}{h(0)} r^{\eta-2}(\theta_c - \theta). \tag{5.12}$$

Using this definition with Eq (5.11), we can solve for the form of the spatial distribution of the transverse velocity, $h(\xi)$. Thus we now have

$$\begin{aligned} p &= g^4(\xi) r^{-\eta}, & \beta_\theta &= h(0)\left(1 - (\eta - 2)\xi\right) r^{2-\eta}, \\ \frac{1}{\Gamma} &= \frac{4g^4(\xi)}{B(\xi)k(\xi)} r^{2-\eta}, & n &= k(\xi) r^{-2}. \end{aligned} \tag{5.13}$$

Note here that $h(0)$ is a negative value, in order to provide collimating solutions for β_θ.

Finally, turning to Eq (5.7) and keeping terms only to lowest order, we can write the perpendicular component of the momentum conservation equation as

$$w\Gamma^2 \left(\frac{\partial \beta_\theta}{\partial r} + \frac{\beta_\theta}{r}\frac{\partial \beta_\theta}{\partial \theta} + \frac{\beta_\theta}{r} \right) + \frac{1}{r}\frac{\partial p}{\partial \theta} = 0. \tag{5.14}$$

Substituting the solutions from Eq (5.13) yields a differential equation that governs the behavior of $g(\xi)$ and $k(\xi)$:

$$\left(\frac{B(\xi)k(\xi)h(0)}{4g^4(\xi)} \right)^2 (3-\eta)\left(1-(\eta-2)\xi\right) + \frac{g'(\xi)}{g(\xi)} = 0, \tag{5.15}$$

where the prime indicates a derivative with respect to ξ. We now explore these results further.

5.5 Results

5.5.1 Radial scaling

Looking at the form of the solutions to Eq (5.13), we can first discuss the evident radial scalings. By construction, the pressure within the layer decreases radially with the same scaling as the pressure of the ambient medium. In the entropy-generating solutions for $\eta < 8/3$ here, the Lorentz factor must scale as $\Gamma \propto r^{\eta-2}$ in order to satisfy energy conservation within the layer, whereas in the isentropic solutions found for $\eta \geq 8/3$ in KBB12, the Bernoulli equation instead forced the Lorentz factor to scale as $\Gamma \propto r^{\eta/4}$.

Figure 5.3 illustrates the scaling of Γ for curves in both of these ranges: the thick line corresponds to $\Gamma(r)$ for $\eta = 8/3$, the curves below correspond to entropy-generating solutions with values of η less than 8/3, and the curves above correspond to isentropic solutions with values of η greater than 8/3. From this plot, we can see that the process of entropy generation in the range of $\eta < 8/3$ slows the acceleration rate of the flow as compared to the constant-entropy solutions in the range of $\eta \geq 8/3$. Nonetheless, in both ranges the Lorentz factor scales always as a positive power of radius, verifying that flow accelerates within the boundary layer as it travels outward in radius. This result supports our picture of the flow described in §5.3.2, wherein the fluid undergoes repeated shocking as a result of being reaccelerated to supersonic velocities.

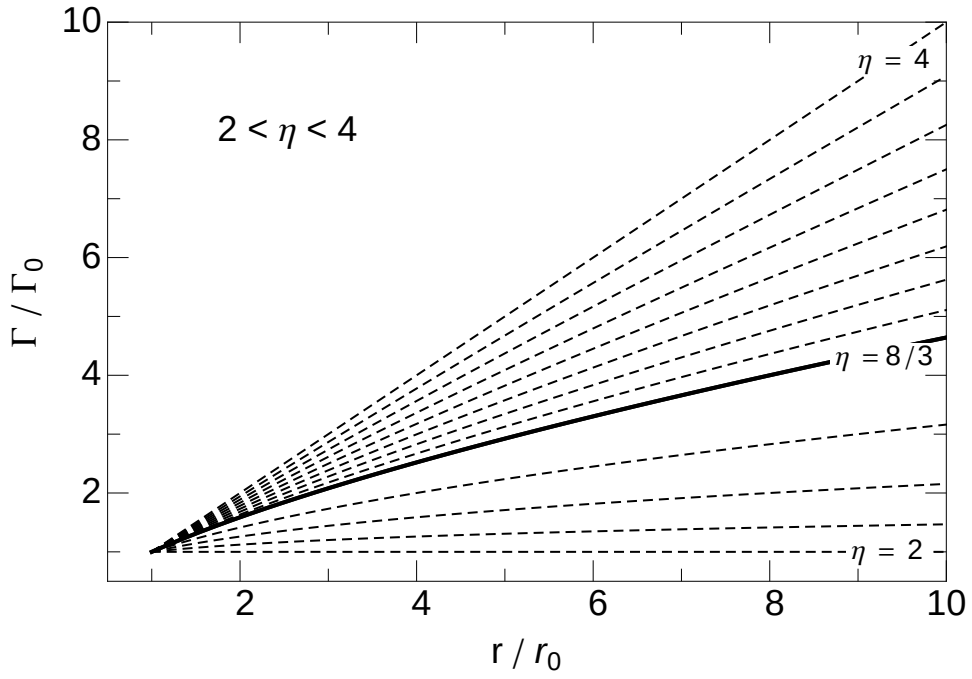

Figure 5.3: Radial scaling of the bulk Lorentz factor for curves with differing values of the pressure power-law index η, ranging from $\eta = 2$ to $\eta = 4$ in increments of $1/6$.

Examining other radial scalings in the $\eta < 8/3$ solutions, we see that the transverse velocity decreases as the fluid travels further from the source, and the density also decreases, as expected. Note that the radial scaling for density here is $n \propto r^{-2}$, which is consistent with an adiabatic equation of state (wherein $p \propto n^{4/3}$) only in the special case where $\eta = 8/3$.

5.5.2 Transverse scaling: a linear family of solutions

The end equations from §5.4.2 admit a wide range of possible solutions, and thus flow can be constructed using an appropriate combination of density profile and varying Bernoulli parameter to fit the physical circumstances of a given system. For the purpose of examining the solutions further, however, let us consider a simple set of solutions closely related to those we explored in KBB12: the solutions that arise when $g(\xi)$ is linear.

5.5.2.1 General linear solutions

Linear solutions are already hinted at in the form that β_θ is demonstrated to take in Eq (5.13); furthermore, examining linear solutions is the simplest approach and will allow us also to draw analogies to the solutions in KBB12. So let us suppose that

$$g(\xi) = 1 - s\xi \tag{5.16}$$

where s is some constant greater than zero. Using this form, Eq (5.15) reduces to

$$B(\xi)k(\xi) = -\frac{4}{h(0)}\left(\frac{s}{3-\eta}\right)^{1/2}\left(\frac{(1-s\xi)^7}{1-(\eta-2)\xi}\right)^{1/2}. \tag{5.17}$$

We use the negative root from Eq (5.15) here because $h(0)$ is negative and from the expression for Γ in Eq (5.13), we see that $B(\xi)k(\xi)$ must be positive to obtain physical results. From here we can

now examine the solutions that arise:

$$\begin{aligned} p &= (1-s\xi)^4\, r^{-\eta} \\ \beta_\theta &= h(0)\,(1-(\eta-2)\xi)\, r^{2-\eta} \\ \frac{1}{\Gamma} &= -h(0)\left(\frac{3-\eta}{s}\right)^{1/2}(1-s\xi)^{1/2}\,(1-(\eta-2)\xi)^{1/2}\, r^{2-\eta} \\ n &= k(\xi) r^{-2} \\ &= -\frac{4}{h(0)}\left(\frac{\eta-2}{3-\eta}\right)^{1/2}\frac{(1-(\eta-2)\xi)^3}{B(\xi)} r^{-2}. \end{aligned} \tag{5.18}$$

A few things are evident looking at these solutions. First, the pressure, transverse velocity, and inverse of the Lorentz factor all clearly drop to zero at finite values of ξ (as does the density, depending on the function chosen for the Bernoulli parameter). Thus the boundary layer that forms is either of width $\Delta\xi = 1/s$ or $\Delta\xi = 1/(\eta-2)$ — whichever is smaller. This is a "hollow cone" solution for the jet, as described in §5.3.1; the jet has a narrow boundary layer that contains a fixed energy flux.

The form of the density profile in this set of solutions remains free; it can be specified either by fixing the profile itself by prescribing $k(\xi)$, or by selecting a physically-motivated function to describe how the Bernoulli parameter $B(\xi)$ evolves. This latter point will be discussed further in §5.5.3.

5.5.2.2 Linear solutions when $s = \eta - 2$

We can further examine a specific example of this set of solutions: that in which $s = \eta - 2$. In this case, the solutions are given by

$$\begin{aligned} p &= (1-(\eta-2)\xi)^4\, r^{-\eta} \\ \beta_\theta &= h(0)\,(1-(\eta-2)\xi)\, r^{2-\eta} \\ \frac{1}{\Gamma} &= -h(0)\left(\frac{3-\eta}{\eta-2}\right)^{1/2}(1-(\eta-2)\xi)\, r^{2-\eta} \\ n &= k(\xi) r^{-2}. \end{aligned} \tag{5.19}$$

We can see that this is a variable-entropy generalization of the solution found in KBB12 for the special case of $\eta = 8/3$; that solution can be reproduced by assuming constant $B(\xi)$, in which case $p \propto n^{4/3}$. The generalized solution here behaves similarly: the flow forms a narrow boundary layer wherein the pressure drops from the value of the external pressure at $\xi = 0$ (the contact discontinuity) to zero at $\xi = 3/2$, implying that the jet material is piled up in a thin sheath around the outside of the flow.

When we instead examine a general η, the pressure and transverse velocity still drop to zero at a finite value of ξ, but the width of the boundary layer that forms is η-dependent: p and β_θ both go to zero when $\xi = 1/(\eta - 2)$. Thus the boundary layer still has a finite width, but that width increases as η decreases from $\eta = 8/3$ to $\eta \to 2$, and the hollow cone structure widens.

We can compare the transverse distribution of pressure in this particular case to that found in KBB12 for $\eta \geq 8/3$. Figure 5.4 illustrates this difference, showing how much more steeply the pressure drops off in the solutions where $\eta < 8/3$ (Figure 5.4(a)) than in the solutions where $\eta \geq 8/3$ (Figure 5.4(b)).

5.5.3 Entropy generation

We can now calculate the specific entropy within the boundary layer using the solutions derived in §5.4, and see if this is consistent with the assumptions we made in constructing the problem, as described in §5.3.2.

The specific entropy within the boundary layer scales as

$$\sigma \propto \ln\left(\frac{p}{n^\gamma}\right) \tag{5.20}$$

where the adiabatic index is $\gamma = 4/3$ in our case of a relativistic jet. In the solutions proposed in this paper, $n \propto r^{-2}$, meaning that the specific entropy scales as $\sigma \propto \ln(r^{8/3-\eta})$. This is a constant for $\eta = 8/3$, which is consistent with the constant-entropy solutions we found in KBB12. For $\eta < 8/3$, the entropy increases with r, which is indeed consistent with the theory that the fluid undergoes a series of entropy-generating shocks when the ambient pressure decreases slowly. Finally, for

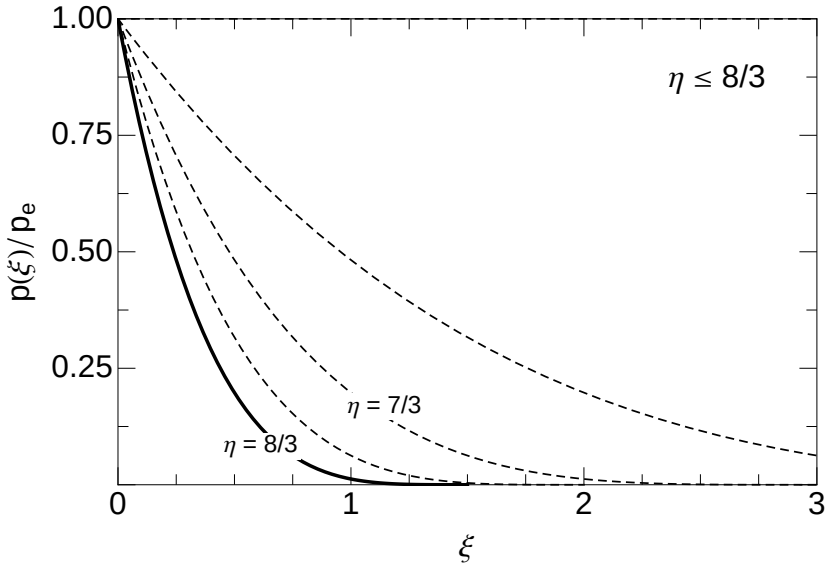

(a)

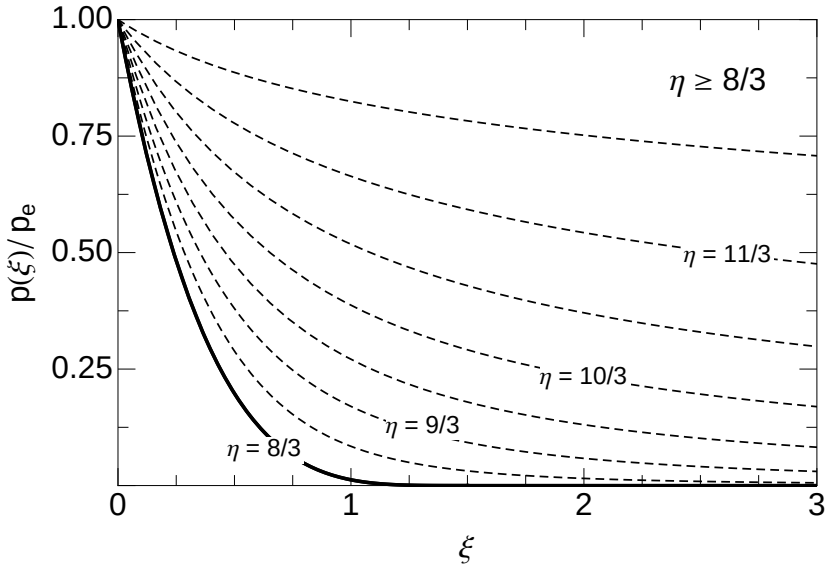

(b)

Figure 5.4: Pressure within the shock as scaled by the external pressure, for curves of constant η. The contact discontinuity is located at $\xi = 0$. (a) Curves for $2 < \eta \leq 8/3$, with η decreasing from the bottom curve up in increments of $1/6$. In these solutions, pressure drops to zero at a finite value of ξ for each curve. (b) For comparison (from KBB12), curves for $8/3 \leq \eta < 4$, with η decreasing from the bottom curve up in increments of $1/6$. In these solutions, pressure decreases asymptotically.

$\eta > 8/3$, entropy is a decreasing function of r, indicating that these solutions don't make sense in this regime.

Given the different behavior of these three different regimes, it is therefore important to select the free parameters for the solutions in a way that is consistent with the physical picture. The Bernoulli function $B(\xi)$ is an initial condition, set by the description of the interior jet flow as it crosses the shock front and enters the boundary layer; $B(\xi)$ remains the same on a streamline, even when crossing a shock. Pressure and density profiles should therefore be selected carefully, both to ensure consistency with the initial flow, and to ensure that the second law of thermodynamics isn't violated.

5.5.4 Additional Isentropic Solutions

Interestingly, we can also find solutions for $\eta > 8/3$ using the approach described in §5.4; the primary difference between these and the $\eta < 8/3$ solutions is that here we can't require energy to be conserved. The resulting solutions for $\eta > 8/3$ take the form

$$\begin{aligned} p &= g^4(\xi) r^{-\eta}, & \beta_\theta &= h(0)\left(1 - \frac{\eta}{4}\xi\right) r^{-\eta/4}, \\ \frac{1}{\Gamma} &= \frac{4g^4(\xi)}{B(\xi)k(\xi)} r^{-\eta/4}, & n &= k(\xi) r^{-3\eta/4}. \end{aligned} \tag{5.21}$$

In this case the flow is isentropic, as in KBB12, because the collimation is too weak to generate multiple shocks. In contrast to KBB12, however, these solutions are not irrotational, and their density profiles are not prescribed.

For these solutions, the energy flux within the boundary layer decreases with increasing radial distance from the source. To create physical solutions, forms of the density and pressure profiles can be chosen that diverge in the transverse direction, as in KBB12, allowing for constant total energy flux within the layer when the bounding shock moves to larger values of ξ with increasing r. Linear solutions like those described in §5.5.2.1, however, are possible; they merely require that the inner boundary is not in fact a shock front. Instead, this boundary must be something akin to a rarefaction front, through which material leaves the boundary layer and rejoins the main jet flow.

For an ambient medium with a pressure profile where $\eta > 8/3$, then, both the irrotational family of solutions found in KBB12 and the family of solutions described above are isentropic, and are reasonable physical descriptions of the flow in this regime.

5.6 Conclusion

Our goal was to obtain solutions that describe boundary-layer flow in a hot, relativistic jet that has lost causal contact with the ambient medium. We first sought solutions that specifically ensured that energy is conserved within the layer. We confirm here that for an external pressure profile of $p_e \propto r^{-\eta}$, when $\eta = 8/3$, linear solutions are possible in which the jet forms a narrow boundary layer of width $\Delta\xi = 1.5$ and behaves as a hollow cone, as described in KBB12, with all of the jet material piled up against the outer edge. This solution conserves energy within the boundary layer and the flow is irrotational, isentropic, and behaves adiabatically.

For a more gradual drop in pressure, where $\eta < 8/3$, the treatment in KBB12 was not sufficient; instead, the solutions demonstrated in this paper are the physical ones. In these solutions, we ensure conservation of energy within the boundary layer, but relax the conditions that the flow must be isentropic and irrotational. As a result, we find solutions in which the flow undergoes repeated shocking, generating entropy as it propagates outward in radius and gradually collimating in the process.

Linear solutions can be found in this regime that behave somewhat similarly to those for $\eta = 8/3$: a boundary layer forms in which the pressure drops to zero at a finite point, prescribing the width of the layer. Here, however, the layer width is dependent upon how steeply the external pressure decreases: as η decreases, the layer becomes broader, and it will continue to widen until the cone of the jet is filled. Furthermore, the rate of acceleration is slowed by the entropy generation, and the flow must no longer behave adiabatically — in fact, the density profile in this regime is completely free, and can be chosen to fit the physical parameters of a given scenario.

Finally, for a steeper drop in external pressure, where $\eta > 8/3$, we find a new family of

solutions that are isentropic, as in KBB12, but for which the flow is not irrotational and the density profile is left free. Linear forms of these solutions result in an energy flux that decreases radially, suggesting that the inner edge of the boundary layer may be a rarefaction front in this case.

This freedom to arbitrarily set up the system allows us to apply this model to a variety of different astrophysical flows; as previously mentioned, any hot, relativistic jets without strong magnetic fields could conceivably be described by this model. The entropy generation included in this model could provide a direct source of internal energy leading to radiation; thus this model is an important first step in establishing the radiation characteristics of these astrophysical flows.

Acknowledgements

This work was supported in part by NSF grant AST-0907872, NASA Astrophysics Theory Program grant NNX09AG02G, and NASA's Fermi Gamma-ray Space Telescope Guest Investigator program.

Chapter 6

Spectral properties of the brightest gamma-ray flares of blazars

6.1 Preface

This chapter consists of components of a paper that will be submitted to Monthly Notices of the Royal Astronomical Society. This project represents my first foray into observational astronomy: in this paper, we examine the spectra of bright blazar flares captured by the *Fermi* Gamma-ray Space Telescope's Large Area Telescope (LAT). In contrast to Chapters 3–5, in which I focused on modeling the steady-state, long-term behavior of relativistic jets, we now explicitly focus on the time-dependent behavior of sudden flaring activity observed from these jets. We attempt to determine what this variability and the behavior of the resulting spectra can tell us about the emission processes driving these flares.

Note About Collaborative Work

Though I am the primary author on this paper, this project was completed under the guidance of postdoctoral researcher Dr. Krzysztof Nalewajko, and this paper is not my sole work; it has been jointly co-written with him.

Abstract

We investigate the spectral properties of the brightest gamma-ray flares of blazars detected by the *Fermi* Large Area Telescope. We search for the presence of spectral breaks and measure the

spectral curvature on typical time scales of a few days. We identify significant spectral breaks in less than half of the analyzed flares, but their parameters do not show any discernible regularities, and in particular they are inconsistent with gamma-ray absorption at any fixed photon energy. More interestingly, we find that the studied blazars are characterized by significant spectral variability. Gamma-ray flares of short duration are often characterized by strong spectral curvature, with the spectral peak located above 100 MeV. Since these spectral variations are observed despite excellent photon statistics, they must reflect temporal fluctuations in the energy distributions of the emitting particles. We suggest that highly regular gamma-ray spectra of blazars integrated over long time scales emerge from a superposition of many short-lived irregular components with relatively narrow spectra.

6.2 Introduction

Blazars, a class of active galactic nuclei, belong to the brightest cosmic sources of high-energy ($\sim \mathrm{GeV}$) gamma-ray radiation. Their gamma-ray emission is produced by non-thermal populations of highly energetic particles in relativistic jets. The mechanism of particle acceleration responsible for the emergence of those populations is not yet understood, but detailed analysis of the gamma-ray data on blazars has the potential to provide more constraints on these processes.

The *Fermi* Large Area Telescope (LAT) has unique capabilities in high-energy astronomy: a very broad spectral range ($\sim 100\ \mathrm{MeV} - 100\ \mathrm{GeV}$), a very wide field of view ($\sim 60^{\circ}$), and the ability to scan the entire sky every 3 hours (Atwood et al., 2009). After several years of its mission, it has collected a vast amount of data on the temporal and spectral behaviour of blazars. Of particular importance are data on the brightest blazars, known as Flat-Spectrum Radio Quasars (FSRQs). Their broad-band spectral energy distributions (SEDs) are strongly dominated by the MeV-GeV gamma-ray band (Fossati et al., 1998), and they reach gamma-ray fluxes of $10^{-5}\ \mathrm{ph\,s^{-1}\,cm^{-2}}$ and higher (Abdo et al., 2011). At such high fluxes, they can be analyzed at very high temporal and/or spectral resolution.

The gamma-ray spectra of FSRQs are typically steep, with average photon indices of $\Gamma \simeq 2.2 - 2.7$ (Abdo et al., 2010b; Ackermann et al., 2011). However, these spectra are not consistent with simple power-laws; they can be better fit by either a log-parabola model, or a broken power-law model. In many blazars, spectral breaks are routinely identified, and they can be parametrized by the observed photon energy at the break $E_{\rm br,obs}$ and the change in the photon index $\Delta\Gamma$. In the initial *Fermi*/LAT data on 3C 454.3, the brightest blazar of the *Fermi* era, a break was identified in spectra integrated over a month of observations with $E_{\rm br,obs} \simeq 2.4$ GeV and $\Delta\Gamma \simeq 1.2$ (Abdo et al., 2009). In the subsequent studies of 3C 454.3, breaks were found with $E_{\rm br,obs} \simeq 1.0 - 2.8$ GeV and $\Delta\Gamma \simeq 0.6 - 1.0$ (Ackermann et al., 2010; Abdo et al., 2011). In other blazars, spectral breaks were identified with break energies $E_{\rm br} \simeq 1.6 - 10$ GeV in the source frame (Abdo et al., 2010b).

It was immediately recognized that such sharp spectral breaks cannot be due to a transition to the fast-cooling regime of electron energy distribution, which predicts a change in photon index of $\Delta\Gamma = 0.5$ (Abdo et al., 2009). Also, it was demonstrated that transition to the Klein-Nishina regime of inverse Compton scattering does not produce a sharp spectral break, but rather a smooth cut-off (Ackermann et al., 2010; Cerruti et al., 2013). The conclusion of Abdo et al. (2009) was that these breaks are most likely due to a break in the underlying electron energy distribution. However, Finke & Dermer (2010) noted that this scenario is incompatible with the observed optical/UV spectra of 3C 454.3. Instead, they proposed that the observed breaks could be explained by a superposition of two spectral components, produced by Comptonization of broad emission lines and direct radiation of the accretion disk.

An interesting alternative was proposed by Poutanen & Stern (2010), who argued that the gamma-ray spectral breaks in blazars could arise from absorption by recombination continua of ionized helium (He II). This model predicts that the observed breaks should be close to $E_{\rm br} \simeq 5$ GeV in the source frame. In a subsequent study of the gamma-ray spectra of 3C 454.3 at several different flux levels, Stern & Poutanen (2011) found a weak anti-correlation between the optical depth for He II continuum, inferred from $\Delta\Gamma$, and the total gamma-ray flux. The implication of strong absorption by ionized helium is that gamma-ray emitting regions should be located very close (~ 0.1 pc) to

the central black hole, possibly shifting to larger distances with increasing gamma-ray flux.

More recent studies have cast doubt on the universal value of break energies measured in the source frame (Harris et al., 2012) and have also suggested that some breaks identified in early studies using *Fermi*/LAT data could be artifacts of inaccurate instrument response functions (Harris et al., 2014). Stern & Poutanen (2014) relaxed their original claim after updated analysis and now argue that only two FSRQs of the nine that they studied display spectral breaks at a consistent energy $E_{\rm br} \simeq 5$ GeV.

Another interesting aspect of the gamma-ray spectra of blazars is the spectral curvature, which can be probed by fitting log-parabola models to the spectra. Such models return two parameters — the curvature index β, and the peak photon energy $E_{\rm peak}$ (see definitions in §6.3). Typical spectra of FSRQs have $E_{\rm peak} < 100$ MeV with $\beta \sim 0.05 - 0.3$ (Ackermann et al., 2011; Harris et al., 2014). Stern & Poutanen (2011) showed for 3C 454.3 that the curvature index is roughly independent of the gamma-ray flux, but that the peak energy is strongly correlated with the gamma-ray flux, ranging between $\sim 10 - 100$ MeV.

In Nalewajko (2013) (hereafter Paper I), a sample was selected of the brightest gamma-ray flares of blazars during the first four years of the *Fermi* mission. The study in Paper I focused on the temporal properties of the flares, such as duration and time asymmetry; however, time variations of the gamma-ray photon index were also investigated. It was demonstrated that many blazar flares exhibit significant variations of the photon index, and that some very short flares (of duration $\lesssim 1$ d) show relatively hard spectra, with $\Gamma \lesssim 2$. The most notable example of such flares is the MJD 55854 event in PKS 1510–089 (Saito et al., 2013), also included in our sample. Additional similar events have been identified recently, and they may represent an important new class of gamma-ray events observed in luminous blazars.

Here, we analyze the spectral properties of the sample of flares selected in Paper I. We focus on two particular aspects: 1) the occurrence and properties of spectral breaks, and 2) spectral curvature and spectral variations in the sample. We begin by describing our analysis of the spectral properties of the flares in Section 6.3. We then present our results on the spectral breaks and the

spectral curvature in Section 6.4. This is followed by a discussion in Section 6.5, and conclusions in Section 6.6.

6.3 Data analysis

We investigate the sample of 40 bright blazar flares selected in Paper I (details of the selection procedure are given therein). Each flare is a period of time when the observed photon flux exceed half of the peak flux. The minimum peak flux for the sample is $7.1 \times 10^{-6}\ \mathrm{ph\,s^{-1}\,cm^{-2}}$. These flares have durations $0.5 - 10$ days, and they are produced by only five blazars: 3C 454.3, PKS 1510–089, PKS 1222+216, 3C 273, and PKS 0402–362.

For each flare period, we integrate the binned SED using the standard analysis tool `gtlike` from the *Fermi*/LAT `ScienceTools` software package (`v9r27p1`). In the analysis, we use the instrument response function `P7SOURCE_V6`, the Galactic diffuse emission model `gal_2yearp7v6_v0`, the isotropic background model `iso_p7v6source`, events of the `SOURCE` class, the region of interest of radius 10°, and all background sources from the 2FGL catalog (Nolan et al., 2012) within 15°. The energy bins are of equal width and uniformly distributed on a logarithmic scale, and they overlap with the logarithmic shift equal to 1/3 of the logarithmic bin length. In cases of insufficient photon statistics, standard 2σ upper limits are calculated. The results are shown in Fig 6.1 in order of decreasing peak flux (as in Paper I).

Next, for each flare we performed maximum likelihood analysis on the unbinned data in the energy range between $E_{\rm min} = 0.1$ GeV and $E_{\rm max} = 10$ GeV by fitting spectral models of a simple power law (SPL), broken power law (BPL), and log parabola (LP). The maximum energy limit $E_{\rm max}$ is chosen due to relatively short integration time scales, on which only a handful of > 10 GeV photons are detected for each flare.

For the SPL fit, we used the PowerLaw2 spectral model from the Fermi analysis tools,[1]

$$\frac{\mathrm{d}N}{\mathrm{d}E} = \frac{N(1-\Gamma)E^{-\Gamma}}{E_{\rm max}^{1-\Gamma} - E_{\rm min}^{1-\Gamma}}, \tag{6.1}$$

[1] `http://fermi.gsfc.nasa.gov/ssc/data/analysis/scitools/source_models.html`

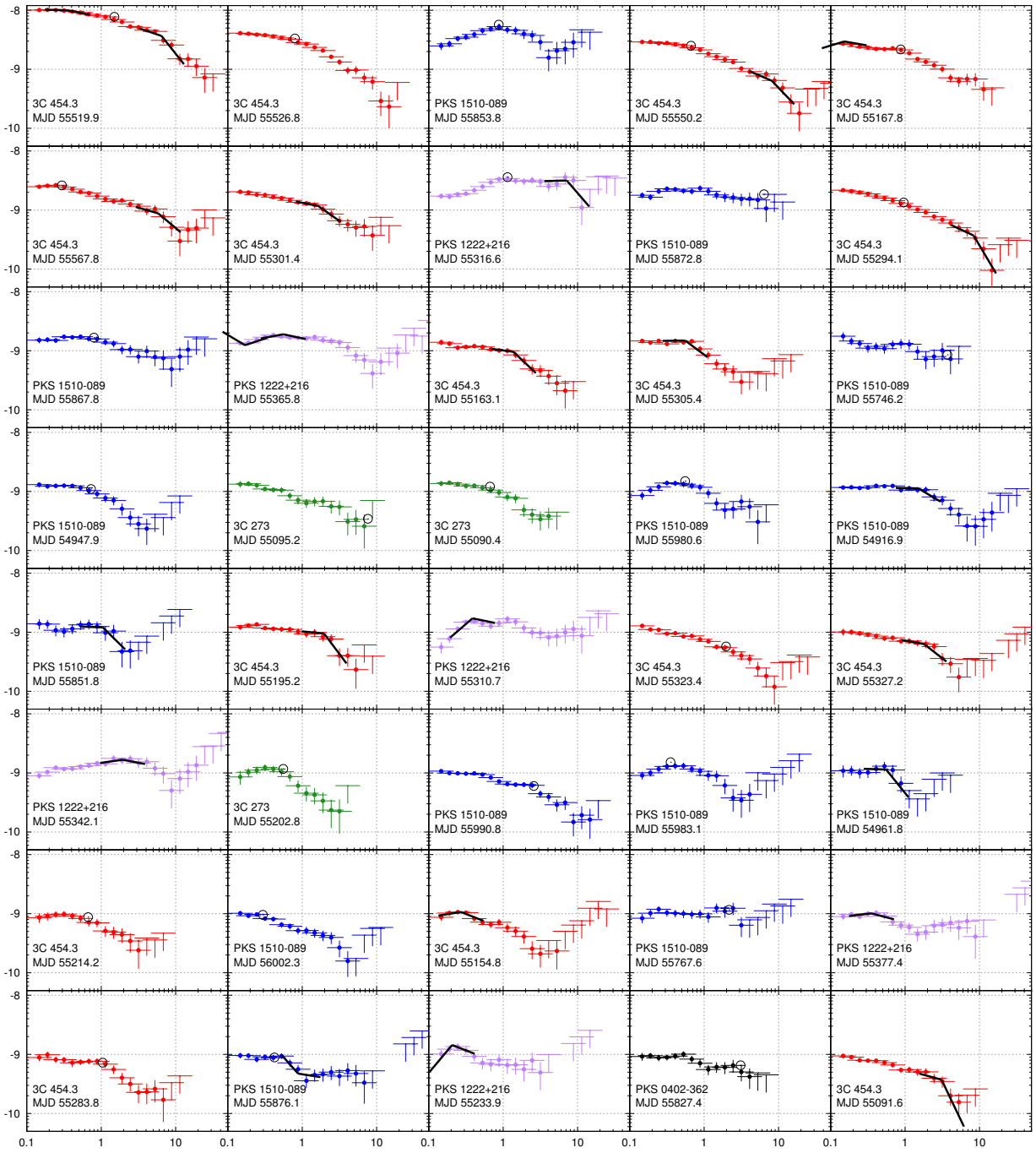

Figure 6.1: Time-integrated flare spectra displaying the flux ($\mathrm{erg\,s^{-1}\,cm^{-2}}$) vs observed energy (GeV) of the 40 brightest gamma-ray blazar flares detected by Fermi. Statistically significant primary spectral breaks (those identified with a BPL fit to the entire spectrum) and secondary spectral breaks (those identified with a BPL fit to only the energy range above or below the primary break energy) are indicated by broken lines that illustrate the value of the spectral index Γ on either side of the break. Primary breaks that are not statistically significant are indicated by open circles. The color of the spectrum indicates the host blazar.

where $\mathrm{d}N/\mathrm{d}E$ is the differential photon flux as a function of photon energy, Γ is the spectral index, and $E_{\min}$ and $E_{\max}$ are the fixed lower and upper bounds of the energy range. Using this model rather than the basic power law fit allowed us to avoid artificially selecting a normalization energy and instead fix the energy range over which we wished to apply the model. In similar fashion, we used the BrokenPowerLaw2 spectral model for the BPL fit,

$$\frac{\mathrm{d}N}{\mathrm{d}E} = N_0 \times \begin{cases} (E/E_{\mathrm{br}})^{-\Gamma_1} & \text{if } E < E_{\mathrm{br}} \\ (E/E_{\mathrm{br}})^{-\Gamma_2} & \text{otherwise,} \end{cases} \tag{6.2}$$

where N_0 is a normalization factor, E_{br} is the break energy, and Γ_1 and Γ_2 are the spectral indices in the range where $E < E_{\mathrm{br}}$ and $E > E_{\mathrm{br}}$ respectively. For the LP fit, we used the LogParabola model,

$$\frac{\mathrm{d}N}{\mathrm{d}E} = N_0 \left(\frac{E}{E_0}\right)^{-(\alpha+\beta \log(E/E_0))}, \tag{6.3}$$

where E_0 is a fixed pivot energy, N_0 is the normalization, β describes the spectral curvature, and α is a parameter related to the peak energy,

$$E_{\mathrm{peak}} = E_0 \exp\left(\frac{2-\alpha}{2\beta}\right). \tag{6.4}$$

We set the pivot energy to $E_0 = 500$ MeV, in keeping with other analyses (e.g. Harris et al. (2012)), after first testing that moving this pivot doesn't have a significant impact on the likelihood value for the fit.

In order to determine which of these three models was the best fit to the data, we performed an Akaike Information Criterion (AIC) test, determining the AIC value for each model:

$$\mathrm{AIC} = 2k - 2\ln\mathscr{L}, \tag{6.5}$$

where k is the number of free parameters in the model, and $\mathscr{L}$ is the maximized value of the likelihood function for the estimated model. The preferred model is then the one with the minimum AIC, and if the difference in the AIC between two fits is such that $\Delta\mathrm{AIC} > 2$, the preference for the model with the minimum AIC is generally considered to be statistically significant (refer to

Harris et al. (2014), Bozdogan (1987), and Lewis et al. (2011) for more information on the AIC and ΔAIC). In our case, if the BPL fit had a $\Delta\text{AIC} > 2$ relative to the other fits, we declared this spectral break significant and recorded the fit parameters in Table 6.1.

Uncertainties in most fit parameters were obtained directly from the fits, with the exception of the parameter $E_{\rm br}$. Uncertainties in $E_{\rm br}$ were instead estimated from the statistical uncertainty corresponding to $-2\Delta L = 1$ for the 1-σ confidence region, where L is the log-likelihood function (see Ackermann et al. (2010), Rolke et al. (2005) for discussion of this technique). In cases where $E_{\rm br}$ was unbound, we rejected the break.

In many cases, the best-fit BPL model with break energy $E_{\rm br1}$ did not yield a significant spectral break, while a candidate break could be seen at $E_{\rm br2} \neq E_{\rm br1}$. A good example of this is flare #10 (3C 454.3, MJD 55294) with $E_{\rm br1} \sim 0.9$ GeV and $E_{\rm br2} \sim 9$ GeV. A candidate break at $E_{\rm br2}$ may not be identified by the global BPL fit due to the overall spectral curvature. This was noted by Stern & Poutanen (2011), who found that spectral breaks can be identified more robustly when the underlying background spectral model is a log-parabola rather than a power-law. In order to account for spectral breaks that could have been missed by the global (**primary**) BPL fits, for every flare in the sample we performed an additional search for **secondary spectral breaks** by fitting the BPL, SPL and LP models separately in the energy ranges $E_{\rm min} < E < E_{\rm br1}$ (**low-energy secondary**) and $E_{\rm br1} < E < E_{\rm max}$ (**high-energy secondary**). In the example of flare #10, a secondary break was indeed identified at $E_{\rm br2} \sim 8.4$ GeV. All statistically significant secondary spectral breaks are included in Table 6.1.

Table 6.1: Statistically significant breaks discovered in the spectra of the 40 brightest Fermi gamma-ray flares. Breaks were recorded if the spectrum was better-fit by a BPL rather than SPL or LP model, with a ΔAIC > 2 for the BPL compared to the next-best fit. $\mathrm{MJD_{peak}}$ is the moment of flux peak, F_{peak} is the peak flux in units of $10^{-6}\ \mathrm{ph\,s^{-1}\,cm^{-2}}$, T is the duration of the flare in days, E_{br} (obs) and E_{br} (source) are the break energies, in GeV, in the observer and source frame respectively, and Γ_1 and Γ_2 are the spectral indices on either side of the break energy. The break classification identifies the break as resulting from a fit to the entire flare spectrum ("primary") or resulting from a fit to only the energies below or above the primary break ("secondary: low" and "secondary: high").

#	Blazar	$\mathrm{MJD_{peak}}$	Break classification	F_{peak}	T	E_{br} (obs)	E_{br} (source)	Γ_1	Γ_2
1	3C 454.3	55520.0	secondary: low	77.2 ± 2.4	3.9	$0.35^{+0.05}_{-0.06}$	$0.65^{+0.09}_{-0.11}$	2.03 ± 0.03	2.25 ± 0.04
1	3C 454.3	55520.0	secondary: high	77.2 ± 2.4	3.9	$6.46^{+0.62}_{-2.07}$	$12.00^{+1.15}_{-3.85}$	2.43 ± 0.10	3.59 ± 0.31
4	3C 454.3	55550.3	secondary: high	23.6 ± 1.3	8.3	$8.12^{+3.79}_{-2.47}$	$15.09^{+7.05}_{-4.59}$	2.54 ± 0.05	3.32 ± 0.43
5	3C 454.3	55167.8	secondary: low	21.8 ± 1.5	4.3	$0.15^{+0.01}_{-0.02}$	$0.28^{+0.02}_{-0.04}$	1.62 ± 0.27	2.22 ± 0.05
6	3C 454.3	55567.8	secondary: high	19.2 ± 1.6	5.4	$5.82^{+1.81}_{-2.22}$	$10.81^{+3.37}_{-4.13}$	2.36 ± 0.05	3.06 ± 0.38
7	3C 454.3	55301.5	primary	16.4 ± 1.8	3.5	$1.64^{+0.51}_{-0.32}$	$3.05^{+0.96}_{-0.60}$	2.25 ± 0.04	2.89 ± 0.20
8	PKS 1222+216	55316.6	secondary: high	15.6 ± 0.9	0.8	$7.16^{+1.58}_{-0.80}$	$10.26^{+2.26}_{-1.14}$	1.97 ± 0.17	3.46 ± 0.64
10	3C 454.3	55294.1	secondary: high	15.3 ± 0.8	9.5	$8.35^{+1.12}_{-2.68}$	$15.52^{+2.08}_{-4.98}$	2.59 ± 0.09	4.13 ± 0.81
12	PKS 1222+216	55365.8	primary	14.2 ± 1.0	2.3	$0.56^{+0.75}_{-0.05}$	$0.80^{+1.08}_{-0.07}$	1.76 ± 0.08	2.27 ± 0.06
12	PKS 1222+216	55365.8	secondary: low	14.2 ± 1.0	2.3	$0.17^{+0.01}_{-0.02}$	$0.24^{+0.01}_{-0.03}$	2.76 ± 0.36	1.58 ± 0.13
13	3C 454.3	55163.1	primary	11.8 ± 1.4	3.0	$1.37^{+0.27}_{-0.28}$	$2.55^{+0.51}_{-0.52}$	2.17 ± 0.06	3.19 ± 0.23
14	3C 454.3	55305.5	primary	11.1 ± 1.5	1.9	$0.56^{+0.22}_{-0.06}$	$1.03^{+0.41}_{-0.10}$	1.98 ± 0.09	2.94 ± 0.15
20	PKS 1510–089	54917.0	primary	9.9 ± 0.7	2.4	$1.50^{+0.30}_{-0.28}$	$2.04^{+0.41}_{-0.38}$	2.03 ± 0.05	2.75 ± 0.17
21	PKS 1510–089	55851.9	primary	9.9 ± 1.0	0.7	$1.05^{+0.25}_{-0.29}$	$1.42^{+0.33}_{-0.39}$	2.04 ± 0.15	3.24 ± 0.48
22	3C 454.3	55195.2	primary	9.7 ± 0.8	2.2	$1.97^{+0.49}_{-0.30}$	$3.66^{+0.92}_{-0.56}$	2.12 ± 0.06	3.68 ± 0.46

25	3C 454.3	55327.2	primary	8.8 ± 1.2	3.1	$1.80^{+0.35}_{-0.33}$	$3.34^{+0.66}_{-0.62}$	2.23 ± 0.06	2.98 ± 0.26
26	PKS 1222+216	55342.1	secondary: high	8.7 ± 0.8	1.6	$1.93^{+1.46}_{-0.71}$	$2.77^{+2.09}_{-1.02}$	1.82 ± 0.08	2.24 ± 0.14
30	PKS 1510–089	54961.8	primary	8.2 ± 0.7	0.6	$0.56^{+0.22}_{-0.11}$	$0.76^{+0.30}_{-0.15}$	2.04 ± 0.24	3.56 ± 0.49
33	3C 454.3	55154.8	primary	7.8 ± 0.9	2.4	$0.27^{+0.04}_{-0.04}$	$0.50^{+0.08}_{-0.07}$	1.79 ± 0.20	2.50 ± 0.09
35	PKS 1222+216	55377.5	primary	7.6 ± 0.7	1.5	$0.35^{+0.12}_{-0.23}$	$0.51^{+0.17}_{-0.33}$	1.86 ± 0.17	2.33 ± 0.10
37	PKS 1510–089	55876.1	secondary: high	7.4 ± 0.8	1.7	$0.61^{+0.53}_{-0.10}$	$0.83^{+0.72}_{-0.14}$	4.54 ± 0.90	2.31 ± 0.16
38	PKS 1222+216	55234.0	primary	7.4 ± 0.8	1.1	$0.21^{+0.03}_{-0.02}$	$0.29^{+0.05}_{-0.02}$	0.50 ± 0.59	2.49 ± 0.13
40	3C 454.3	55091.6	primary	7.1 ± 0.8	5.5	$3.09^{+0.76}_{-0.84}$	$5.75^{+1.41}_{-1.57}$	2.35 ± 0.05	4.63 ± 0.97

6.4 Results

6.4.1 Spectral breaks

In analyzing the spectra of the 40 flares, we found that none were best fit by a SPL model, 31 were best fit by a BPL model, and nine were best fit by a LP model. Of the 31 BPL-favored spectra, the BPL model was significantly favored over other models in 15 cases. The breaks from two of these cases were rejected because they were unbound, but the 13 remaining primary breaks are recorded in Table 6.1. Ten additional statistically significant breaks were found by the secondary analysis. They are also recorded in the table (labeled to identify them as secondary breaks found either on the low- or high-energy side of the primary break of the spectrum), for a total of 23 significant breaks detected in the 40 flares. Figure 6.1 displays the binned spectrum for each of the 40 flares and illustrates the location of any significant primary and secondary breaks, as well as the values of the spectral index Γ on either side of the breaks. The primary breaks that are not significant are also noted on the spectra for reference.

As part of the analysis of the spectral breaks of these flares, we sought to test the 'double absorber' model put forward by Poutanen & Stern (2010). This model predicts two increases in the opacity of the broad-line region to gamma-ray-energy photons: one at ~ 5 GeV (in the source frame) due to He II recombination, and one at ~ 20 GeV due to H I recombination. These opacity increases result in changes in the photon index that should be seen clearly as breaks in the flare spectra. Because our analysis does not extend beyond 10 GeV due to relatively short integration time scales, we do not attempt to comment on the presence of the proposed break due to H I, however, we analyze the breaks we found in the $0.1 - 10$ GeV range to search for a preference for breaks near 5 GeV. In Figure 6.2, we plot the distribution of the redshift-corrected break energies against the peak flux of the flare. As can be seen, there is no indication for a break preference at 5 GeV or any other fixed energy in the source frame. Instead, the break energies seem to be spread uniformly between $0.2 \text{ GeV} < E_{\rm br} < 20 \text{ GeV}$. We do not find any indication for a correlation between $E_{\rm br}$ and other parameters of the flares, such as peak flux, duration, or time asymmetry.

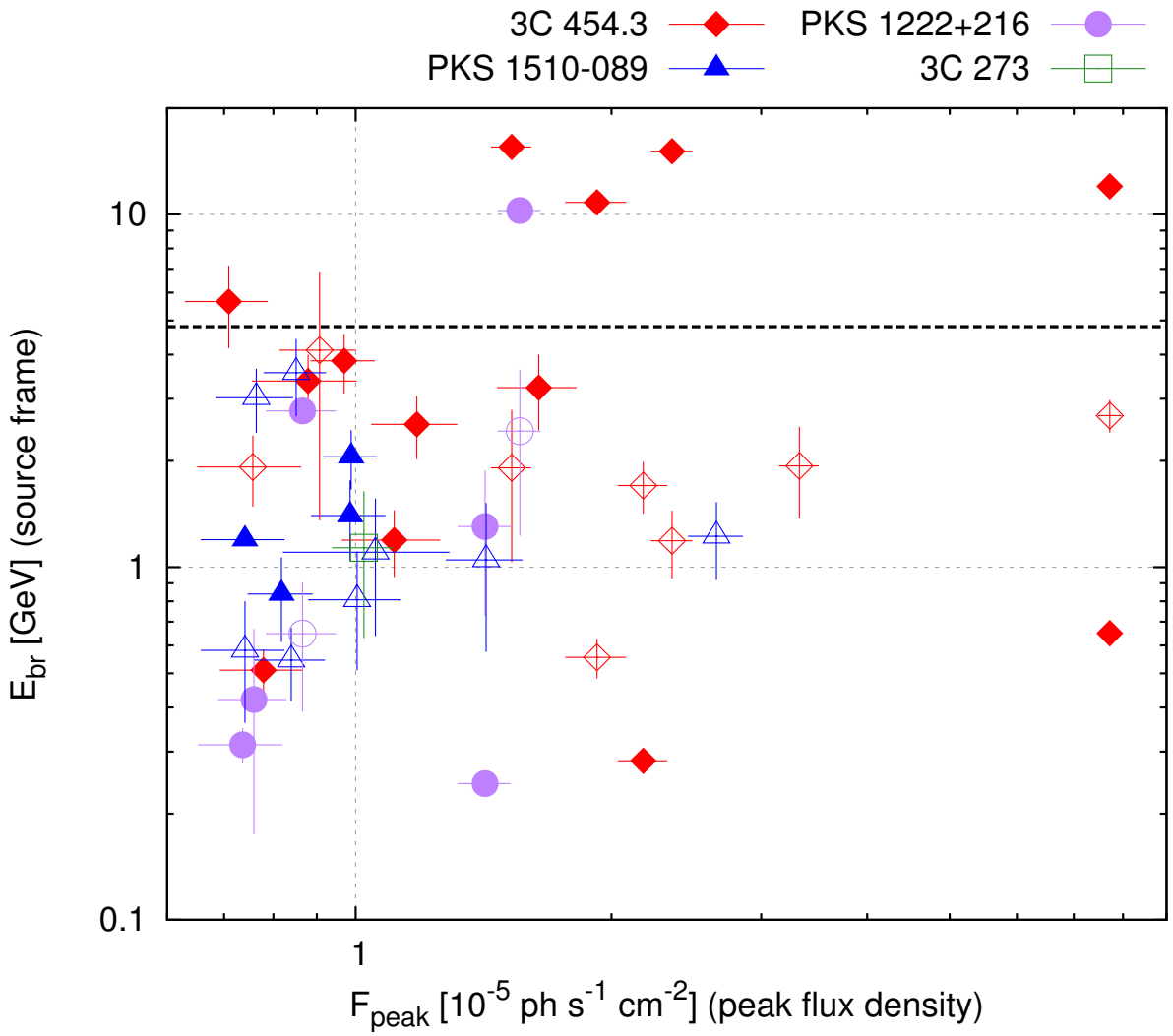

Figure 6.2: Distribution of the source-frame break energy $E_{\rm br}$ (GeV) vs. the peak flux F_{peak} (10^{-5} ph s^{-1} cm^{-2}) of the flare, plotted for all identified spectral breaks in the top 40 Fermi gamma-ray flares. The shape and color of each point indicate the host blazar. Solid symbols indicate statistically significant primary and secondary breaks, whereas unfilled symbols indicate primary breaks that were not statistically significant.

In Figure 6.3, we plot the distribution of the break amount, or change in the photon index $\Delta\Gamma$ at the break, vs. peak flux. For two spectral breaks, we found $\Delta\Gamma < 0$ (negative breaks), indicating spectral hardening with increasing energy. Both of these breaks are secondary, and they reflect local spectral features. For the positive breaks, we find that $0.5 \lesssim \Delta\Gamma \lesssim 2$. The value of $\Delta\Gamma = 0.5$ can be understood theoretically as resulting from a break in the electron energy distribution $N(\gamma) \propto \gamma^{-p}$ by $\Delta p = 1$, which could be due to the transition from inefficient to efficient cooling. While a substantial number of significant spectral breaks are close to this value in our data, roughly the same number of breaks are clearly inconsistent with it. The value of $\Delta\Gamma$ does not seem to be correlated with other parameters of the flare such as observed flux, duration or time asymmetry. Stern & Poutanen (2011) showed that in the case of 3C 454.3 the value of $\Delta\Gamma$, interpreted as a measure of optical depth for absorption from the He II continuum, is weakly anticorrelated with the gamma-ray luminosity (or flux). We do not find any evidence for this in our results.

6.4.2 Spectral curvature

In analyzing the flare spectra, our second goal was to examine the spectral curvature of the 40 flares. Table 6.2 contains flare details and fit parameters from the LP model applied to each of the 40 flares across the full energy range. The spectral curvature parameter β spans the range of $\sim 0.05 - 0.3$, which is consistent with the finding that none of the flares has a gamma-ray spectrum best described by SPL model. It also means that all the gamma-ray spectra are concave, which is natural for spectra dominated by a single spectral component. Interestingly, we find a very broad range of the spectral peak values, with $0.03 \text{ GeV} < E_{\rm peak} < 2 \text{ GeV}$. The very low values $E_{\rm peak} < 0.1 \text{ GeV}$ are often insignificant, as they are derived from an extrapolation of the LP model beyond the observed energy range. Nevertheless, these low estimates correspond to the typical shape of the gamma-ray spectra of FSRQ blazars, where the unobserved SED peak is generally thought to lie somewhere in the $\sim 1 - 10 \text{ MeV}$ range (Fossati et al., 1998; Abdo et al., 2010c). The cases where $E_{\rm peak} > 0.1 \text{ GeV}$ would in general be considered to be atypical.

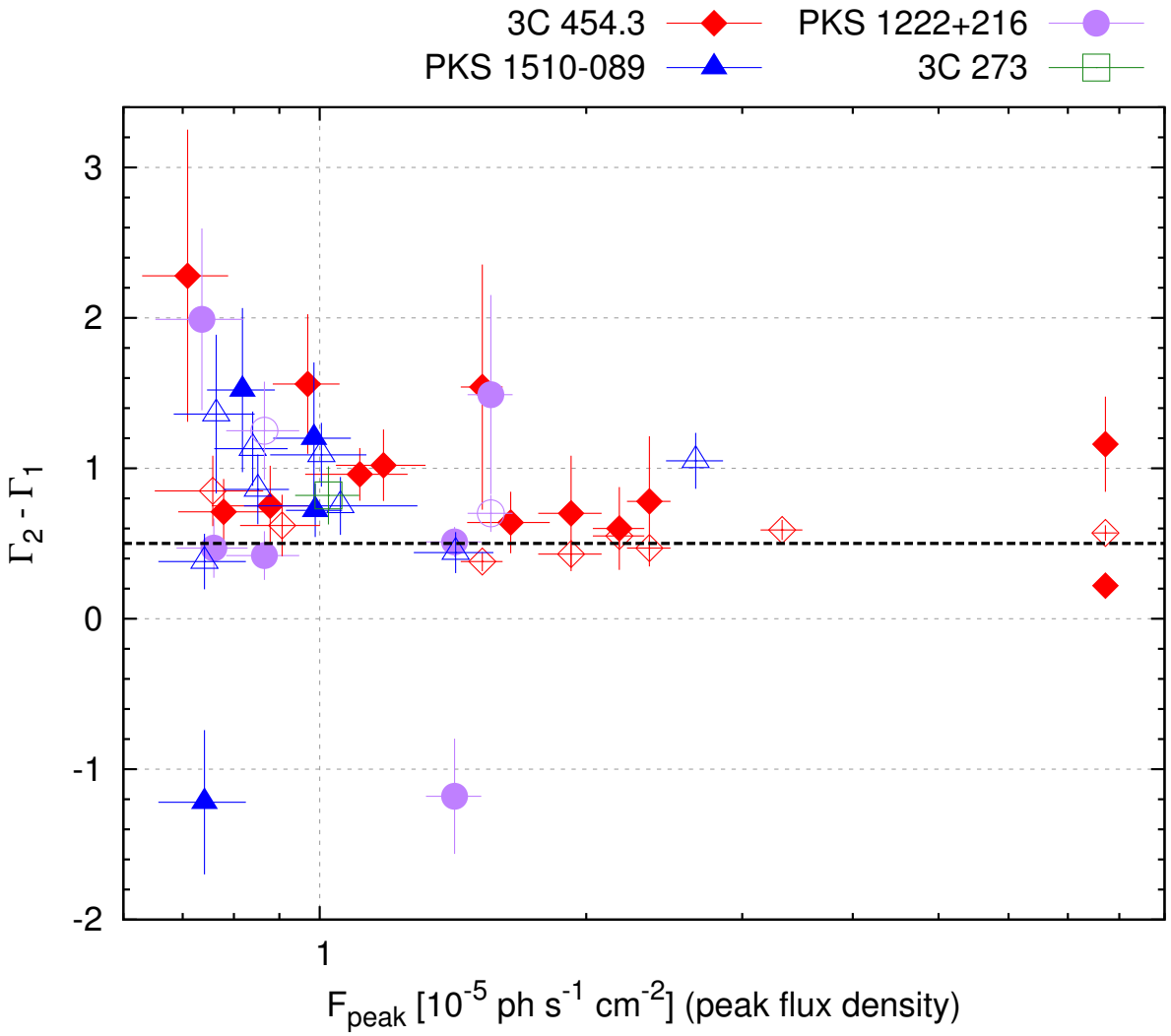

Figure 6.3: Distribution of the change in photon index $\Delta\Gamma = \Gamma_2 - \Gamma_1$ versus the peak flux F_{peak} (10^{-5} ph s^{-1} cm^{-2}) of the flare, plotted for all identified spectral breaks in the 40 brightest Fermi gamma-ray flares. The shape and color of each point indicate the host blazar. Solid symbols indicate statistically significant primary and secondary breaks, whereas unfilled symbols indicate primary breaks that were not statistically significant. The dotted line denotes $\Delta\Gamma = 0.5$, the value expected from a cooling break associated with radiative losses.

Table 6.2: Log-parabola fit parameters for the brightest gamma-ray flares of blazars. $\mathrm{MJD_{peak}}$ is the moment of flux peak, F_{peak} is the peak flux in units of $10^{-6}\ \mathrm{ph\,s^{-1}\,cm^{-2}}$, t_1 is the flux doubling time scale, t_2 is the flux halving time scale, $T = (t_1 + t_2)$ is the flare duration, α is the spectral index at the pivot energy, and β is the spectral curvature. All times are in units of days.

#	Blazar	$\mathrm{MJD_{peak}}$	F_{peak}	t_1	t_2	T	α	β	E_{peak}
1	3C 454.3	55520.0	77.2 ± 2.4	2.9	1.0	3.9	2.20 ± 0.01	0.09 ± 0.01	0.17 ± 0.02
2	3C 454.3	55526.9	33.3 ± 1.8	1.1	3.9	5.0	2.31 ± 0.02	0.13 ± 0.02	0.15 ± 0.03
3	PKS 1510–089	55853.8	26.6 ± 2.0	0.2	0.4	0.6	1.76 ± 0.08	0.23 ± 0.05	0.85 ± 0.18
4	3C 454.3	55550.3	23.6 ± 1.3	3.2	5.1	8.3	2.27 ± 0.02	0.11 ± 0.01	0.14 ± 0.02
5	3C 454.3	55167.8	21.8 ± 1.5	1.2	3.1	4.3	2.29 ± 0.03	0.11 ± 0.02	0.14 ± 0.04
6	3C 454.3	55567.8	19.2 ± 1.6	2.9	2.5	5.4	2.25 ± 0.02	0.08 ± 0.02	0.09 ± 0.04
7	3C 454.3	55301.5	16.4 ± 1.8	1.3	2.2	3.5	2.32 ± 0.04	0.07 ± 0.03	<0.10
8	PKS 1222+216	55316.6	15.6 ± 0.9	0.4	0.4	0.8	1.69 ± 0.05	0.13 ± 0.03	1.67 ± 0.56
9	PKS 1510–089	55872.8	15.3 ± 1.2	0.2	0.7	0.9	2.00 ± 0.06	0.14 ± 0.04	0.51 ± 0.11
10	3C 454.3	55294.1	15.3 ± 0.8	5.9	3.6	9.5	2.36 ± 0.02	0.08 ± 0.01	0.05 ± 0.02
11	PKS 1510–089	55867.8	14.2 ± 1.5	0.5	1.5	2.0	2.11 ± 0.06	0.09 ± 0.04	0.27 ± 0.12
12	PKS 1222+216	55365.8	14.2 ± 1.0	1.0	1.3	2.3	1.97 ± 0.04	0.09 ± 0.03	0.60 ± 0.14
13	3C 454.3	55163.1	11.8 ± 1.4	2.0	1.0	3.0	2.30 ± 0.05	0.13 ± 0.04	0.16 ± 0.07
14	3C 454.3	55305.5	11.1 ± 1.5	0.8	1.1	1.9	2.36 ± 0.06	0.22 ± 0.05	0.22 ± 0.05
15	PKS 1510–089	55746.2	11.1 ± 1.4	0.4	0.5	0.9	2.26 ± 0.09	0.08 ± 0.07	<0.25
16	PKS 1510–089	54948.0	10.6 ± 2.3	0.9	1.3	2.2	2.35 ± 0.06	0.15 ± 0.05	0.16 ± 0.07
17	3C 273	55095.3	10.3 ± 0.9	0.4	1.6	2.0	2.39 ± 0.06	0.07 ± 0.05	<0.09
18	3C 273	55090.5	10.2 ± 0.9	0.4	1.2	1.6	2.36 ± 0.07	0.21 ± 0.06	0.21 ± 0.06
19	PKS 1510–089	55980.6	10.0 ± 1.3	0.5	0.8	1.3	2.11 ± 0.08	0.28 ± 0.07	0.41 ± 0.06
20	PKS 1510–089	54917.0	9.9 ± 0.7	1.9	0.5	2.4	2.12 ± 0.04	0.10 ± 0.03	0.28 ± 0.08
21	PKS 1510–089	55851.9	9.9 ± 1.0	0.2	0.5	0.7	2.26 ± 0.12	0.16 ± 0.10	0.22 ± 0.14
22	3C 454.3	55195.2	9.7 ± 0.8	0.6	1.6	2.2	2.23 ± 0.06	0.16 ± 0.04	0.24 ± 0.06
23	PKS 1222+216	55310.7	9.6 ± 0.8	0.5	0.7	1.2	1.73 ± 0.08	0.21 ± 0.05	0.96 ± 0.24
24	3C 454.3	55323.5	9.1 ± 0.9	4.2	1.8	6.0	2.36 ± 0.04	0.08 ± 0.03	0.05 ± 0.04
25	3C 454.3	55327.2	8.8 ± 1.2	1.9	1.2	3.1	2.29 ± 0.05	0.08 ± 0.04	0.08 ± 0.08
26	PKS 1222+216	55342.1	8.7 ± 0.8	0.8	0.8	1.6	1.78 ± 0.05	0.08 ± 0.03	1.93 ± 1.16

27	3C 273	55202.9	8.7 ± 1.1	0.3	0.6	0.9	2.54 ± 0.12	0.33 ± 0.11	0.22 ± 0.07
28	PKS 1510–089	55990.8	8.5 ± 0.7	5.2	1.1	6.3	2.26 ± 0.03	0.08 ± 0.02	0.10 ± 0.05
29	PKS 1510–089	55983.1	8.4 ± 0.8	0.5	0.4	0.9	2.10 ± 0.09	0.24 ± 0.07	0.41 ± 0.08
30	PKS 1510–089	54961.8	8.2 ± 0.7	0.3	0.3	0.6	2.62 ± 0.18	0.32 ± 0.17	0.19 ± 0.11
31	3C 454.3	55214.3	8.0 ± 0.9	0.8	0.8	1.6	2.37 ± 0.09	0.23 ± 0.08	0.22 ± 0.08
32	PKS 1510–089	56002.4	7.8 ± 1.0	1.8	0.9	2.7	2.40 ± 0.06	0.10 ± 0.04	0.07 ± 0.06
33	3C 454.3	55154.8	7.8 ± 0.9	0.5	1.9	2.4	2.30 ± 0.06	0.09 ± 0.05	0.10 ± 0.10
34	PKS 1510–089	55767.6	7.6 ± 0.8	0.4	0.5	0.9	1.98 ± 0.09	0.17 ± 0.07	0.54 ± 0.14
35	PKS 1222+216	55377.5	7.6 ± 0.7	0.4	1.1	1.5	2.15 ± 0.07	0.05 ± 0.04	<0.26
36	3C 454.3	55283.9	7.6 ± 1.1	1.3	1.4	2.7	2.30 ± 0.07	0.15 ± 0.05	0.19 ± 0.08
37	PKS 1510–089	55876.1	7.4 ± 0.8	0.7	1.0	1.7	2.28 ± 0.07	0.05 ± 0.05	<0.12
38	PKS 1222+216	55234.0	7.4 ± 0.8	0.7	0.4	1.1	2.20 ± 0.11	0.18 ± 0.09	0.29 ± 0.12
39	PKS 0402–362	55827.5	7.3 ± 1.0	0.3	1.8	2.1	2.18 ± 0.08	0.19 ± 0.07	0.32 ± 0.09
40	3C 454.3	55091.6	7.1 ± 0.8	4.4	1.1	5.5	2.41 ± 0.04	0.07 ± 0.03	<0.07

In Figures 6.4 and 6.5, we show the distributions of β and $E_{\rm peak}$, respectively, vs. the flare duration T. We find that flare duration has a strong influence on the shape of the gamma-ray spectrum. Flares longer than $\simeq 2.5$ d have gently curved spectra with $\beta \sim 0.1$ and $E_{\rm peak} \lesssim 0.1$ GeV, whereas shorter flares can have a stronger curvature with $E_{\rm peak} > 0.1$ GeV. As was noted in Paper I, most of the long flares were produced by 3C 454.3, and they also tend have more consistent average photon indices $\langle \Gamma \rangle \simeq 2.3$, and more symmetric distribution of the time asymmetry parameter. On the other hand, the short flares are more typical for blazars PKS 1510-089 and PKS 1222+216. The latter source stands out by producing flares with the highest $E_{\rm peak}$ values.

6.5 Discussion

In this work we focus on the gamma-ray spectra of blazars integrated during the highest observed gamma-ray fluxes on relatively short time scales of $T < 10$ d. This is a consequence of the flare definition adopted in Paper I, and this approach distinguishes this work from most studies of gamma-ray spectra of blazars that focus on maximizing the photon statistics by integrating the spectra on much longer time scales (months – years). The results of studies performed on longer time scales may not be applicable on shorter time scales. A glance at Figure 6.1 reveals many irregularities that are absent in the neat long-term results presented, e.g., by Abdo et al. (2010b). In the face of such irregularities, we should not expect that these spectra can be well fit by simple spectral models like SPL, BPL or LP. Instead, we should expect at most to produce better or worse approximations of the real spectra with these models.

Of course, one should carefully consider whether these irregularities may be due to any statistical or systematical errors in the analysis of the *Fermi*/LAT data. From the standard maximum likelihood analysis, we know how many reconstructed photons contribute to each flux measurement, so the photon statistics do not concern us. The systematic errors are less understood, and the Fermi Collaboration provides only crude estimates based on the in-orbit calibration studies (Ackermann et al., 2012), but these values ($\sim 10\%$) are much lower than the observed amplitudes of

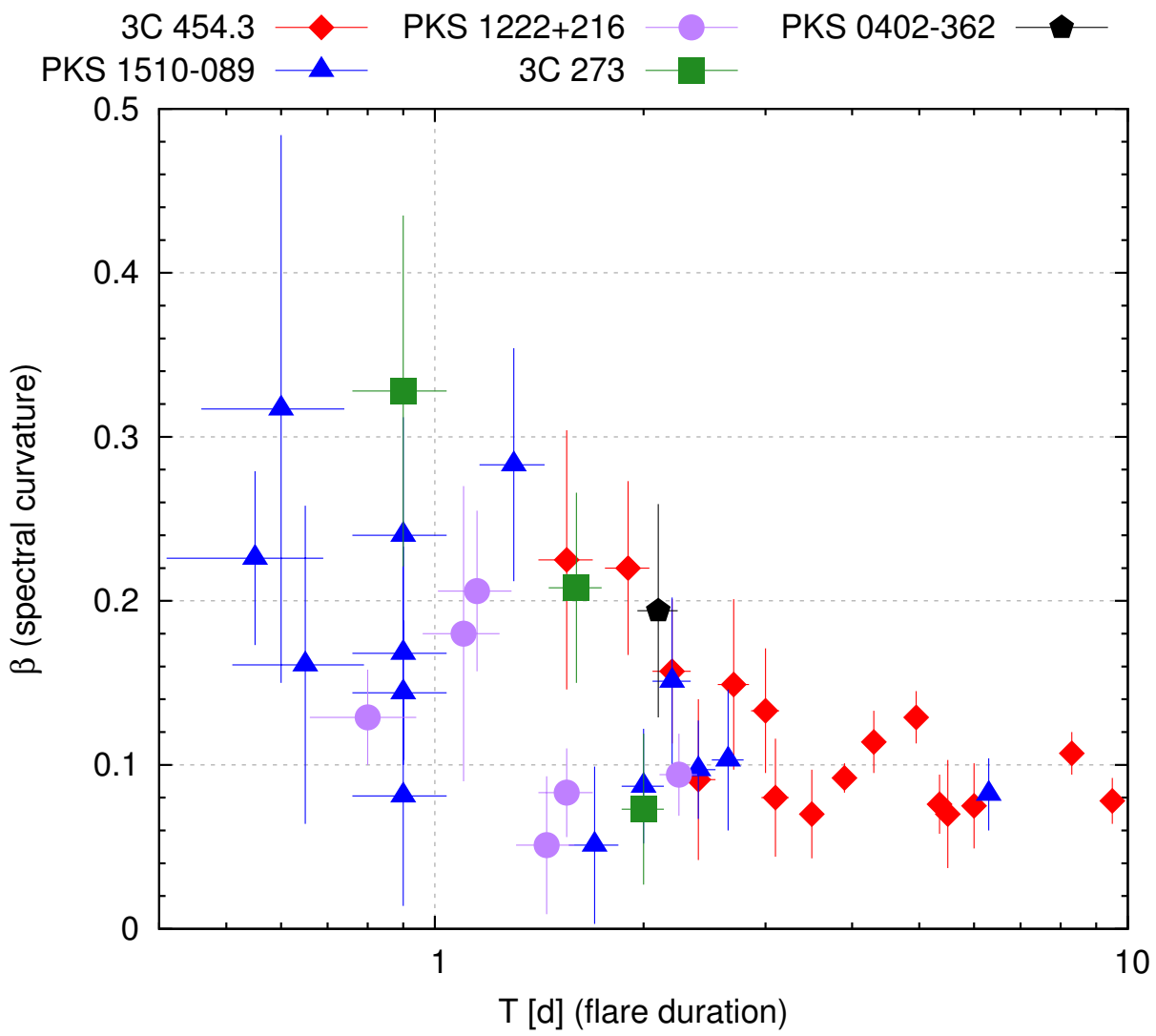

Figure 6.4: Distribution of the spectral curvature β (resulting from a log parabola fit to the spectrum) versus the duration T (days) of the flare, plotted for the 40 brightest Fermi gamma-ray flares. The shape and color of each point indicate the host blazar.

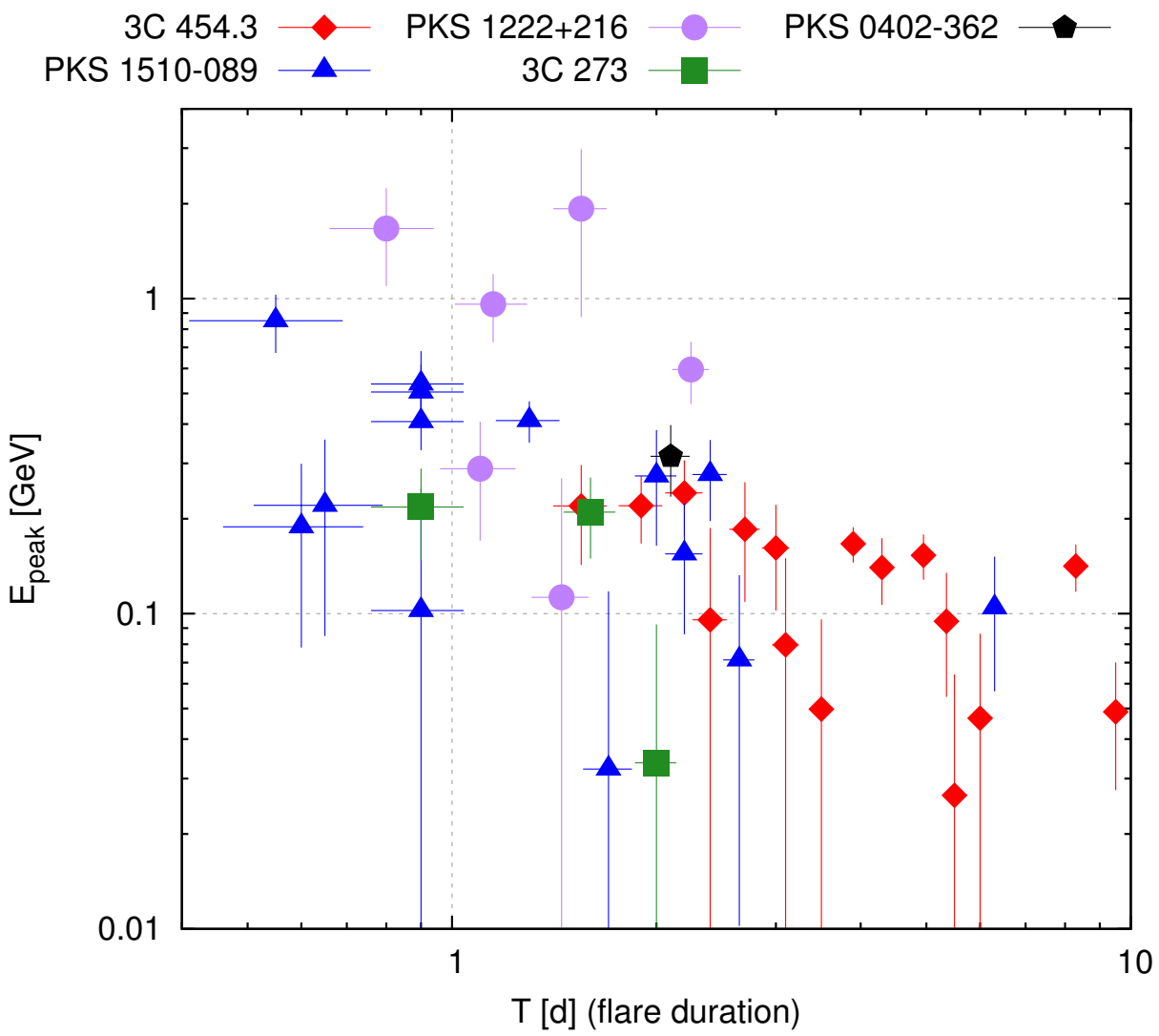

Figure 6.5: Distribution of the spectral peak position $E_{\rm peak}$ (resulting from a log parabola fit to the spectrum) versus the duration T (days) of the flare, plotted for the 40 brightest Fermi gamma-ray flares. The shape and color of each point indicate the host blazar.

the spectral fluctuations. That the power density spectra of bright blazars are power laws without any breaks (Abdo et al., 2010a), including 3C 454.3 in the high state (Ackermann et al., 2010), suggests that flux measurements are equally accurate at all relevant time scales. We will therefore assume that the observed spectral fluctuations are a real property of blazars, and not instrumental artifacts.

Our systematic and unbiased search for the occurrence of spectral breaks returned results that can be characterized as random. The broad distributions of break energies $E_{\rm br}$ and break amounts $\Delta\Gamma$, and the lack of clear correlations with other flare parameters, suggests that there is no unique physical mechanism behind them. In the double absorber model (Poutanen & Stern, 2010), spectral breaks should be observed at consistent break energy $E_{\rm br} \simeq 5$ GeV in the source frame at all times, unless the gamma-ray radiation is produced far outside the broad-line region. Our results do not indicate any preference for this $E_{\rm br}$ value, which is consistent with the results of Harris et al. (2012). The irregularity of the break parameters suggests that they reflect the random spectral fluctuations observed in the binned spectra. At much longer integration time scales, more regular spectral breaks could arise due to non-uniform statistics of such fluctuations.

The main finding of this work is that the spectra of long flares ($T > 2$ d) are more regular than the spectra of short flares ($T < 2$ d), which is illustrated by the distribution of the parameters β and $E_{\rm peak}$ of the log-parabola fits to the individual spectra (Figs. 6.4 and 6.5). The short flares often have their spectral peak within the *Fermi*/LAT band ($E_{\rm peak} > 0.1$ GeV), which is not the case for the long-term average spectra of FSRQ blazars (Abdo et al., 2010b). This may have profound implications for the theoretical picture of dissipation and particle acceleration in relativistic AGN jets. The regular (gently broken power-law) gamma-ray spectra of blazars observed on long time scales may generally be superpositions of many simple components. Each of those components may have a narrowly peaked particle energy distribution and produce a short subflare contributing to the overall observed light curve. If the emission of such a component is coherent in photon energy and time, it may also be coherent in space, emitted from compact independent regions within the jet.

In Paper I, a dichotomy was revealed between the temporal properties of the brightest gamma-ray flares of blazars. On one hand, most flares produced by 3C 454.3 are long, with complex light curves (multiple subflares of comparable peak flux), without clear time asymmetry. On the other hand, most flares produced by PKS 1510-089 and PKS 1222+216 are short, with simple light curves, and a tendency for the flux decay time scale to be longer than the flux raising time scale. This dichotomy was suggested to be an observational effect, with the viewing angle of the jet much smaller in the case of 3C 454.3, resulting in the more uniform Doppler beaming of all emitting regions. Now we add to this picture the systematic differences between the observed gamma-ray spectra. The spectra of long flares are more regular than the spectra of short flares, as the former consist of more elementary narrow components. The interpretation of the source dichotomy in terms of the viewing angle is consistent with this, as more uniform Doppler beaming is required to observe more spectral components at comparable flux levels.

6.6 Conclusions

We performed a spectral analysis with the *Fermi*/LAT of the sample (selected in Paper I) of the 40 brightest gamma-ray flares of blazars (FSRQs) detected in the first four years of the *Fermi* mission. The gamma-ray spectra are integrated over relatively short time scales $T < 10$ d, and they show significant and variable departures from the long-term average spectra of the same sources. We performed a uniform search for the occurrence of spectral breaks. The break energies show a broad distribution and no preference for the fixed value of 5 GeV in the source frame predicted by the double-absorber model of Poutanen & Stern (2010). In order to compare the basic structures of the observed spectra, we fitted them with a log parabola model and found an interesting trend of the model parameters with the flare duration. Short flares ($T < 2$ d) often show a strong spectral curvature with the SED peak within the *Fermi*/LAT range $E_{\rm peak} > 0.1$ GeV, while all long flares show a mild spectral curvature with a SED peak below the LAT range. The dichotomy between typical properties of flares observed in sources 3C 454.3 vs. PKS 1510-089 and others, first

described in Paper I, is extended to include differences between the observed gamma-ray spectra.

We suggest that the irregular gamma-ray spectra observed by the *Fermi*/LAT for short blazar flares reflect compact individual emitting regions within the relativistic jets that have a narrow energy distribution of emitting particles. The superposition of many such spectral components peaking at different energies would then result in the regular power-law spectra observed over long time scales.

Acknowledgements

This work is based on the publicly available data from the *Fermi* Large Area Telescope operated by NASA and Department of Energy in collaboration with institutions from France, Italy, Japan, and Sweden. S.K. was supported by NSF grant AST-0907872, NASA Astrophysics Theory Program grant NNX09AG02G, and NASA's Fermi Gamma-ray Space Telescope Guest Investigator program. K.N. was supported by NASA through Einstein Postdoctoral Fellowship grant number PF3-140130 awarded by the Chandra X-ray Center, which is operated by the Smithsonian Astrophysical Observatory for NASA under contract NAS8-03060.

PART II

Science Communication

Chapter 7

Preface to Part II

7.1 Background

With federal support for science dwindling in the United States, it is now more critical than ever to provide training for current and future scientists to advocate for science — but such training requires first establishing more effective ways to communicate how science is done, describe the impact of current scientific research, and convey its importance. Science communication research, a field that crosses disciplinary boundaries at the interface between science and society, and the topic of the second half of this thesis, works to address these concerns. The following section provides some important background in science communication theory.

7.1.1 A Definition of Science Communication

Science communication is a surprisingly complicated concept to define, as any communication that involves different audiences, and in particular the general public, is complex and highly contextual (Burns et al., 2003). Schirato & Yell (1997) proposes the following definition of communication: "...the practice of producing and negotiating meanings, a practice which always takes place under specific social, cultural and political conditions." This definition captures the complexities of interacting with differing audiences under varying circumstances, and the phrase "negotiating meanings" in particular touches on the important distinction between communication as a one-way flow of information versus communication as a two-way dialog.

Burns et al. (2003) proposes a contemporary definition of science communication as "the use of appropriate skills, media, activities, and dialogue to produce one or more of the following personal responses to science:

- **Awareness**, including familiarity with new aspects of science
- **Enjoyment** or other affective responses, e.g. appreciating science as entertainment or art
- **Interest**, as evidenced by voluntary involvement with science or its communication
- **Opinions**, the forming, reforming, or confirming of science-related attitudes
- **Understanding** of science, its content, processes, and social factors

Science communication may involve science practitioners, mediators, and other members of the general public, either peer-to-peer or between groups.

7.1.2 Importance of Science Communication

There are quite a few arguments for the necessity of effective communication of science. A common consideration in science communication literature is the existence of moral and ethical responsibility to increase the science literacy of the public. Increased science knowledge is not only generally useful, but also permits the public to make intelligent decisions both in science policy (Treise & Weigold, 2002) and in their personal lives (Nelkin, 1995). Furthermore, there is an issue of accountability: scientific research is largely funded by public money, so scientists have an obligation to communicate the outcomes of their research to society.

Effective communication between scientists and across research groups is imperative for scientific collaboration and sharing of ideas, but scientists also benefit from communicating their research with the general public. Continued funding is often dependent upon the public — and policy makers — being convinced of the worth of scientists' research; this message is particularly clear today as we see the impact of the recent US government budget cuts to science funding. Furthermore, communicating with the public can provide personal benefits for scientists as well:

evidence suggests that scientists who are quoted in the media are more likely to be cited in the formal scientific literature (Phillips & others., 1991; Kiernan, 2003).

Finally, examples abound of the dangerous consequences that can arise when scientists fail to communicate effectively, from the public perception of vaccines (Offit & Coffin, 2003) and climate change (Nisbet, 2009), to the criminal trial and sentencing of scientists in the wake of the deadly 2009 L'Aquila earthquake in Italy (Povoledo & Fountain, 2012). It is clear from these examples that the process of relaying information from scientists to the general public must be undertaken with great care.

7.1.3 Who Should Communicate Science?

Science communication has been historically governed by a linear model (see Figure 7.1): a sequential transport of information from the scientists (producers of the information), to professional communicators such as public information officers, to journalists, to the general public (receivers of the information). This model is funnel-like; a simplification of information occurs at each step of the process (Christensen, 2007).

The news media were at one time seen as having the potential to create a country of science-literate citizens (Treise & Weigold, 2002). In the past several decades, however, this is less popular of a view. Evidence suggests that much of the public appears to be scientifically illiterate (Hartz & Chappell, 1997; Paisley, 1998), implying that the process of communication fails at some level. Most science journalists don't have a scientific education background (Weigold, 2001). Scientists often assign the blame for communication failure to journalists; surveys indicate that scientists don't consider the media to portray science accurately or effectively (Basken, 2009; Besley & Nisbet, 2013).

Perhaps as a result, there has been an unprecedented level of encouragement in the last few decades for scientists to learn to communicate with the public directly (Davies, 2008; Besley et al., 2012; Dudo, 2012). In 1985, a report was issued by the Royal Society (The Royal Society, 1985; now known as the Bodmer Report, after the chair of the working group) evaluating public

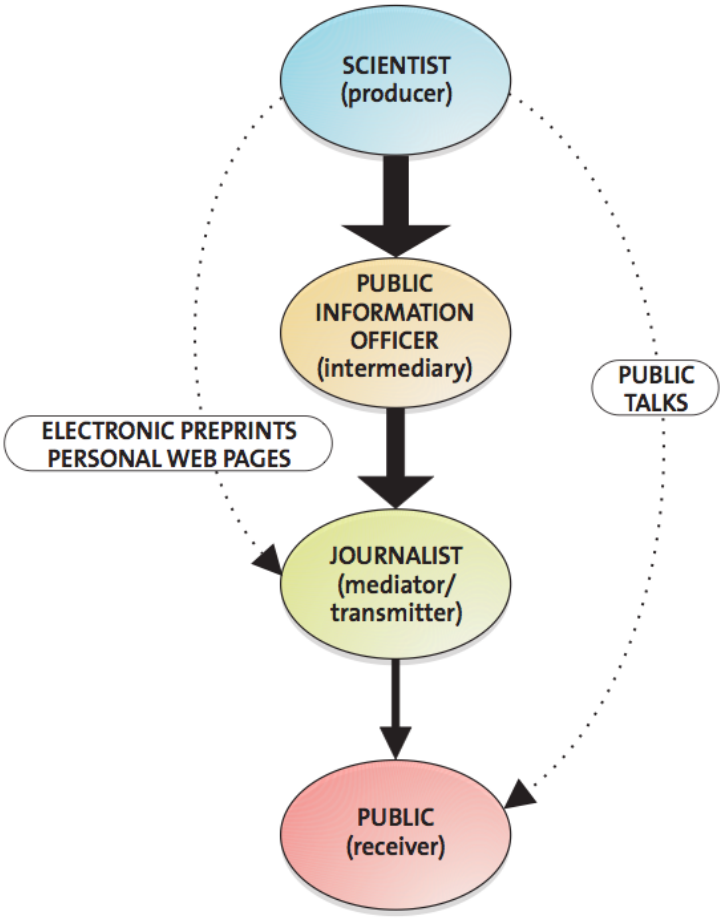

Figure 7.1: Diagram of the linear model of science communication, from Christensen (2007). Information is sequentially transported from the scientist (producer) to the public (receiver).

understanding of science and the role that scientists should have in improving it. The report argued that "scientists must learn to communicate with the public, be willing to do so, and indeed consider it their duty to do so" (The Royal Society, 1985, p.6). This report played a large role in beginning to lift the stigma associated with public outreach activities, and initiated a wave of funding and interest amongst scientists for science communication that has maintained momentum to present day.

Positive attitudes toward science communication among scientists are significantly more evident in the wake of the Bodmer Report and subsequent studies. In a study of nearly 1700 scientists

performed in 2000, 84% declared that they felt they had a duty to communicate their research findings to the public, and a surprising 69% felt that they themselves should have the main responsibility for that communication (The Wellcome Trust, 2000).

7.1.4 Impediments to Scientists as Communicators

There exist, however, impediments to the goal of mobilizing scientists as science communicators. Some major factors, as self-reported by participants in the Royal Society's 2006 survey of 1400+ professional science researchers, include lack of time, lack of peer support, and issues of discomfort, exposure and vulnerability (The Royal Society, 2006; Bowater & Yeoman, 2013). Even amongst the scientists for whom these factors are not a deterrent, there exists a still more troublesome impediment: lack of training. In Hartz & Chappell (1997), Neal Lane, former director of the National Science Foundation, is quoted as saying

> With the exception of a few people ... we don't know how to communicate with the public. We don't understand our audience well enough — we have not taken the time to put ourselves in the shoes of a neighbor, the brother-in-law, the person who handles our investments — to understand why it's difficult for them to hear us speak. We don't know the language and we haven't practiced it enough. (cited in Hartz and Chappell 1997, p. 38)

Figure 7.2, reproduced from the book "The Hands-On Guide for Science Communicators" (Christensen, 2007), illustrates the different environments in which the three major actors in science communication (namely, scientists, public information officers, and journalists) work. These differences also serve to illustrate the reshaping of science communication understanding that a scientist must undergo in order to effectively communicate with the public: a scientist must learn to exhibit many of the values of a journalist when communicating with non-specialist audiences.

Baram-Tsabari & Lewenstein (2013), p.80, phrased this issue another way:

> ...[S]cientists may need to "unlearn" the communication skills they have acquired as scientists. If learning the discourse of science is essential to becoming a scientist, learning the discourse of public communication of science is essential for scientists engaging with the public. This process can only take place in sociocultural environments that value such practices.

Scientist	PIO	Journalist
Values advanced knowledge	Uses the advanced knowledge in a broad context	Values diffuse knowledge
Values technical language	Reshapes technical language into simple language	Values simple language
Values near certain information	Uses facts, but also more speculative indications to give perspective	Values indications
Values quantitative information	Balances facts with emotional and personal accounts	Values qualitative information
Values near complete information	"Cuts through" when the results are trustworthy, but perhaps still not complete	Values incomplete information
Values narrow information	Uses the frontline narrow science to open doors to the broader context	Values comprehensive broad spectrum information
Specialist	Specialist in communicating science to the general public	Generalist
Theorist	Understands theory and applies it in the real world context	Pragmatist
Values knowledge for knowledge's sake	Focuses on the knowledge that is relevant to society	Focuses on what is relevant to society
Is cumulative	Is very picky with which information to accumulate	Is non-cumulative
Is slow	Can develop stories over long time, but always delivers on time	Is fast
Enjoys high professional status	Respects all other actors	Is in the lower ranks of professional status

Figure 7.2: The different environments in which the three major actors in science communication (scientists, public information officers, and journalists) work. Figure reproduced from Christensen (2007).

> Unfortunately, the two discourses are sometimes in tension: One rewards jargon, the other penalizes it; one rewards precision, the other accepts approximation; one rewards quantification, the other rewards storytelling and anecdotes.

How, then, do scientists receive the appropriate training necessary for this reframing of their view of science communication?

7.1.5 Availability of Communication Training for Scientists

Despite this evident need for professional communication training among scientists, there are currently few programs designed to provide scientists with effective science communication skills. A study commissioned by the Royal Society in 2006, for instance, shows that out of a sample of nearly 1500 professional scientists, 73% had never received any formal training in communicating science to the non-specialist public. Of those who reported having received training, most were only trained in the specific case of interacting directly with the press (The Royal Society, 2006).

An NSF-funded project to compile data on existing science communication programs is being conducted by COMPASS, an organization focused on improving connections between scientists and the wider world through communication and policy work.[1] At least one website has also attempted to gather such information,[2] and a formal report from both of these two groups is in production at this time. But the majority of the programs that currently exist target scientists already established professionally (e.g. Basken, 2009; Besley & Tanner, 2011), and furthermore, none of the prominent science communication training programs have performed any systematic evaluation of their courses' learning outcomes (as reported in Baram-Tsabari & Lewenstein, 2013).

In the remaining chapters of this thesis, I attempt to address this problem by presenting thorough evaluations of two different science communication training programs that both target very early-career scientists.

[1] http://compassblogs.org/blog/2013/04/01/gradscicomm-how-compass-is-answering-the-national-demand-for-science-communication-training/

[2] http://www.com.uri.edu/scicom/

7.2 Statistical methods

I include here a brief overview of the statistical methods employed while analyzing the data in the subsequent two studies. For more information, see the references contained within this section. A general overview of statistical methods used in discipline-based research can also be found in Slater et al. (2011) and in Ding & Liu (2012).

7.2.1 Types of quantitative data

The nature of quantitative data in education research makes it very different to deal with than quantitative data in astrophysics research. A scales of measure taxonomy first proposed by Stevens (1946) argues that quantitative data generally falls into one of four categories: nominal, ordinal, interval, or ratio. According to this taxonomy,

- **Nominal data** is discrete and has no order. It is sometimes also referred to as a type of "categorical" data. An example of nominal data collected in our studies is much of the demographic data, such as gender or nationality, where the data consists of independent categories that have no natural ranking.

- **Ordinal data** is another type of categorical data that can be sorted, allowing for rank-ordering, but the difference between the data cannot be quantified. An example of ordinal data might be Likert-scale responses indicating agreement with a statement on a five-point scale ranging from "strongly disagree" to "strongly agree"; these responses can be ranked, but the degree of difference between "strongly agree" and "agree", for example, may not be the same as the degree of difference between "agree" and "neutral".

- **Interval data**, on the other hand, can be rank-ordered and has well-defined spacing between options; it is continuous on a scale of equal intervals. Examples of interval data include things like temperature (where the difference between $1\,^{\circ}$C and $2\,^{\circ}$C is the same as the difference between $41\,^{\circ}$C and $42\,^{\circ}$C) or date (where the difference between July 21 and

July 22 is the same as the difference between October 3 and October 4).

- **Ratio data** has all of the properties of interval data, but also possesses a meaningful zero value to which the data on the scale can be compared. While temperature has no well-defined zero point ($20\,^{\circ}$C is not twice as hot as $10\,^{\circ}$C), ratio data can be compared in this way: the distance from Ithaca, NY to Boulder, CO is roughly 1.5 times the distance from Boulder to Santa Barbara, CA; the mass of the black hole Sgr A* is 4.3 million times the mass of the Sun.

In traditional scientific research, most data typically falls into the categories of interval and ratio data. As a result, we can manipulate the data with mathematical operations, and the results still hold useful meaning in interpreting the data (Ding & Liu, 2012). Education research data, on the other hand, often falls into the categories of nominal and ordinal data, and care must be exercised when this data is analyzed. Even our scoring of writing samples in the following studies, in which students were assigned a grade on a five-point scale in each of various categories, is not technically interval data; the difference between two students scoring 4 points and 5 points in the category of jargon, for instance, might not be the same as the difference between two students scoring 2 points and 3 points in the same category — as much as we might like these intervals to be the same, and as much as we might attempt to design the rubric in such a way that they are. In spite of this, researchers often tend to treat scores like these as being a close enough approximation of interval data, **if the scores of the students follow a Gaussian distribution**, that statistics appropriate for interval data can be used to analyze them (Ding & Liu, 2012).

7.2.2 Parametric vs. non-parametric statistical analysis

The emphasized portion of the previous sentence is critical: the underlying distribution of the scores must follow a Gaussian distribution in order for most standard statistics to be applied. Statistics that assume a normal distribution of the variable in the population from which data is collected are known as **parametric** statistics. When data is continuous and the sample size is

sufficiently large, it is often safe to assume a normal underlying distribution, in which case statistics that rely on the mean and standard deviation of the data are appropriate. If the data is categorical, however, or the sample size is small, the the normality assumption does not hold. In these cases, **non-parametric** statistics must be used for analysis, as these do not make any assumptions about the underlying distributional properties. Non-parametric statistics tend to instead examine the data in the form of frequencies (Ding & Liu, 2012).

Lack of normality is a pervasive issue in education research (Meissel, 2014); it is argued that the majority of data collected within the social sciences doesn't meet the conditions required to assume normality (Micceri, 1989). For those who prefer a little more visual imagery in their background reading: Micceri (1989), in fact, suggests that the likelihood of collecting normal data in applied settings is comparable to the likelihood of an encounter with a unicorn. I will attempt in the following sections not to cry "unicorn" unnecessarily, and to instead identify data that cannot be analyzed parametrically. I will describe now the primary statistics that we employed when analyzing our data.

7.2.3 Interrater reliability

In the case of the second study presented in the remainder of this thesis, the writing samples collected from students were analyzed independently by two individual raters, whose scores were then averaged. When multiple raters are involved in assigning scores, a question is raised: how can one establish whether or not the two graders are scoring consistently? Better yet, can the degree of agreement between the scorers be quantified?

Classical test theory (Lord, 1959; Novick, 1966) assumes that an assigned score consists of true score plus a measurement error, which prevents one from observing the true score directly. This measurement error can be produced by a number of things — including the instability of a measuring instrument when measurements are made by different coders. This is known as inter-rater reliability.

The goal of interrater reliability analysis is to determine what fraction of the variance in an

assigned score is due to variance in the true score, after the variance due to measurement errors between coders has been removed (Novick, 1966). Finding an interrater reliability rating of 0.7, for instance, indicates that 70% of the observed variance is due to true variance, and 30% is due to error variance as a result of differences in ratings between coders.

How does one establish interrater reliability? A statistic often reported in this case is percent agreement — or, for a slightly more relaxed constraint, percent agreement **within some interval** (for instance, the percent of the time two raters' scores for a sample fall within 1 point of each other). The problem with this method of reporting is that it doesn't take into account the probability of agreement by chance, and it can therefore overestimate the amount of agreement (see Cohen, 1960; Krippendorff, 1980; Hallgren, 2012).

An alternative was suggested by Cohen (1960); Cohen argued for use of a statistic now known as Cohen's kappa (κ), which is given by

$$\kappa = \frac{P(a) - P(e)}{1 - P(e)}. \tag{7.1}$$

Here $P(a)$ is the percent agreement that is observed, and $P(e)$ is the percent agreement that is expected by chance. $P(a)$ and $P(e)$ can be established for a given set of scores by creating a contingency table and comparing score frequencies: $P(a)$ is given by the fraction of total scores during which the two raters' scores agree, and $P(e)$ can be found by taking the sum — over all possible scores — of the expected frequencies of agreement by chance. These expected frequencies of agreement by chance are given by the product of the two raters' frequencies with which they assign the particular score (i.e., if Rater 1 assigns a "YES" 60% of the time and Rater 2 assigns a "YES" 30% of the time, then the expected frequency of agreement for a "YES" rating is $0.6 \times 0.3 = 0.18$).

As an example, if Rater 1 assigns scores of (1, 1, 0) to three students' samples, and Rater 2 assigns scores of (1, 0, 0) to those same three samples, then the observed agreement is $P(a) = \frac{2}{3}$, and the expected agreement is $P(e) =$ (expected frequency of agreement by chance for a score of 1) + (expected frequency of agreement by chance for a score of 0) $= \left(\frac{2}{3} \times \frac{1}{3}\right) + \left(\frac{1}{3} \times \frac{2}{3}\right) = \frac{4}{9}$. Thus the Cohen's κ for this example is $\kappa = (\frac{2}{3} - \frac{4}{9})/(1 - \frac{4}{9}) = \frac{2}{5} = 0.4$.

Possible resulting values of Cohen's κ range from -1 to 1, where 1 is perfect agreement, 0 is completely random agreement, and -1 is perfect disagreement. A commonly-adapted general means of interpreting Cohen's κ is given by Landis & Koch (1977), who suggest that 0.00 to 0.20 indicates slight agreement, 0.21 to 0.40 indicates fair agreement, 0.41 to 0.60 indicates moderate agreement, 0.61 to 0.80 indicates substantial agreement, and 0.81 to 1.00 indicates almost perfect or perfect agreement. Using this scheme, Rater 1 and Rater 2 in the example above thus demonstrate only fair agreement. It should also be noted that some other analyses, e.g. Krippendorff (1980), use even more conservative cutoffs.

Often in the case of ordinal or interval data, we might want to quantify the **amount** of disagreement between the raters. As an example, if Rater A and Rater B gave the same sample scores of 2 and 5, respectively, you might want the interrater reliability to reflect a greater degree of disagreement than if Rater A gave the sample a score of 2 and Rater B a score of 3. In this case, we can assign weighting to the score discrepancy, as proposed in Cohen (1968). This produces a statistic known as the weighted Cohen's κ, given by

$$\kappa = 1 - \frac{\sum_{i=1}^{k} \sum_{j=1}^{k} w_{ij} x_{ij}}{\sum_{i=1}^{k} \sum_{j=1}^{k} w_{ij} m_{ij}}, \tag{7.2}$$

where the w_{ij} are elements of the weight matrix, the x_{ij} are elements of the observed matrix, and the m_{ij} are elements of the expected matrix (refer to Cohen (1968) for details). Different kinds of weighting can be applied, but in this study we choose to treat our scores as roughly interval, and we assign linear weighting accordingly: if the two raters' scores differ by one point, the weight is 1; if the raters' scores differ by two points, the weight is 2, etc.

As Cohen's κ is generally considered to be a fairly conservative estimate of agreement, we quote both percent agreement as well as the weighted Cohen's κ statistic in §9.4.1, in order to present the most complete picture of the interrater reliability within this study.

7.2.4 Statistical significance

In the studies that follow in the remainder of this thesis, we employ primarily pre- and post-training comparisons to analyze the potential impact of the training we provide the students. With such measurement tools, we would like to be able to report whether the distribution of student scores/responses in the pre-training test/survey question is significantly different, statistically, from the distribution in the post-training test/survey question. Without taking statistical significance into account, we could be fooling ourselves into thinking that student abilities or attitudes have improved when what we're actually observing is random fluctuations.

The standard approach used to test for statistical significance in the difference between pre and post scores is known as the paired t-test. By using paired data for each student, each student functions as his or her own control, lowering the level of unexplained variance. With a paired t-test, the differences between the two scores in each pair (i.e., the pre and the post score) are calculated. The null hypothesis is typically that the two score distributions are identical, and therefore that the average difference will be zero. The statistic t is then given by

$$t = \frac{\langle X_D \rangle}{s_D/\sqrt{N}}, \tag{7.3}$$

where $\langle X_D \rangle$ is the average pair difference, s_D is the standard deviation for that distribution, and N is the sample size. Under the null hypothesis, this statistic follows a t-distribution with $N-1$ degrees of freedom; thus the value of t can be converted into a p-value, which describes the probability that such a value could have been found by chance, even if there were no difference between the two score distributions. Typical convention for the field of education research is that $p < 0.05$ implies that the difference is statistically significant, and the null hypothesis that the two distributions are the same can be rejected at the 95% confidence level (Coe, 2002).

The paired t-test, however, relies on the assumption that the underlying scores are distributed normally. If sample sizes are small, or there are significant outliers, this assumption doesn't hold true and the t-test is not reliable. In this case, an analogous non-parametric test can be used: the Mann-Whitney test, which compares two independent sets of ordinal data (see e.g. Wallace, 2011

for an example of use of this test, and a statistical methods book such as Wilcox, 1987 for a more complete description of the Mann-Whitney test than what follows).

The Mann-Whitney test can be applied by combining all the scores, both pre and post, for all students and rank-ordering the group as a whole. The null hypothesis for the test is that when the data is then split back into the original pre and post groups, the distribution of ranks will be the same in each group, and the two rank-totals (found by summing up the ranks in each group) will be the same. The alternative hypothesis is — ideally — that the higher ranks will primarily be found in the post-training group, and the two rank-totals will be significantly different. The test statistic associated with the Mann-Whitney test is U, which reflects the difference between the two rank-totals and is given by the following formulas:

$$U_1 = N_1 N_2 + \frac{N_1(N_1+1)}{2} - R_1 \tag{7.4}$$

$$U_2 = N_1 N_2 + \frac{N_2(N_2+1)}{2} - R_2 \tag{7.5}$$

$$U = \min(U_1, U_2), \tag{7.6}$$

where N_1 and N_2 are the sample sizes of the pre- and post-training scores and R_1 and R_2 are the rank-totals for each of the two groups.

As with the t statistic, the U statistic can then be converted into a p-value that tells you the probability that the null hypothesis — in this case, that the two score distributions are the same — could be true by chance. This conversion can happen in one of two ways, depending on the sample size:

(1) If the sample sizes are small (typically $N \leq 20$) then you can use a lookup table of critical U values for the Mann-Whitney test. If the U value found is smaller than the critical U value in the $p = 0.05$ table, then the result is significant, and we reject the null hypothesis that the pre- and post-training scores are the same.

(2) If the sample sizes are large, it can be assumed that the U statistic is approximately normally

distributed. In this case, the mean and standard deviation of U are given by

$$\mu = \frac{N_1 N_2}{2} \tag{7.7}$$

$$\sigma^2 = \frac{N_1 N_2 (N_1 + N_2 + 1)}{12}, \tag{7.8}$$

and the p-value associated with the U value can be found assuming this normal distribution.

A note about ties: if the data set being analyzed contains a large number of tied scores, two things should be observed. First, the appropriate treatment for ranking ties is, for each group of ties, to assign the average rank for all the scores in the tied group. For example, the scores (0, 1, 1, 2, 2, 2, 3) would be assigned the ranks (1, 2.5, 2.5, 5, 5, 5, 7). Secondly, if the sample sizes are large and one wishes to treat the U statistic as normally distributed, the following revised version of the variance gives better results:

$$\sigma^2 = \frac{N_1 N_2}{N^2 - N} \left(\frac{N^3 - N}{12} - \sum \frac{f^3 - f}{12} \right), \tag{7.9}$$

where $N = N_1 + N_2$ and the sum is taken over all scores where ties exist and f is the number of ties at that level.

Tests such as the paired t-test and the Mann-Whitney test, then, are a useful means of determining whether two sets of scores are statistically significantly different. Once you've established this, however, you may want to examine **how** different the two sets of scores are. This can be done with effect size.

7.2.5 Effect size

Statistical significance combines two independent aspects: effect size and sample size. As a result, statistical significance increases both when there is a greater effect, and when the size of the sample increases. For purposes of better understanding **only** the amount by which student responses change between the pre and post test, without having sample size conflated in the measurement, we look at effect size.

Effect size is commonly measured using Cohen's d statistic (Cohen, 1977), which describes the separation of the mean pre- and post-training scores in terms of the standard deviation of the pre-training scores:

$$d = \frac{\langle \text{post} \rangle - \langle \text{pre} \rangle}{\sigma_{\text{pre}}} \tag{7.10}$$

As with all statistics, interpretation of effect size must not be done blindly, but a commonly-used rule of thumb — introduced by Cohen himself — is that a measure of Cohen's $d = 0.2$ constitutes a small effect, $d = 0.5$ a medium effect, and $d = 0.8$ a large effect. For reference, $d = 0.2$ would mean that 58% of the post-test scores were higher than the mean of the pre-test scores, $d = 0.5$ would mean that 69% are higher, and $d = 0.8$ would mean 79% are higher.

For non-normal data, however, Cohen's d can give a misleading picture; Cohen's d statistic relies on the two distributions of scores being normal and having the same standard deviation (see, e.g., Coe, 2002 for a discussion of this). For data that is not normal, we instead need a non-parametric equivalent of Cohen's d in order to discuss effect size.

An alternative was suggested by Cliff, 1993, known as Cliff's δ. Cliff's δ is a robust and intuitive alternative to Cohen's d, and can be used regardless of the distribution of the underlying scores. Indeed, it is just as effective as Cohen's d even if the scores are normally distributed; it is just somewhat more complex to calculate (Meissel, 2014). Cliff's δ is effectively a dominance statistic: it is obtained by calculating the non-overlapping area of two distributions by counting cases. The formula is given by:

$$\delta = \frac{\#(x_{i1} > x_{j2}) - \#(x_{i1} < x_{j2})}{N_1 N_2}, \tag{7.11}$$

where the x_{i1} are the scores within the post test group and the x_{j2} are the scores within the pre test group. This statistic thus subtracts the number of instances of dominance in the pre test group from the number of instances of dominance in the post test group, and reports this as a fraction of the total possible comparisons.

Cliff's δ can range between -1 and 1, where the extremes imply no overlap between the pre and post test distributions, and 0 implies perfect overlap, suggesting that there has been no change.

A positive Cliff's δ implies a gain: the class's scores have shifted higher in the post test than they were in the pre test; a negative Cliff's δ implies the opposite. An interesting advantage to Cliff's δ, reflected in these results, is that it measures the size of an effect over the entire distribution of both groups, rather than only measuring the size of the effect for those in the center of the distribution — a problem exhibited by parametric tests such as Cohen's d (Meissel, 2014).

It should be noted that effect size, as measured by Cliff's δ, and statistical significance, as measured by Mann-Whitney's U statistic, are not independent (Cliff, 1993). In fact, one can easily be calculated from the other, as shown below:

$$\delta = \frac{2U}{N_1 N_2} - 1. \tag{7.12}$$

Examining the effect size of the score shift between the pre- and post-training scores provides us with one means of judging how much the students gained or lost over the span of the study. Effect sizes can also be compared across classes, with caution, to provide a broad view of the pedagogical impact of the training. We may want another way of examining the difference between pre and post scores within each class, however; for that, we turn to normalized gain.

7.2.6 Normalized gain and normalized change

For another means of examining the change in scores over the span of the study, we employ a statistic known as **normalized change** (first introduced in Marx & Cummings, 1998). The reader familiar with education research might instead recognize the statistic of **normalized gain** (for the seminal work on normalized gain, see Hake, 1998). Normalized gain is typically used to evaluate how a student's score on a pre-test compares to that on a post-test, and it is given by the following formula:

$$g = \frac{\mathrm{post} - \mathrm{pre}}{100 - \mathrm{pre}}, \tag{7.13}$$

where 'post' and 'pre' are the student's post-test and pre-test scores out of 100%, respectively. Normalized gain thus describes the amount a student learned as a fraction of the amount that they **could** have learned.

When matched data (i.e., data that includes both a pre-test and a post-test for each student in the sample) is available, then it makes the most sense to examine the average of individual student gains. Unfortunately, this statistic can be heavily skewed by the few students who score exceptionally well on the pre-test — a student with a perfect pre-test score has an individual gain of $-\infty$ regardless of their post-test score. In order to avoid having to drop the data associated with these students, many researchers prefer to instead use average normalized gain: in this case one computes the overall normalized gain of the class average, rather than computing the average of the normalized gains of individual students. The average normalized gain is given by

$$\langle g \rangle = \frac{\langle \mathrm{post} \rangle - \langle \mathrm{pre} \rangle}{100 - \langle \mathrm{pre} \rangle}, \tag{7.14}$$

where $\langle \mathrm{post} \rangle$ and $\langle \mathrm{pre} \rangle$ are respectively the class-averaged post-test and pre-test scores out of 100% (see Bao, 2006 for further discussion of the difference between the average of individual normalized gains and the normalized gain of the class average).

Though average normalized gain exhibits some benefits, it still has several constraints, as discussed in Marx & Cummings (2007). Its primary limitation is that results can become difficult to interpret if students perform more poorly on the post-test than on the pre-test. Marx & Cummings (2007) proposed a statistic they called 'normalized change' instead, in order to better handle negative gains. The formula for normalized change is given by

$$g = \begin{cases} \dfrac{\mathrm{post} - \mathrm{pre}}{100 - \mathrm{pre}} & \text{if post} > \text{pre} \\ \dfrac{\mathrm{post} - \mathrm{pre}}{\mathrm{pre}} & \text{if post} < \text{pre} \\ \mathrm{drop} & \text{if post} = \text{pre} = 100 \text{ or } 0 \\ 0 & \text{if post} = \text{pre otherwise.} \end{cases} \tag{7.15}$$

Thus if a student's score increases, g still reflects the student's gain as a fraction of maximum possible gain, but if a student's score decreases, g now reflects the loss symmetrically, as a fraction of the maximum possible loss. This definition of g also removes the students who scored perfectly on the pre-test or the post-test, with the argument that these students' performance is beyond the scope of the measurement instrument.

Using normalized change when analyzing students' pre-training and post-training writing samples allows us to return to using matched data and calculating the average of individual changes, rather than a change of the average score, which we believe captures students' gain more realistically. Thus, where possible, we choose to measure average normalized change rather than normalized gain of the average.

Chapter 8

ComSciCon: Training Graduate Students to Communicate Science

8.1 Preface

The material presented in this chapter will be included in a paper to be submitted to the journal Science Communication, and was completed under the guidance of Dr. Seth Hornstein. In this work, I evaluate the effectiveness of ComSciCon 2013, a science communication workshop for science, technology, engineering and math (STEM) graduate students. I co-founded and co-organized this workshop with a group of nine graduate students from Harvard and MIT (listed in the acknowledgements) in the summer of 2013. Many of the training methods used at ComSciCon 2013 were later adapted for use in the classroom in my study in the following chapter, Chapter 9. My evaluation of ComSciCon was therefore largely intended as a preliminary study to assess the effectiveness of these training and evaluation tactics. This is discussed further in Chapter 9.

Abstract

Effective science communication is imperative for the sharing of scientific ideas, continued funding and support from policy makers, and education of the public. Science graduate students are a prime group to target for communication training, as they will be our future scientists, educators, and education/public outreach (E/PO) professionals. To provide such training, we created Communicating Science 2013, a professional development workshop for STEM graduate students. This workshop taught graduate students from around the nation to effectively communicate science to both their peers and the public. To learn about graduate students' attitudes toward science

communication and establish the workshop's efficacy, we surveyed the participants both before and after the workshop. This assessment probed topics such as communication preparation the participants have already received, how science communication is perceived in their home department, and what participants hoped to gain from the workshop. We describe the workshop and report the assessment results here.

8.2 Introduction

8.2.1 About ComSciCon 2013

The Communicating Science 2013 Conference, or ComSciCon 2013, was a multi-day science communication workshop for graduate students in science, technology, engineering and math (STEM) fields. It was held in June 2013 in Cambridge, Massachusetts, for a group of 50 graduate students that was selected from a pool of over 700 applicants. ComSciCon 2013 was fully organized by a team of nine graduate students to address the lack of training and professional development opportunities for young scientists who wish to learn to communicate with their peers and with the public more effectively. The various components of ComSciCon are detailed in §8.3.2.

8.2.2 Research Goals

In performing a study of the participants of ComSciCon 2013, we had multiple objectives. Our aims included both performing a comprehensive evaluation of ComSciCon itself (for the sake of improving the workshop in future iterations) as well as probing the backgrounds and environments of STEM graduate students, and testing and evaluating various science communication training tactics. An outline of our research goals follows:

(1) Survey the environment that currently exists for STEM graduate students who are interested in science communication.

   (a) How do ComSciCon participants perceive the support of their field, department, and peers?

(b) What training have the participants already received in science communication?

(c) How do the attitudes of ComSciCon participants compare to a cross-section of professional scientists (i.e., scientists surveyed in the United Kingdom in The Royal Society, 2006)?

(2) Test science communication training tactics for STEM graduate students, with the intent of future application to larger and broader audiences (see Chapter 9).

(a) What are some appropriate training tactics?

(b) How well are our methods received?

(c) How effective are our methods?

(3) Evaluate the general ComSciCon workshop format and establish if it is effective, sustainable, and able to have a lasting impact.

8.3 Methods

8.3.1 Sample Selection and Participant Demographics

ComSciCon 2013 participants were selected from a pool of more than 700 applicants enrolled in a STEM (Science, Technology, Engineering and Math) graduate program at an accredited U.S. university. The goal of ComSciCon 2013 was not only to train students to be more effective science communicators, but also to build a network of students who are both interested in science communication and able to propagate the ideas presented at the workshop. As a result, ComSciCon organizers selected participants from the applicant pool by identifying students who have already proven themselves to be exceptionally dedicated to the goal of effective science communication. Applicants submitted a writing sample and a description of their current education and public outreach activities, both of which were used to select for the top students demonstrating strong science communication skills and obvious initiative in leading science communication projects. As a result

of this selection process, we believe that participants of ComSciCon 2013 represent a rather specialized subset of STEM graduate students: ones who were already particularly capable and interested in science communication prior to the workshop.

Of the final selection of 50 ComSciCon 2013 participants, 48 agreed to participate in this study. These 48 students were distributed throughout the STEM fields (see Table 8.3.1), and roughly 85% of them were in the third year or higher of their program. The study participants are ethnically distributed similar to the national averages for STEM doctorate recipients[1] : roughly 82% identified as white, 17% identified as Asian, and 4% identified as other ethnicities (multiple selections were possible). Study participants were heavily gender-skewed compared to national statistics, however: 29% of participants were male and 71% female (compared to a national average of 62% male and 38% female for 2012 STEM doctorate recipients).

STEM Field	Participants (N=48)
Biology	29 %
Physics/Astronomy	25 %
Geology/Earth Science	15 %
Social Science	10 %
Chemistry	8 %
Engineering	8 %
Mathematics	2 %
Computer Science	2 %

Table 8.1: Breakdown of study participants by STEM field.

8.3.2 Provided Training: Components of ComSciCon

Training for participants was administered over the course of a 2.5-day workshop. Below we describe the primary components of the workshop and the specific training and benefits associated with each one.

[1] based on data from `http://www.nsf.gov/statistics/sed/2012/data_table.cfm`

8.3.2.1 Panel Sessions

ComSciCon participants attended seven panel sessions featuring 21 professional science communicators. Panel sessions included topics such as engaging non-scientific audiences, interacting with the media, sharing science with scientists, non-academic publishing, and communicating using multimedia. The list of panelists spanned a broad range of science communication professions and included journalists, editors, press officers, educators, and science fiction authors. During panel sessions, the experts spoke about about their work and backgrounds and answered questions from workshop participants.

One benefit from these sessions is that participants — many of whom had already expressed strong interest in careers with science communication emphasis — were exposed to a variety of career options and introduced to contacts within these careers. The other primary benefit was that each expert discussed personal observations from his or her experiences as well as general advice for effective science communication; it is in the panel sessions that students gained, from a broad variety of sources, the majority of the workshop's theoretical training in science communication strategies.

8.3.2.2 Pop Talks

Workshop participants were each required to give a one-minute talk about their research, targeted at the level of the general public, to the rest of the group. Each member of the audience was armed with two signs that they could hold up during the talk: one that read "JARGON," to flag language that was too specialized for a general audience, and one that read "AWESOME," to identify when the presenter explained something particularly well.

The pop talk sessions were the primary source of hands-on training for the students, providing them with a means of putting into practice the theoretical training they had been receiving during the panel sessions. Arming the audience with signage allowed the presenter to receive instantaneous feedback during his or her talk and thereby adjust accordingly.

8.3.2.3 Write-a-Thon

At the end of the first day of the workshop, students participated in a "write-a-thon": a several-hour session during which they each created an original piece of science writing for the general public, using the lessons that they had learned that day. The following day, they met in small groups to peer-edit each other's work. After participants updated their drafts, they met with the experts from the panel sessions to receive professional feedback on their writing. They were later encouraged to pursue publishing opportunities (with some provided as publishers partnering with ComSciCon) for the pieces that they created during the workshop; roughly a quarter of participants took advantage of these opportunities and had their work published within six months of the workshop's conclusion.

This portion of the workshop was intended as further practical application of the theoretical training participants had received, this time focusing on written rather than oral communication skills. The iterative process of peer-editing and feedback from the expert science communicators allowed students to continue to improve their communication skills beyond their first attempt. The publishing opportunities made available after the workshop were intended to provide students with a means of finalizing the project that they began at ComSciCon and increase their profile within the science communication community.

8.3.2.4 Poster Session

ComSciCon participants were invited to take part in an electronic poster session on the final day of the workshop. Roughly 20 attendees submitted poster presentations that described the communication and outreach initiatives that they were leading, and the posters were displayed on digital poster boards during a several-hour period of time near the end of the workshop.

The primary benefit of the poster session was to allow students to network with each other, discussing current and previous projects, and potentially building new collaborations. A side benefit was that students, in presenting their posters to each other, were able to continue to practice the

Table 8.2: Learning goals targeted in Baram-Tsabari & Lewenstein (2013).

Clarity	Use appropriate language, address, readability, use basic explanations as appropriate, avoid jargon, and acknowledge prior knowledge
Content	Select appropriate content: engaging, interesting, and relevant to particular audience. Include scientific information, as well as nature of science, scientific method, and implications
Style	Use style aspects creatively: humor, emotions, anecdotes, and local references
Analogy	Develop analogic strategies for explaining complex topics
Narrative	Use complex narrative tools as appropriate, such as character development, conflict, and resolution

science communication skills they had learned over the course of the workshop.

8.3.3 Instruments and Measures

Two primary tools are being used to answer the research questions proposed in this study: writing samples and an attitudes survey. Study participants were asked both before and immediately after the workshop to provide a $100 - 200$ word paragraph describing their current STEM research as though to a member of the general public. These writing samples were then analyzed using a rubric based on the learning goals in the written science communication assessment tool developed in Baram-Tsabari & Lewenstein (2013). This instrument quantitatively analyzes the consistency of a writing sample with a specific set of learning goals for written science communication; we selected a subset of this tool's learning goals appropriate for evaluating ComSciCon's impact. Examples of learning goals that we chose to target are listed in Table 8.2.

Because the initial writing samples were part of the application process (see Appendix B.1 for the application text), and participants were selected from the pool of applicants partially based on the quality of this writing sample (as described in §8.3.1), comparison is inherently difficult — by definition, participants' initial samples already exhibit many characteristics of effective science communication! As a result, we chose to focus on a few specific characteristics that were discussed by the professional science communicators during the panel sessions at ComSciCon, and measure

their presence or absence in the participants' writing before and after the workshop. Those characteristics are:

(1) Jargon: Did the author avoid using any jargon terms without defining them?

(2) Relevance: Did the author answer the question "Why should the reader care?"

(3) Connection: Did the author use any analogies, metaphors, or other ways of connecting to the reader's experiences?

(4) Hook: Did the author use some sort of hook at the start of their summary to reel in the reader?

(5) Appeal: Did the author use some form of humor, narrative, or other aspect of appeal to keep the reader's attention?

To gauge students' perception of the environment that currently exists for them as science communicators, as well as to better understand their own attitudes toward science communication and to be able to compare them to other professional scientists, each study participant completed an attitudes survey both before and immediately after the workshop, as well as an additional survey that was administered six months later. All three surveys are reproduced in Appendix B.2 for reference. These surveys probed topics such as previous training the attendees had received in science communication, the state of the field for students interested in science communication today, and how the participants felt the workshop had affected their abilities to communicate science. Many of the questions addressing students' attitudes toward science communication and outreach were based on a survey developed in 2006 by the Royal Society and administered to a group of nearly 1500 research scientists at higher-education institutes (The Royal Society, 2006).

8.4 Results and Discussion

As a component of ComSciCon 2013, participants were asked to fill out a survey both before and after the workshop, as described in §8.3.3. Their responses, as well as analysis of their writing

samples before and after the workshop, are discussed in this section.

8.4.1 General Goals and Beliefs of Participants

8.4.1.1 Perceived Support for Communicators

ComSciCon attendees were asked to report how supportive they considered other scientists to be of those who take part in activities that engage the general public. This question was intended to gauge the state of the field for young scientists today who attempt to pursue science communication and outreach activities during the course of their academic careers. Figure 8.1 summarizes the responses from participants.

Responses tended to indicate a reasonably supportive environment. $72 - 78\%$ of participants who expressed a view reported their scientific fields, faculty in their department, and advisors to be either “fairly supportive” or “very supportive”. That percentage is even higher — 91% — when describing their peers. These numbers are slightly larger than those in the Royal Society study: 71% of UK scientists who expressed a view considered the researchers in their department to be “fairly supportive” or “very supportive” toward those who take part in activities that engage the general public.

It should be noted, however, that there may be a selection effect at work here: participants are a select group who feel comfortable openly attending ComSciCon. In contrast, there may be students who are concerned that attending a science communication training workshop would cause them to be viewed negatively in their field, in their department, or by their advisors or peers. As such, ComSciCon participants may be reporting a more positive environment toward science communication than can be expected as the average.

8.4.1.2 Career Goals

Survey responses indicated that ComSciCon 2013 participants were a very interesting population. The selection criteria for ComSciCon are such that only students with a demonstrated interest

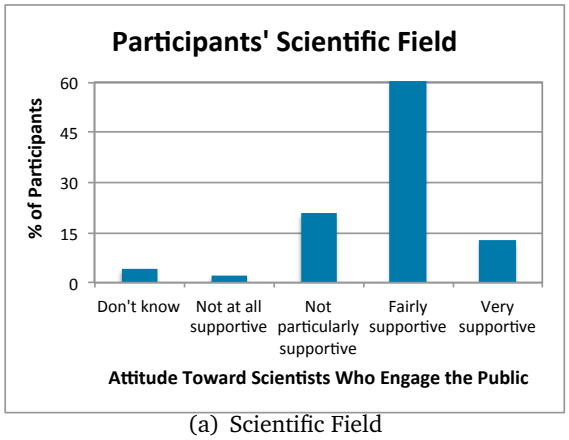

(a) Scientific Field

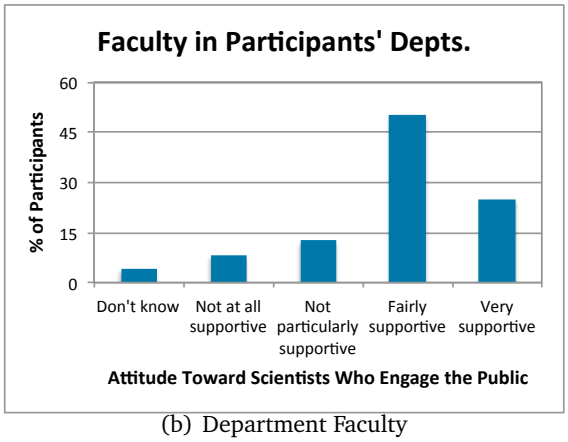

(b) Department Faculty

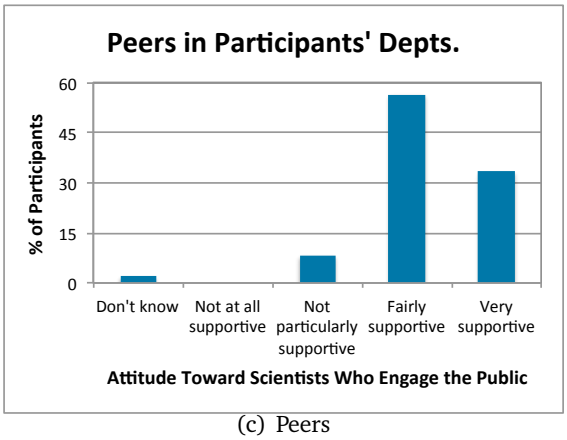

(c) Peers

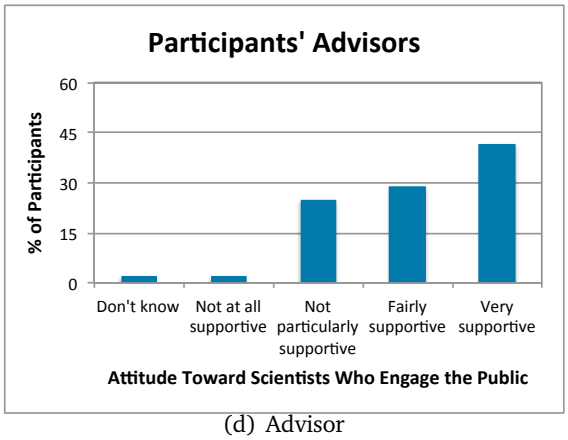

(d) Advisor

Figure 8.1: Perceived level of support for scientists who engage the public, from a) participants' scientific fields, b) faculty in participants' departments, c) peers in participants' department, and d) participants' advisors.

in science communication were admitted as participants, and yet students' interests and goals are by no means uniform. As an example, the career goals of ComSciCon participants are shown in Figure 8.2. These goals clearly represent a broad distribution of interests — from students who intend to transition to a career such as science journalism that is fully science-communication-based, to students who intend to remain in academia but hope to become more effective science communicators as part of their professional development. Similarly, when asked to report the number of hours the students intend to spend on communicating science with non-experts in their future careers, responses were distributed across the spectrum of possible answers, from $0-2$ hours/week to $20+$ hours/week.

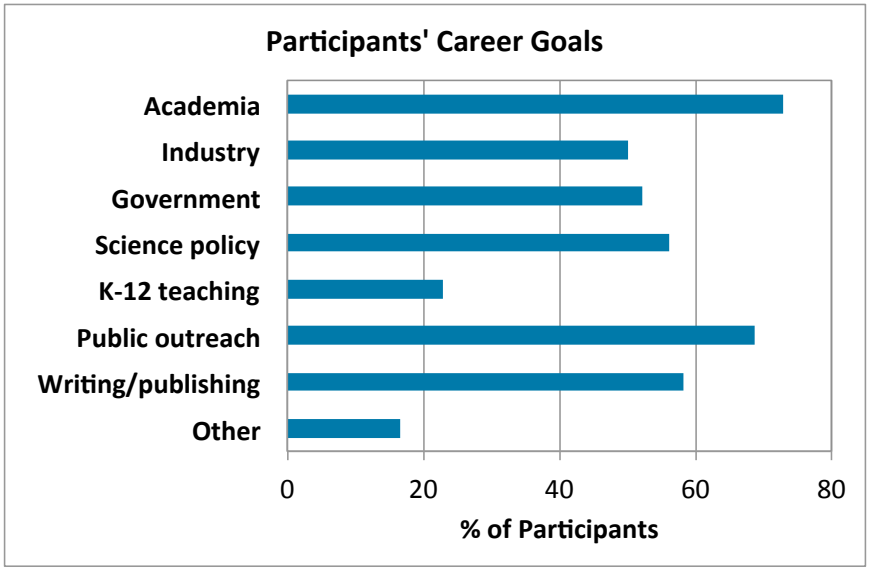

Figure 8.2: Participants' self-reported career goals. N=48; multiple selections were possible.

We consider this to be a very positive indicator: this means that ComSciCon is able to target both students who plan to remain in academia and those who intend to leave it. We hope that this will increase ComSciCon's impact as the ideas from the training are able to spread to a larger population of scientists.

8.4.1.3 Attitudes Toward Science Communication

Despite the wide spread of career goals, ComSciCon participants exhibited some specific attitudes that reflected their common interest in science communication. We compare some of their responses here to what we consider to be a broad cross-section of professional scientists: the 1400+ professional science researchers at higher education institutes in the United Kingdom surveyed in 2006 by the Royal Society for a report on factors affecting science communication by scientists and engineers (The Royal Society, 2006).

In general, both ComSciCon participants and the professional scientists surveyed by the Royal Society believed that "scientists have a moral duty to engage with the non-specialist public about the social and ethical implications of their research" and that "funders of scientific research should help scientists" with this communication; roughly $70 - 80\%$ of both the ComSciCon participants and the professional scientists agreed with these statements (selected "strongly agree" or "agree").

When asked who should be doing the communication of science with the public, however, 81% of ComSciCon participants disagreed with the suggestion that it is best done by trained professionals and journalists, compared to only 44% of the professional scientists; similarly, 88% of ComSciCon participants disagreed that it is best done by senior researchers, compared to only 54% of the professional scientists.

When asked about the personal impact of engagement with the public, 96% of ComSciCon participants reported that engaging with the non-specialist public in science was personally rewarding, and 90% agreed that public engagement could help their careers. In contrast, only 63% and 38% of the professional scientists agreed with these statements, respectively. In addition, ComSciCon participants are significantly more engaged in public outreach than the general cross-section of professional scientists; when given a list of types of public outreach activities and asked to select those that they had participated in within the past year, 91% of ComSciCon participants selected at least one, compared to 74% of the Royal Society professional scientists surveyed.

8.4.1.4 Previous Training

In spite of ComSciCon participants' skew toward interest and active engagement in outreach and science communication activities, when participants were asked what training they had previously received in science communication, 27% reported that they had never before received any formal communication training, and 44% had only received formal training in communicating with other scientists, but not with groups such as the public, school children, or the media. Figure 8.3 summarizes their responses.

If so few of these students selected specifically for their background in science communication activities have had formal training, what does this imply about the general population of STEM graduate students? We argue that these responses illustrate the need for programs such as ComSciCon to provide communication training to young scientists as a part of their professional development.

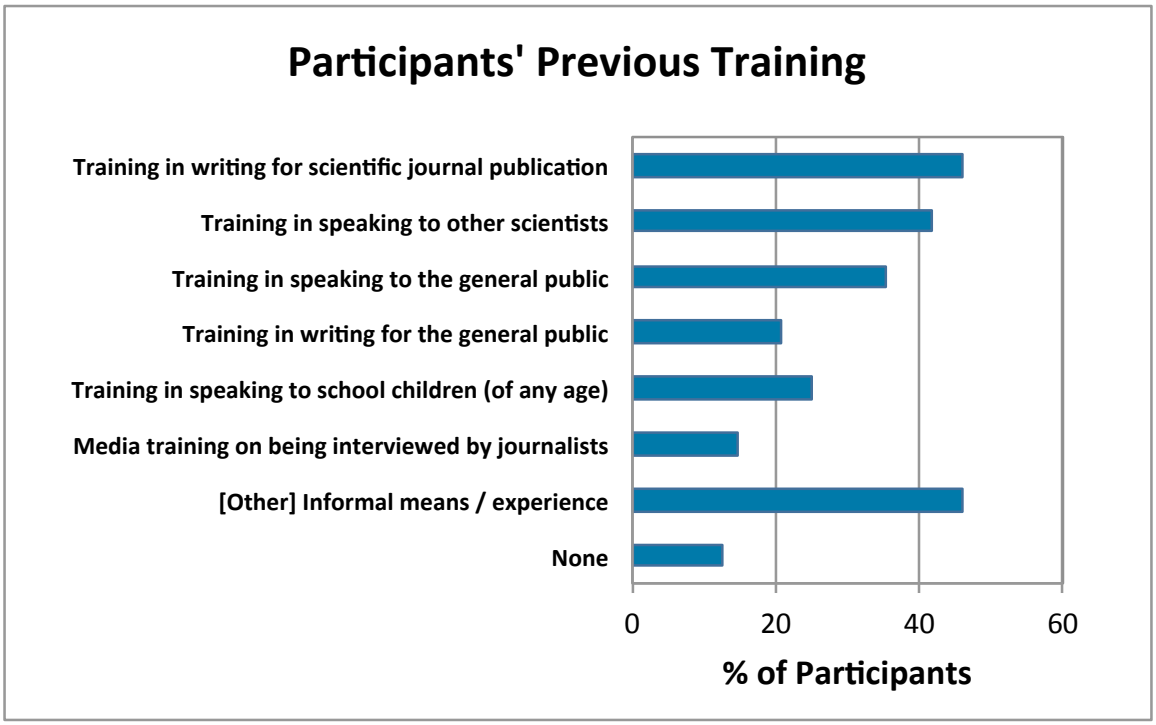

Figure 8.3: Participants' self-reported previous training in science communication. N=48; multiple selections were possible.

8.4.2 Self-reported Impact

ComSciCon participants exhibited no statistically significant change (as measured by a Mann-Whitney test) in any of their general attitudes toward science communication and public engagement after participating in the workshop. As participants already had very positive views toward public engagement and science communication before the workshop, this is perhaps an unsurprising result.

Before the workshop, participants were asked to report what they felt would increase their confidence in science communication. The responses generally fell into one of four categories: 1) formal training, 2) practice, 3) critical evaluation of their communication attempts, and 4) success in their attempts at communication (e.g., having an article accepted for publication). ComSciCon provided each of these things: formal training from professional science communicators in the panel sessions, practice both in written communication from the write-a-thon and in oral communication from the pop talks, critical evaluation of both of these activities by peers and professionals, and the opportunity for for success — many participants' articles have since been published in outlets partnering with ComSciCon, such as Scientific American, Natural History Magazine, and Astronomy Magazine. Did participants' confidence increase after the workshop as a result?

ComSciCon participants were asked to report their level of confidence in their science communication skills in several categories, the first of which was their confidence submitting an article to a popular science publication such as Wired, Popular Science, Scientific American, or Discover. The distribution of their confidence ratings before and after the workshop are shown in Figure 8.4. When the distributions are compared using a Mann-Whitney test, they are found to be different samples at the 95% confidence level — students' confidence gain after the workshop is statistically significant. The effect size for the shift in confidence is quite large: the Cliff's δ is 0.48, indicating there is only 52% overlap between the pre and post distributions.

Similarly, participants' reports of their confidence communicating with scientists and their confidence communicating with the public also showed gains after the workshop; the results are

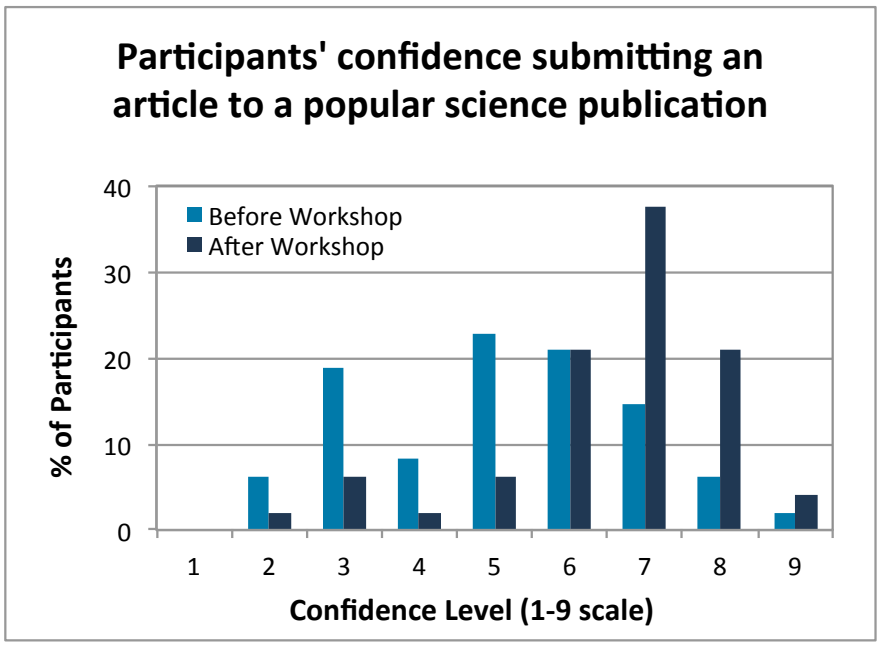

Figure 8.4: Participants' self-reported confidence submitting an article to a popular science magazine. Confidence before the workshop is shown by the lighter bars, confidence after the workshop is shown by the darker bars.

shown in Figure 8.5. The Cliff's δ values for the gain in participants' confidence communicating with scientists and confidence communicating with the public are 0.52 and 0.33 respectively, suggesting that these, too, are fairly meaningful pedagogical shifts.

8.4.3 Writing Sample Analysis

ComSciCon participants wrote a $100-200$ word paragraph summarizing their research topics for an audience of the general public, once in their application for ComSciCon, and once immediately after the workshop. Of the 48 study participants, 41 authorized use of both of their writing samples in this study. We compare those samples now in order to establish whether participants' writing styles changed after the science communication training.

The categories of jargon, relevance, connection, hook, and appeal (as described in §8.3.3) were each evaluated on a binary scale: students were assigned a 1 if the characteristic was present, and 0 if it was not. The results from before and after ComSciCon are shown in Figure 8.6.

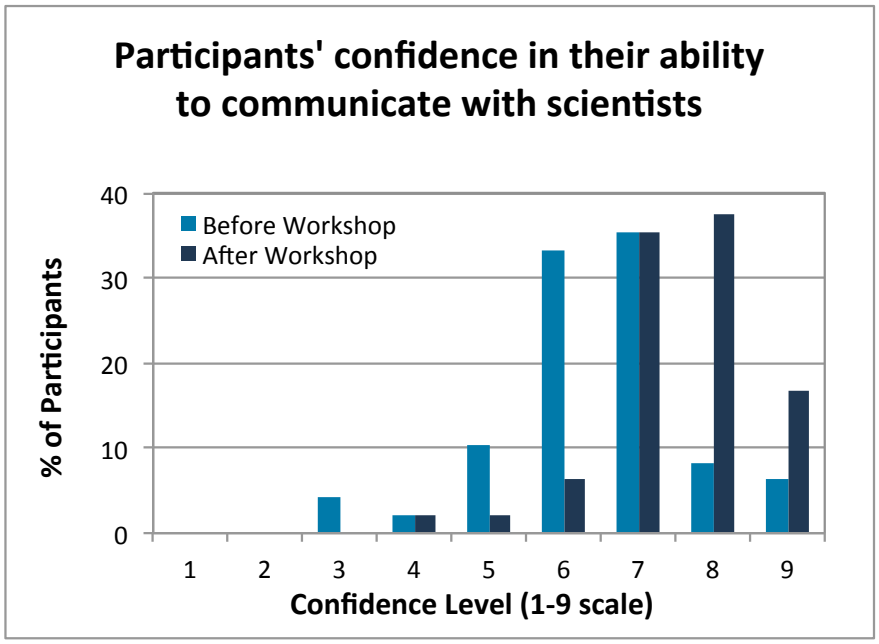

(a)

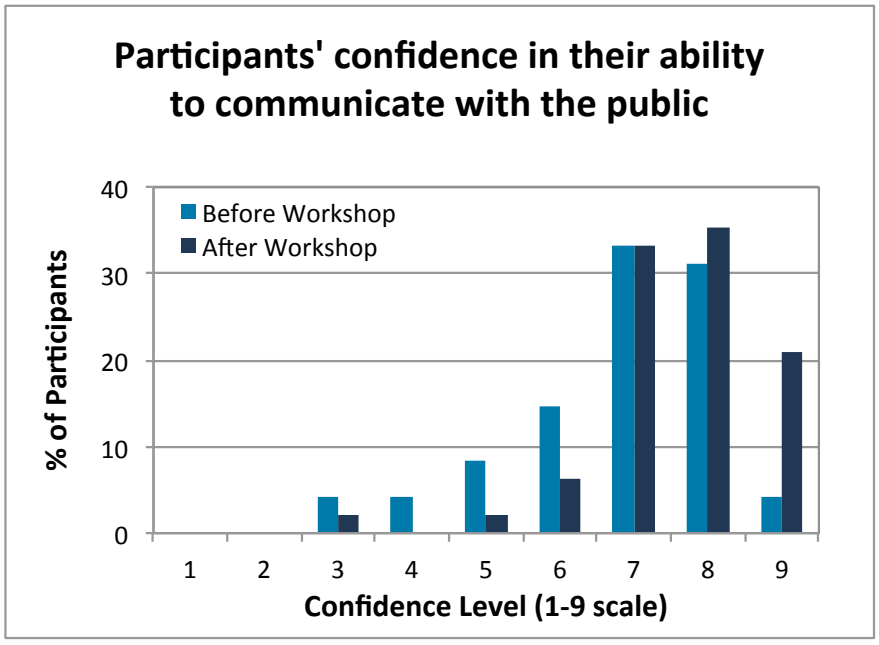

(b)

Figure 8.5: Participants' reported confidence in a) their ability to communicate with scientists, and b) their ability to communicate with the general public. Confidence before the workshop is shown by the lighter bars, confidence after the workshop is shown by the darker bars.

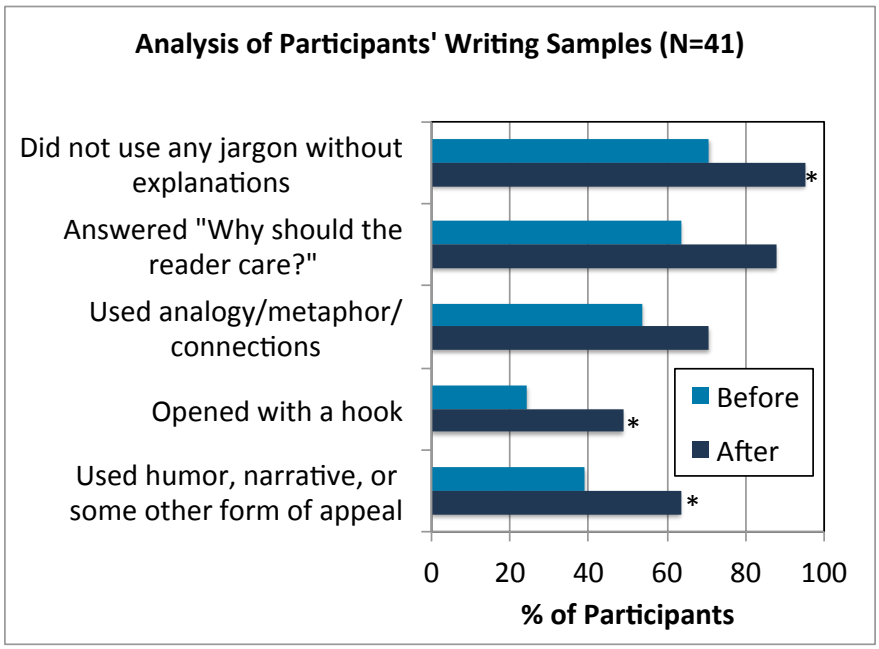

Figure 8.6: Scores for participants (N=41) in five categories evaluating targeted learning goals. Asterisks indicate categories where the shift in scores is statistically significant.

It can be seen from the figure that students' scores improved in all five of the categories; the improvement is statistically significant at the 95% confidence level for the categories of jargon, hook and appeal. The normalized gain (see §7.2.6) of the average score is calculated for each category and displayed in Table 8.3; as can be seen, the average scores increased a substantial percentage of the amount that they could have increased.

Table 8.3: Normalized gain of participants' average score (N=48) in each of the five categories evaluation.

Category	Norm. Gain
Jargon	83 %
Relevance	67 %
Connection	37 %
Hook	32 %
Appeal	40 %

In general, participants' writing samples were greatly improved in all five categories after the workshop. The decrease in the use of jargon was one of the most evident enhancements, and was unsurprising given the amount of improvement we saw in students' awareness of jargon as they

practiced their pop talks in front of each other during the workshop.

8.4.4 Follow-Up

ComSciCon participants were contacted six months after the completion of ComSciCon 2013 and asked to complete a follow-up survey; 35 participants opted to do so. Students were asked about how ComSciCon had affected various aspects of their lives and goals.

One question with a particularly interesting response was that asking students to report how participating in ComSciCon had changed their career plans. Of the 35 participants who responded, 9 reported that their career plans were unchanged. For the remaining 26 participants whose career plans did change, however, the influence of their participation in ComSciCon was completely variable. For some students, being exposed to new information caused them to consider careers they hadn't before. For others, that same exposure resulted in them discovering that they **didn't** want to pursue that career after all. Some students realized that remaining in academia was important to them, while others realized that they wanted to leave it, or they wanted a career with a blend of research and outreach components. The three main effects of ComSciCon on career plans seem to be 1) that it made participants seriously contemplate what was and was not important to them in a career, 2) that participants were provided with more information about the options available to them, and 3) that participants were effectively given the opportunity to try being science writers for a day (via the Write-a-Thon). The combination of these three items, however, appears to have had a different impact on each participant individually.

Participants were also asked how their participation in ComSciCon 2013 had changed their work over the past six months. Several reported having started a research blog in which they used explanations of their work, often intended for the general public, as a means of organizing their thoughts about their research. Others suggested that it had reframed how they thought about their research and provided context for their work, as a result of having to think about the relevance of their work to the general public. Still others reported that their writing skills had generally improved since the workshop, which helped them when writing scientific papers. Finally, many

stated that their skills communicating with other scientists in their field had improved as a result of the workshop.

Participants were next asked how participation in ComSciCon had advanced their professional goals. Students reported the benefit of an increase in connections due to the networking that occurred at the workshop, the addition of résumé items as a result of publication after ComSciCon, improved writing skills, and increased confidence communicating and presenting.

In order to probe whether connections from ComSciCon had evolved into any continued relationships, participants were asked to report whether they had had any further interaction with the professional science communicator panelists or other participants since the conclusion of the workshop. Only 26% of participants reported any sort of interaction with ComSciCon panelists after the workshop ended, but 74% reported continued interactions with other participants. In addition, five of the 35 who responded also became organizers for the following year's workshop, ComSciCon 2014.

8.5 Conclusion and the Future of ComSciCon

Evidence from the participant surveys clearly demonstrates that, though ComSciCon participants appear to be a unique group in their shared interest and background in public engagement and science communication, they had nonetheless received very little formal training in how to effectively communicate science. Their responses also generally indicated a positive perceived view of science communicators in their departments and fields. The clear need for programs that provide formal training for future scientists in how to communicate science clearly with different audiences, as well as the apparent support for science communicators, suggests that now is an excellent time for the implementation of such programs as ComSciCon.

Overall, the model for ComSciCon was very well received. ComSciCon training specifically addressed the primary needs expressed by participants in order to feel more confident as communicators. Feedback both from ComSciCon 2013 participants and the invited panelists indicate that

the workshop was successful in providing useful information to participants, improving their abilities and their confidence in science communication, and providing the opportunity for networking with professionals and peers who share their interests, in many cases forming lasting relationships.

In addition to the self-reported increase in confidence, we see evidence of the success of ComSciCon training tactics in the improved writing skills of participants; participants generally increased their abilities to write without jargon, explain the relevance of their research to their audience, make connections to their audience's past experiences, and use elements of appeal in their writing to hook their audience and keep them interested. The improvement demonstrated by participants in this study suggests that we should consider thinking about how to adapt some of these elements of training into larger and broader programs.

Finally, we are pleased to see that ComSciCon appears to be a partially self-sustaining effort. Participants from ComSciCon 2013 became organizers for the following year's workshop, and financial support from sponsoring institutes has continued beyond the initial installment. ComSciCon 2014 included an additional component to the workshop on how participants could implement a local version of ComSciCon at their home institutes, thereby continuing to pass the information learned at ComSciCon on. We hope that this growth and support continues, so that science communication training can become a standard part of STEM students' professional development.

Acknowledgements

SK was funded by University of Colorado Boulder's Center for STEM Learning for this work. SK would like to thank the sponsors of ComSciCon: Harvard's Graduate School of Arts & Sciences, Faculty of Arts & Sciences, and Department of Astronomy; MIT's Office of the Dean for Graduate Education; University of Colorado Boulder's College of Arts and Sciences, College of Engineering, Office of the Vice Chancellor for Research, Office for University Outreach, and Graduate School; and the Microsoft New England Research and Development Center. The organizers of ComSciCon 2013 were: co-chairs Nathan Sanders (Harvard) and Shannon Morey (MIT); Courtney Dressing, Maria

Drout, Christopher Faesi, Elisabeth Newton, and Sukrit Ranjan (Harvard); Kara Manke (MIT); and Susanna Kohler (University of Colorado Boulder). Faculty advisors were Alyssa Goodman (Harvard) and Marcia Bartusiak (MIT).

Chapter 9

Effects of Adding Science Communication Training to Astronomy Classes

9.1 Preface

This chapter contains the bulk of my science communication research work; the material presented here will be included in a paper to be submitted to the Journal of Research in Science Teaching, and was completed under the guidance of Dr. Seth Hornstein. In this chapter, I adapt some of the training methods and assessment tools presented in Chapter 8 to be used on a larger and broader scale in STEM classrooms. I then implement science communication training in five astronomy classes and evaluate the impact that this training has on students' science communication skills and attitudes.

Abstract

The ability of scientists to effectively communicate with the public is imperative to our society, yet there exist few programs designed to provide scientists with the corresponding training. To explore this need, we target very-early-career scientists by integrating science communication training into five undergraduate/graduate science classes. By analyzing writing samples and gauging participants' attitudes toward science communication throughout the semester-long classes, we demonstrate that integrating a small amount of written science communication training into existing science classes is sufficient to produce measurable improvement in students' written public science communication skills. We present a description of the training and the impact on students' abilities and attitudes toward science communication here.

9.2 Introduction

9.2.1 About This Study

Effective science communication is an important professional skill for future scientists, but as we have already established, there exist few training programs for scientists who wish to improve their abilities. We also believe that students beginning their science careers should not have to seek out special professional development opportunities in order to increase their science communication skills; training in effective science communication should be a normal component of science education at the undergraduate or graduate level..

Unfortunately, most science instructors don't have the time to devote to an excessive component of professional development in their classes, nor do they necessarily have the background to teach strategies for strong science communication with different audiences. Here, we develop training materials that take up only a small amount of class time and could potentially be implemented by instructors in any STEM course at the undergraduate or graduate level.

We test these materials in five astronomy major classes: three at the undergraduate and two at the graduate level. We then assess the effectiveness of this science communication training in improving the students' skills at communicating with the general public, as well as the impact the training had on their attitudes toward science communication.

9.2.2 Preliminary study

A preliminary study has already been executed testing some of the training materials and assessment tools that are adapted here. The preliminary study was the evaluation of ComSciCon 2013, a science communication workshop for STEM graduate students. While the sample in that study, a subset of the participants of ComSciCon, are a relatively select group, their responses to the training — as well as the improvements measured in their abilities to communicate with the general public after the training — have provided us with useful insight into which training tactics were most successful and whether our assessment tools were appropriate for our measurement

goals.

One example of a successful tactic from ConSciCon was “pop talks”, an activity wherein students give one-minute talks about their research or another scientific topic of choice as though to a general audience. Their peers then flag language not appropriate for a general audience by holding up signs labeled with the word “JARGON”. Our analysis of ComSciCon suggested that this training activity was particularly well-received, and a significant improvement in students’ abilities to communicate without using jargon in their writing occurred after the training. As a result of this outcome, we adapted pop talks to be included in the training materials used in the classroom in the study presented here.

Our evaluation of ComSciCon hinged upon two primary measurement tools: a rubric used to evaluate the writing samples of participants, and a survey designed to gauge the attitudes of students toward science communication. We have used similar measurement tools in the study presented here, based on the effectiveness of the tools used in the ComSciCon evaluation; our rubric, for instance, has been upgraded to a more sophisticated version as a result of measurement limitations in the evaluation of ComSciCon. The surveys were adapted to be relevant to a broad range of students in varying stages of their academic careers.

9.2.3 Research goals

In administering science communication training broadly to several hundred students spread across five astronomy classes and evaluating the result, we wanted to learn several things. Our two primary research questions were:

(1) **Is integrating a small amount of written science communication training into existing science classes for majors sufficient to produce measurable improvement in students’ written public science communication skills?**

(2) **Is there an optimal time in the undergraduate/early-graduate career to provide this training?**

In addition, some of our other research goals were:

- Determine what a typical student (i.e., one selected from a broad distribution of class levels, majors, academic backgrounds, etc.) in a STEM class thinks about science communication.
- Determine what a typical student in a STEM class perceives the environment to be for those who engage in science communication activities.
- Establish if attitudes toward science communication change after students receive training.
- Determine if there are any differences in how STEM majors and non-majors should be trained to communicate science effectively.

9.3 Methods

Five classes containing primarily astronomy-major undergraduate students and astrophysics graduate students were selected, and the students in these classes were provided with a small amount of science communication training over the span of a single semester. We then assessed the impact that this training had on the students' written science communication skills and their attitudes toward science communication.

9.3.1 Participants

Participants were all undergraduate or graduate students enrolled in one of five astronomy courses at University of Colorado Boulder. All students enrolled in these classes were exposed to the science communication training described in the next session, but each student was given the ability to opt out of having his or her data included in this study. The five classes, the level of the students in each class, and the approximate enrollment of each class are detailed in Table 9.1.

It should be noted that ASTR 2030 was an unusual class, both due to the fact that it contained mixed levels of students (with roughly an equal number of students falling into the freshman/sophomore category and the junior/senior category), and due to the fact that it contained

Table 9.1: Description of the specific undergraduate and graduate classes targeted in this study.

Course	Primary enrollment classification	Approx. enrollment
ASTR 1030: Accelerated Intro to Astronomy 1	Freshmen majors	95
ASTR 2030: Black Holes	Mixed-level majors/non-majors	125
ASTR 3710: Solar System Formation/Dynamics	Junior/senior majors	50
ASTR 5110: Atomic and Molecular Processes	First-year graduate students	10
ASTR 5120: Radiative and Dynamical Processes	Second-year graduate students	10

both STEM majors as well as a large contingent of non-majors (with a roughly equal split between "STEM major" and "non-STEM major"). We asked students to self-report their major and year, and used this information to examine study results for this class both as a whole and separately for STEM majors and non-majors.

9.3.2 Training

All students in these five classes were provided with science communication training over the span of the semester-long course. This training was designed to be unobtrusive in the context of the overall course and create as little disruption for the class instructors as possible. The training consisted of four components:

(1) In-class lecture/discussion

For each course, 15 minutes in each of two separate class periods were spent discussing both the reasons why public science communication is an important skill for scientists (as described in §7.1.2) and the specific elements of effective communication of science (e.g., minimizing of jargon, presenting connections to everyday life, using effective analogies, etc., as described in Baram-Tsabari & Lewenstein (2013) and other studies such as Bowater & Yeoman (2013)). These lessons were taught in a guest-professor format during normal class time, and they included both lecture and active-engagement components. See Appendix C.1.1 for sample lesson plan outlines from these in-class lectures.

(2) Reading assignments

Students were assigned to read two articles popularizing recent scientific results topically related to their class (see Sanders et al. (2012) for an example source). This was intended to demonstrate how professional writers have distilled information from scientific research papers. See Appendix C.1.3 for a sample reading assignment.

(3) Writing assignments

Four or five homework assignments were given during the semester, in which students were asked to write a short (100-200 word) paragraph summarizing an assigned scientific subject, article, paper, etc. that we selected in collaboration with the course instructor to be both topically related to the class and appropriate to the class level. See Appendix C.1.4 for a sample writing assignment.

(4) Peer-review

For each of the writing assignments after the first one, students completed anonymous peer-review assessment of two classmates' work based on a rubric developed in accordance with the key points of the training. The goal of the peer-review assignments was to give the students feedback on their own writing, reinforce the lessons from the in-class lecture/discussion, and further expose them to examples of both good and bad writing. See Appendix C.3 for the rubric provided to students for use while peer-reviewing.

9.3.3 Instruments and measures

As part of the study we attempted to evaluate both the efficacy of the training provided over the semester and how students' attitudes toward science communication might have changed by the end of the semester. The tools we used to analyze these aspects are presented here.

9.3.3.1 Evaluation of efficacy of training

The first of the five writing assignments was given before the first in-class lecture/discussion occurred, so that it could be used as a pre-training writing sample. The last of the five assignments

Table 9.2: Learning goals targeted in the science communication training provided to study participants. These seven elements are also those on which students' writing samples were later evaluated.

Jargon	Is the writer being careful to avoid or explain words that the public might not know?
Readability	Does the writer avoid run-on sentences and make his/her message clear?
Correctness	Is the writer presenting correct information?
Relevance	Has the writer told you why you should care about this?
Organization	Does the writer's paragraph build upon itself in a clear, logical way?
Connection	Does the writer use analogies or make connections to things his/her audience might have experienced in everyday life?
Appeal	Does the writer somehow hook the reader, use humor in his/her writing, tell a story, or do something else to interest his/her audience?

was used as a post-training writing sample, and the efficacy of the science communication training was then assessed by comparing the two samples for each student. The rubric used to evaluate the writing samples was originally developed based on the written science communication assessment tool presented in Baram-Tsabari & Lewenstein (2013), an instrument that quantitatively analyzes the consistency of a writing sample with a specific set of learning goals for written science communication. The specific learning goals that we chose to focus on for our target group in this study are detailed in Table 9.2; they were selected in accordance with generally accepted best practices specifically for training scientists to more effectively communicate with the public (e.g. Baram-Tsabari & Lewenstein, 2013; Bowater & Yeoman, 2013; Baron, 2010; Dean, 2009).

The samples were evaluated independently by two researchers familiar with the use of rubrics to evaluate student writing, and checks were conducted to improve interrater reliability (see §7.2). Interrater reliability was calculated two ways. For purposes of grading, we sought to ensure that the two raters' scores were typically within one point of each other. This was tested periodically during sample evaluation, and if the percent agreement between the two raters was not high enough, scoring tactics were reviewed before progressing. The overall percent agreement of the two raters for all of the sample sets was typically above 90%, and the weighted Cohen's κ (given by Eq (7.2)) was typically between 0.5 and 0.7, which is generally interpreted to indicate "moderate" to

"substantial" agreement (e.g. Landis & Koch, 1977). After all samples were scored by both raters, the two raters' scores were averaged to produce the final set of scores.

9.3.3.2 Evaluation of attitudes toward science communication

Students' attitudes toward science communication were measured at the beginning and end of the semester in each class using a survey adapted from that commissioned by the Royal Society in 2006 to probe the attitudes of professional scientists toward public engagement (see The Royal Society, 2006 for details). The content of the survey that we developed can be viewed in Appendix C.2.

There were two goals of administering this survey to the students: first, to expand upon the information obtained from the preliminary study by determining what a broad cross-section of STEM students' attitudes toward science communication and public engagement are, as well as what sort of environment currently exists for students interested in public engagement and science education; and second, to determine if any of the students' attitudes change after the they have been exposed to a semester of science communication training (which, as mentioned in §9.3.2 and can be seen in Appendix C.1.1, includes a lecture component discussing the importance of — and reasons for — communicating science).

9.4 Results and Discussion

As previously discussed, the two primary measures in this study were the students' pre-training and post-training writing samples and their pre-training and post-training attitude survey responses. For the writing samples, we chose to only analyze matched data to be able to make more robust comparisons; students who only submitted pre or post writing samples were excluded from the data set. For the attitudes surveys, we took a different approach: because the attitudes surveys administered before and after training were not identical (some questions only applied in the pre-training case, and some questions only applied in the post-training case), having matched

Table 9.3: Summary of the study sample sizes for each participating class, for the primary measuring instruments of the study. The first column indicates the number of paired pre- and post-training writing samples, and the second and third columns indicate the number of pre- and post-training attitudes surveys completed.

Course	Number of Writing Samples	Number of Pre Survey Respondents	Number of Post Survey Respondents
ASTR 1030	53	58	55
ASTR 2030	80	71	80
ASTR 3710	34	38	36
ASTR 5110	11	12	11
ASTR 5120	10	9	10

data was less important. For this reason, we chose to retain all survey responses to maximize the sample size; thus our survey data is unmatched. Our final sample sizes are presented in Table 9.3.

9.4.1 Writing sample analysis

The inset text below illustrates an example pre- and post-training writing sample produced by a student enrolled in one of the graduate-level courses.

> PRE
> (Summary of: Worseck et al., 2011)
> This study constrained the end of the epoch of helium reionization to a redshift (z) of 2.7. Similar to the reionization of hydrogen in the intergalactic medium by the energetic UV photons from hot stars, helium is 'reionized' in the early universe by quasars that supply the energy necessary to excite helium from a first-ionized to a second-ionized phase (the helium now has no electrons). Using the COS (Cosmic Origins Spectrograph) on Hubble, the group examined the spectra of two quasars (the nucleus of a distant galaxy), revealing the presence of characteristic absorption features of He II; these absorption features are then used in combination with three older quasar sightlines to construct a picture of the optical depth of He II. The optical depth is indicative of absorption in the intergalactic medium, where a greater optical depth/absorption exhibits the presence of He II that is not yet fully reionized. This study concluded using the spectral signatures of helium reionization as well as optical depth measurements that reionization is occurring at $z > 2.7$. This study is relevant both for the understanding of quasars themselves as well as the composition of the early universe.
>
> POST
> (Summary of: Ramirez et al., 2014)
> The climate of our sister planet, Mars, has remained a mystery to astronomers

> for decades; we want to know if there was once running water on the surface and why it all disappeared. Using both images from spacecraft orbiting Mars and experiments on Martian surface material conducted by rovers, scientists are able to conclude that liquid water existed on mars billions of years ago. Scientists see valleys on Mars that are analogous to Earth's Grand Canyon, which was formed from rushing rivers. For rivers to exist on Mars, the Martian atmosphere must have been thicker billions of years ago. But up until now, astronomers have been unable to model an atmosphere that grows thick enough to protect the liquid water from freezing. A team of scientists out of Penn State considered molecular hydrogen in addition to the usual carbon dioxide, and it did the trick; they were able to simulate a Martian atmosphere capable of supporting liquid water. This study is important because understanding Mars' climate evolution will help climate scientists on Earth understand our own evolving climate as well as the potential disastrous effects of human-induced climate change.

The difference in the student's writing style between the pre and post sample is evident here; it can be seen that the student made gains in learning to write with less jargon, clearly explain the point of the study and why it matters, and appeal to the reader. We now attempt to quantify these changes across the set of students who participated in this study.

9.4.1.1 General outcomes

The pre- and post-training distributions of scores are shown for all five classes in Figures 9.1–9.5; these are included so that the reader may obtain a visual sense of how the distributions changed for each class between the beginning and end of the semester. To quantify the difference, the average normalized change (given by Eq (7.15)) for the students in each class is reported in Table 9.4 for each of the seven categories. In both the figures and the table, starred categories correspond to those that demonstrate a statistically significant difference at the 95% confidence level between the pre- and post-training score distributions, as measured by a Mann-Whitney test (see §7.2.4).

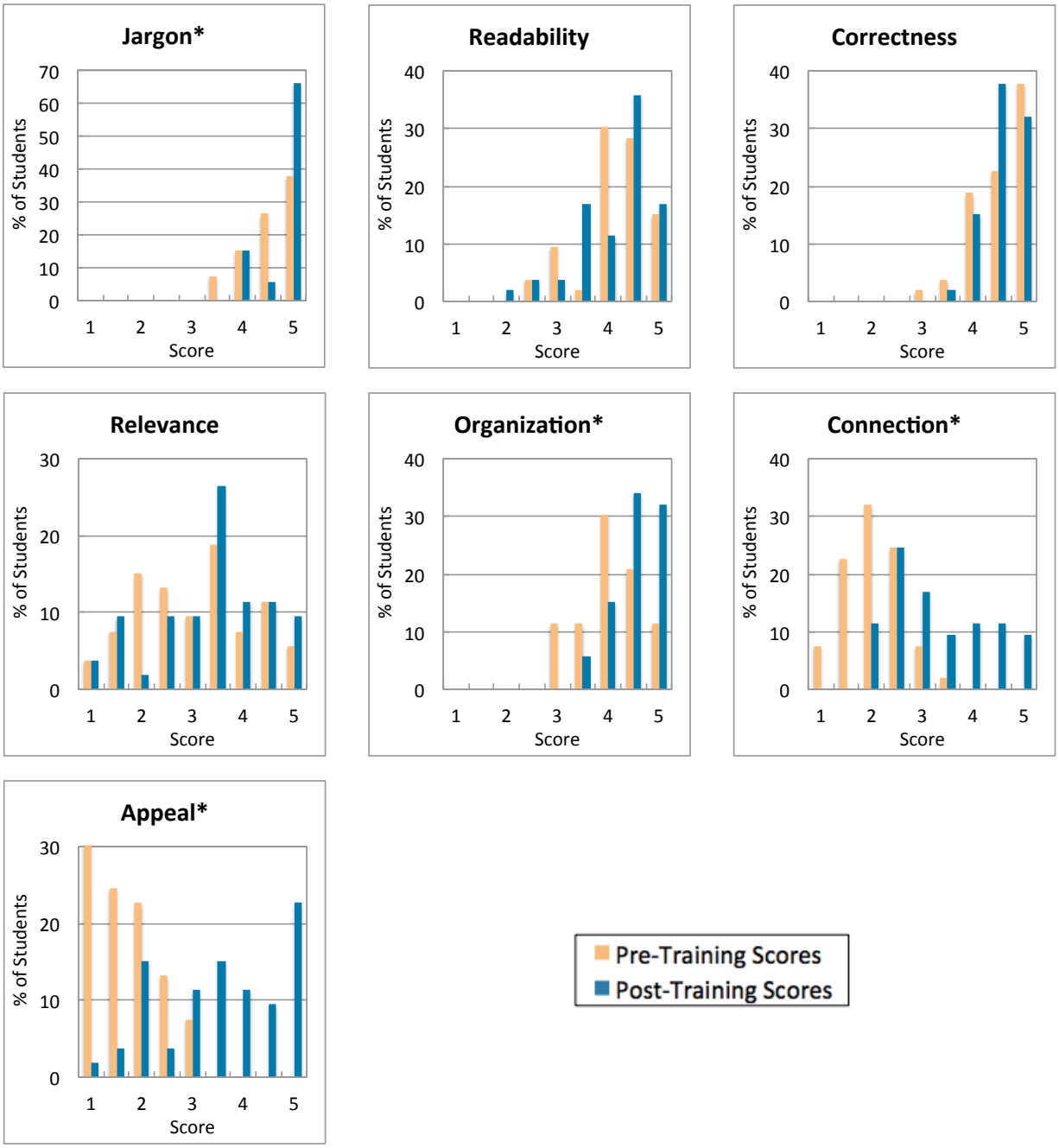

Figure 9.1: ASTR 1030 (N=53) pre- and post-training writing sample score distributions. Categories with an asterisk after the title demonstrate a statistically significant difference between the pre and post scores.

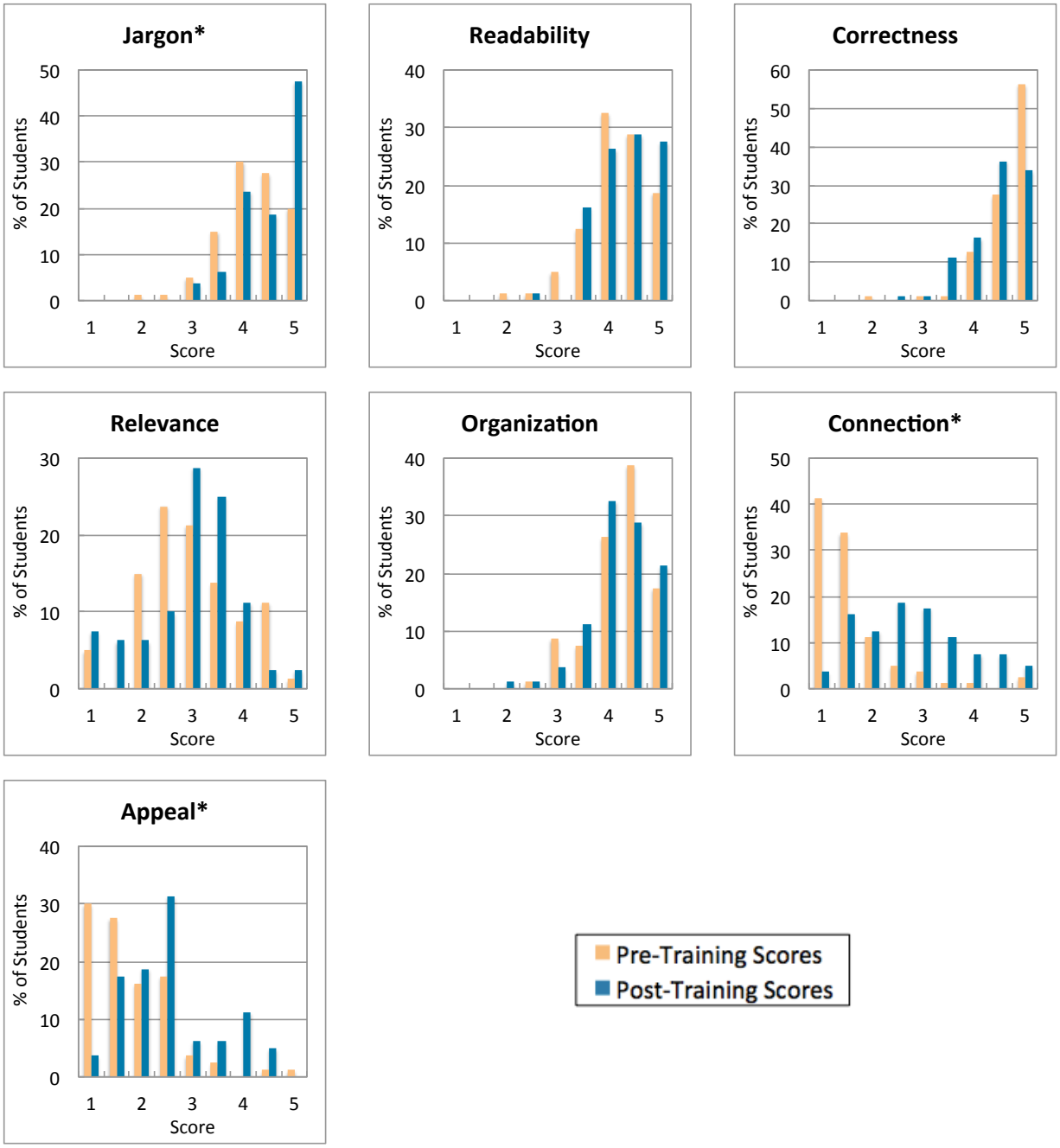

Figure 9.2: ASTR 2030 (N=80) pre- and post-training writing sample score distributions. Categories with an asterisk after the title demonstrate a statistically significant difference between the pre and post scores.

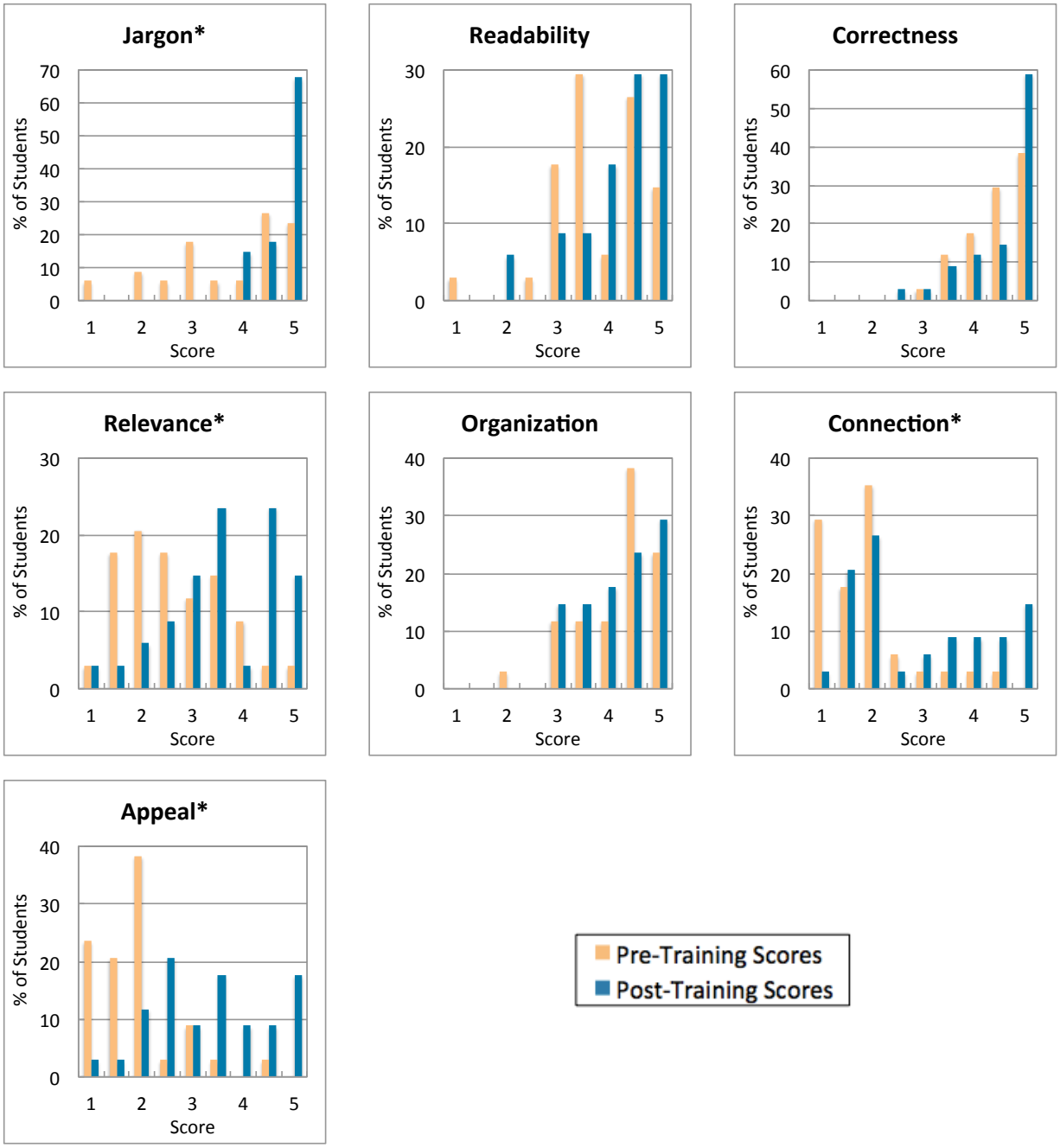

Figure 9.3: ASTR 3710 (N=34) pre- and post-training writing sample score distributions. Categories with an asterisk after the title demonstrate a statistically significant difference between the pre and post scores.

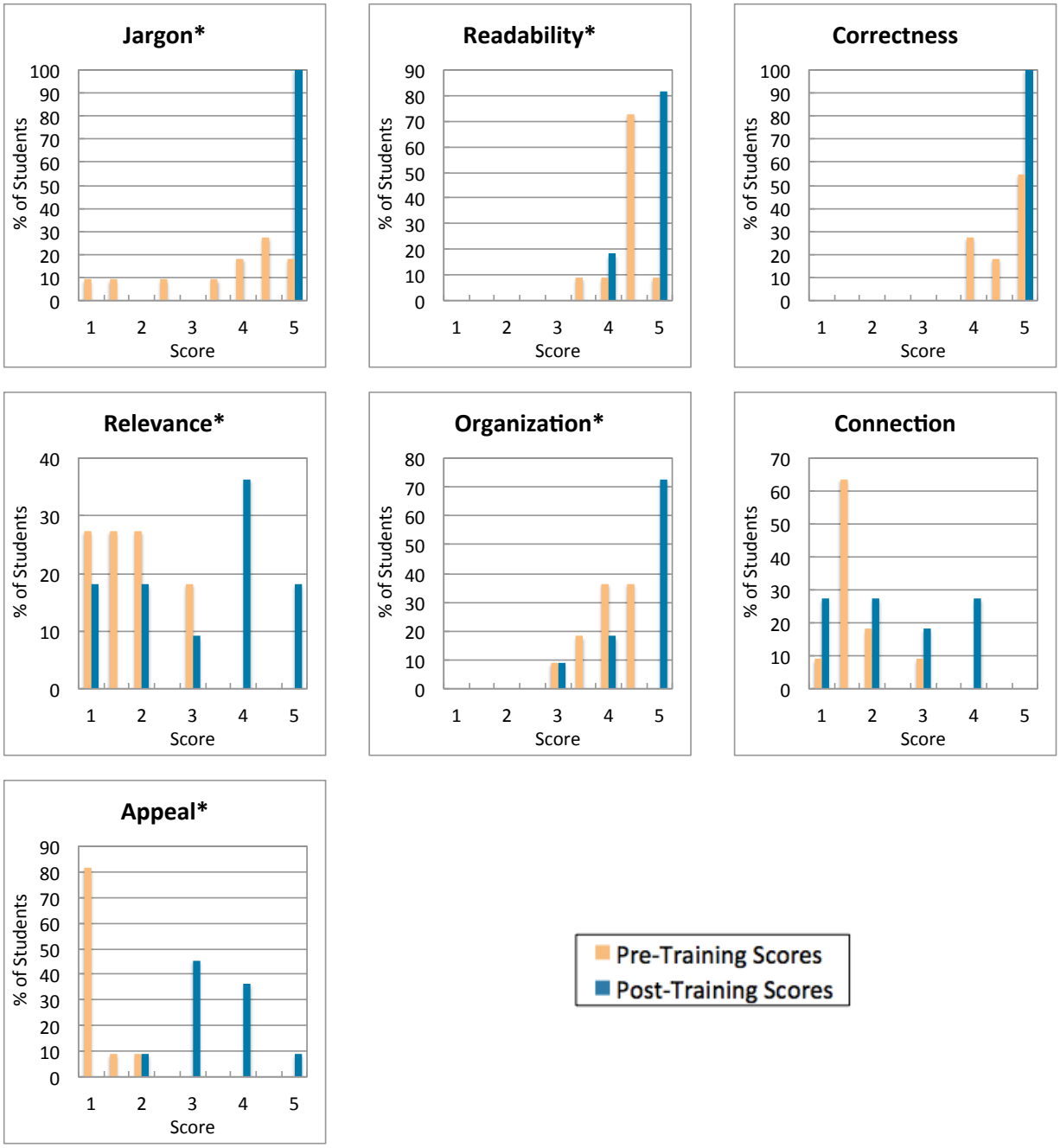

Figure 9.4: ASTR 5110 (N=11) pre- and post-training writing sample score distributions. Categories with an asterisk after the title demonstrate a statistically significant difference between the pre and post scores.

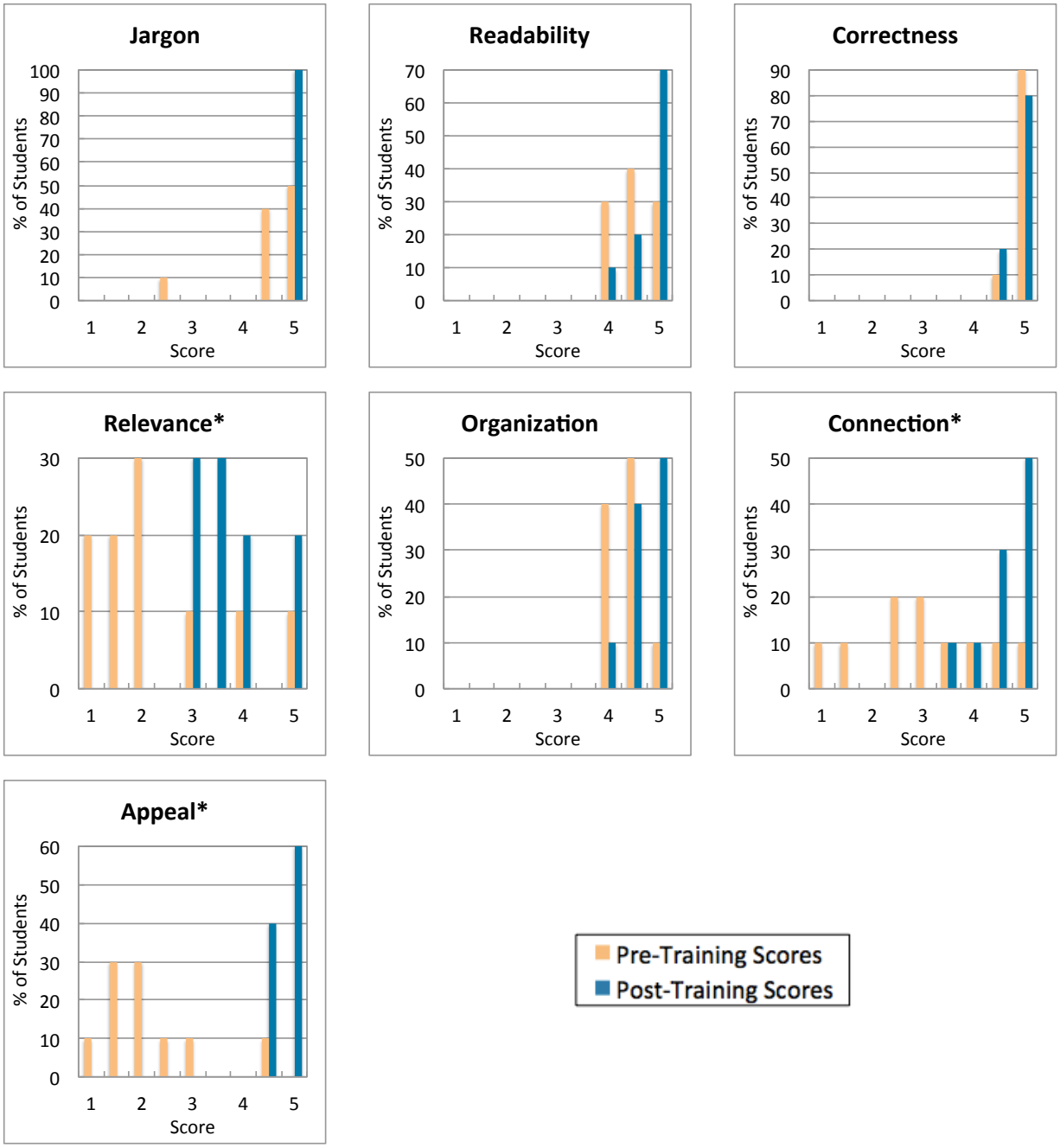

Figure 9.5: ASTR 5120 (N=10) pre- and post-training writing sample score distributions. Categories with an asterisk after the title demonstrate a statistically significant difference between the pre and post scores.

Table 9.4: Average normalized change g (in %), as described by Eq (7.15), for the five classes studied. Positive values correspond to an average gain, and negative values correspond to an average loss. Asterisks indicate that the pre- and post-test score distributions were statistically significantly different.

	Jar	Read	Cor	Rel	Org	Con	App
ASTR 1030	64*	21	29	17	51*	42*	56*
ASTR 2030	47*	31	9	5	21	32*	20*
ASTR 3710	81*	40	41	39*	22	32*	43*
ASTR 5110	100*	78*	100	44*	72*	17	60*
ASTR 5120	100	61	-5	53*	61	71*	85*

Looking at the distributions and the gains, the greatest overall improvement is seen in the categories of jargon, relevance, connection and appeal. As the distributions are clearly not Gaussian, we choose to measure the average effect size using Cliff's δ. The average effect sizes for these four categories are $\delta = 0.50$, 0.38, 0.59, and 0.79 respectively, which means that the pre and post distributions for these scores exhibit only 50%, 62%, 41%, and 21% overlap. For reference, the equivalent overlaps in a normal distribution would correspond to values of Cohen's d (i.e., the number of standard deviations separating the pre and post peaks) of roughly 0.9, 0.6, 1.1, and 1.9, respectively — which are actually quite large effect sizes.

Scores in the categories of organization and readability also improved somewhat, primarily at the graduate student level, but rarely at a statistically significant level. For the most part, students already possessed basic skills in organizing their thoughts and writing clearly, and these abilities only marginally improved over the span of the semester.

One of the concerns commonly expressed about writing for the general public is that, as a result of the effort to make the topic appealing and jargon-free, much of the scientific correctness of the topic can be lost (e.g. Dean, 2009). We were therefore especially interested to see if scores in the category of correctness would be anticorrelated with scores in topics such as jargon, connection, and appeal. While there is a small net loss in correctness in one of the graduate classes, none of the final correctness scores are statistically significantly different from the pre-training scores.

9.4.1.2 Comparison of different class levels

The average pre and post scores for each class is shown in Figure 9.6; the data with a statistically significant difference between the pre and post scores are indicated by asterisks. Caution should be exercised when comparing score data between classes, as each class was given different writing assignments, and differences in scores between classes are therefore at least partially dependent on this factor. In spite of this, we would like to get a sense of general trends in differences between the different class levels.

To attempt to remove some of the bias that comes from the fact that students in different classes had different assignments, we can focus on the differences in average normalized change between classes: how does the amount that students improved — out of the amount that they **could** have improved — compare between classes? In particular, are there obvious differences between the lower-division classes (1030 and 2030) and the upper-division classes (which I will use to mean 3710 and the graduate classes, 5010 and 5120)?

The distribution of the individual students' normalized changes was statistically significantly different for lower-division vs. upper-division students in the categories of jargon, readability, correctness, relevance, and appeal; upper-division students consistently improved more in these categories than did lower-division students. Looking at the information on gains contained in table 9.4, as well as the raw averages shown in Figure 9.6, it seems that the categories of relevance and appeal in particular reflect significantly greater gains in the upper-level students than in the lower-level students.

Jargon, in particular, is an interesting category: gains are higher in upper-division classes, which is in part due to the lower-division students using little jargon to begin with — the lower-division students scored an average of 4.3 out of 5 in the category of jargon on the pretest. We suspect this is largely due to two factors: they don't yet know the jargon of their field, and the articles that they were assigned to summarize didn't contain much jargon in the first place. In contrast, the articles assigned to the upper-division students were much more jargon-heavy, and

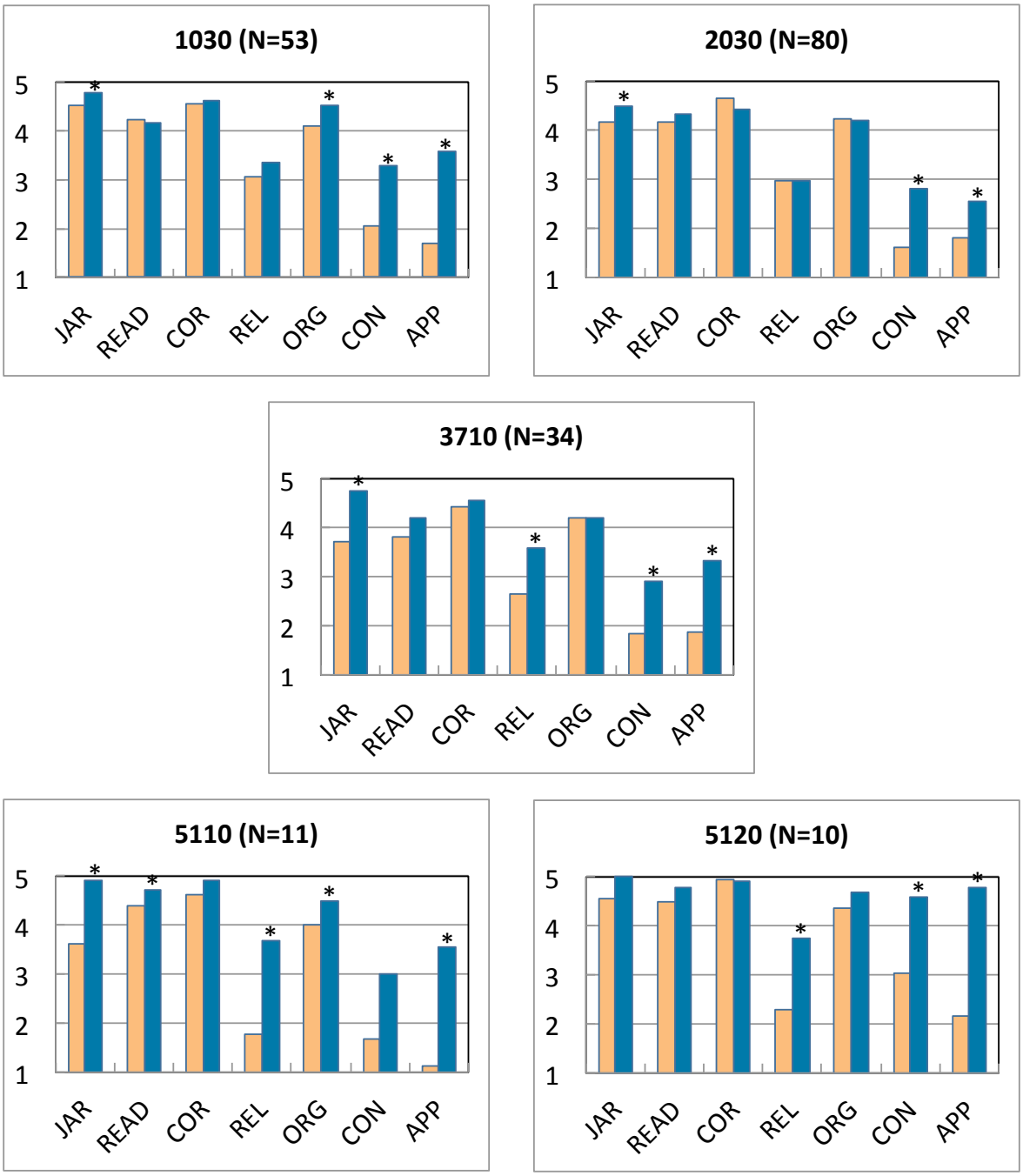

Figure 9.6: Average class pre- and post-training scores for each of the five classes. Asterisks indicate data where the difference between the pre and the post scores is statistically significant.

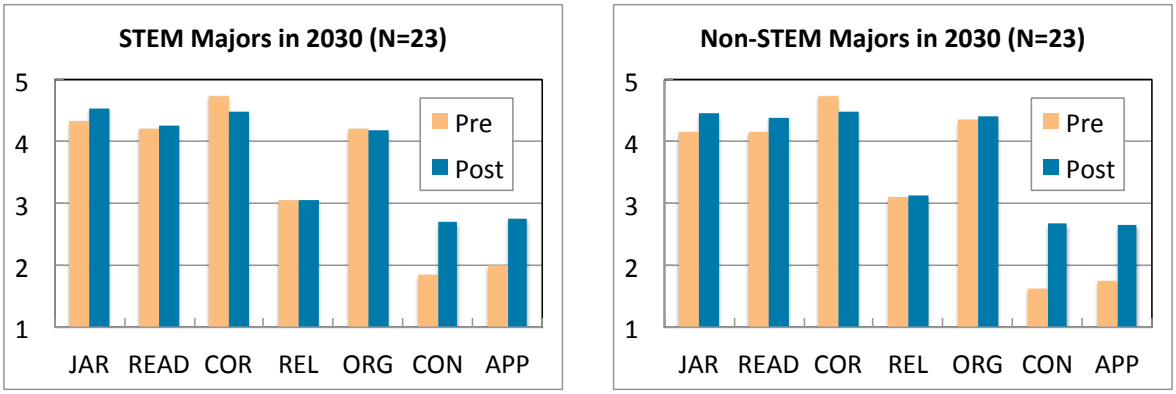

Figure 9.7: Comparison of the average scores for self-identified STEM majors and non-majors in ASTR 2030.

these students are already accustomed to expressing themselves using jargon in their field.

9.4.1.3 Comparison of STEM majors vs. non-majors

Of the 80 writing samples we had available to analyze in ASTR 2030 — the only class with a heavily mixed demographic — 46 students opted to provide information about their declared major. This group included 23 self-identified STEM majors and 23 non-majors; the average scores for these two sets of students are shown in Figure 9.7. Using only this sample, we analyzed the scores in each of these two sets of students independently. A Mann-Whitney test clearly demonstrates that the distribution of scores for majors is statistically indistinguishable from those for non-majors, both for the pre-training writing sample and the post-training sample.

Though we are dealing with small-number statistics (N=46), we suggest that these results may indicate that the set of students who are STEM majors and those who are non-majors do not generally need to be treated differently during training in a lower-division class; in the context of our study, they seem to enter with a similar knowledge base and react the same way to the training over the span of the semester. Larger studies comparing majors to non-majors are necessary, however, to draw any firm conclusions.

9.4.2 Attitudes survey analysis

All students in the five target classes were asked to optionally respond to an attitudes survey at the beginning of the semester, before any science communication training had been administered, and again at the end of the semester after all the training had been completed. The surveys probed topics such as the students' perception of the importance of science communication, the previous training the students had received in science communication, and how the students felt the training had affected their abilities to communicate science.

9.4.2.1 Importance of science communication

Both before the training and after, students were asked the question, "How important do you consider it to be for scientists to be able to communicate with the general, non-specialist public?" Somewhat surprisingly, even before any discussion of or training in science communication had occurred, responses were extremely positive: on a scale of 1 (not important) to 9 (very important), a remarkable 92% of students selected a score of 7, 8 or 9. Responses are shown, broken down by class, in Figure 9.8. Responses were effectively unchanged when the students were surveyed again at the end of the semester.

9.4.2.2 Previous training

Students were asked what, if any, training they had previously received in science communication; Figure 9.9 summarizes their responses. Unsurprisingly, the higher the level of the students, the more training they typically had received: while an average of 67% of undergraduate students reported having received no formal science communication training, only 29% of graduate students reported the same. The training that appears to be most commonly provided to students, however, pertains only to communicating with scientists; 71% of undergraduates and 60% of graduates reported either no formal training, or only training associated with communicating with scientists. These numbers are slightly lower than those quoted by the Royal Society in their 2006 report (The

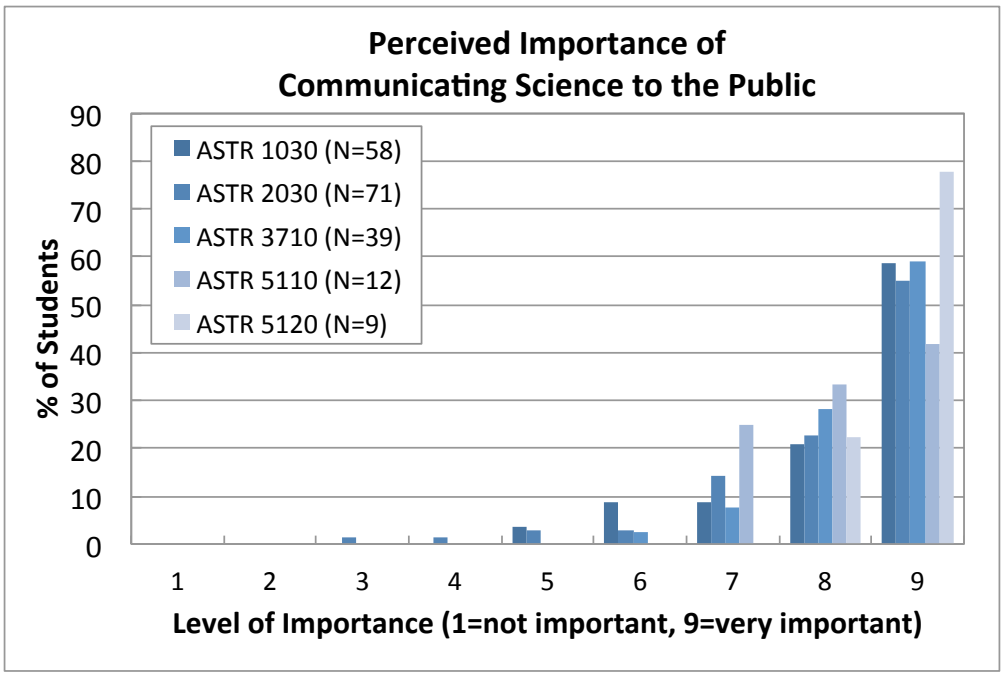

Figure 9.8: Students' initial (pre-training) responses to the question "How important do you consider it to be for scientists to be able to communicate with the general, non-specialist public?"

Royal Society, 2006), wherein 73% of the 1400+ professional scientists surveyed reported that they had never had any formal training in communicating with the non-specialist public. This may indicate that, in the past decade, some progress has been made in development of programs that provide science communication training to young scientists. Nonetheless, the percentage of students who had not received any training in communicating with the public is still quite high.

9.4.2.3 Support for communicators

Students were also asked to report how supportive they considered others to be of those who take part in activities that engage the general public. This question was intended to gauge the state of the field for young scientists today who attempt to pursue science communication and outreach activities during the course of their academic careers. Figure 9.10 summarizes the responses from participants.

Responses generally indicated that students perceive a reasonably supportive environment

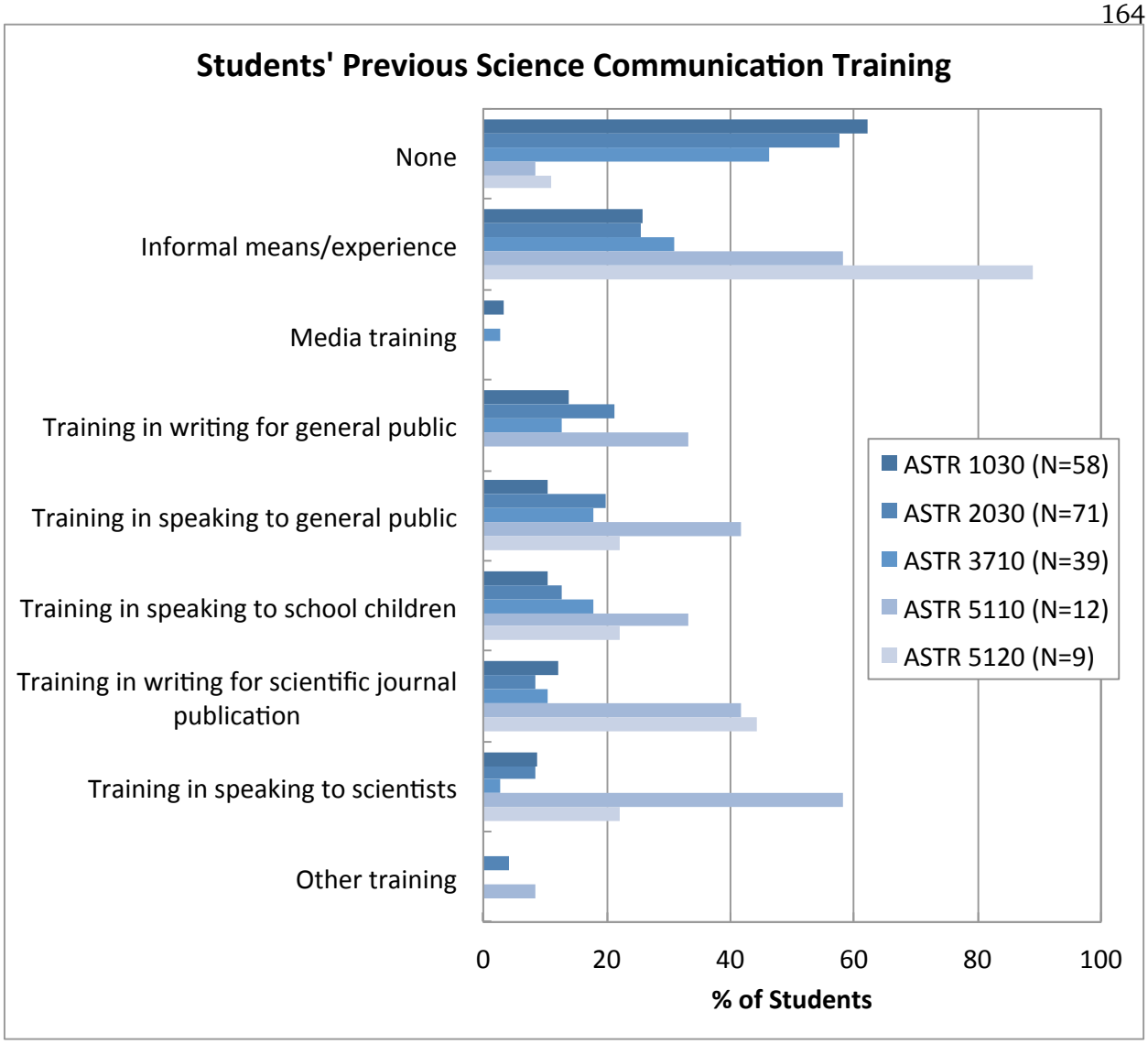

Figure 9.9: Students' self-reported previous training in science communication.

for science communicators. When averaged across the classes, $74-91\%$ of students who expressed a view reported their scientific fields, faculty in their department, peers in their department, and their advisors to be either "very supportive" or "supportive". This is a more somewhat more positive general outlook than that reported by the group of 1400+ professional scientific researchers interviewed in the United Kingdom in 2006; of the UK scientists who expressed a view, only 71% reported that the researchers in their department were "very supportive" or "fairly supportive" toward those who take part in activities that engage the non-specialist public.

Looking at the breakdown by class level, a large percentage of the students in all classes ($88-100\%$ of those who expressed a view) seemed to agree that the faculty in their department were supportive of science communicators (as measured by a response of "very supportive" or "supportive"). In the remaining categories, a far greater percentage of graduate students (ASTR 5110 and 5120) indicated support of science communicators by their peers (92-100%) and advisors ($88-100\%$) than by their field as a whole ($50-67\%$). In contrast, a larger percentage of undergraduates (ASTR 1030, 2030 and 3710) reported support of science communicators by their field ($80-86\%$) than by their peers ($76-84\%$) or — for students actively engaged in research — their advisors ($64-77\%$).

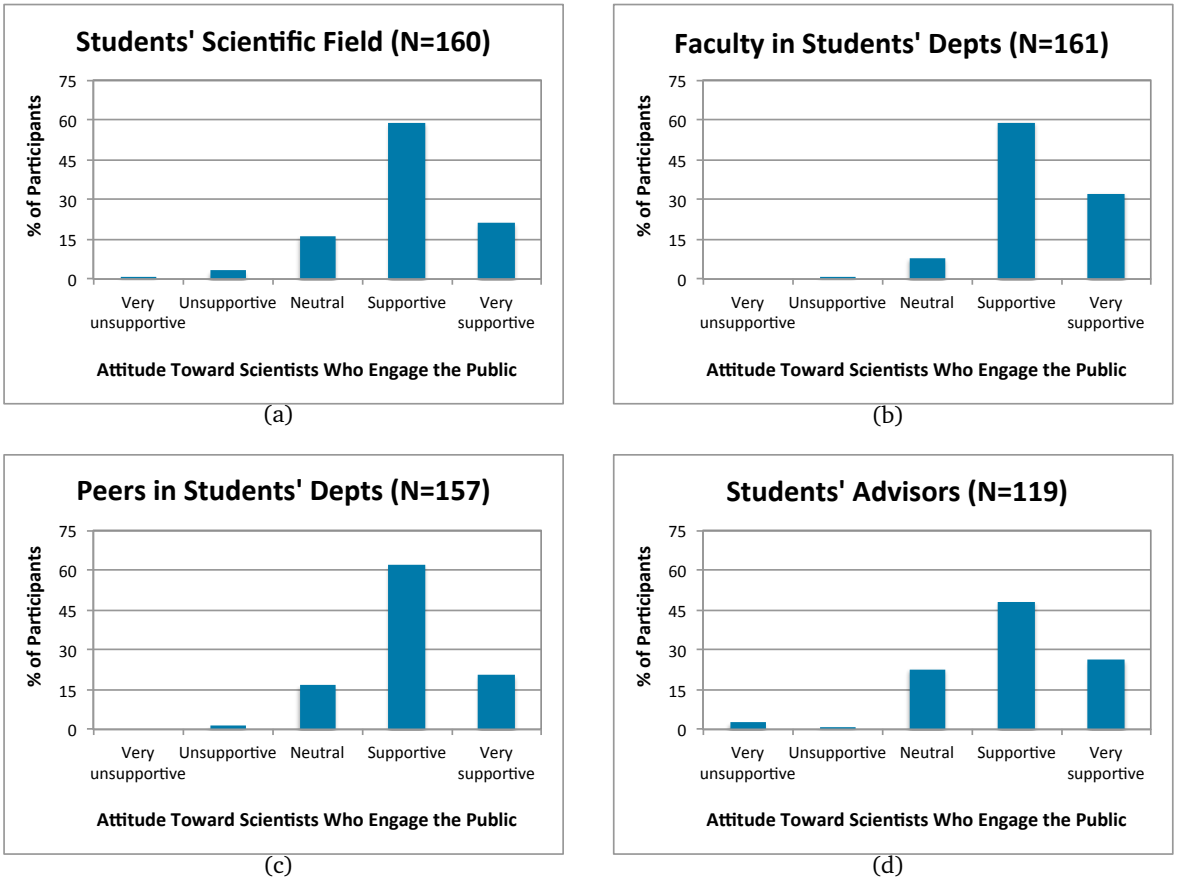

Figure 9.10: Perceived level of support for scientists who engage the public, from a) students' scientific fields, b) faculty in students' departments, c) peers in students' department, and d) students' advisors. N=160, 161, 157, and 119 for these categories respectively, for students who expressed a view (i.e., answered the question and did not select "don't know").

In general, current students seem to be far more optimistic than past generations about the opinions of scientists regarding those who participate in public engagement and communication activities. In response to the statement "Scientists who communicate a lot are not well regarded by other scientists," 72% of the students who expressed a view disagreed with the statement, compared to the 11% who agreed with it. In contrast, only 56% of the professional scientists asked the same question in the 2006 Royal Society report disagreed, and 21% agreed (The Royal Society, 2006).

9.4.2.4 Confidence Communicating

Students were asked to report their level of confidence in their science communication skills in several categories. The first category asked how comfortable they would feel submitting an article to a popular science publication, such as Wired, Popular Science, Scientific American, or Discover. Figure 9.11 displays the students' aggregate responses before and after the training. The difference in the two distributions is statistically significant, with an effect size given by a Cliff's δ of 0.38.

The difference in class levels manifests itself generally as a higher degree of confidence for upper levels. For lower-division students, only 22% reported a confidence level above 5 (on a scale of 1-9, where 9 is "very confident") prior to training, and 55% reported a score above 5 after training. In contrast, for upper-division students, those averages were 39% and 65%, respectively.

Trends in students' self-reported confidence in communicating both with scientists and with the general public were similar: both showed a significant gain between the pre-training and post-training surveys. The aggregate responses can be seen in Figure 9.12; the effect size for the shift in confidence in communicating with scientists is $\delta = 0.31$, and the effect size for the shift in confidence communicating with the general public is $\delta = 0.26$. Here again, students at higher class levels on average reported higher levels of confidence, both before and after the training. The exception is post-training scores for confidence communicating with the public: more than 90% of both lower-division and upper-division students reported a confidence level above 5.

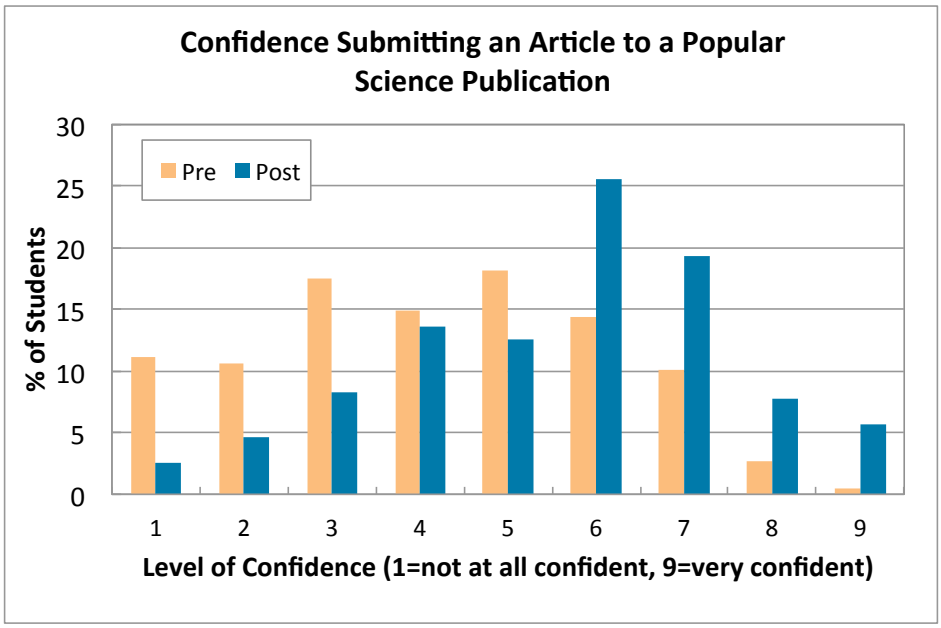

Figure 9.11: Students' confidence submitting an article to a popular science publication. Responses are aggregated for all students, with N=188 for the pre-training responses and N=192 for the post-training responses.

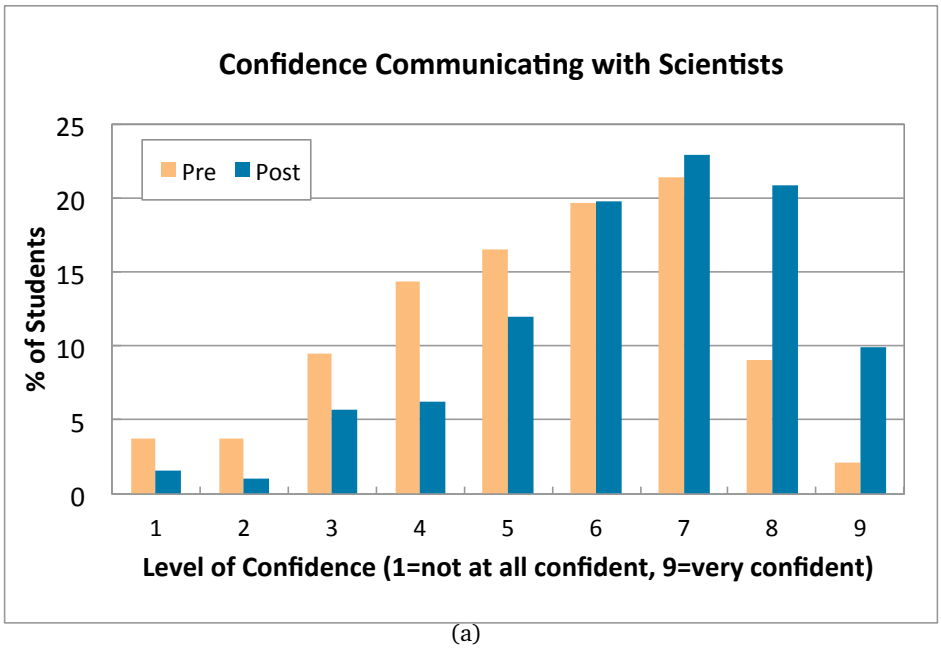

(a)

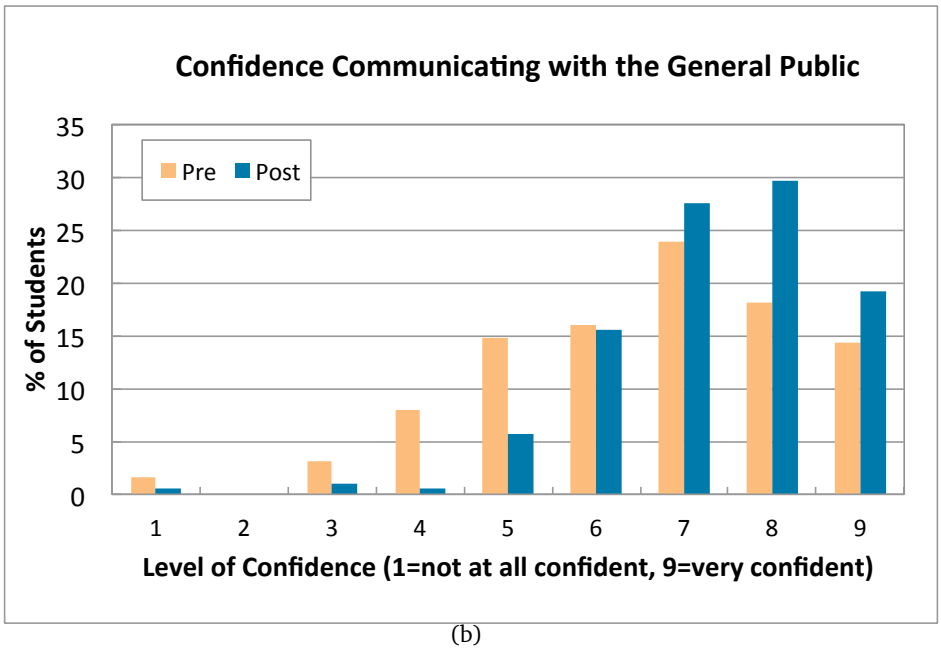

(b)

Figure 9.12: Students' reported confidence in their ability to a) communicate with scientists, and b) communicate with the general public. Responses are aggregated for all students, with N=188 for the pre-training responses and N=192 for the post-training responses.

9.4.2.5 Impressions of Training Impact

Finally, at the end of the semester students were asked to report their level of agreement with two statements: 1) I feel like I better understand the reasons why science communication is important now compared to the beginning of the semester, and 2) I feel like I better understand the elements of good science communication with the public now compared to the beginning of the semester. These questions were basically intended to gauge whether or not the students considered the training to have been worthwhile and/or effective.

Responses to these questions are shown in Figure 9.13. An average of 61% of all students agreed (selected "strongly agree" or "agree") that they better understood the importance of science communication at the end of the semester, compared to an average of 13% who disagreed (selected "disagree" or "strongly disagree"). An average of 78% agreed that they better understood the elements of good science communication with the public at the end of the semester, compared to an average of 11% who disagreed.

There was no significant difference between lower-division and upper-division students in their responses to these questions. In addition, there was no significant difference between STEM majors and non-majors in ASTR 2030 in their responses to these questions (calculated from a sample size of N=27 majors and N=30 non-majors).

9.5 Conclusion

In this study we selected five undergraduate and graduate astronomy courses offered at University of Colorado Boulder and added a small amount of science communication training to each one. The training consisted of 30 minutes of in-class lecture time, two out-of-class reading assignments, four or five writing assignments given as homework, and two or three peer-grading assignments also done out of class. This training was designed to tie in to the topical class material and create as little disruption to the normal class instruction and goals as possible. We have presented in this paper an analysis of the results from this experiment, with our primary goal being to

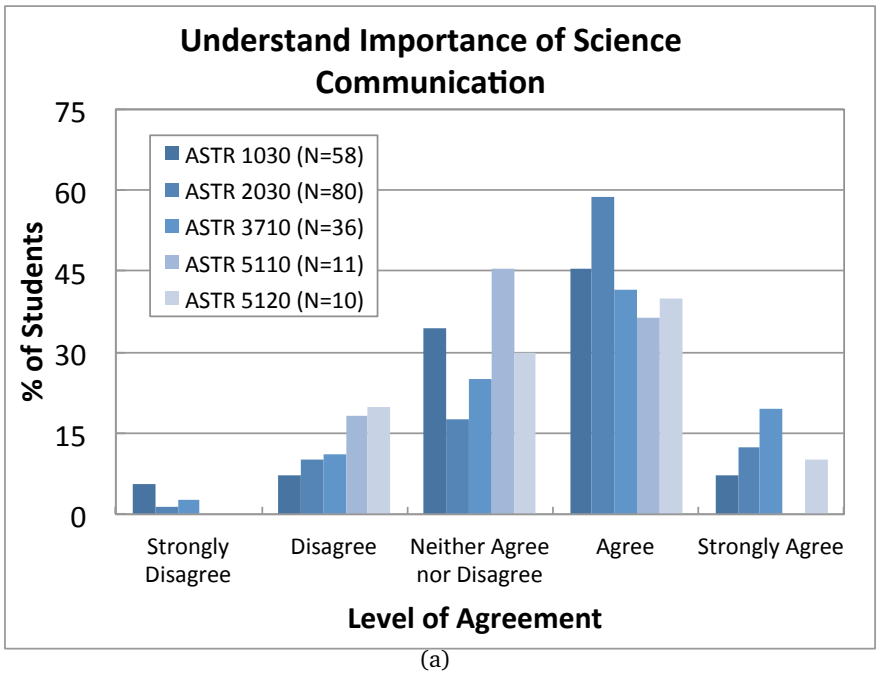

(a)

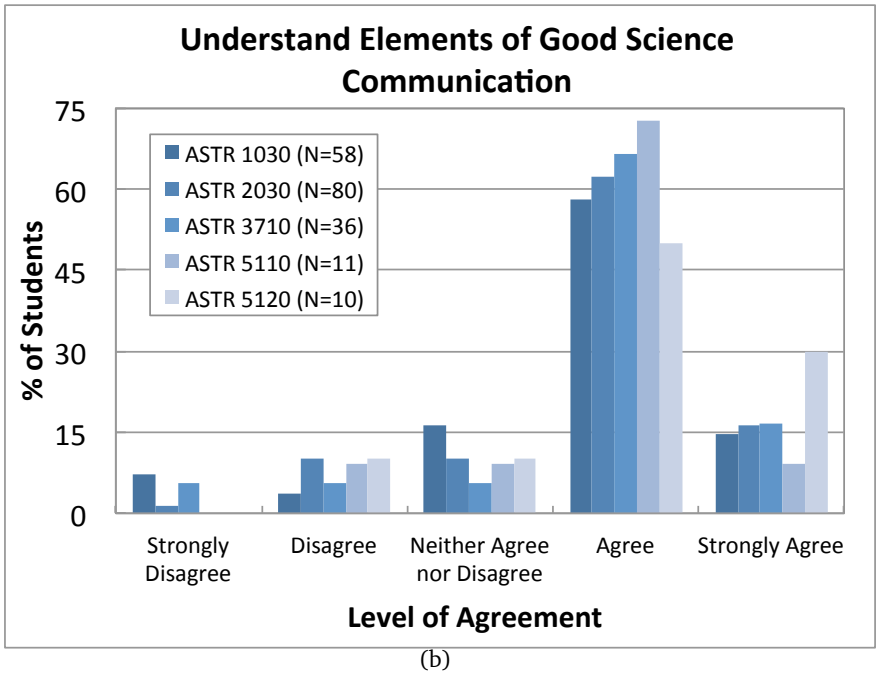

(b)

Figure 9.13: Students' post-training agreement with the statements a) "I feel like I better understand the reasons why science communication is important now compared to the beginning of the semester," and b) "I feel like I better understand the elements of good science communication with the public now compared to the beginning of the semester."

determine whether this minimal science communication training is enough to effect change in a) students' written ability to communicate science to the general public, and b) students' attitudes toward science communication. Our secondary goal was to determine if there exists a specific time in students' careers when it is most appropriate to provide them with science communication training.

9.5.1 Success of Training

The primary result of our analysis is that students' writing for the general public significantly improved over the span of the semester in several categories. The biggest changes can be seen in students' abilities to write with minimal jargon, to express the relevance of the science topic to the reader, to write using elements of appeal, and to use analogies and connections to which the reader can relate. Perhaps more importantly, students did not become significantly less able to express scientific topics **correctly** as a result of their increased skills in writing for the general public; thus there do not seem to have been any negative consequences as a result of the students having received this training.

Students' attitudes toward science communication were not significantly changed over the course of the semester — but this is largely because they entered the training with already very positive attitudes toward science communication and public engagement in general. Student survey responses seem to indicate not only that they personally have a positive view of the importance of science communication, but also that they believe that scientists in general are far more supportive of science communicators than has been the view in the past (e.g. The Royal Society, 2006). Whether this implies that the "Sagan Effect" of science communicators being ill-regarded by the scientific community has diminished in recent years, or whether it simply means that the students are still too early in their scientific careers to yet have encountered this mindset, is unclear.

Students were overall very receptive to the science communication training and provided positive feedback. Their reported confidence in communicating significantly improved after the training — both in the category of communicating with the public, which was the primary focus of the training, and in the category of communicating with scientists, which was much less em-

phasized. Moreover, students generally reported at the end of the semester that they felt they had gained knowledge of both why science communication is important and how to communicate effectively.

9.5.2 Timing of Training

Perhaps surprisingly, there was no significant difference between lower-division and upper-division (in which we include graduate-level) students in their perceptions of the importance of science communication or their attitudes towards this training. We expected there to be greater resistance to these concepts amongst the upper-division students, but this does not appear to be the case based on the survey responses we received: lower- and upper-division students all consistently agreed upon the importance of science communication and about the usefulness of the training that they received over the semester.

Analysis of the writing samples of lower-division and upper-division students separately revealed a few key differences between the two groups, however. Upper-division students demonstrated a greater improvement than lower-division students in the abilities to communicate with elements of appeal, to communicate with minimal jargon, and to communicate the relevance of the scientific topic to the reader. A likely explanation is that many habits of professional scientists — such as communicating with peers using field-specific jargon, or writing with the primary purpose of communicating as much information as compactly as possible — are developed gradually in science students as they progress in their careers. In the process of becoming accustomed to these professional habits, they also become less able to relate effectively to a non-specialist audience.

9.5.3 Recommendations

The fact that so few students reported having previously received any formal training in communicating science with a non-specialist audience serves to illustrate the lack of formal training programs in place. These numbers, combined with the students' clear recognition of the importance of science communication, indicates the need for such programs to provide communication training

to young scientists as a part of their professional development.

In spite of the difference in gains between lower-division and upper-division students, the fact remains that both groups demonstrated significant improvement in their abilities to communicate with the public and their confidence in doing so — as well as their confidence in communicating with scientists. We see no reason, therefore, not to introduce science communication training at a basic level into any undergraduate- or graduate-level science class; we believe that the training presented here can be relatively easily implemented by any instructor and used to complement the science material in the class. We hope that the results shown in this paper will provide a starting point for discussion on how to encourage broad implementation of similar training in university STEM classes.

Acknowledgements

SK was funded by University of Colorado Boulder's Center for STEM Learning through a Chancellor's Award. SK thanks Fran Bagenal, Mitch Begelman, Phil Armitage, Andrew Hamilton, and Rosalba Perna for their generous cooperation in allowing their classes to be included in this study. SK also thanks Briana Ingermann for assistance with writing-sample analysis and Noah Finkelstein for helpful discussions about this project.

Chapter 10

Conclusion

This thesis investigated two types of causality and communication: the physics of relativistic astrophysical outflows, and the implementation of science communication training for undergraduate and graduate students in STEM fields.

In Chapter 3 we presented two models for the pressure confinement and resulting acceleration of a hydrodynamic, ultrarelativistic jet that has lost causal contact with its environment. In this scenario a shocked boundary layer forms where the jet impacts the ambient medium; one of our models considered the jet structure under the assumption that the pressure within the boundary layer is a function only of the radial distance from the source, and does not have any horizontal structure, whereas the other model allowed for the development of a transverse pressure gradient across the layer. We found a set of solutions fully describing the boundary layer flow in both cases, and demonstrated that, when pressure is allowed to vary across the boundary layer, changing how steeply the pressure drops off outside of the jet affects whether the jet fills to the axis or instead piles up all of its material in a narrow sheath around its outer edge.

In Chapter 4 we expanded upon the model in Chapter 3 by adding the effects of a toroidal magnetic field threading the jet. We demonstrated that the boundary layer will always become magnetically dominated far from the source, and we found a set of solutions fully describing the boundary layer flow in this limit. We showed that the magnetic case differed in structure from the hydrodynamic case: the magnetically-dominated boundary layer becomes thinner with increasing radius, and it is bounded on the inside not by a shock front, but by a rarefaction front through

which material leaves the boundary layer and rejoins the jet. In spite of this, the layer contains a sharp pressure gradient and functions as an insulating buffer between the jet and the ambient environment.

In Chapter 5 we revisited the work in Chapter 3 and asked what would happen if we relaxed some of our original assumptions, such as that the flow must be irrotational, isentropic, and adiabatic. We showed that in the case where the external pressure decreases slowly, solutions can be constructed wherein the entropy increases within the boundary layer with increasing distance from the source, presumably due to multiple shocks driven into the flow as it gradually collimates. We demonstrated that the acceleration rate of the jet slowed as a result, and that this process provides a source of internal energy that could be channeled into radiation.

In Chapter 6 we considered time-dependent properties of relativistic outflows, rather than the steady-state views presented in the previous chapters. We investigated the spectral properties of the 40 brightest gamma-ray flares detected by the *Fermi* Large Area Telescope in the first four years of its mission. We identified the significant spectral breaks and demonstrated that they occur at broadly-distributed energies, disfavoring the model of spectral break production by absorption. We also found that the flares exhibited significant spectral variability and argued, based on our analysis, that the highly regular gamma-ray spectra of blazars integrated over long time scales emerge from a superposition of many short-lived components with relatively narrow spectra.

In Chapter 8 we evaluated a science communication workshop for STEM graduate students and used this evaluation to assess the current environment for students interested in science communication, as well as whether or not our training tactics in the workshop were effective and well-received. We found that, despite the students being an elite group of science communicators, they had received little formal training previously, indicating a need for such training programs. We demonstrated that students after the workshop had significantly improved their skills in communicating without jargon and explaining the relevance of their research to a general audience in an interesting way, and we showed that their confidence in various forms of communication had also increased.

In Chapter 9 we took the idea of science communication training for students one step further, and analyzed a program wherein science communication training was inserted into five astronomy classes for undergraduate and graduate students. We found the training to be successful: in spite of the training being fairly minimal and not taking up much class time, it had the outcome that students improved their ability to communicate without jargon, while acknowledging the big picture, in a way that keeps the interest of a general audience. We found that the greatest impact was on upper-division and graduate classes, but we suggest that because this training positively impacted all levels and had no negative consequences, it could (and should!) be implemented in any STEM classroom.

Bibliography

Abdo, A. A., et al. 2009, ApJ, 699, 817

—. 2010a, ApJ, 722, 520

—. 2010b, ApJ, 710, 1271

—. 2010c, ApJ, 716, 30

—. 2011, ApJ, 733, L26

Ackermann, M., et al. 2010, ApJ, 721, 1383

—. 2011, ApJ, 743, 171

—. 2012, ApJS, 203, 4

Aharonian, F., et al. 2005, A&A, 430, 865

Alexander, D. M., & Hickox, R. C. 2012, New Astronomy Reviews, 56, 93

Aloy, M. A., Janka, H.-T., & Müller, E. 2005, A&A, 436, 273

Atwood, W. B., et al. 2009, ApJ, 697, 1071

Bao, L. 2006, American journal of physics, 74, 917

Baram-Tsabari, A., & Lewenstein, B. V. 2013, Science Communication, 35

Barkov, M. V., & Baushev, A. N. 2011, New Astronomy, 16, 46

Baron, N. 2010, Escape from the ivory tower: a guide to making your science matter (Island Press)

Basken, P. 2009, Chronicle of Higher Education, 55

Beckwith, K., Hawley, J. F., & Krolik, J. H. 2008, ApJ, 678, 1180

—. 2009, ApJ, 707, 428

Begelman, M. C. 1995, Proceedings of the National Academy of Science, 921, 11442

—. 1998, ApJ, 493, 291

Begelman, M. C., Blandford, R. D., & Rees, M. J. 1984, Reviews of Modern Physics, 56, 255

Begelman, M. C., Fabian, A. C., & Rees, M. J. 2008, MNRAS, 384, L19

Begelman, M. C., & Li, Z.-Y. 1994, ApJ, 426, 269

Benford, G. 1978, MNRAS, 183, 29

Beskin, V. S. 2009, MHD Flows in Compact Astrophysical Objects: Accretion, Winds and Jets (Springer)

Beskin, V. S., Kuznetsova, I. V., & Rafikov, R. R. 1998, MNRAS, 299, 341

Besley, J. C., & Nisbet, M. 2013, Public Understanding of Science, 22, 644

Besley, J. C., Oh, S. H., & Nisbet, M. 2012, Public Understanding of Science, 22, 971

Besley, J. C., & Tanner, A. H. 2011, Science Communication, 33, 239

Blandford, R. D. 1976, MNRAS, 176, 465

Blandford, R. D., & Payne, D. G. 1982, MNRAS, 199, 883

Blandford, R. D., & Znajek, R. L. 1977, MNRAS, 179, 433

Bowater, L., & Yeoman, K. 2013, Science Communication: A Practical Guide for Scientists, First Edition (West Sussex, UK: John Wiley & Sons, Ltd)

Bozdogan, H. 1987, Psychometrika, 52, 345

Bridle, A. H., & Perley, R. A. 1984, ARA&A, 22, 319

Bromberg, O., Granot, J., Lyubarsky, Y., & Piran, T. 2014, MNRAS, 443, 1532

Bromberg, O., & Levinson, A. 2007, ApJ, 671, 678

—. 2009, ApJ, 699, 1274

Bromberg, O., Nakar, E., Piran, T., & Sari, R. 2011, ApJ, 740, 100

Burns, T. W., O'Connor, D. J., & Stocklmayer, S. M. 2003, Public Understanding of Science, 12, 183

Cerruti, M., Dermer, C. D., Lott, B., Boisson, C., & Zech, A. 2013, ApJ, 771, L4

Chiueh, T., Li, Z.-Y., & Begelman, M. C. 1991, ApJ, 377, 462

Christensen, L. L. 2007, The hands-on guide for science communicators (Springer)

Cliff, N. 1993, Psychological Bulletin, 114, 494

Coe, R. 2002, Education-line

Cohen, J. 1960, Educational and Psychological Measurement, 20, 37

—. 1968, Psychological bulletin, 70, 213

—. 1977, Statistical power analysis for the behavioral sciences (rev (Lawrence Erlbaum Associates, Inc)

Cohen, M. H., Cannon, W., Purcell, G. H., Shaffer, D. B., Broderick, J. J., Kellermann, K. I., & Jauncey, D. L. 1971, ApJ, 170, 207

Contopoulos, J. 1995, ApJ, 446, 67

Contopoulos, J., & Lovelace, R. V. E. 1994, ApJ, 429, 139

Coughlin, E. R., & Begelman, M. C. 2014, ApJ, 781, 82

Davies, S. R. 2008, Science Communication

Dean, C. 2009, Am I making myself clear? A scientist's guide to talking to the public (Harvard University Press)

Ding, L., & Liu, X. 2012, in Getting Started in PER, 3rd edn., Vol. 2 (American Association of Physics Teachers)

Dixon, W. G. 1978, Special relativity: the foundation of macroscopic physics. (Cambridge Univ. Press)

Doeleman, S. S., et al. 2012, Science, 338, 355

Dudo, A. 2012, Science Communication, 35, 476

Eichler, D. 1982, ApJ, 263, 571

—. 1993, ApJ, 419, 111

Fabian, A. C. 1999, Proceedings of the National Academy of Sciences, 96, 4749

Finke, J. D., & Dermer, C. D. 2010, ApJ, 714, L303

Fossati, G., Maraschi, L., Celotti, A., Comastri, A., & Ghisellini, G. 1998, MNRAS, 299, 433

Georganopoulos, M., & Marscher, A. P. 1998, ApJ, 506, 621

Goldstein, A., et al. 2011, ArXiv e-prints

Gomez, J. L., Marti, J. M. A., Marscher, A. P., Ibanez, J. M. A., & Marcaide, J. M. 1995, ApJ, 449, L19

Hake, R. R. 1998, American journal of Physics, 66, 64

Hallgren, K. A. 2012, Tutorials in quantitative methods for psychology, 8, 23

Harris, J., Chadwick, P. M., & Daniel, M. K. 2014, MNRAS, 441, 3591

Harris, J., Daniel, M. K., & Chadwick, P. M. 2012, ApJ, 761, 2

Hartz, J., & Chappell, R. 1997, Worlds apart: How the distance between science and journalism threatens America's future (First Amendment Center)

Hawley, J. F., & Krolik, J. H. 2006, ApJ, 641, 103

Heyvaerts, J., & Norman, C. 1989, ApJ, 347, 1055

Hoyle, F., Burbidge, G. R., & Sargent, W. L. W. 1966, Nature, 209, 751

Jorstad, S. G., Marscher, A. P., Mattox, J. R., Wehrle, A. E., Bloom, S. D., & Yurchenko, A. V. 2001, ApJS, 134, 181

Jorstad, S. G., et al. 2005, AJ, 130, 1418

Junor, W., Biretta, J. A., & Livio, M. 1999, Nature, 401, 891

Kaspi, S., Smith, P. S., Maoz, D., Netzer, H., & Jannuzi, B. T. 1996, The Astrophysical Journal Letters, 471, L75

Kiernan, V. 2003, Science Communication, 25, 3

Kohler, S., & Begelman, M. C. 2012, MNRAS, 426, 595

Kohler, S., Begelman, M. C., & Beckwith, K. 2012, MNRAS, 422, 2282

Koide, S. 2004, ApJ, 606, L45

Komissarov, S. S. 1994a, MNRAS, 269, 394

—. 1994b, MNRAS, 266, 649

—. 1999, MNRAS, 308, 1069

—. 2011, Mem. Soc. Astron. Italiana, 82, 95

Komissarov, S. S., Barkov, M. V., Vlahakis, N., & Königl, A. 2007, MNRAS, 380, 51

Komissarov, S. S., & Falle, S. A. E. G. 1997, MNRAS, 288, 833

Komissarov, S. S., Vlahakis, N., Königl, A., & Barkov, M. V. 2009, MNRAS, 394, 1182

Kompaneets, A. S. 1960, Soviet Physics Doklady, 5, 46

Krippendorff, K. 1980, Content Analysis: An Introduction to Its Methodology (SAGE Publications)

Landau, L. D., & Lifshitz, E. M. 1959, Fluid mechanics (Butterworth-Heinemann)

Landis, J. R., & Koch, G. G. 1977, biometrics, 159

Lazzati, D., & Begelman, M. C. 2005, ApJ, 629, 903

Levinson, A., & Eichler, D. 2000, Physical Review Letters, 85, 236

Lewis, F., Butler, A., & Gilbert, L. 2011, Methods in Ecology and Evolution, 2, 155

Lithwick, Y., & Sari, R. 2001, ApJ, 555, 540

Lord, F. M. 1959, Psychometrika, 24, 1

Lovelace, R. V. E. 1976, Nature, 262, 649

Lyubarsky, Y. 2009, ApJ, 698, 1570

—. 2011, Phys. Rev. E, 83, 016302

Maraschi, L., Ghisellini, G., & Celotti, A. 1992, ApJ, 397, L5

Marscher, A. 2010, in Lecture Notes in Physics, Vol. 794, The Jet Paradigm, ed. T. Belloni (Springer Berlin / Heidelberg), 173–201, 10.1007/978-3-540-76937-8_7

Marscher, A. P. 2006, in American Institute of Physics Conference Series, Vol. 856, Relativistic Jets: The Common Physics of AGN, Microquasars, and Gamma-Ray Bursts, ed. P. A. Hughes & J. N. Bregman, 1–22

Marx, J., & Cummings, K. 1998, AAPT Announcer, 29, 81

Marx, J. D., & Cummings, K. 2007, American Journal of Physics, 75, 87

McKinney, J. C., & Blandford, R. D. 2009, MNRAS, 394, L126

Meier, D. 2003, in New Views on Microquasars, ed. P. Durouchoux, Y. Fuchs, & J. Rodriguez, 165

Meissel, K. L. D. 2014, PhD thesis, The University of Auckland

Micceri, T. 1989, Psychological Bulletin, 105, 156

Micono, M., Bodo, G., Massaglia, S., Rossi, P., Ferrari, A., & Rosner, R. 2000, A&A, 360, 795

Nalewajko, K. 2013, MNRAS, 430, 1324

Nalewajko, K., & Sikora, M. 2009, MNRAS, 392, 1205

Narayan, R., McKinney, J. C., & Farmer, A. J. 2007, MNRAS, 375, 548

Nelkin, D. 1995, Selling science–How the press cover science and technology

Nisbet, M. C. 2009, Environment: Science and Policy for Sustainable Development, 51

Nolan, P. L., et al. 2012, ApJS, 199, 31

Novick, M. R. 1966, Journal of Mathematical Psychology, 3, 1

Offit, P., & Coffin, S. E. 2003, Vaccine, 22, 1

Paisley, W. J. 1998, Science Communication, 20, 70

Perucho, M., Martí, J. M., Cela, J. M., Hanasz, M., de La Cruz, R., & Rubio, F. 2010, A&A, 519, A41

Phillips, D. P., & others. 1991, New England Journal of Medicine, 325, 1180

Piran, T. 2004, Reviews of Modern Physics, 76, 1143

Poutanen, J., & Stern, B. 2010, ApJ, 717, L118

Povoledo, E., & Fountain, H. 2012, New York Times

Proga, D., MacFadyen, A. I., Armitage, P. J., & Begelman, M. C. 2003, ApJ, 599, L5

Ramirez, R. M., Kopparapu, R., Zugger, M. E., Robinson, T. D., Freedman, R., & Kasting, J. F. 2014, Nature Geoscience, 7, 59

Rolke, W. A., López, A. M., & Conrad, J. 2005, Nuclear Instruments and Methods in Physics Research A, 551, 493

Rosswog, S., & Brüggen, M. 2007, Introduction to high-energy astrophysics (Cambridge University Press Cambridge)

Saito, S., Stawarz, Ł., Tanaka, Y. T., Takahashi, T., Madejski, G., & D'Ammando, F. 2013, ApJ, 766, L11

Sanders, N. E., et al. 2012, AER, 1, 01020

Sari, R., Piran, T., & Halpern, J. P. 1999, ApJ, 519, L17

Schirato, T., & Yell, S. 1997, Communication and Cultural Literacy: An Introduction (Allen & Unwin)

Sikora, M., Begelman, M. C., & Rees, M. J. 1994a, ApJ, 421, 153

—. 1994b, ApJ, 421, 153

Slater, S., et al. 2011, Discipline-Based Science Education Research: A Scientist's Guide (W. H. Freeman)

Stern, B. E., & Poutanen, J. 2011, MNRAS, 417, L11

—. 2014, ArXiv e-prints

Stevens, S. S. 1946, Science, 103, 677

Tchekhovskoy, A., Metzger, B. D., Giannios, D., & Kelley, L. Z. 2014, MNRAS, 437, 2744

Tchekhovskoy, A., Narayan, R., & McKinney, J. C. 2010, New Astronomy, 15, 749

The Royal Society. 1985, The Public Understanding of Science (London, England: The Royal Society)

—. 2006, Factors affecting science communication: A survey of scientists and engineers (London, England: The Royal Society)

The Wellcome Trust. 2000, The Role of Scientists in Public Debate Report (London: Wellcome Trust)

Tomimatsu, A. 1994, PASJ, 46, 123

Treise, D., & Weigold, M. F. 2002, Science Communication, 23, 310

Wagner, S. J., et al. 1995, A&A, 298, 688

Wallace, C. S. 2011, PhD thesis, University of Colorado Boulder

Weigold, M. F. 2001, Science Communication, 23

Wilcox, R. R. 1987, New statistical procedures for the social sciences: Modern solutions to basic problems (Psychology Press)

Worseck, G., et al. 2011, The Astrophysical Journal Letters, 733, L24

Zakamska, N. L., Begelman, M. C., & Blandford, R. D. 2008, ApJ, 679, 990

Zauderer, B. A., et al. 2011, Nature, 476, 425

Appendix A

Additional Derivations

A.1 Derivation of Governing Equations under the Kompaneets Approximation

The following is a more detailed derivation of Eqs 3.5–3.6 from Chapter 3. These are coupled differential equations that describe the shock front and contact discontinuity of the boundary layer surrounding an ultrarelavtistic jet that has lost causal contact, in the specific limit where the boundary layer is treated as having constant pressure across its width, known as the Kompaneets approximation.

We begin again from the relativistic oblique shock-jump conditions across the shock front:

$$n_j \Gamma_j \beta_{j,x} = n_s \Gamma_s \beta_{s,x} \tag{A.1}$$

$$w_j \Gamma_j^2 \beta_{j,x} = w_s \Gamma_s^2 \beta_{s,x} \tag{A.2}$$

$$w_j \Gamma_j^2 \beta_{j,x}^2 + p_j = w_s \Gamma_s^2 \beta_{s,x}^2 + p_s \tag{A.3}$$

$$\beta_{j,y} = \beta_{s,y} \tag{A.4}$$

where the x-direction is chosen perpendicular to the shock front and the y-direction is tangential (see Figure 3.1). Here $w \equiv \epsilon + p$ where ϵ is the total proper energy density, given by $\epsilon = \rho + 3p$. Considering the case of an ultrarelativistic gas in the regime where the jet is still accelerating, we assume that $nmc^2 \ll p$ and the equation of state is $p = \epsilon/3$, such that $w \approx 4p$. Thus the energy jump condition (A.2) and momentum conservation (A.3) become

$$p_j \Gamma_j u_{j,x} = p_s \Gamma_s u_{s,x} \tag{A.5}$$

$$4 p_j u_{j,x}^2 + p_j = 4 p_s u_{s,x}^2 + p_s \tag{A.6}$$

where $u_x \equiv \Gamma\beta_x$ is the four-velocity component along the shock normal. Eq (A.5) is now rewritten as

$$\frac{p_s}{p_j} = \frac{u_{j,x}^2}{u_{s,x}^2}\chi \tag{A.7}$$

with $\chi \equiv \dfrac{\beta_{s,x}}{\beta_{j,x}}$. Combining this and Eq (A.6), we eliminate $u_{s,x}$ and obtain an expression for the pressure ratio which involves only $u_{j,x}$ and χ:

$$\frac{p_s}{p_j} = 1 + 4u_{j,x}^2(1-\chi). \tag{A.8}$$

We now work to eliminate χ by recalling the definition of the Lorentz factor Γ for the jet and shock regions:

$$\Gamma_{j(s)}^2 \equiv \frac{1}{a - \beta_{j(s),x}^2} \tag{A.9}$$

where we have defined a as $a \equiv 1 - \beta_{j,y}^2$ and employed the shock jump condition $\beta_{j,y} = \beta_{s,y}$. Using this and the definition $u_x^2 \equiv \beta_x^2\Gamma^2$, Eq (A.7) becomes

$$\frac{p_s}{p_j} = \frac{\frac{a}{\beta_{j,x}^2} - \chi^2}{(\frac{a}{\beta_{j,x}^2} - 1)\chi} = \frac{1 + u_{j,x}^2(1-\chi^2)}{\chi}. \tag{A.10}$$

Equating Eq (A.8) and Eq (A.10), we find the following two solutions for χ:

$$\chi = \begin{cases} 1 \\ \dfrac{u_{j,x}^2 + 1}{3u_{j,x}^2}. \end{cases} \tag{A.11}$$

The shock solution is the second of these two, giving the correct relativistic result of $\chi \to \frac{1}{3}$ as $u_{j,x}^2 \to \infty$. Denoting the angle Ψ_j as the angle between a given jet streamline and the tangent to the shock front, we can write

$$\beta_{j,x} = |\boldsymbol{\beta}_j| \sin\Psi_j \approx \sin\Psi_j \tag{A.12}$$

for ultrarelativistic flow. Substituting this and the solution for χ back into Eq (A.10), we obtain

$$\frac{p_s}{p_j} = \frac{8u_{j,x}^2 - 1}{3} = \frac{8\Gamma_j^2 \sin^2\Psi_j - 1}{3}. \tag{A.13}$$

Now examining the geometry of the problem, we recognize that $\sin\Psi_j$ can be represented in terms of θ_j and α_j, respectively the angle the streamline makes with the z-axis and the angle that the shock tangent makes with the z-axis. By noting that $\sin\Psi_j = \sin(\theta_j - \alpha_j)$ and $\tan\alpha_j = \frac{dr_j}{dz}$, and assuming conical streamlines such that $\tan\theta_j = \frac{r_j}{z}$, we write

$$\sin^2\Psi_j \quad = \quad \frac{\left(r_j - z\frac{dr_j}{dz}\right)^2}{\left(r_j^2 + z^2\right)\left(1 + \left(\frac{dr_j}{dz}\right)^2\right)}. \tag{A.14}$$

Solving for $\sin^2\Psi_j$ in Eq (A.13) and equating this to the geometric solution above, we obtain our final differential equation governing the shape of the inner shock wall,

$$\frac{\left(r_j - z\frac{dr_j}{dz}\right)^2}{\left(r_j^2 + z^2\right)\left(1 + \left(\frac{dr_j}{dz}\right)^2\right)} \quad = \quad \frac{1}{8\Gamma_j^2}\left(3\frac{p_s}{p_j} + 1\right), \tag{A.15}$$

labeled as Eq (3.5) in Chapter 3.

As noted at the beginning of this section, the pressure ratio has a dependence upon r and z:

$$\frac{p_s}{p_j} \quad = \quad \frac{p_{s,0}}{p_{j,0}}\frac{z^{-\eta}}{(\cos\Theta_0)^{-4}\,(r^2+z^2)^{-2}}, \tag{A.16}$$

where $\frac{p_{s,0}}{p_{j,0}}$ is the pressure ratio at the initial impact point and $(\cos\Theta_0)^{-4}$ is a normalization term. Similarly, the free expansion in the interior of the jet results in the Lorentz factor scaling as

$$\Gamma_j \quad = \quad \Gamma_{j,0}\cos\Theta_0(r^2+z^2)^{1/2} \tag{A.17}$$

with $\Gamma_{j,0}$ describing the Lorentz factor at the initial impact point. Inserting these expressions back into Eq (A.15), we can analytically solve for $\frac{dr_j}{dz}$ and later numerically integrate this to find $r_j(z)$.

To solve for the shape of the outer wall of the shocked layer, the contact discontinuity, we use a slight modification of the method described in BL07. Energy-momentum conservation ensures that

$$\nabla\cdot\mathbf{F}_s = 0, \tag{A.18}$$

where $\mathbf{F}_s$ is the energy flux, or the zeroth component of the energy-momentum tensor, within the shocked layer. We can integrate this equation over a volume of the shocked boundary layer of

the jet, bounded on either side by the shock r_j and the contact discontinuity r_c, and bounded on the bottom and top by horizontal planes at z and $z + dz$. But by Gauss's theorem, this integral is equivalent to an integral of the flux through the surfaces of the bounded volume, which can further be written out in terms of the individual surfaces:

$$\begin{aligned} 0 &= \int_V (\nabla \cdot \mathbf{F}_s) dV && \text{(A.19)} \\ &= \int_S (\mathbf{F}_s \cdot \hat{\mathbf{n}}) dS && \text{(A.20)} \\ &= \left(\int_{r_j}^{r_c} (\mathbf{F}_s \cdot \hat{\mathbf{z}}) 2\pi r dr \right) \Big|_{z+dz} + \left(\int_{r_j}^{r_c} (\mathbf{F}_s \cdot (-\hat{\mathbf{z}})) 2\pi r dr \right) \Big|_z \\ &\quad + \int_{\partial\Omega_j} (\mathbf{F}_s \cdot \hat{\mathbf{n}}_j) dS_j + \int_{\partial\Omega_c} (\mathbf{F}_s \cdot \hat{\mathbf{n}}_c) dS_c, && \text{(A.21)} \end{aligned}$$

where $\hat{\mathbf{n}}_{j(c)}$ is a unit vector normal to the shock (contact discontinuity) surface, $\partial\Omega_{j(c)}$ denotes integration over the portion of the shock (contact discontinuity) surface enclosed between z and $z + dz$, and $dS_{j(c)}$ is the corresponding surface area element. Here the terms in Eq (A.21) refer to the flux through the top surface, bottom surface, shock surface, and contact discontinuity surface of the bounded volume, respectively.

Denoting the relativistic flux through these surfaces by

$$\mathbf{F} = w\Gamma^2 \boldsymbol{\beta} = 4p\Gamma^2 \boldsymbol{\beta}, \tag{A.22}$$

we can first note that the last integral in Eq (A.21) will be equal to zero since, by definition, the velocity is parallel to the contact discontinuity, meaning that $\boldsymbol{\beta}_s \cdot \hat{\mathbf{n}}_c = 0$. We may further interpret Eq (A.21) by noting that the surface element at the shock (contact discontinuity) surface can be written as

$$dS_{j(c)} = 2\pi r_{j(c)} \frac{dz}{\cos \alpha_{j(c)}}, \tag{A.23}$$

where $\alpha_{j(c)}$ is the angle the tangent to the shock (contact discontinuity) makes with the z-axis, as described previously (see Figure 3). As $\boldsymbol{\beta}_j \cdot \hat{\mathbf{n}}_j = -|\boldsymbol{\beta_j}| \sin \Psi_j$, we now have

$$\left(\int_{r_j}^{r_c} (4p_s \Gamma_s^2 \beta_{s,z}) 2\pi r dr \right) \Big|_z^{z+dz} = \int_z^{z+dz} (4p_j \Gamma_j^2 |\boldsymbol{\beta}_j| \sin \Psi_j) 2\pi r_j \frac{dz}{\cos \alpha_j}. \tag{A.24}$$

In order to make this problem analytically tractable, we now assume that the flow parameters within the shock depend only on the vertical distance z. Thus we are able to perform the integral over r on the left-hand side of Eq (A.24). Now examining the right-hand side we see that, for a small interval dz, the integral can be closely approximated by evaluating the integrand at z and multiplying it by the interval dz. Thus we have

$$p_s\Gamma_s^2\beta_{s,z}(r_c^2 - r_j^2)\Big|_z^{z+dz} = 2p_j\Gamma_j^2|\boldsymbol{\beta}_j|r_j\frac{\sin\Psi_j}{\cos\alpha_j}dz. \tag{A.25}$$

Dividing both sides of the equation by dz and employing the definition of d/dz to transform the left-hand side, we achieve the final equation governing the contact discontinuity:

$$\frac{d}{dz}\left(p_s\Gamma_s^2\beta_{s,z}(r_c^2 - r_j^2)\right) = 2p_j\Gamma_j^2|\boldsymbol{\beta}_j|r_j\frac{\sin\Psi_j}{\cos\alpha_j}, \tag{A.26}$$

which is Eq (3.6) in Chapter 3.

Appendix B

ComSciCon Materials

B.1 ComSciCon 2013 Application

Science Communication Workshop 2013 Application

Graduate students in all fields of science and engineering are invited to apply.
For more information about the workshop, please visit: http://workshop.astrobites.com/

First Name:

Last Name:

Email Address:

Phone Number:

University:

Current Position:

- Graduate Student (Masters)
- Graduate Student (Ph.D.)
- Other

Expected Graduation Date:

Field of Study:
Choose the one with which you most identify

- Astronomy/astrophysics
- Biology
- Chemistry

- Computer Science
- Engineering: Biological
- Engineering: Chemical
- Engineering: Civil
- Engineering: Mechanical
- Engineering: Other
- Geology/Earth Science
- Materials Science
- Mathematics
- Physics
- Social Science

Would you be able to attend the entire workshop?
The workshop will run from June 13-15, 2013 in Cambridge, MA

- yes
- no

Would you need to travel to attend the workshop?

- No, I live in or near Cambridge, MA
- Yes, I would need to travel and would require accommodations

What city and state would you be traveling from?

- I would not need travel assistance or accommodations
- Other:

Your Experience Communicating Science

Please briefly describe (1-2 sentences each) two experiences you have had communicating science to an audience other than researchers in your field. These could be long-term or short-term experiences, oral or written projects, online or in person, for K-12 students or adults, etc.

- **Communication Experience #1** (1-2 sentences only):
- **Communication Experience #2** (1-2 sentences only):

Short Answer Questions

Why do you want to attend this workshop? In what way will it assist you in your future career?
Please write no more than 150 words.

Writing sample prompt: how would you describe your research to the general public?
Please write no more than 100 words.

Additional Comments
This will not be considered when evaluating your application; please use this space to list any questions or concerns you have about the workshop.

B.2 Surveys

Survey #1 (Pre-Workshop)

Personal Information

Your name will be used only to match your responses from the pre-and post-workshop surveys. All identifying information will be separated from your responses to the remainder of the survey.

Name

Current University

Email

Press Info: We're interested in contacting local media outlets about ComSciCon 2013! Please list newspapers that service your local area. Include both university papers and city or regional papers.

If we contact these papers, may we give them your contact information?

Demographics

The following optional questions are for statistical purposes only.

Gender

- Male
- Female
- Other:

Ethnicity

- I am Hispanic or Latino
- I am not Hispanic or Latino

Race
(Choose one or more)

- American Indian or Alaska Native
- Asian
- Black or African American

- Native Hawaiian or Other Pacific Islander
- White
- Other

Citizenship

- US citizen
- Permanent US resident
- International

Personal Background
(Questions $1-3$ of 18)

(1) **Year in graduate school you will be beginning in Fall 2013**

- 1
- 2
- 3
- 4
- 5
- 6 or higher

(2) **Field of Study**

Choose the one with which you most identify

- Astronomy/astrophysics
- Biology
- Chemistry
- Computer Science
- Engineering: Biological
- Engineering: Chemical
- Engineering: Civil
- Engineering: Mechanical
- Engineering: Other
- Geology/Earth Science
- Materials Science
- Mathematics
- Physics
- Social Science

(3) **Career Goals**

Check all possible careers you are considering.

- Academia
- Industry
- Government
- Science policy
- K-12 teaching
- Public outreach
- Writing/publishing

- Other:

ComSciCon 2013
(Questions $4-6$ of 18)

(4) **Why are you attending ComSciCon 2013?**

(5) **What is the main thing you hope to get out of the workshop?**

(6) **Which panel(s) or speaker(s) are you most looking forward to? Why?**
As a reminder, the panels are:

- Session 1: Engaging Non-Scientific Audiences
- Session 2: Science Writing for a Cause
- Session 3: Communicating Science Through Fiction
- Session 4: Sharing Science with Scientists
- Session 5: Interacting with the Media
- Session 6: World of Non-Academic Publishing
- Session 7: Communicating with Multimedia and the Web

Science Communication Background
(Questions $7-12$ of 18)

(7) **What training, if any, have you had in communicating science before now? Check all that apply. Do not include any teaching training you may have had.**

- None
- Media training on being interviewed by journalists
- Training in writing for the general public
- Training in writing for scientific journal publication
- Training in speaking to the general public
- Training in speaking to other scientists
- Training in speaking to school children (of any age)
- Informal means / experience
- Other:

(8) **If you indicated that you have had science communication training, who provided it?**

(9) **On a scale of 1 (not at all confident) to 9 (very confident), how comfortable would you feel submitting an article to a popular science publication (e.g. Wired, Popular Science, Scientific American, Discover)?**

(10) **On a scale of 1 (not at all confident) to 9 (very confident), how confident are you in:**

- **Your ability to communicate with scientists?**
- **Your ability to communicate with the general public?**

(11) **How do you think you gained the science communication skills you have?**

(12) **What do you think would make you more confident in your science communication skills?**

Science Communication Attitudes
(Questions $13-18$ of 18)

(13) **How important do you feel it is that you personally, in your current post, directly engage with each of the following groups about your research? Please rate importance on a scale of 1 (not important) to 5 (very important).**

(a) General journalists (e.g. press, TV, radio, etc)
(b) Schools and school teachers
(c) Young people outside of school
(d) Policy makers
(e) Industry/business community (other than where directly concerned with funding your research)
(f) The general, non-specialist public
(g) Non-governmental organizations (e.g. nonprofits)

(14) **Thinking about public engagement with, and communication about, science, roughly how many times in the past 12 months have you done each of the following?**
Scale:

- **None**
- **Once**
- **2-3 times**
- **4-5 times**
- **More than 5 times**

(a) Worked with teachers/schools (including writing educational materials)
(b) Given a public lecture, including being part of a panel
(c) Taken part in a public dialogue event/debate

(d) Been interviewed on radio
(e) Been interviewed by a newspaper journalist
(f) Written for the non-specialist public (including for the media, articles and books)
(g) Engaged with policy makers
(h) Engaged with non-governmental organizations (e.g. nonprofits)
(i) Worked with science centers/museums
(j) Judged competitions
(k) Given a talk to the scientific community
(l) Written for the scientific community (in any form)

(15) **How important do you think it is that you personally, in your current post, engage directly with the non-specialist adult public on each of the following? Please rate importance on a scale of 1 (not important) to 5 (very important)**

(a) The scientific findings of your research
(b) Areas of further research
(c) Policy and regulatory issues
(d) The wider social and ethical implications of your research findings for society
(e) The potential benefits of your work to individuals
(f) The scientific process/the nature of science
(g) Scientific uncertainty
(h) The enjoyment and excitement of doing science
(i) The relevance of science to everyday life
(j) To raise awareness of career options in science

(16) **Below are some things scientists have said about engaging with the non-specialist public about science and engineering. Please indicate whether you agree or disagree for each statement.**

Scale:

- **Strongly Agree**
- **Agree**
- **Neither**
- **Disagree**
- **Strongly Disagree**
- **Don't know**

(a) Scientists who communicate a lot are not well regarded by other scientists
(b) Funders of scientific research should help scientists to communicate with the non-specialist public
(c) Scientists have a moral duty to engage with the non-specialist public about the social and ethical implications of their research

(d) I don't think my research is interesting to the non-specialist public

(e) The main reason to engage with the non-specialist public is to get their support for science and engineering

(f) I simply don't have time to engage with the non-specialist public

(g) I would not want to be forced to take a public stance on the issues raised by my research

(h) Engagement with the non-specialist public is best done by trained professionals and journalists

(i) Engaging the non-specialist public in science is personally rewarding

(j) My research is too specialized to make much sense to the non-specialist public

(k) I would need help to develop a science engagement project

(l) I would be happy to take part in a science engagement activity that was organized by someone else

(m) Public engagement could help with my career

(n) Engaging with the non-specialist public is best done by senior researchers

(o) There are no personal benefits for me in engaging with the non-specialist public

(17) **How supportive do you perceive the following groups/individuals to be towards those who take part in activities that engage the general, non-specialist public?**

Scale:

- **Very supportive**
- **Fairly supportive**
- **Not particularly supportive**
- **Not at all supportive**
- **Don't know**

(a) Your field as a whole

(b) Faculty in your department

(c) Your advisor

(d) Your peers in your department

(18) **How much time, on average, do you intend to spend on communicating science to non- experts in your future career?**

- $0-2$ hrs/week
- $2-5$ hrs/week
- $5-10$ hrs/week
- $10-20$ hrs/week
- $20+$ hrs/week

Survey #2 (Post-Workshop)

Personal Information
Your name, university, and email will be used only to match your responses from the pre- and post-workshop surveys. All identifying information will be separated from your responses to the remainder of the survey.

Name

Current University

Email

Career Goals
(Question 1 of 22)

(1) **Career Goals**

Check all possible careers you are considering.

- Academia
- Industry
- Government
- Science policy
- K-12 teaching
- Public outreach
- Writing/publishing
- Other:

ComSciCon 2013
(Questions $2-12$ of 22)

(2) **Why did you attend ComSciCon2013?**

(3) **What was the most memorable thing you learned?**

(4) **How do you think you will apply this new knowledge?**

(5) **Which panel(s) or speaker(s) had the greatest impact on you and why?**
As a reminder, the panels were:

- Session 1: Engaging Non-Scientific Audiences

- Session 2: Science Writing for a Cause
- Session 3: Communicating Science Through Fiction
- Session 4: Sharing Science with Scientists
- Session 5: Interacting with the Media
- Session 6: World of Non-Academic Publishing
- Session 7: Communicating with Multimedia and the Web

(6) **Which was your least favorite panel and why?**

(7) **What was the best piece of advice you received in this workshop?**

(8) **Do you think this workshop was the appropriate length?**

(9) **Is there anything you wish had been a part of this workshop that wasn't?**

(10) **Do you have any suggestions for improving this workshop?**

(11) **Do you have any suggestions for future panel topics and/or panelists?**

(12) **Do you have any other comments about ComSciCon 2013?**

Science Communication Confidence
(Questions $13-14$ of 22)

(13) **On a scale of 1 (not at all confident) to 9 (very confident), how comfortable would you feel submitting an article to a popular science publication (e.g. Wired, Popular Science, Scientific American, Discover)?**

(14) **On a scale of 1 (not at all confident) to 9 (very confident), how confident are you in:**

- **Your ability to communicate with scientists?**
- **Your ability to communicate with the general public?**

Science Communication Attitudes
(Questions $15-18$ of 22)

(15) **How important do you feel it is that you personally, in your current post, directly engage with each of the following groups about your research? Please rate importance on a scale of 1 (not important) to 5 (very important).**

(a) General journalists (e.g. press, TV, radio, etc)
(b) Schools and school teachers
(c) Young people outside of school

(d) Policy makers

(e) Industry/business community (other than where directly concerned with funding your research)

(f) The general, non-specialist public

(g) Non-governmental organizations (e.g. nonprofits)

(16) **How important do you think it is that you personally, in your current post, engage directly with the non-specialist adult public on each of the following? Please rate importance on a scale of 1 (not important) to 5 (very important)**

(a) The scientific findings of your research

(b) Areas of further research

(c) Policy and regulatory issues

(d) The wider social and ethical implications of your research findings for society

(e) The potential benefits of your work to individuals

(f) The scientific process/the nature of science

(g) Scientific uncertainty

(h) The enjoyment and excitement of doing science

(i) The relevance of science to everyday life

(j) To raise awareness of career options in science

(17) **Below are some things scientists have said about engaging with the non-specialist public about science and engineering. Please indicate whether you agree or disagree for each statement.**

Scale:

- **Strongly Agree**
- **Agree**
- **Neither**
- **Disagree**
- **Strongly Disagree**
- **Don't know**

(a) Scientists who communicate a lot are not well regarded by other scientists

(b) Funders of scientific research should help scientists to communicate with the non-specialist public

(c) Scientists have a moral duty to engage with the non-specialist public about the social and ethical implications of their research

(d) I don't think my research is interesting to the non-specialist public

(e) The main reason to engage with the non-specialist public is to get their support for science and engineering

(f) I simply don't have time to engage with the non-specialist public

(g) I would not want to be forced to take a public stance on the issues raised by my research

(h) Engagement with the non-specialist public is best done by trained professionals and journalists

(i) Engaging the non-specialist public in science is personally rewarding

(j) My research is too specialized to make much sense to the non-specialist public

(k) I would need help to develop a science engagement project

(l) I would be happy to take part in a science engagement activity that was organized by someone else

(m) Public engagement could help with my career

(n) Engaging with the non-specialist public is best done by senior researchers

(o) There are no personal benefits for me in engaging with the non-specialist public

(18) **How much time, on average, do you intend to spend on communicating science to non- experts in your future career?**

- $0-2$ hrs/week
- $2-5$ hrs/week
- $5-10$ hrs/week
- $10-20$ hrs/week
- $20+$ hrs/week

Writing Sample
(Questions $19-20$ of 22)

(19) **Writing sample prompt: how would you describe your research to the general public?**

(20) **May we also include the writing sample from your ComSciCon application in this study?**

Networking
(Questions $19-20$ of 22)

(21) **Below is a list of all workshop participants. Please indicate which of these participants you had ALREADY interacted with BEFORE the workshop, and the level of the interaction.**

(22) **Below is a list of all workshop participants. Please indicate which of these participants you interacted with DURING the workshop, and the level of the interaction.**

Survey #3 (6-Month Follow-Up)

Personal Information

Your name will be used only to match your responses from the pre-and post-workshop surveys. All identifying information will be separated from your responses to the remainder of the survey.

Name

Current University

Email

Career Goals
(Question 1 of 8)

(1) **Career Goals**
Check all possible careers you are considering.

- Academia
- Industry
- Government
- Science policy
- K-12 teaching
- Public outreach
- Writing/publishing
- Other:

ComSciCon 2013
(Questions $2-5$ of 8)

(2) **How has your participation in ComSciCon 2013 changed your work over the last 6 months?**

(3) **How has your participation in ComSciCon 2013 advanced your professional goals?**

(4) **How has your participation in ComSciCon 2013 changed your career plans?**

(5) **Thinking about public engagement with, and communication about, science, roughly how many times in the past 12 months have you done each of the following?**
Scale:

- **None**
- **Once**
- **2-3 times**
- **4-5 times**
- **More than 5 times**

(a) Worked with teachers/schools (including writing educational materials)
(b) Given a public lecture, including being part of a panel
(c) Taken part in a public dialogue event/debate
(d) Been interviewed on radio
(e) Been interviewed by a newspaper journalist
(f) Written for the non-specialist public (including for the media, articles and books)
(g) Engaged with policy makers
(h) Engaged with non-governmental organizations (e.g. nonprofits)
(i) Worked with science centers/museums
(j) Judged competitions
(k) Given a talk to the scientific community
(l) Written for the scientific community (in any form)

Contact
(Questions $6-7$ of 18)

(6) **Have you had any further communication with any of the *speakers* from ComSciCon 2013? If yes, how many? Please describe the level of communication (one email, multiple emails, one phone conversation, etc). Please list the speakers with whom you've communicated, if you can!**

(7) **Have you had any further communication with any of the other *attendees* from ComSciCon 2013? If yes, how many? Please describe the level of communication (one email, multiple emails, one phone conversation, etc). Please list the attendees with whom you've communicated, if you can!**

Press
(Question 8 of 8)

(8) **To your knowledge, did a paper in your local area cover ComSciCon 2013?**

Appendix C

Science Communication Training in the Classroom Materials

C.1 Sample Training Materials

C.1.1 Sample Lesson Plan Outlines

Lesson Plan #1

Outline of topics that will be covered:

(1) Intro: Example of bad science communication

(2) Brainstorm ideas with class: Why is it important to be able to communicate science to others? Some suggestions:

  (a) promoting a scientifically-literate society

  (b) promoting a science-oriented society: need to convince policy makers and voters that funding scientific research is worthwhile

  (c) moral obligation: taxpayer funding should be justified

  (d) moral obligation: what are some examples of what happens when science communication doesn't happen effectively?

    (i) public perception of vaccines

    (ii) public perception of climate change

    (iii) aftermath of the L'Aquila earthquake

(3) Discuss: What makes for good science communication with the public?

  (a) **Jargon:** Are you being careful to avoid or explain words that the public might not know?

  (b) **Readability:** Are you avoiding run-on sentences and making your message clear?

  (c) **Correctness:** Are you presenting correct information?

  (d) **Relevance:** Have you told me why I should care about this?

  (e) **Organization**: Does your paragraph build upon itself in a clear, logical way?

  (f) **Connection**: Are you using analogies or making connections to things your audience might have experienced in everyday life?

(g) **Appeal**: Do you somehow hook the reader, use humor in your writing, or tell a story to interest your audience?

Lesson Plan #2

Goal: expose students to examples that reinforce the aspects of good science communication taught in the previous lesson (**jargon, readability, correctness, relevance, organization, connection, appeal**).

First activity: Break into groups and have students practice giving one-minute talks describing a basic scientific concept. Arm each student with two cards, one that reads "jargon" and one that reads "awesome", which they can hold up during the one-minute talks to flag jargon and let students know when they're explaining things well.

Second activity: Have students examine two writing samples about the same topic: one that uses many traits of good science communication and one that uses few such traits. Have students rate each one using the seven-level rubric, and discuss what the writers did/didn't do well.

C.1.2 In-Class Handout

ASTR XXXX Handout
Fall 2013

Aspects of Good Science Communication

(1) **Jargon**

Are you being careful to avoid or explain words that the public might not know?

Here's an example of a jargon-heavy research description:

> My research is on the relativistic blazar jets that are emitted from AGN. These jets are observed to travel at velocities that are within a fraction of a percent of c, but the cause of their acceleration and collimation is unclear.

Here's a better way to describe the same research to an audience that isn't likely to be familiar with astrophysical terms:

> My research is on the extremely fast-moving jets that are emitted from the centers of some very active galaxies. These jets are moving almost at the speed of light, but we're not sure what causes them to reach these enormous speeds. We also don't know why the jets are shaped in a tight column instead of spraying out in all directions.

Avoiding jargon is not the same as "dumbing things down" — it just means being aware of your audience and whether or not they're familiar with words that have specialized meanings. If your audience is a group of astronomers, "dark matter" might not be jargon, but "polymer" might be. If your audience is a group of chemists, the opposite may be true.

(2) **Readability**

Are you avoiding run-on sentences and making your message clear?

When writing for the public, the rule of thumb is to try to stick with one idea per sentence. When you use complicated compound sentences, the main point often ends up getting lost.

(3) **Correctness**

Are you presenting correct information?

This one's pretty self-explanatory:

> The newly-discovered exoplanet is teeming with fluffy green rabbits. Scientists hope to be able to send astronauts armed with carrots to this planet by 2017.

is only good science communication if it's true (which would be awesome).

(4) **Relevance**

Have you told me why I should care about this?

This version may get the information across:

> We are currently approaching the end of the 11-year solar cycle, at which point the Sun's magnetic field will flip its polarity.

But this version tells people why they should care:

> We are currently approaching the end of the 11-year solar cycle, at which point the Sun's magnetic field will flip its polarity. This part of the cycle is when the Sun will be the most active, which can result in solar storms and space weather that might affect astronauts in space, or even knock out power grids on Earth.

(5) **Organization**

Does your paragraph build upon itself in a clear, logical way?

Here's an example of an organized explanation that first presents the main idea and then provides supporting details:

> There are two main aspects of the game of soccer that would change on Mars: the force with which players would need to kick the ball, and players' ability to "bend" the ball. Players would have to change how hard they kick the ball because the acceleration due to gravity on Mars is much lower than that on Earth. This means that a ball given a specific initial angle and velocity would fly considerably further on Mars than on Earth. The players' ability to bend the ball would change because bending relies on air resistance to deflect a spinning ball's path. Since the Martian atmosphere is much thinner than Earth's, there would be significantly less air resistance on the ball in flight — effectively preventing bending.

(6) **Connection**

Are you using analogies or making connections to things your audience might have experienced in everyday life?

This could come in the form of an analogy or metaphor:

> Small daily flares are observed from the black hole in the center of our galaxy. One proposed explanation for these flares is that Sgr A* frequently snacks on passing asteroids.

Or a connection to common knowledge:

> The radiation dose from these incoming muons on an average-sized life form is slightly more than a ten-millionth of a Sievert (a measurement of radiation). For comparison, a ten-millionth of a Sievert is roughly the same radiation you're exposed to by eating a banana, 1 Sievert will produce mild radiation sickness in humans, and a level of 4-5 Sieverts is fatal to humans.

Or a connection to a previous event or recent news story:

> Space debris poses a threat in a number of ways. First, it has the potential to collide with the ISS: just this June astronauts had to take shelter in the Soyuz capsule due to concern about a piece of approaching space junk. The debris can also deorbit in an unpredictable way and, if large enough, survive the atmosphere and reach Earth's surface — remember the satellite that made headlines last month, or ROSAT's very recent demise?

(7) **Appeal**

Do you somehow hook the reader, use humor in your writing, or tell a story to interest your audience?

There are lots of ways to hook a reader! One option is to open with a compelling question:

> Looking for something fun to consider today? Try this on for size: what happens to life on Earth if a gamma-ray burst points at us from within our own galaxy?

Humor could come in the form of ironic language or understatement:

> Ionization of the atmosphere and depletion of the ozone layer would probably result in insta-sunburn, mutations and cancer, and disintegration of the food chain as we know it — all of which would be somewhat unfortunate.

And here's an example of using storytelling to open an article:

> On an air force base in California, there is a building from which the positions and trajectories of approximately 22,000 pieces of space junk are continually monitored. Every spent rocket booster, or defunct satellite — in fact, every man-made object in Earth's orbit that's larger than 10cm in diameter — is carefully tracked. And while that sounds like a lot of debris, that's only a small fraction of what is out there.

C.1.3 Sample Reading Assignment

Read the article on gamma-ray bursts, linked below. Besides reading for content, also pay attention to things that the author does and doesn't do well in writing for the general public.

Remember, some things to consider when writing for the general public include:

(1) **Jargon:** Is the writer being careful to avoid or explain words that the public might not know?

(2) **Readability:** Does the writer avoid run-on sentences and make his/her message clear?

(3) **Correctness:** Is the writer presenting correct information?

(4) **Relevance:** Has the writer told you why you should care about this?

(5) **Organization**: Does the writer's paragraph build upon itself in a clear, logical way?

(6) **Connection**: Does the writer use analogies or make connections to things his/her audience might have experienced in everyday life?

(7) **Appeal**: Does the writer somehow hook the reader, use humor in his/her writing, or tell a story to interest his/her audience?

Article: `http://www.nytimes.com/2003/06/20/science/20GAMM.html`

C.1.4 Sample Writing Assignment

Read the article on imaging black holes, linked below. Then write a paragraph (between 100 and 200 words) summarizing it at a level that a member of the general, non-specialist public will be able to understand.

Remember, some things to consider when writing for the general public include:

(1) **Jargon:** Is the writer being careful to avoid or explain words that the public might not know?

(2) **Readability:** Does the writer avoid run-on sentences and make his/her message clear?

(3) **Correctness:** Is the writer presenting correct information?

(4) **Relevance:** Has the writer told you why you should care about this?

(5) **Organization**: Does the writer's paragraph build upon itself in a clear, logical way?

(6) **Connection**: Does the writer use analogies or make connections to things his/her audience might have experienced in everyday life?

(7) **Appeal**: Does the writer somehow hook the reader, use humor in his/her writing, or tell a story to interest his/her audience?

Article: `http://www.nbcnews.com/science/incredible-technology-how-see-invisible-black-hole-6C10654146`

Enter your paragraph here (100-200 words):

C.2 Attitudes Surveys

Attitudes Survey #1

Personal Information

Your name and student number will be used only to match your responses from the pre-and post-workshop surveys. All identifying information will be separated from your responses to the remainder of the survey.

Name:
Student Number:

Demographics

The following optional questions are for statistical purposes only.

Gender

- Male
- Female
- Other:

Ethnicity

- I am Hispanic or Latino
- I am not Hispanic or Latino

Race
(Choose one or more)

- American Indian or Alaska Native
- Asian
- Black or African American
- Native Hawaiian or Other Pacific Islander
- White
- Other

Citizenship

- US citizen
- Permanent US resident
- International

Academic Background
(Questions 1-2 of 10)

(1) **Year in school**

- freshman
- sophomore
- junior
- senior
- 5th year or above undergrad
- grad student

(2) **Field of Study**

Choose the one with which you most identify

- Astronomy/astrophysics
- Other STEM (science/technology/engineering/math) field
- Non-STEM field
- Undeclared

Science Communication Background
(Questions 3-7 of 11)

(3) **What training, if any, have you had in communicating science before now? Check all that apply. Do not include any teaching training you may have had.**

- None
- Media training on being interviewed by journalists
- Training in writing for the general public
- Training in writing for scientific journal publication
- Training in speaking to the general public
- Training in speaking to other scientists
- Training in speaking to school children (of any age)
- Informal means / experience
- Other:

(4) **If you indicated that you have had science communication training, who provided it?**

(5) **What experiences, if any, have you had in communication before now? Check all that apply.**

- Teaching (K-12)
- Teaching (university-level teaching assistant or instructor)
- Tutoring
- Giving public talks
- Giving scientific talks
- Publishing a paper
- Participating in public outreach events
- Participating in debate club/team or similar
- Taking an acting class or performing in plays, etc.
- Taking a journalism class or writing for a newpaper, etc.
- Writing for a blog
- Other experiences:

(6) **On a scale of 1 (not at all confident) to 9 (very confident), how comfortable would you feel submitting an article to a popular science publication (e.g. Wired, Popular Science, Scientific American, Discover)?**

(7) **On a scale of 1 (not at all confident) to 9 (very confident), how confident are you in:**

- **Your ability to communicate with scientists?**
- **Your ability to communicate with the general public?**

Science Communication Attitudes
(Questions 8-11 of 11)

(8) **On a scale of 1 (not at all important) to 9 (very important), how important do you consider it to be for scientists to be able to communicate with the general, non-specialist public?**

(9) **How important do you think it is for scientists to engage directly with the non-specialist adult public on each of the following? Please rate importance on a scale of 1 (not important) to 5 (very important).**

(a) The scientific findings of their research
(b) Areas of further research
(c) Policy and regulatory issues
(d) The wider social and ethical implications of their research findings for society
(e) The potential benefits of their work to individuals
(f) The scientific process/the nature of science
(g) Scientific uncertainty
(h) The enjoyment and excitement of doing science

(i) The relevance of science to everyday life

(j) To raise awareness of career options in science

(10) **Below are some things scientists have said about engaging with the non-specialist public about science and engineering. Please indicate whether you agree or disagree for each statement.**

Scale:

- **Strongly Agree**
- **Agree**
- **Neither**
- **Disagree**
- **Strongly Disagree**
- **Don't know**

(a) Scientists who communicate a lot are not well regarded by other scientists

(b) Funders of scientific research should help scientists to communicate with the non-specialist public

(c) Scientists have a moral duty to engage with the non-specialist public about the social and ethical implications of their research

(d) A lot of scientific research isn't interesting to the non-specialist public

(e) The main reason to engage with the non-specialist public is to get their support for science and engineering

(f) Engagement with the non-specialist public is best done by trained professionals and journalists

(g) A lot of scientific research is too specialized to make much sense to the non-specialist public

(h) In order to communicate with the public, scientists need to determine the public's opinions on science issues

(i) Public engagement could help with scientists' careers

(j) Engaging with the non-specialist public is best done by senior researchers

(k) The main reason to engage with the non-specialist public is to provide them with information

(l) There are no personal benefits for scientists engaging with the non-specialist public

(m) If the general public understood science better then there would be more public support of science

(n) It is important to get public input into science policy issues

(11) **(Answer if you are in a STEM field only) How supportive do you perceive the following groups/individuals to be towards those who take part in activities that engage the general, non-specialist public?**

Scale:

- **Very supportive**
- **Fairly supportive**
- **Not particularly supportive**
- **Not at all supportive**
- **Don't know**

(a) Your field as a whole
(b) Faculty in your department
(c) Your peers in your department
(d) Your advisor (select "Don't know" if you don't have an advisor)

Attitudes Survey #2

Personal Information
Your name and student number will be used only to match your responses from the pre-and post-workshop surveys. All identifying information will be separated from your responses to the remainder of the survey.

Name:
Student Number:

Science Communication Training
(Questions 1-7 of 10)

(1) **On a scale of 1 (not at all useful) to 9 (very useful), rate how useful you found the science communication training in the class.**

(2) **What would have made the training more useful?**

(3) **Do you have any other comments about the science communication training?**

(4) **Rate your agreement with the following statement: I feel like I better understand the reasons why science communication is important now compared to the beginning of the semester.**

- Strongly Disagree
- Disagree
- Neither
- Agree
- Strongly agree

(5) **Rate your agreement with the following statement:I feel like I better understand the elements of good science communication with the public now compared to the beginning of the semester.**

- Strongly Disagree
- Disagree
- Neither
- Agree
- Strongly agree

(6) **On a scale of 1 (not at all confident) to 9 (very confident), how comfortable would you feel submitting an article to a popular science publication (e.g. Wired, Popular Science, Scientific American, Discover)?**

(7) **On a scale of 1 (not at all confident) to 9 (very confident), how confident are you in:**

- **Your ability to communicate with scientists?**
- **Your ability to communicate with the general public?**

Science Communication Attitudes
(Questions 8-10 of 10)

(8) **On a scale of 1 (not at all important) to 9 (very important), how important do you consider it to be for scientists to be able to communicate with the general, non-specialist public?**

(9) **How important do you think it is for scientists to engage directly with the non-specialist adult public on each of the following? Please rate importance on a scale of 1 (not important) to 5 (very important).**

(a) The scientific findings of their research
(b) Areas of further research
(c) Policy and regulatory issues
(d) The wider social and ethical implications of their research findings for society
(e) The potential benefits of their work to individuals
(f) The scientific process/the nature of science
(g) Scientific uncertainty
(h) The enjoyment and excitement of doing science
(i) The relevance of science to everyday life
(j) To raise awareness of career options in science

(10) **Below are some things scientists have said about engaging with the non-specialist public about science and engineering. Please indicate whether you agree or disagree for each statement.**

Scale:

- **Strongly Agree**
- **Agree**
- **Neither**
- **Disagree**
- **Strongly Disagree**
- **Don't know**

(a) Scientists who communicate a lot are not well regarded by other scientists
(b) Funders of scientific research should help scientists to communicate with the non-specialist public
(c) Scientists have a moral duty to engage with the non-specialist public about the social and ethical implications of their research

(d) A lot of scientific research isn't interesting to the non-specialist public

(e) The main reason to engage with the non-specialist public is to get their support for science and engineering

(f) Engagement with the non-specialist public is best done by trained professionals and journalists

(g) A lot of scientific research is too specialized to make much sense to the non-specialist public

(h) In order to communicate with the public, scientists need to determine the public's opinions on science issues

(i) Public engagement could help with scientists' careers

(j) Engaging with the non-specialist public is best done by senior researchers

(k) The main reason to engage with the non-specialist public is to provide them with information

(l) There are no personal benefits for scientists engaging with the non-specialist public

(m) If the general public understood science better then there would be more public support of science

(n) It is important to get public input into science policy issues

C.3 Rubric

Skill	Score of 1 means	Score of 3 means	Score of 5 means
Jargon Is the writer being careful to avoid or explain words that the public might not know?	Most sentences contain jargon without explanations, making paragraph difficult to read.	Some sentences contain jargon without explanations, but the paragraph is still understandable.	No sentences contain jargon without explanations, making the paragraph easy to read.
Readability Does the writer avoid run-on sentences and make his/her message clear?	Most sentences are run-on sentences or are difficult to read, and the writer's message is obscured as a result.	Some sentences are run-on sentences or are difficult to read, but the writer's message still comes across after a few read-throughs.	Writer does not use run-on sentences, and his/her message is very clear.
Correctness Is the writer presenting correct information?	Many sentences contain incorrect information.	Some sentences contain incorrect information.	Writer's information is entirely correct.
Relevance Has the writer told you why you should care about this?	Writer does not explain the relevance of the information to the reader or discuss why the reader should care about it.	Writer makes an effort to explain the relevance of the information to the reader, but the point he/she is making isn't clear.	Writer clearly explains the relevance of the information to the reader and discusses why the reader should care about it.
Organization Does the writer's paragraph build upon itself in a clear, logical way?	Writer's paragraph has no logical order and doesn't make any sense as a whole.	Some structure and logical flow is evident in the paragraph, but it's still choppy, disorganized, or confusing.	The paragraph is well structured, with each sentence logically following from the previous one.
Connection Does the writer use analogies or make connections to things his/her audience might have experienced in everyday life?	The writer makes no attempt at analogies, metaphors, or connections to everyday life.	The writer attempts analogy, metaphor or connection to everyday life, but not in a way that helps the reader's understanding of the subject.	The writer uses analogy, metaphor and everyday experiences clearly and accurately, in a way that successfully helps the reader to understand the subject.
Appeal Does the writer somehow hook the reader, use humor in his/her writing, or tell a story to interest his/her audience?	The writer makes no attempt at narrative, humor, or some sort of hook to interest the reader.	The writer makes a moderate attempt at narrative, humor, or some type of hook.	The writer uses good narrative, clever humor, or an enticing hook to successfully interest his/her audience.